



**U.S. Army  
Environmental  
Center**

# **Unexploded Ordnance Advanced Technology Demonstration Program at Jefferson Proving Ground (Phase II)**

**DISTRIBUTION STATEMENT A**

Approved for public release  
Distribution Unlimited

**June 1996**



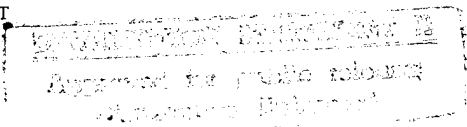
**DTIC QUALITY INSPECTED 1**

Distribution Unlimited; Approved for Public Release

## REPORT DOCUMENTATION PAGE

Form Approved  
OMB No. 0704-0188

Public reporting burden for this collection of information is estimated to average 1 hour per response, including the time for reviewing instructions, searching existing data sources, gathering and maintaining the data needed, and completing and reviewing the collection of information. Send comments regarding this burden estimate or any other aspect of this collection of information, including suggestions for reducing this burden to Washington Headquarters Services, Directorate for Information Operations and Reports, 1215 Jefferson Davis Highway, Suite 1204, Arlington, VA 22204-4302, and to the Office of Management and Budget, Paperwork Reduction Project (0704-01881), Washington, D.C. 20503.

1. AGENCY USE ONLY (Leave Blank)	2. REPORT DATE 17 June 1996	3. REPORT TYPE AND DATES COVERED	
4. TITLE AND SUBTITLE Unexploded Ordnance Advanced Technology Demonstration Program at Jefferson Proving Ground (Phase II)		5. FUNDING NUMBERS	
6. AUTHOR(S)		7. PERFORMING ORGANIZATION NAME(S) AND ADDRESS(ES) Naval Explosive Ordnance Disposal Technology Division Project Manager: Gerard Snyder 301/743-6855 Senior Engineer: Andy Pedersen 301/743-6856 2008 Stump Neck Road Indian Head, Md 20640-5070	
8. PERFORMING ORGANIZATION REPORT NUMBER		9. SPONSORING/MONITORING AGENCY NAME(S) AND ADDRESS(ES) U.S. Army Environmental Center Project Officer: Kelly Rigano 410/612-6868 Aberdeen Proving Ground, MD 21010-5401	
10. SPONSORING/MONITORING AGENCY REPORT NUMBER SFIM-AEC-ET-CR-96170		11. SUPPLEMENTARY NOTES  Supporting Contractors:   PRC Environmental Management, Inc.                      PRC Inc. 200 East Randolph Drive    801 N. Strauss Avenue Suite 4700    Indian Head, MD 20640 Chicago, IL 60601	
12a. DISTRIBUTION/AVAILABILITY STATEMENT Unlimited distribution			12b. DISTRIBUTION CODE "A"
13. ABSTRACT (Maximum 200 words) The report summarizes the results of unexploded ordnance technology demonstrations conducted at Jefferson Proving Ground, Indiana, during May through September 1995. The purpose of this Congressionally-mandated program was to identify and evaluate innovative and cost-effective systems for the detection, identification, and remediation of sites which contain UXO.			
14. SUBJECT TERMS Unexploded Ordnance, Munitions, Demonstration, Innovative Technology, Detection, Remediation		15. NUMBER OF PAGES	
16. PRICE CODE		17. SECURITY CLASSIFICATION OF REPORT Unclassified	
18. SECURITY CLASSIFICATION OF THIS PAGE Unclassified		19. SECURITY CLASSIFICATION OF ABSTRACT Unclassified	
20. LIMITATION OF ABSTRACT Unlimited		20. LIMITATION OF ABSTRACT Unlimited	

NSN 7540-01-280-5500

Standard Form 298 (Rev 12-94)  
Prescribed by ANSI Sta 239-18  
298-102

# 19960703 011

Report No. SFIM-AEC-ET-CR-96170

**Unexploded Ordnance  
Advanced Technology  
Demonstration Program at  
Jefferson Proving Ground  
(Phase II)**

**June 1996**

**Distribution Unlimited; Approved for Public Release**

## TABLE OF CONTENTS

<u>Section</u>	<u>Page</u>
EXECUTIVE SUMMARY .....	ES-1
1.0 INTRODUCTION .....	1-1
1.1 PROGRAM BACKGROUND .....	1-1
1.2 DEMCNSTRATION OBJECTIVES .....	1-4
2.0 SITE BACKGROUND .....	2-1
2.1 SITE DESCRIPTION .....	2-1
2.1.1 Topographic, Physiographic, and Geologic Properties .....	2-1
2.1.2 Ecologic Characteristics .....	2-2
2.1.3 Compliance with Environmental Regulations .....	2-3
2.1.4 Climatic Patterns .....	2-3
2.2 HISTORIC SITE USE .....	2-4
3.0 DEMONSTRATION TECHNICAL APPROACH .....	3-1
3.1 SITE PREPARATION .....	3-1
3.2 DEMONSTRATOR SELECTION PROCESS .....	3-4
3.3 DEMONSTRATION PROCEDURES .....	3-4
3.4 QUALITY ASSURANCE AND QUALITY CONTROL .....	3-5
3.4.1 Target Emplacement .....	3-5
3.4.2 Target Validation .....	3-6
3.4.3 Data Transmittal Control .....	3-6
3.4.4 Data Submittal and Algorithm Validation .....	3-6
4.0 PERFORMANCE EVALUATION METHODOLOGY .....	4-1
4.1 APPROACH .....	4-1
4.1.1 Target Matching Algorithms .....	4-2
4.1.2 Detection Performance .....	4-3



**TABLE OF CONTENTS**  
(continued)

<u>Section</u>	<u>Page</u>
4.1.3 Localization Performance .....	4-6
4.1.4 Identification and Classification Performance .....	4-8
4.2 PERFORMANCE ASSESSMENT .....	4-10
4.2.1 Performance Assessment Plots .....	4-10
4.2.2 Confidence Intervals .....	4-12
5.0 DEMONSTRATION RESULTS .....	5-1
5.1 MAGNETOMETER SENSOR SYSTEMS .....	5-1
5.1.1 Aerodat Inc. ....	5-1
5.1.1.1 Technology Description .....	5-1
5.1.1.2 System Assessment .....	5-3
5.1.1.3 Measured Performance .....	5-4
5.1.2 Australian Defence Industries, Pty. Ltd. ....	5-9
5.1.2.1 Technology Description .....	5-9
5.1.2.2 System Assessment .....	5-10
5.1.2.3 Measured Performance .....	5-11
5.1.3 Geometrics, Inc. ....	5-16
5.1.3.1 Technology Description .....	5-16
5.1.3.2 System Assessment .....	5-18
5.1.3.3 Measured Performance .....	5-19
5.1.4 Polestar Technologies, Inc. ....	5-24
5.1.4.1 Technology Description .....	5-24
5.1.4.2 System Assessment .....	5-25
5.1.4.3 Measured Performance .....	5-26
5.1.5 Scintrex, Inc. ....	5-27
5.1.5.1 Technology Description .....	5-27
5.1.5.2 System Assessment .....	5-27
5.1.5.3 Measured Performance .....	5-30

**TABLE OF CONTENTS**  
(continued)

<u>Section</u>	<u>Page</u>
5.1.6 Vallon GmbH .....	5-34
5.1.6.1 Technology Description .....	5-34
5.1.6.2 System Assessment .....	5-36
5.1.6.3 Measured Performance .....	5-37
5.2 ELECTROMAGNETIC INDUCTION SENSOR SYSTEMS .....	5-42
5.2.1 Bristol Aerospace Ltd. ....	5-42
5.2.1.1 Technology Description .....	5-42
5.2.1.2 System Assessment .....	5-43
5.2.1.3 Measured Performance .....	5-44
5.2.2 GeoPotential .....	5-49
5.2.2.1 Technology Description .....	5-49
5.2.2.2 System Assessment .....	5-50
5.2.2.3 Measured Performance .....	5-51
5.2.3 Parsons Engineering Science, Inc. ....	5-56
5.2.3.1 Technology Description .....	5-56
5.2.3.2 System Assessment .....	5-57
5.2.4.3 Measured Performance .....	5-58
5.3 GROUND PENETRATING RADAR SENSOR SYSTEMS .....	5-63
5.3.1 Airborne Environmental Surveys, Inc. ....	5-63
5.3.1.1 Technology Description .....	5-63
5.3.1.2 System Assessment .....	5-65
5.3.1.3 Measured Performance .....	5-66
5.3.2 Kaman Sciences Corporation .....	5-71
5.3.2.1 Technology Description .....	5-71
5.3.2.2 System Assessment .....	5-72
5.3.2.3 Measured Performance .....	5-73

**TABLE OF CONTENTS**  
(continued)

<u>Section</u>	<u>Page</u>
5.3.3 SRI International .....	5-78
5.3.3.1 Technology Description .....	5-78
5.3.3.2 System Assessment .....	5-79
5.3.3.3 Measured Performance .....	5-80
5.4 MAGNETOMETER AND ELECTROMAGNETIC INDUCTION .....	5-86
5.4.1 Australian Defence Industries, Pty. Ltd. ....	5-86
5.4.1.1 Technology Description .....	5-86
5.4.1.2 System Assessment .....	5-87
5.4.1.3 Measured Performance .....	5-88
5.4.2 Geo-Centers, Inc. ....	5-93
5.4.2.1 Technology Description .....	5-93
5.4.2.2 System Assessment .....	5-95
5.4.2.3 Measured Performance .....	5-97
5.4.3 Geophex Ltd. ....	5-101
5.4.3.1 Technology Description .....	5-101
5.4.3.2 System Assessment .....	5-103
5.4.3.3 Measured Performance .....	5-104
5.5 ELECTROMAGNETIC INDUCTION AND GROUND PENETRATING RADAR SENSOR SYSTEMS .....	5-108
5.5.1 Coleman Research Corporation .....	5-108
5.5.1.1 Technology Description .....	5-108
5.5.1.2 System Assessment .....	5-110
5.5.1.3 Measured Performance .....	5-111
5.6 REMEDIATION SYSTEMS .....	5-116
5.6.1 Concept Engineering Group, Inc. ....	5-116
5.6.1.1 Technology Description .....	5-116
5.6.1.2 System Assessment .....	5-117
5.6.1.3 Measured Performance .....	5-119

**TABLE OF CONTENTS**  
(continued)

<u>Section</u>	<u>Page</u>
5.6.2 Wright Laboratory .....	5-121
5.6.2.1 Technology Description .....	5-121
5.6.2.2 System Assessment .....	5-122
5.6.2.3 Measured Performance .....	5-124
6.0 COMPARISONS AND CONCLUSIONS .....	6-1
6.1 PERFORMANCE STATISTICS SUMMARY .....	6-1
6.2 ADDITIONAL PERFORMANCE STATISTICS .....	6-8
6.3 OPERATIONAL SUMMARY .....	6-9
6.4 SUMMARY AND CONCLUSIONS .....	6-11
REFERENCES .....	REF-1

**APPENDIXES**

Appendix

- A PERFORMANCE MEASUREMENT ALGORITHM DESCRIPTIONS
- B FENCE LINE AREA EXTRACTIONS 16A- AND 16B-HECTARE AREAS
- C DERIVATION OF  $P_{\text{random}}$
- D JPG CONTROLLED SITE 16B-HECTARE DEMONSTRATION AREA  
TARGET ANOMALY INVESTIGATION
- E MINE DETECTION STATISTICS
- F DEMONSTRATOR COST

GLOSSARY .....	GL-1
----------------	------

## LIST OF FIGURES

<u>Figure</u>	<u>Page</u>
ES-1	Plot of Demonstrator Probability of Detection (Ordnance) versus False Alarm Ratio . . . . . ES-10
ES-2	Individual Demonstrator Localization Performance . . . . . ES-11
ES-3	Individual Demonstrator Probability of Correct Identification (Classification by Type) . . . . . ES-12
2-1	Location of Jefferson Proving Ground . . . . . 2-5
2-2	Area Location Map . . . . . 2-6
3-1	16B-Hectare (40B-Acre) Demonstration Area . . . . . 3-7
4-1	Fence Line Extraction for 16A-Hectare Area with Sample Demonstrator Data . . . . . 4-14
4-2	Fence Line Extraction for 16B- and 32-Hectare Area with Sample Demonstrator Data . . . . . 4-15
4-3	Cumulative Distribution of Distance Between Nearest Neighbor Baseline Items at 16A-Hectare Area . . . . . 4-16
4-4	Cumulative Distribution of Distance Between Nearest Neighbor Baseline Items at 16B-Hectare Area . . . . . 4-17
4-5	Sample Receiver Operating Characteristics (ROC) Curve . . . . . 4-18
4-6	Sample Signal and Noise Distribution with Mean Signal to Noise Ratio (SNR) = 2 . . . . . 4-19
4-7	Sample Signal and Noise Distribution with Mean Signal to Noise Ratio (SNR) = 3 . . . . . 4-20
4-8	Sample Plot Illustrating Detection as a Function of Depth and Size (Diameter) – Trend Indicated . . . . . 4-21
4-9	Sample Plot Illustrating Detection as a Function of Depth and Size (Diameter) – No Trend Indicated . . . . . 4-22
4-10	Plot of Demonstrator Probability of Detection (Ordnance) versus False Alarm Ratio . . . . . 4-23
5.1.1-1	Aerodat Inc., Airborne Detection System . . . . . 5-2
5.1.1-2	Aerodat Target Declarations . . . . . 5-6
5.1.1-3	Aerodat Detection Ability . . . . . 5-8
5.1.2-1	Australian Defence Industries, Pty. Ltd., TM-4 Imaging Magnetometer . . . . . 5-9
5.1.2-2	ADI Magnetometer Target Declarations . . . . . 5-13
5.1.2-3	ADI Magnetometer Detection Ability . . . . . 5-15
5.1.3-1	Geometrics, Inc. G-858 Magnetometer . . . . . 5-16
5.1.3-2	Geometrics Ground Penetrating Radar System . . . . . 5-17
5.1.3-3	Geometrics Target Declarations . . . . . 5-21
5.1.3-4	Geometrics Detection Ability . . . . . 5-23
5.1.4-1	Polestar Technologies, Inc., Magnetometer System . . . . . 5-24
5.1.5-1	Scintrex, Inc., Smartmag Magnetometer System . . . . . 5-28
5.1.5-2	Scintrex Target Declarations . . . . . 5-31
5.1.5-3	Scintrex Detection Ability . . . . . 5-33
5.1.6-1	Vallon GmbH Multisensor Vehicle . . . . . 5-34
5.1.6-2	Vallon Man-Portable Sensor Positioning System . . . . . 5-35
5.1.6-3	Vallon Target Declarations . . . . . 5-39
5.1.6-4	Vallon Detection Ability . . . . . 5-41
5.2.1-1	Bristol Aerospace Ltd., Pulse Induction Sensor Array . . . . . 5-42
5.2.1-2	Bristol Target Declarations . . . . . 5-46
5.2.1-3	Bristol Detection Ability . . . . . 5-48
5.2.2-1	GeoPotential Electromagnetic Induction Instrument . . . . . 5-49

**LIST OF FIGURES**  
(continued)

<u>Figure</u>	<u>Page</u>
5.2.2-2 GeoPotential Target Declarations .....	5-53
5.2.2-3 GeoPotential Detection Ability .....	5-55
5.2.3-1 Parsons Engineering Science, Inc., EM-61 Electromagnetic Unit .....	5-56
5.2.3-2 Parson Target Declarations .....	5-60
5.2.3-3 Parson Detection Ability .....	5-62
5.3.1-1 Airborne Environmental Surveys, Inc., Airborne Ground Penetrating Radar System .....	5-63
5.3.1-2 Digital Airborne Imaging Spectrometer System .....	5-64
5.3.1-3 AES Target Declarations .....	5-68
5.3.1-4 AES Detection Ability .....	5-70
5.3.2-1 Kaman Sciences Corporation Towed Ground Penetrating Radar .....	5-71
5.3.2-2 Kaman Target Declarations .....	5-75
5.3.2-3 Kaman Detection Ability .....	5-77
5.3.3-1 SRI International Airborne Ground Penetrating Radar System .....	5-78
5.3.3-2 SRI Target Declarations .....	5-83
5.3.3-3 SRI Detection Ability .....	5-85
5.4.1-1 ADI EM-61 Electromagnetic Time-Domain Unit .....	5-86
5.4.1-2 ADI Magnetometer & EM Target Declarations .....	5-90
5.4.1-3 ADI Magnetometer & EM Detection Ability .....	5-92
5.4.2-1 Geo-Centers, Inc., Surface Towed Ordnance Locator System .....	5-93
5.4.2-2 Geo-Centers EM-61 Electromagnetic Unit .....	5-94
5.4.2-3 Geo-Centers Schiebel EM Sensors .....	5-95
5.4.2-4 Geo-Centers Target Declarations .....	5-98
5.4.2-5 Geo-Centers Detection Ability .....	5-100
5.4.3-1 Geophex Ltd. G-858 Magnetometer .....	5-101
5.4.3-2 Geophex Ltd. GEM-2 Electromagnetic Unit .....	5-102
5.4.3-3 Geophex Target Declarations .....	5-105
5.4.3-4 Geophex Detection Ability .....	5-107
5.5.1-1 Coleman Research Corporation Towed Multi-Sensor Array System .....	5-108
5.5.1-2 Coleman Target Declarations .....	5-113
5.5.1-3 Coleman Detection Ability .....	5-115
5.6.1-1 Concept Engineering Group, Inc. Soft Trencher System .....	5-117
5.6.2-1 Wright Laboratory Remote Excavation Vehicle .....	5-121
6-1 Individual Demonstrator Probability of Detection (Ordnance) .....	6-13
6-2 Individual Demonstrator False Alarm Rate .....	6-14
6-3 Plot of Demonstrator Probability of Detection (Ordnance) versus Probability of False Alarm .....	6-15
6-4 Optimal Performance Statistics by Demonstrator .....	6-16
6-5 Individual Demonstrator Localization Performance .....	6-17
6-6 Individual Demonstrator Probability of Correct Identification (Classification by Type) .....	6-18
6-7 Individual Demonstrator Probability of Correct Classification by Size .....	6-19
6-8 Individual Demonstrator Probability of Correct Classification by Class .....	6-20
6-9 Demonstrator Probability of Detection (Ordnance) Versus False Alarm Ratio .....	6-21

## LIST OF TABLES

<u>Table</u>		<u>Page</u>
ES-1	DEMONSTRATED DETECTION TECHNOLOGIES .....	ES-4
ES-2	DEMONSTRATOR SYSTEM AND LOCALIZATION PERFORMANCE .....	ES-5
ES-2	FRACTION OF DEMONSTRATOR TARGET REPORTS IDENTIFIED AND CLASSIFIED .....	ES-6
1-1	DEMONSTRATED TECHNOLOGIES .....	1-3
5.1.1-1	PERFORMANCE STATISTICS FOR AERODAT .....	5-7
5.1.2-1	PERFORMANCE STATISTICS FOR ADI (MAGNETOMETER DATA) .....	5-14
5.1.3-1	PERFORMANCE STATISTICS FOR GEOMETRICS .....	5-22
5.1.5-1	PERFORMANCE STATISTICS FOR SCINTREX .....	5-32
5.1.6-1	PERFORMANCE STATISTICS FOR VALLON .....	5-40
5.2.1-1	PERFORMANCE STATISTICS FOR BRISTOL .....	5-47
5.2.2-1	PERFORMANCE STATISTICS FOR GEOPOTENTIAL .....	5-54
5.2.3-1	PERFORMANCE STATISTICS FOR PARSONS .....	5-61
5.3.1-1	PERFORMANCE STATISTICS FOR AES .....	5-69
5.3.2-1	PERFORMANCE STATISTICS FOR KAMAN .....	5-76
5.3.3-1	PERFORMANCE STATISTICS FOR SRI .....	5-84
5.4.1-1	PERFORMANCE STATISTICS FOR ADI (MAGNETOMETER AND EM INDUCTION) .....	5-91
5.4.2-1	PERFORMANCE STATISTICS FOR GEO-CENTERS .....	5-99
5.4.3-1	PERFORMANCE STATISTICS FOR GEOPHEX .....	5-106
5.5.1-1	PERFORMANCE STATISTICS FOR COLEMAN .....	5-114
5.6.1-1	CONCEPT ENGINEERING GROUP, INC. - 16A-HECTARE AREA .....	5-120
5.6.2-1	WRIGHT LABORATORY - 16A-HECTARE AREA .....	5-125
6-1	DEMONSTRATOR DETECTION AND LOCALIZATION BY SENSOR TYPE .....	6-2
6-2	DEMONSTRATOR IDENTIFICATION AND CLASSIFICATION (TYPE, SIZE, AND CLASS) BY SENSOR TYPE .....	6-3
6-3	DEMONSTRATOR OPTIMAL PERFORMANCE EVALUATION SYSTEM .....	6-5
6-4	DEMONSTRATOR IDENTIFICATION AND CLASSIFICATION INFORMATION PROVIDED .....	6-7
6-5	SUMMARY OF DEMONSTRATOR AREA COVERAGE .....	6-11

## **EXECUTIVE SUMMARY**

This report presents results of the Phase II controlled site unexploded ordnance (UXO) advanced technology demonstration (ATD) conducted at U.S. Army Jefferson Proving Ground (JPG) in Madison, Indiana. The purpose of the UXO ATD program is to assess the capabilities of technologies useful for the detection, identification, and remediation of UXO. Performance data gathered as a result of the ATDs can be used by the Government to aid in selecting effective and efficient systems for UXO clearance in response to the global UXO problem.

### **Problem Statement and Description of the UXO Clearance Technology Program**

In the United States, millions of hectares of Government-owned and formerly owned properties contain buried UXO. Bombs, missiles, mines, projectiles, submunitions, rockets, and other types of ordnance have been the result of operations conducted at functional test ranges, impact ranges, training areas, and disposal areas. Properties requiring cleanup include installations identified for base realignment and closure (BRAC), formerly used defense sites, and active installations that are considering alternate uses for properties containing UXO. The Department of Defense (DoD) has estimated that UXO cleanup efforts in the United States alone may cost \$28 to \$48 billion.

In addition, more than 60 countries report a need to remediate a wide range of UXO, including land mines and ordnance from World Wars I and II. As of December 1994, the State Department estimated that 80 to 110 million land mines remain uncleared, primarily in undeveloped countries. This UXO results in approximately 10,000 deaths and 30,000 injuries each year. The presence of UXO also denies countries the use of agricultural land and other resources.

In response to this need, the U.S. Army Environmental Center (USAEC) and the Naval Explosive Ordnance Disposal Technology Division (NAVEODTECHDIV) established the UXO Clearance Technology Program to demonstrate, evaluate, and characterize advanced technology for UXO clearance.



## **Summary of the Program Objective and Background**

In recent years, U.S. Congress has recognized the need for using more effective, reliable, safe, and economical systems and technology for UXO clearance. In fiscal year 1993, USAEC efforts in demonstrating, evaluating, and enhancing UXO clearance technology were greatly expanded to address a congressional mandate to demonstrate and evaluate the performance of commercially available and government-enhanced systems designed for UXO clearance.

In fiscal year 1994, USAEC created a 48 hectare controlled test site containing inert ordnance at JPG. The test site was comprised of a 16-hectare area designed for ground demonstrations and a 32-hectare area designed for airborne demonstrations. At these two areas, inert ordnance, nonordnance, and debris were buried at precise but unpublished locations, depths, and orientations that are representative of realistic conditions at sites containing UXO. The types of ordnance emplaced at the site ranged from mines and submunitions less than 5 inches in diameter to 2,000-pound bombs. Ground-based demonstrators were allotted 40 hours to survey 16 hectares, airborne demonstrators were allotted 40 hours to survey 32 hectares, and remediation demonstrators were allotted 40 hours to excavate as many targets as possible during that time and demonstrate their unique capabilities. Detection demonstrator data were then compared with defined "target" locations.

The objectives of the 1994 Phase I ATD project included identifying and evaluating commercial, prototype, and operational technologies for UXO detection, identification, and remediation; establishing a technology performance baseline; and understanding the performance of current UXO clearance technology. The demonstration results also identified areas that require further research and development.

## **Discussion of Phase II Objectives, Process, and Demonstrations**

Congress appropriated additional funding in fiscal year 1994 to continue the program for a second phase. As with Phase I, the Phase II demonstrations were conducted at JPG. The objectives for Phase II again included evaluating technologies effective for detecting, identifying, and remediating UXO, as well as measuring these results against the Phase I baseline. The demonstration areas were modified for Phase II, including the creation of a second ground demonstration area within the air demonstration area. To ensure site integrity for this phase of the demonstrations, several changes were made to both areas as inert ordnance items were

excavated and removed and new inert ordnance items were emplaced. During Phase II, 15 UXO detection systems and two remediation systems were demonstrated from May through September 1995, following procedures similar to Phase I. Table ES-1 summarizes the detection technologies and transport systems demonstrated at the controlled site. Detection system technologies included four magnetometer systems, three electromagnetic (EM) induction systems, three ground-penetrating radar (GPR) systems, and five multi-sensor systems. Of the detection systems, six were man-portable, two were vehicle-towed, four were combined man-portable and vehicle-towed (multimodal), and three were airborne. Two remediation systems were demonstrated: a remote backhoe and a soft trencher. This report summarizes the operational performance of both detection and remediation systems based on field oversight and their measured performance based on data analysis.

### **Measured Performance Results**

After surveying their assigned area, each of the demonstrators was to process their data and report the locations of suspected targets. For each target location, the demonstrators were to supply estimates of the depth, type (ordnance or nonordnance), size (small, medium, or large), and class (bomb, projectile, mortar, or cluster). After receiving the demonstrators' reported targets, these results were compared to the baseline to determine probability of detection, false alarm ratio, mean radial and depth error, and the fraction of detections that were correctly identified or classified.

Tables ES-2 and ES-3 summarize demonstrator performance with respect to detection, localization, identification, and classification. Several conclusions can be drawn from data analysis of the demonstration results. The best performance in detecting ordnance was demonstrated by Parsons Engineering Science, Inc. (Parsons), using an EM induction system and Geometrics, Inc. (Geometrics), using a magnetometer system. Demonstrators employing GPR exhibited poor detection capabilities. Systems employing a combination of magnetometer and EM induction sensors had a narrow range of high  $P_D$  values (0.65 - 0.72) (see Table ES-2). All of the airborne demonstrators showed poor detection capabilities, regardless of sensor type employed.

**TABLE ES-1  
DEMONSTRATED DETECTION TECHNOLOGIES**

Demonstrator	Transport						Sensor System		
	Ground			Aerial			Magnetometer	EM	GPR
	Vehicle-Towed	Man-Portable	Rotary-Wing	Fixed-Wing					
Aerodat Inc.			✓			✓			
Airborne Environmental Surveys, Inc.			✓					✓	
Australian Defence Industries, Pty. Ltd.		✓				✓	✓		
Bristol Aerospace Ltd.	✓						✓		
Coleman Research Corporation	✓	✓					✓	✓	
Geo-Centers, Inc.	✓	✓				✓	✓		
Geometrics, Inc. <sup>1</sup>	✓	✓				✓		✓	
Geophex Ltd.		✓				✓	✓		
GeoPotential		✓					✓		
Kaman Sciences Corporation	✓							✓	
Parsons Engineering Science, Inc.		✓					✓		
Polestar Technologies, Inc.		✓				✓			
Scintrex, Inc.		✓				✓			
SRI International			✓						
Valloum GmbH	✓	✓				✓		✓	

Note: <sup>1</sup> Geometrics's GPR system was demonstrated in the field, but results were not included for analysis.

**TABLE ES-2  
DEMONSTRATOR SYSTEM AND LOCALIZATION PERFORMANCE**

Sensor Type	Demonstrator	System Performance		Localization	
		P <sub>D</sub> (Ord)	False Alarm Ratio <sup>1</sup>	Horizontal (Radial) (m)	Vertical ( Depth ) (m)
Magnetometer (MAG)	Geometrics	0.83	3.96	0.65	0.62
	ADI (MAG)	0.63	8.88	0.74	0.68
	Vallon	0.57	68.5	0.83	0.98
	Scintrex	0.50	10.1	0.94	0.87
	Aerodat	0.02	18.5	2.29	2.07
	Parsons	0.85	4.68	0.79	0.72
Electromagnetic	Bristol	0.62	6.97	1.04	0.97
	GeoPotential	0.11	13.0	1.30	0.80
	AES	0.05	3.11	2.76	0.99
Ground-Penetrating Radar (GPR)	SRI	0.01	27.7	3.49	2.42
	Kaman	0.00	NA	NA	NA
	Geo-Centers	0.72	20.7	0.81	0.88
Magnetometer and Electromagnetic (EM)	Geophex	0.71	3.41	0.91	0.62
	ADI (MAG and EM)	0.65	9.35	0.74	0.68
EM and GPR	Coleman	0.29	9.56	1.41	1.00

Notes:

NA Not applicable because no ordnance items were detected

<sup>1</sup> False alarms per UXO items detected

**TABLE ES-3  
FRACTION OF DEMONSTRATOR TARGET REPORTS IDENTIFIED AND CLASSIFIED**

Demonstrator	Identification		Size			Class			
	Nonordnance		Large	Medium	Small	Bombs	Projectiles	Mortars	Clusters
Geometrics <sup>1</sup>	0.00		0.74	0.54	0.80	NA	NA	NA	NA
ADI (MAG)	0.11		0.65	0.57	0.96	0.77	0.42	0.35	0.00
Vallon <sup>2</sup>	NA		0.17	0.88	0.38	0.33	0.00	0.00	0.00
Scintrex	0.00		0.50	1.00	0.25	0.75	0.40	0.33	NA
Aerodat <sup>2</sup>	NA		NA	NA	NA	NA	NA	NA	NA
Parsons	0.10		0.16	0.75	0.23	0.12	0.57	0.25	0.00
Bristol <sup>2</sup>	NA		NA	NA	NA	NA	NA	NA	NA
GeoPotential <sup>1</sup>	0.00		0.00	0.50	0.33	0.50	0.60	0.33	NA
AES	NA		0.75	0.00	0.33	1.00	1.00	0.00	NA
SRI <sup>2</sup>	NA		NA	NA	NA	NA	NA	NA	NA
Kaman <sup>2</sup>	NA		NA	NA	NA	NA	NA	NA	NA
Geo-Centers <sup>1</sup>	0.00		0.67	0.80	0.86	0.93	0.76	0.00	0.00
Geophex <sup>2</sup>	0.23		0.88	0.38	0.43	NA	NA	NA	NA
ADI (MAG & EM)	0.11		0.65	0.53	0.92	0.77	0.38	0.35	0.00
Coleman <sup>1</sup>	0.00		0.14	0.25	0.92	0.33	0.87	0.00	0.00

Notes:

NA Not applicable

<sup>1</sup> Demonstrator reported all target types as "ordnance."

<sup>2</sup> Demonstrator did not provide type, size, and/or class information for declarations or listed them as "unknown."

The false alarm ratio, defined as the number of false alarms divided by the number of ordnance items detected, assesses the impact of a demonstrator's false alarms on a remediation effort. The ratio defines the number of nonordnance items that would be excavated for every ordnance item. False alarm ratios for the Phase II demonstrators ranged from approximately 3 to 70, differing greatly between the various systems. Although the GPR systems had the lowest false alarm ratios, this was outweighed by their low detection capabilities ( $P_D$  values). The highest false alarm ratio was produced by a ground-portable magnetometer system.

Figure ES-1 presents a plot of  $P_D$  versus false alarm ratio for the demonstrators. The plot shows demonstrators with better detection performance in the upper left corner, and those with poorer performance in the lower right corner. Both of the best performers (Parsons and Geometrics) employed advanced data processing, which may have contributed to their good performance.

Figure ES-2 illustrates the localization capability of the various sensor types. The figure depicts the mean horizontal positions and mean vertical depth errors in meters. With the exception of airborne systems, magnetometer sensors and a combination of magnetometer and EM induction sensors proved to have the best localization capability.

With respect to identification (classification by type), few demonstrators showed any capability to discriminate between ordnance and nonordnance (see Table ES-3). Geophex Inc., had the best identification performance, with a 0.23 probability of correctly classifying nonordnance (Figure ES-3). Most demonstrators providing class information were more successful at correctly identifying bombs and projectiles than other ordnance classes. Although many of the demonstrators detected clusters, none exhibited the ability to correctly classify them. It is possible that the resolution of their systems or processing is not sufficient to resolve closely spaced clusters of ordnance items.

The two remediation demonstrators were successful at excavating targets within the given 24 hours. The remote excavation vehicle system demonstrated an average rate of 0.57 hour per hole including ordnance removal. The soft trencher demonstrated an average rate of 0.75 hour per hole without ordnance removal, at depths ranging from 0.03 to 3.81 meters.

## Field Operations

The capabilities and limitations of the various detection systems were influenced by the transportation mode utilized, the terrain at the demonstration areas, and the weather conditions. Man-portable systems were more durable and were able to access the entire site successfully; however these systems were limited by the speed and stamina of the field equipment operator. Vehicle-towed systems covered the site quickly but were often subject to breakdowns that caused time-consuming delays. Multimodal systems were able to easily traverse open areas with vehicle systems and use man-portable platforms in heavy vegetation areas. Airborne systems, while yielding the best coverage rates, proved to have very low detection capabilities. Both remediation systems were prone to frequent breakdowns.

## Summary

Currently available site characterization and remediation tools are not adequate to effectively and economically respond to the UXO problem. First, although survey rates for the more effective systems are on the order of 0.40 hectares per hour, a significant amount of ordnance will remain undetected. Even the best system demonstrated during Phase II failed to detect 15 percent of the ordnance items. Second, the inability to distinguish nonordnance from ordnance results in high false alarm ratios; this means that most of the effort to excavate buried UXO will be nonproductive. For example, some of the better performers had false alarm ratios ranging from 3.41 to 4.68. Even with these results, for every excavation producing a UXO item, approximately three to five holes would be excavated that would not contain UXO. Finally, the excavation process itself is a limiting factor to remediation as detection systems can locate suspected targets up to 20 times faster than they can be excavated.

As it becomes necessary to address the growing number of UXO sites worldwide, more capable technologies will be needed to assist in site restoration and risk reduction processes. The UXO ATD project constitutes an important first step in a series of testing and evaluation projects to help meet this need. The two phases of this project have identified key technology issues and lessons learned that need to be addressed to meet DoD needs:

- $P_D$  must be improved while a reduction in false alarms is realized.

- False alarms must be reduced through more sophisticated processing and better discrimination techniques.
- Classification capabilities must be improved to make remediation more cost-effective.
- Advanced data processing and data fusion from multi-sensor platforms must be investigated.
- Site survey speed must be increased without compromising detection capability.
- To be useful, large area survey technologies such as airborne systems must be improved.
- Remediation rates must be improved in order to make facility cleanup possible.
- New approaches for remediating surface and subsurface UXO are needed.
- Systems need to be evaluated under varying environmental and topographic conditions.
- Systems need to be evaluated according to specific performance capabilities and strengths.

The Phase I results showed that there was very limited detection capability, excessively high false alarm rates, and minimal discrimination and classification ability. Of the 25 systems tested during Phase I of the UXO ATDs, the best technology could only detect approximately 65 percent of the inert ordnance emplaced at the controlled test site. To achieve this detection rate, however, the system reported nearly 60 false alarms per UXO item detected, and demonstrated no ability to discriminate between UXO and clutter and debris.

Phase II results showed some improvement as the best systems detected approximately 85 percent of the emplaced ordnance and reported about 4 false alarms per UXO item detected. This significant increase in detection and corresponding reduction in false alarms from Phase I to Phase II was principally attributed to the proper selection and application of technology for the JPG environment. However, as in Phase I, none of the systems demonstrated any significant ability to classify UXO or discriminate between UXO and clutter and debris.



**Figure ES-1**  
**Plot of Demonstrator Probability of Detection (Ordnance) versus False Alarm Ratio**

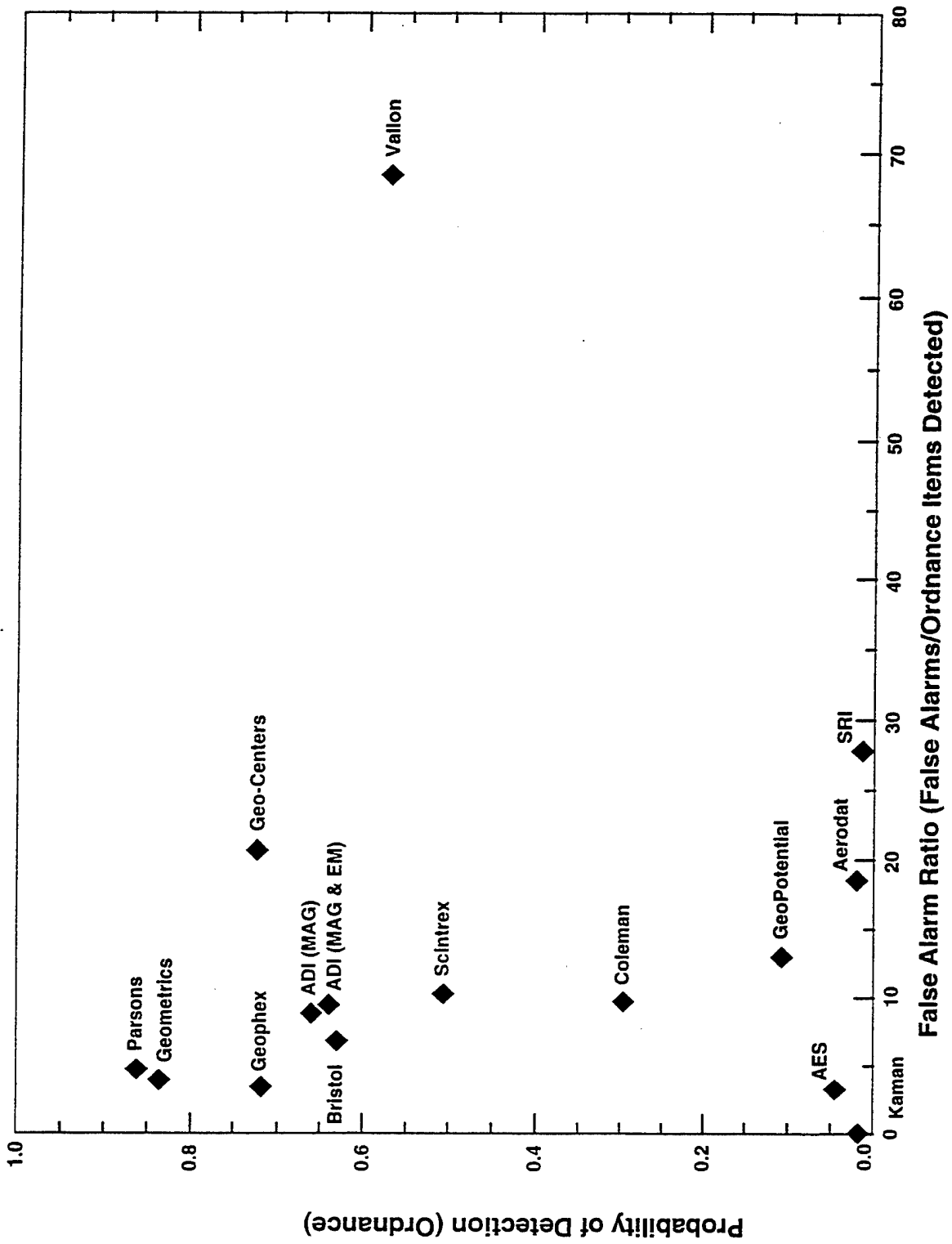


**Figure ES-2  
Individual Demonstrator Localization Performance**

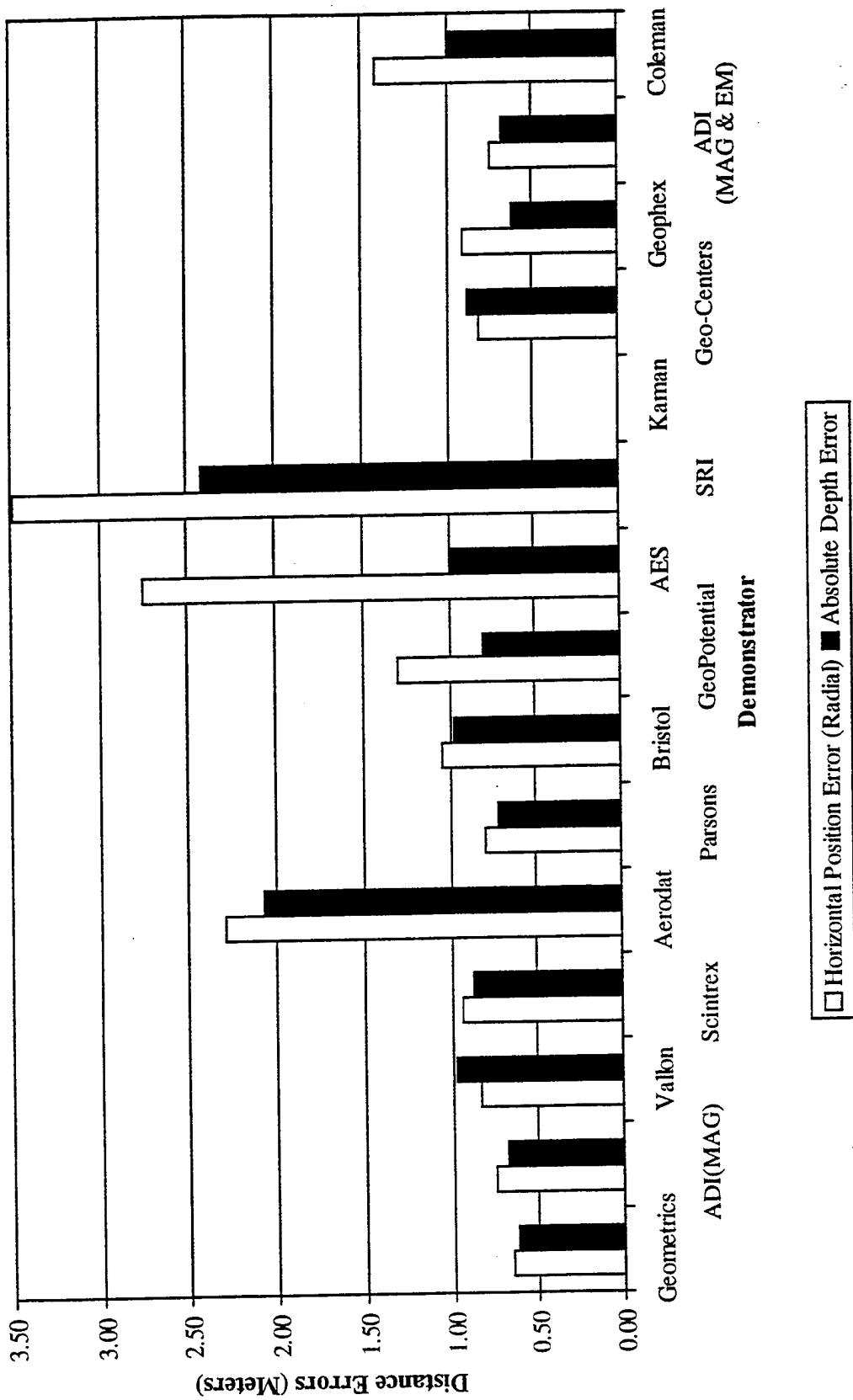
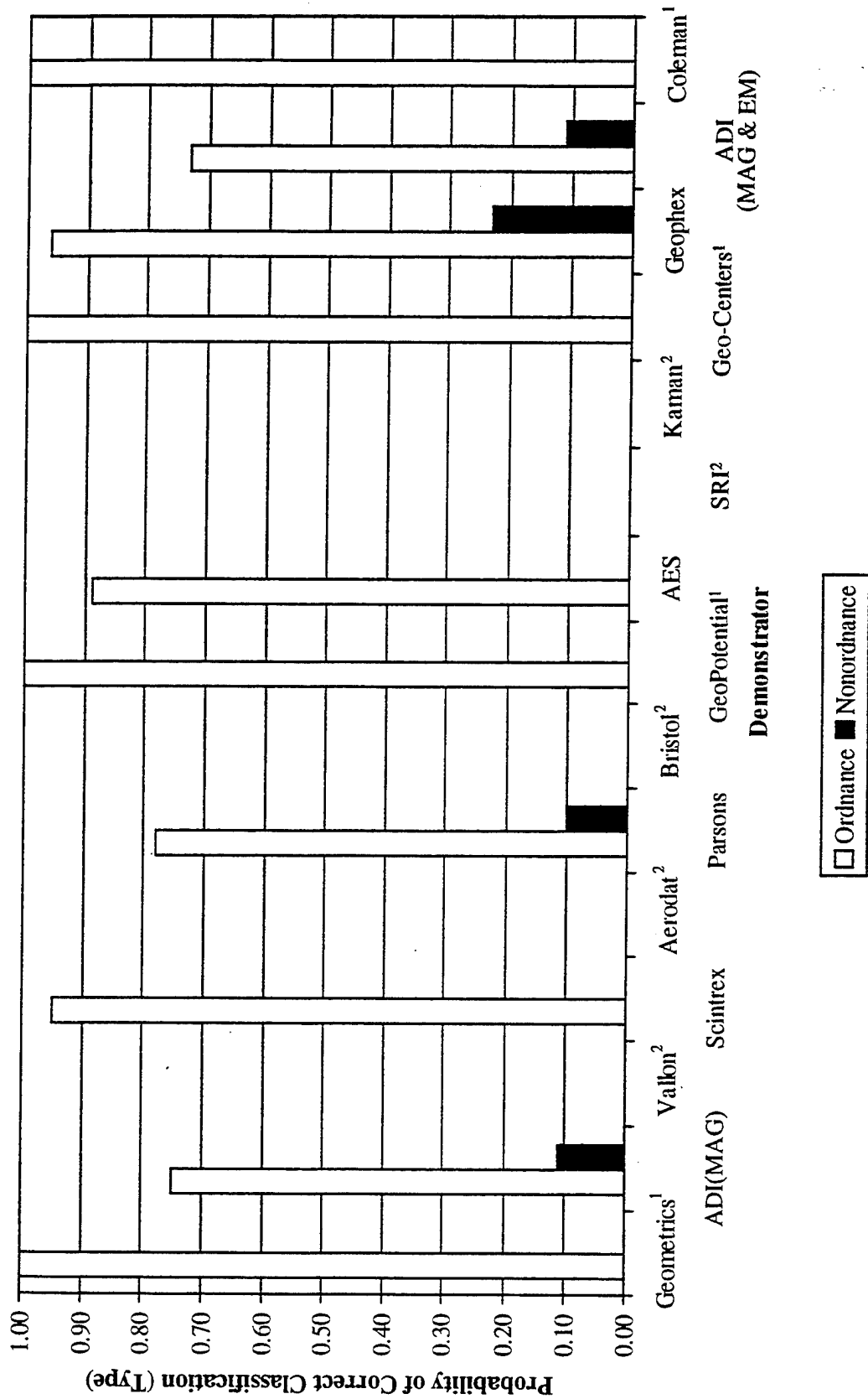


**Figure ES-3  
Individual Demonstrator Probability of Correct Identification (Classification by Type)**



Notes: <sup>1</sup> Demonstrator reported all target declarations as "ordnance"  
<sup>2</sup> Demonstrator did not provide type information for declarations or listed as "unknown"

## 1.0 INTRODUCTION

Many hectares of previously owned or currently owned U.S. Department of Defense (DoD) sites contain unexploded ordnance (UXO) as a result of military training and testing activities conducted to maintain mission readiness. The types of ordnance at these sites range from centuries-old cannonballs to currently used rockets, projectiles, bombs, mortars, submunitions, and mines.

The U.S. Army Environmental Center (USAEC) has established and currently manages the UXO Clearance Technology Program to address UXO issues. The goal of this program is to enhance, demonstrate, and evaluate UXO identification and remediation technologies to provide the Government with more reliable, accurate, safe, and cost-effective methods for UXO characterization and clearance. USAEC has designated the Naval Explosive Ordnance Technology Division (NAVEODTECHDIV) as the technical lead for this program.

### 1.1 PROGRAM BACKGROUND

In response to the congressional mandate in HR 5504, USAEC and NAVEODTECHDIV established the Advanced Technology Demonstration (ATD) program to identify and evaluate technologies for UXO detection, identification, and remediation (U.S. House of Representatives [USHR] 1992a, 1992b, 1992c). In fiscal year 1994, USAEC and NAVEODTECHDIV created two controlled demonstration sites at the Jefferson Proving Ground (JPG) in Madison, Indiana. Phase I of the UXO ATD program was conducted from April through October 1994; Phase II was conducted from May through September 1995.

In preparation for the Phase I demonstrations, two controlled test site areas were prepared: a 16-hectare (40-acre) area for ground system demonstrations and a 32-hectare (80-acre) area for airborne system demonstrations. These areas are referred to as "controlled" because the emplaced items provide a known baseline for the performance measurement of clearance technologies. The areas were surveyed, and a 30.5- by 30.5-meter (100- by 100-foot) grid system was established in each area. The areas were then prepared by emplacing inert ordnance and nonordnance items at depths and orientations typical of UXO-contaminated areas. The position of each emplaced item was measured by a licensed surveyor and recorded in a target database to provide a baseline against which demonstrator performance could be measured.

For Phase I, 29 systems were demonstrated from April through October 1994 (USAEC 1995). The systems demonstrated included man-portable, vehicle, combination man-portable and vehicle (multi-modal), airborne, and remediation systems. In addition, a variety of sensor technologies were demonstrated, including magnetometer systems, electromagnetic induction systems, ground penetrating radar systems, infrared systems, and combinations of the above.

Phase II was open to all technology developers. Demonstrators who participated in Phase I were eligible for Phase II only if significant improvements or changes had been made to their system. Proposals were evaluated in a manner similar to Phase I; selection criteria included technical approach, experience, and best value to the Government. A total of 17 systems were accepted by the government panel for Phase II.

Phase II was conducted from May through September 1995. The 17 systems demonstrated in Phase II included three airborne systems, six man-portable systems, two vehicle-towed systems, four combined man-portable and vehicle-towed (multimodal) systems, and two remediation systems. The 15 detection technologies used magnetometer systems, electromagnetic induction, and ground penetrating radar systems, as shown in Table 1-1. This report discusses Phase II of the UXO detection, identification, and remediation ATDs.

To ensure data uniformity, each demonstrator was requested to submit data in a standardized data entry software program. Measures of effectiveness were developed to provide a technically meaningful framework for assessing demonstrator performance. The measures were based on a target-matching algorithm (TMA) developed for this project and were expressed as target detection ratios (percentages of emplaced targets located by each demonstrator); classification ratios (percentages of emplaced targets correctly identified by each demonstrator); error ratios (percentages of each demonstrator's reported targets declared to be incorrectly identified ordnance); and additional data, such as the size, class, depth, and relative orientation of each target. Demonstrator data were collected, entered into the target database, and analyzed using the TMA. Phase I results were presented in Report No. SFIM-AEC-ET- CR-94120 dated December 1994. Ground based system overall detection ratios ranged from 1 to 65 percent. Airborne systems received overall detection ratios between 0 and 8 percent. The remediation systems demonstrated during Phase I operated at a slow rate (between 4 and 11 targets in 40 hours), but proved successful in excavating targets.

**TABLE 1-1**

**DEMONSTRATED TECHNOLOGIES**

Demonstrator	Magnetometer	Electromagnetic Induction	Ground Penetrating Radar
<b>Airborne Systems</b>			
Aerodat Inc.	X		
Airborne Environmental Surveys, Inc.			X
SRI International			X
<b>Man-Portable Systems</b>			
Australian Defence Industries, Pty. Inc.	X	X	
Geophex Ltd	X	X	
GeoPotential		X	
Parsons Engineering Science, Inc.		X	
Polestar Technologies, Inc.	X		
Scintrex, Inc.	X		
<b>Vehicle Systems</b>			
Bristol Aerospace Ltd.		X	
Kaman Sciences Corp.			X
<b>Multimodal Systems</b>			
Coleman Research Corp.		X	X
Geo-Centers, Inc.	X	X	
Geometrics, Inc.	X		X
Vallon GmbH (in cooperation with Security Search Products)	X		

## 1.2

### DEMONSTRATION OBJECTIVES

The objectives of the Phase II UXO-ATD program were to obtain system capability and performance data on UXO detection and remediation technologies. The data objectives for demonstrators were:

- to report the location of targets detected in the test area
- to localize targets detected within the test area
- to discriminate ordnance from nonordnance targets
- to classify ordnance targets detected in the test area
- and in the case of remediation demonstrators, excavate or remove ordnance items.

The objectives of the evaluators of the Phase II data were:

- to evaluate overall system and technology performance and provide system capability and limitation information to the user community
- to evaluate individual sensor performance, providing useful information for demonstration contractors and end users of the technology, as well as, potentially indicate directions for future sensor technology improvement
- to compare system performance against the Phase I baseline
- to identify promising technologies that can be used to provide more economical, safe, and effective UXO clearance
- to identify research and development efforts that would provide the Government with the greatest return on investment

## 2.0 SITE BACKGROUND

### 2.1 SITE DESCRIPTION

JPG is located about 5 miles north of Madison, Indiana, in Jefferson, Ripley, and Jennings Counties (See Figure 2-1). The facility covers about 22,365 hectares (55,265 acres) and includes firing lines, impact areas, buildings, and roadways.

As discussed in Section 1.1, two areas within JPG were selected for demonstrations during Phase I of the UXO-ATD program. A 16-hectare area in the northwest quarter of Section 36, Township 6 North, Range 10 East was designed for demonstrations of ground systems. A 32-hectare area at the center of Section 14, Township 5 North, Range 10 East was designed for demonstrations of airborne systems. The areas are located adjacent to access roads on the east side of the facility (see Figure 2-2).

#### 2.1.1 Topographic, Physiographic, and Geologic Properties

Topographic relief in Jefferson County is influenced by the Ohio and Muscatatuck River watersheds. The Ohio River watershed, located in the eastern third of Jefferson County, is very dissected and is characterized by narrow, sloping ridges and steep hillsides with terraces. The Muscatatuck River watershed, located in the western two-thirds of Jefferson County, is characterized by broad, nearly level ridges and moderately sloping hillsides. The major tributary of the Ohio River in Jefferson County is Indian-Kentuck Creek, which drains the eastern third of the county (USDA 1985b).

Physiographically, the demonstration areas are nearly level with a slightly undulating surface, marked by minor erosional features from surface water runoff. Both areas are well-vegetated with grasses, shrubs, and trees. No tributaries to the Ohio or Muscatatuck Rivers dissect the demonstration areas.

The demonstration areas are located on the uplands, in areas of sparse forestation. Both areas are located adjacent to access roads along the east side of the facility. Drainage at the 16A-hectare area is to the west into Big Creek. Drainage at the 32-hectare area is to the east into West Fork Creek.



Surficial soils are situated on a flat plain known as the Illinoisan till plain (Indiana Department of Natural Resources [IDNR] no date). The plain consists of glacial till deposited during Illinoisan glaciation. The glacial deposits are underlain by Silurian-aged Laurel Dolomite bedrock. The Laurel Dolomite is about 14 meters (45 feet) thick, gray, and cherty. Below the bedrock, Silurian- and Ordovician-aged interbedded limestone and shale extends from 91 to 121 meters (300 to 400 feet). Depth to bedrock at the demonstration areas ranges from 1.5 to 9 meters (5 to 30 feet) below ground surface (PRC 1994).

Native soils at the 16-hectare and the 32-hectare areas consist mainly of Avonburg and Cobbsfork silt loams. Avonburg soils are nearly level, deep, and somewhat poorly drained soils situated on smooth uplands. Areas of this soil type are broad and irregular in shape and cover 8 to 80 hectares (20 to 200 acres) (USDA 1985b). Cobbsfork soils are nearly level, deep, and poorly-drained soils situated on tabular divides in uplands; Cobbsfork soils are prone to ponding. Areas of this soil type are broad and irregularly shaped, ranging from 16 to 810 hectares (40 to 2,000 acres) in size (USDA 1985a).

Cobbsfork soils have a very high available water capacity and very slow permeability. Avonburg soils have a moderate available water capacity and very slow permeability. In both soil types, the water table is typically perched at or near the surface during most of the year. Both the Avonburg and Cobbsfork soils are low in organic matter, and they are acidic, friable, and best suited for grass and tree development (USDA 1985a and 1985b).

### 2.1.2 Ecologic Characteristics

JPG consists primarily of poorly drained flats in various stages of succession from open fields to regrowth forested flatwoods. Flatwoods are forested areas that occur on level or nearly level soils that are poorly drained and have a shallow perched water table. Some wooded stream valleys with better drainage are also present at JPG. Vegetative community types that have been inventoried by the IDNR Division of Nature Preserves include bottomland forests, upland forests, and cliffs along these major drainages (IDNR no date).

JPG lies within the Bluegrass Natural Region, as identified by IDNR. This natural region is identified and named for its similarities in physiography and natural communities to the Bluegrass Region of Kentucky. Most of the natural region was originally forested, although a few glade, cliff, and barren remnants are known, as well as nonforested aquatic communities. The areas used for the UXO demonstrations can be

classified as Bluegrass Till Plain Flatwoods. These natural communities are forested areas on level or nearly level soils that are poorly drained and acidic, with a shallow perched water table (IDNR no date).

### 2.1.3 Compliance with Environmental Regulations

On February 25, 1994, NAVEODTECHDIV and JPG signed a Record of Environmental Consideration (REC) in accordance with the environmental regulations of Army Regulation 200-2 and the National Environmental Policy Act. The REC provided a categorical exclusion for the creation of the controlled site at JPG and for its use in the demonstrations. Wetlands, endangered species, and archaeological investigations were conducted as part of the REC. The REC states that no effect on these resources is expected as a result of the demonstrations; therefore, no further environmental documentation was required. Because the Phase II activities were similar in nature and planned for the same locations as those for Phase I, the REC was determined to apply to Phase II as well.

### 2.1.4 Climatic Patterns

Climate in Jefferson, Ripley, and Jennings Counties is cold in winter and hot in summer. Winter precipitation consists mainly of snow, which aids in soil moisture accumulation and minimizes drought conditions in summer months. In winter, the average temperature is about 2°C (35 °F); the average daily minimum temperature is about -4°C (25°F). In summer, the average temperature is about 24°C (75°F); the average daily maximum temperature is about 30°C (85°F).

The total annual precipitation is about 107 centimeters (42 inches), with about 55 centimeters (22 inches) falling from April through September. Thunderstorms occur about 50 days per year; tornados and severe weather also occur occasionally. These types of storms are usually local and short in duration and can cause severe damage locally (USDA 1985a, 1985b).

The average seasonal snowfall is about 33 centimeters (13 inches). The average relative humidity in midafternoon is about 60 percent. Humidity is higher at night, and the average at dawn is about 80 percent. The sun shines 70 percent of the time in summer and 40 percent in winter. Prevailing winds are from the south. Average wind speed is highest in spring at 16 kilometers (10 miles) per hour (USDA 1985a, 1985b).

## 2.2

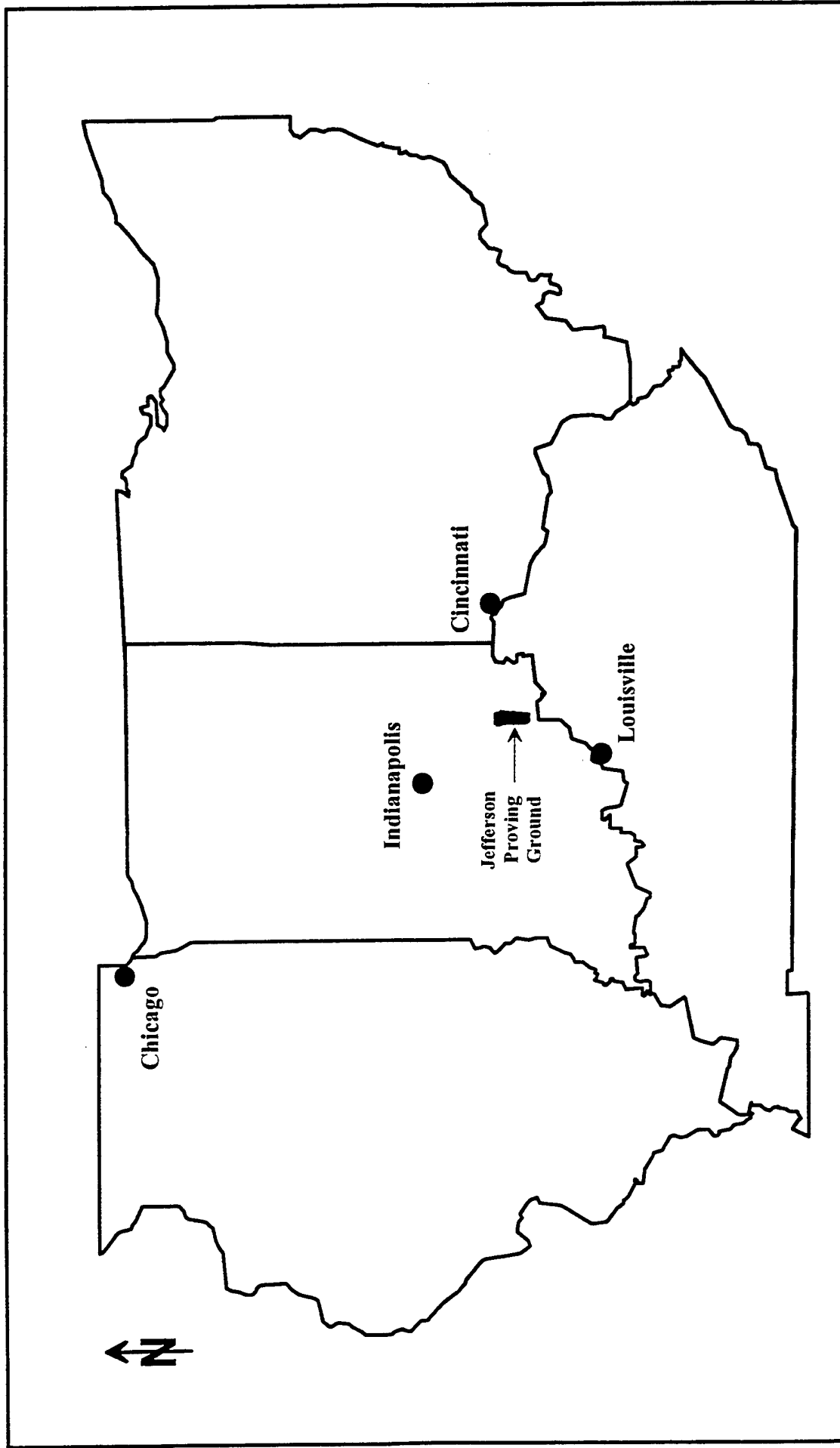
### HISTORIC SITE USE

An extensive survey of historical data related to the site indicates that farming was the predominant land use. The land was typified by relatively small, dispersed farmsteads and communities. Both woodland and agricultural tracts occurred in the two controlled site areas. In 1940, the federal government acquired the land; the first round of ammunition was tested at JPG on May 10, 1941 (USAEC 1995).

As part of the background investigation for the Phase I UXO ATD program, an archaeological investigation was performed in November 1993. This study revealed that both areas were used for agricultural purposes before the federal government acquired the land. One site identified at the 32-hectare area was believed to be a historic farmstead that was abandoned in 1941. The farmhouse was moved from the JPG property to the east, along Highway 421. Two other sites identified in the study were of indeterminate historic affiliation. None of the sites identified were eligible for listing on the National Register of Historic Places (Anslinger 1993).

Geophysical and geotechnical surveys were conducted in 1994 to establish area conditions and identify hazardous conditions. These surveys were conducted as part of the preparation for Phase I of the UXO ATD program. The survey results identified no hazardous conditions to preclude the use of these areas as controlled demonstration areas. However, given the nature and mission of JPG, a considerable amount of the total base area has undoubtedly been affected by munition testing and related activities.

Until September 1995, JPG served as a munitions testing facility of the Test and Evaluation Command, U.S. Army Material Development and Readiness Command. During the period of operation, JPG's mission was to check, investigate, and evaluate various test items to determine whether they conformed to specifications (JPG 1980). Between 1942 and 1995, JPG conducted a variety of munitions tests throughout the base. Although neither of the areas used for the controlled site are specifically located where these tests took place, they may be within the "fan" area of several of the impact fields. The controlled site areas are believed to have been only minimally affected by historical activities conducted at JPG.

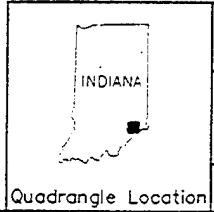
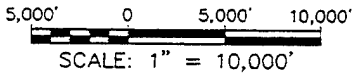
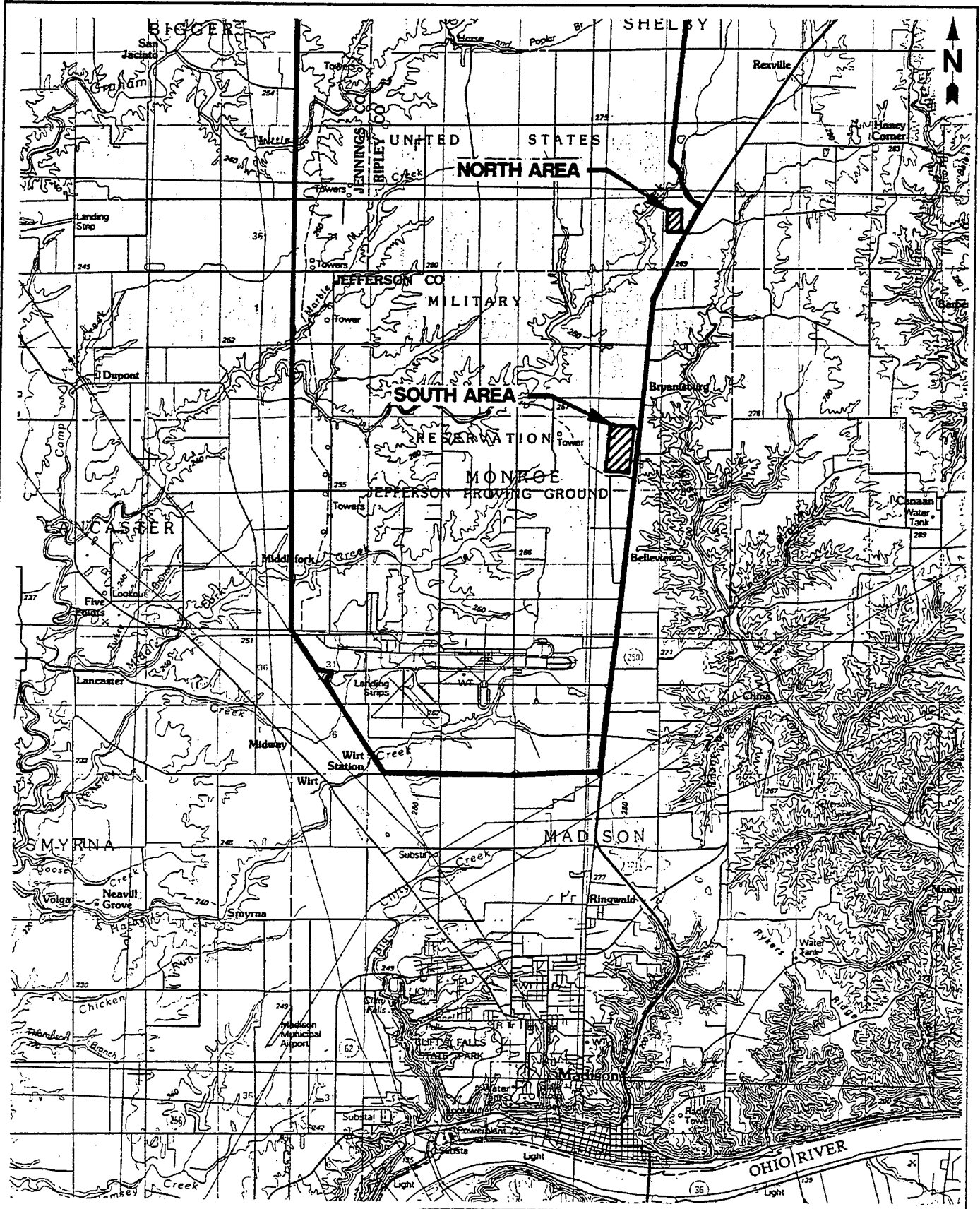


JEFFERSON PROVING GROUND  
MADISON, INDIANA

**FIGURE 2-1**  
LOCATION OF JEFFERSON PROVING GROUND

**PRC** ENVIRONMENTAL MANAGEMENT, INC.

Map Not to Scale



JEFFERSON PROVING GROUND  
MADISON, INDIANA

**FIGURE 2-2**  
**AREA LOCATION MAP**

SOURCE: MODIFIED FROM USGS, 30 X 60 MINUTE  
MADISON, INDIANA-KENTUCKY, QUADRANGLE, 1990

Quadrangle Location **PRC** ENVIRONMENTAL MANAGEMENT, INC.

### 3.0 DEMONSTRATION TECHNICAL APPROACH

#### 3.1 SITE PREPARATION

The sites were prepared for Phase I of the controlled site UXO ATD by mowing the tall grass, herbs, and woody vegetation that covered both demonstration areas. Some small sapling trees and brush thickets remained. A JPG survey crew then surveyed both areas using a total station survey instrument. A grid system was established at both areas on a 30.5- by 30.5-meter (100- by 100-foot) pattern. A stake was driven at each grid node to mark the corner locations. Each stake was marked with the grid node's alphanumeric code. A piece of 5-centimeter (2-inch)-diameter polyvinyl chloride (PVC) pipe about 30 centimeters (12 inches) long was driven into the ground at each grid node until it was flush with the ground surface. The PVC pipes were used to hold the stakes in place. Ground surface elevation was measured to the closest 3 centimeters (about 0.1 foot) at each grid node and recorded.

Permanent benchmarks (or first order survey monuments) were established at each area to provide precise positioning aids for target emplacement by the government and for target location by the demonstrator. Three geodetic benchmarks were established within the 16-hectare area, and four were established at the 32-hectare area. The node stakes were also used as benchmarks to measure elevations and locations of inert ordnance and debris items during emplacement.

After the areas were mowed and the monuments were established, an aerial survey was performed to collect topographic measurements and identify locations of vegetation and terrain features. Elevation data points were established throughout and around the edges of each grid so that a detailed contour model of each demonstration area could be constructed. Topographic maps of both areas were produced for use by the demonstrators.

Inert ordnance and nonordnance items comprising the baseline target set were then emplaced at both demonstration areas. The areas were designed to simulate three different UXO scenarios: a military training area, an ordnance disposal site, and a formerly used defense site. A small sample of mines were also emplaced in both areas to assess the plastic mine detection capabilities of the various systems. The table below lists the types of inert ordnance emplaced at the two areas.

Ordnance	Classification Size	Range of Emplacement depths (meters)
Bombs	2,000-pound (lb), 1,000-lb, 750-lb, 500-lb, and 250-lb	0.15 - 5.37
Projectiles	8-inch, 175-millimeter (mm), 155-mm, 152-mm, 106-mm, 105-mm, 90-mm armor-piercing and high explosive anti-tank (HEAT), and 76-mm HEAT	0.22 - 4.17
Rocket warheads	5-inch and 2.75-inch	0.15 - 0.47
Mortars	4.2-inch, 81-mm, and 60-mm	0.01 - 1.43
Submunitions	M-42 armor defeating bomblets	0 - 0.87
Land mines	TS-50 and VS-50 antipersonnel mines	0 - 0.04
Aircraft cannon	30-mm and 20-mm rounds	0.05 - 1.83

Before inert ordnance were emplaced, research was conducted to determine realistic depths and orientations for the ordnance items. The following guidelines were used to emplace ordnance:

- General purpose bombs (250 to 2,000 lb) have been found at depths exceeding 6 meters (m) (20 ft), at no predicable orientation to the surface plane.
- Projectiles (76 mm to 8 inch) are typically found at depths from 0.3 to 3.7 meters (m) (1 to 12 ft); orientation is horizontal to, or at a slight angle from, the surface plane.
- Air-launched rockets (2.75 and 5 inch) are generally found at depths of 1 to 2.4 m (3 to 8 ft); orientation is typically between 45 and 90 degrees from the plane of the surface due to the angle of trajectory.
- Mortar rounds are generally found within 120 cm (48 in) of the surface; orientation is typically between 45 and 90 degrees from the plane of the surface due to the high angle of trajectory.
- Submunitions are generally small, with no standard size or shape, and are dispensed from cluster bombs or artillery rounds; they are generally found on the surface, although they may be buried by secondary explosions.
- 20 mm and 30 mm aircraft- and ground-delivered flat trajectory gunfire typically results in the projectile penetrating the ground no more than 30.5 centimeters (cm) (12 in), resting horizontal to the plane of the ground surface.

Sources of false alarms (e.g., fragments, building materials, and scrap metal) were also emplaced at the controlled site. In addition to the inert nonordnance items, other sources of false alarms were also introduced. For example, many active sensors can detect disturbed soil, therefore, some holes were dug and the soil replaced without emplacing a target. All of the locations were surveyed and recorded. After all targets were emplaced and surveyed, both demonstration areas were tilled and reseeded to present a uniform appearance and prevent visual detection by the demonstrators.

A demonstrator reference area (DRA) was also established near the 16-hectare area. Four inert ordnance items were emplaced in the corners of the DRA. The ordnance types, locations, and depths were given to the demonstrators to enable them to calibrate their systems.

Several changes were made in the UXO ATD program after the completion of Phase I. To ensure site integrity for Phase II, the demonstration areas were modified, including the creation of a second 16-hectare ground demonstration area within the boundaries of the 32-hectare area. The original 16-hectare area is referred to as 16A-hectare area to differentiate it from the second 16B-hectare area created for Phase II ground demonstrations.

In spring 1995, several changes were made to the 16A-hectare area. Numerous inert ordnance items originally emplaced for Phase I of the UXO ATD program were excavated and moved to new locations. As ordnance items were excavated and removed, the locations were noted. In addition, a number of new inert ordnance items were emplaced at new locations. Once these changes were made at the 16A-hectare area, a new target map was produced.

The 16B-hectare area was established for returning ground-based demonstrators by using part of the north end (7.2 hectares) and part of the south end (8.8 hectares) of the 32-hectare area, for a total area of about 16 hectares (see Figure 3-1). Four of the Phase I demonstrators selected for Phase II were assigned to the 16B-hectare area to minimize any advantages over first-time demonstrators. The quantities and types of ordnance emplaced in the 16B-hectare area were similar to those emplaced in the 16A-hectare area. A new target map was created reflecting the changes made (PRC 1995a).



### **3.2 DEMONSTRATOR SELECTION PROCESS**

For Phase II of the UXO ATD program, potential candidates were identified through a *Commerce Business Daily* solicitation (CBD 1994). Interested parties were then sent information packages that included information about the site along with a description of the criteria for selection. A total of 42 proposals were submitted for Phase II of the UXO ATD program.

Criteria for proposal consideration included the following: corporate experience, key personnel, system and technology description, support and quality control, ability to meet the government's requirements, and cost. Based on these criteria, the government review panel selected 18 demonstrators. Two vendors canceled and one government laboratory (Wright Laboratory) was added for a total of 17 demonstrators for Phase II.

### **3.3 DEMONSTRATION PROCEDURES**

All demonstrators chosen were provided with a demonstration work plan (DWP) that outlined operations and safety procedures and responsibilities for the parties involved in the demonstrations. Specifically, the DWP provided site background, demonstration responsibilities, evaluation criteria, and data validation information. A data entry disk was provided to each demonstrator to ensure standard data submission to the government for evaluation. Demonstrators were also provided with copies of various forms used by PRC during oversight of the activities. In addition, the Safety, Health, and Emergency Response Plan (SHERP) was included in the DWP for use by demonstrators (PRC 1995b).

The SHERP served as a guide for all government representatives, support personnel, and demonstrators. At the beginning of each demonstration period, all demonstration team members were required to attend a comprehensive health, safety, and operations briefing. As part of the daily routine, each demonstration team member was required to acknowledge their compliance with the SHERP by signature before field activities began. Each demonstration area was assigned a site safety officer who was responsible for SHERP compliance. An EOD technician was part of the support team to address any ordnance issues.

Demonstrators were provided with daily weather forecasts, including data collected from the on-site weather station and reports from U.S. Weather Bureaus in Indianapolis, Indiana, and Louisville, Kentucky. Forecasts

included the daily high and low temperatures, relative humidity, wind speed and direction, chance of precipitation, and likelihood of severe weather.

Demonstrators were given a specified amount of time to collect data, based on the type of technology to be demonstrated. Detection technology demonstrators with ground systems were given 40 hours to cover the assigned 16-hectare area. Demonstrators were not permitted to remove any objects from the site during the demonstration.

Detection technology demonstrators with airborne systems had 24 hours to characterize the 32-hectare area. Specific air routes, flight plans, ground tracks, and air speeds were established for the airborne demonstrations to avoid conflicts with ongoing Indiana Air National Guard training.

Remediation technology demonstrators had 24 hours to demonstrate the system's capability. Demonstrators were provided with baseline targets to remediate.

### **3.4 QUALITY ASSURANCE AND QUALITY CONTROL**

The quality assurance program plan (QAPP) for Phase II outlined quality assurance (QA) and quality control (QC) procedures for the UXO ATD program. The QAPP defined rigorous standard procedures for conducting a controlled test program. The primary focus of the QAPP was on the accuracy of the emplaced baseline target set (inert ordnance type, location, and orientation), target validation, the transmission of data from the demonstrator to the government, and the validation of algorithms to assess system performance.

#### **3.4.1 Target Emplacement**

All inert ordnance and nonordnance were serialized and emplaced in accordance with a site layout plan. The location of all baseline targets were accurately determined by a licensed surveyor to an accuracy of 5 centimeters in three dimensional space. All maps were controlled by the Government to ensure site integrity.

### **3.4.2 Target Validation**

As part of the QA procedures, remediation demonstrators were directed to specific targets. Locations where ordnance was excavated were recorded. In this way, the remediation demonstrations also served the purpose of target validation. As each target was unearthed, PRC personnel verified and recorded the location, depth, size, class, and serial number of the target. No discrepancies were found to exceed the QAPP requirements.

### **3.4.3 Data Transmittal Control**

Chain-of-custody procedures were implemented to ensure accurate data transmittal. All data not transmitted in person were transmitted using a courier service equipped with a unique tracking system for shipment items. This approach allowed data transmittals to be tracked between parties.

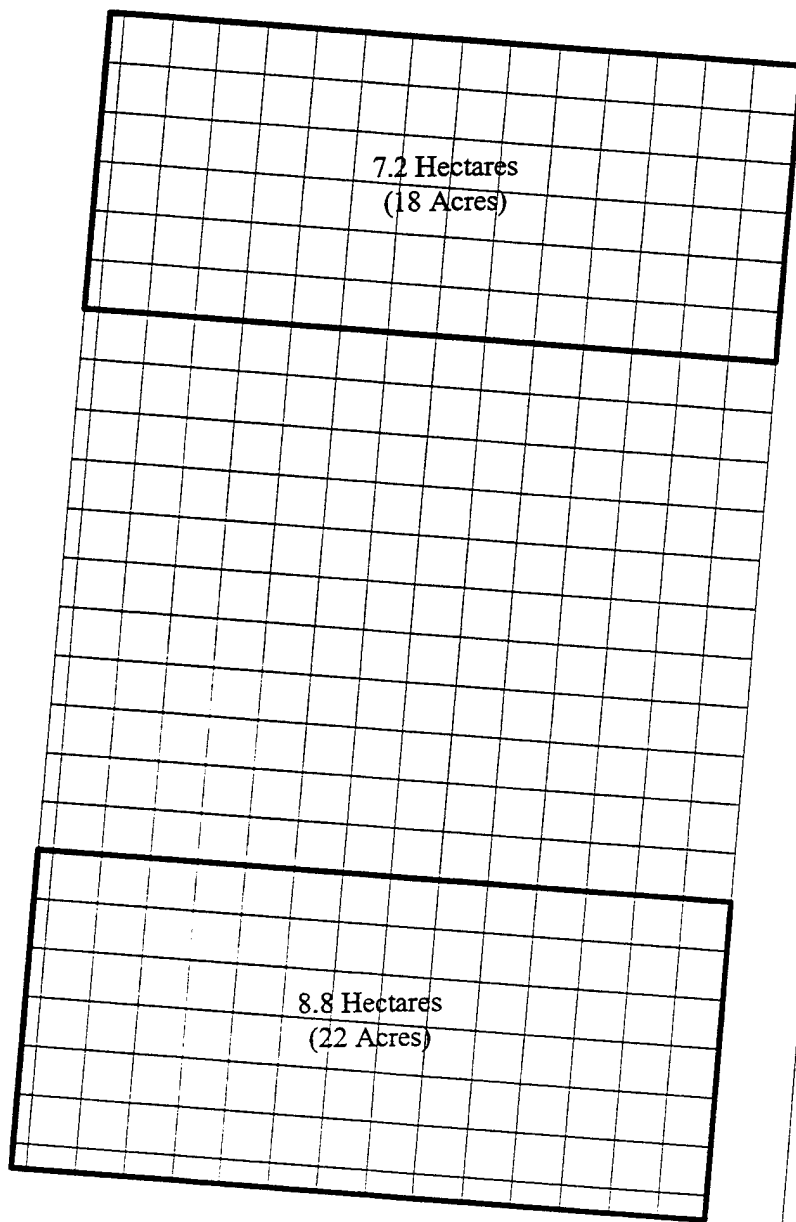
### **3.4.4 Data Submittal and Algorithm Validation**

Two computer software programs were developed for use during the demonstrations: the data entry program and the target matching algorithm (TMA). The data entry program provided a means for the demonstrator to electronically record data at the controlled site and then provide the data for analysis in a standard data submission format. The data entry disk included demonstration condition data, target baseline data, demonstrator target data, validated target data, site operational and logistical data, and demonstrator descriptive data. The data entry program enabled the demonstrators to collect and report their target and descriptive data consistently and reliably. Subsequent to demonstrator submittal of data, a copy of the data was returned to each demonstrator for verification of data accuracy. If necessary, any discrepancies or inconsistencies were resolved.

The TMA was designed to measure demonstrator effectiveness in locating known (baseline) targets at the controlled site demonstration areas. During the operation of the algorithm, each demonstrator's target predictions are compared to baseline target positional data using the x, y, and z coordinate system. The Institute for Defense Analysis (IDA) and PRC selected the algorithms to be used and validated the computer code used to assess demonstrator performance. Before the TMA and the computer code were used to assess demonstrator performance, they were validated internally by PRC and externally by IDA. A more thorough explanation of the TMA and its application is provided below in Section 4.0.



Support Trailer



East Perimeter Road

7.2 Hectares  
(18 Acres)

8.8 Hectares  
(22 Acres)

JEFFERSON PROVING GROUND  
MADISON, INDIANA

FIGURE 3-1  
16B-HECTARE (40B-ACRE)  
DEMONSTRATION AREA

NOT TO SCALE

**PRC** ENVIRONMENTAL MANAGEMENT, INC.

## 4.0 PERFORMANCE EVALUATION METHODOLOGY

The techniques, criteria, and methods used to evaluate individual detection demonstrator performance for Phase II of the UXO ATD program at JPG are based in large part on those developed for the UXO ATD Phase I analysis by Automated Research Systems Ltd. (USAEC 1994) and the Institute for Defense Analysis (IDA 1995; USAEC 1995). The remediation evaluation methodology is discussed with the respective results in Section 5.0.

### 4.1 APPROACH

The effectiveness of UXO characterization systems, such as magnetometers, electromagnetic induction sensors, or ground penetrating radar, depends on their performance in three general categories:

(1) detection -- the ability to detect targets; (2) localization -- the ability to accurately determine the detected target's location in three-dimensional space; and (3) identification and classification -- the ability to discriminate between UXO and non-UXO targets and to determine the characteristics of targets identified as UXO. These performance categories used for Phase II follow the evaluation criteria used to compare demonstrator performance during Phase I (USAEC 1995). Area coverage and cost information, are provided as a historical record and are not used to assess system performance.

Demonstrators were evaluated against the baseline target set for the areas of the site they surveyed. The JPG 16A, 16B, and 32 hectare sites are divided into grid cells that are 30.5- by 30.5- meters (100- by 100- feet) square. If a demonstrator surveyed less than 50 percent of a particular grid cell, those items from the baseline target set along with any of that demonstrator's reported targets were excluded from the performance assessment.

Remnants of a metal fence were detected by demonstrators at each test area. All demonstrator reported targets and baseline items contained within an 8-meter wide (26 feet) swath, which encompassed each fence segment, were excluded from the performance analysis. Figures 4-1 and 4-2 indicate fence segment locations on the 16A- and 16B-hectare areas, respectively, along with reported target locations from one of the demonstrators. Appendix B describes the algorithm used to remove the reported targets and baseline items and the rationale for so doing.

After identifying the portion of the baseline target set based on the area covered by the demonstrator and removing the data around the fence lines, TMAs were applied to demonstrator reported targets to determine which demonstrator reported targets were scored as detections of baseline items and which were not. These algorithms are briefly described in Section 4.1.1 below and in greater detail in Appendix A. After scoring the demonstrator reported targets, demonstrator performance was determined in each of the three categories. This performance analysis and associated statistical measures are presented in the following subsections.

#### 4.1.1 Target Matching Algorithms

Two of these TMAs, "*CLOSEST*" and "*GROUP*," were selected for use in the Phase II analysis (USAEC 1995 and IDA 1995). These algorithms were developed and validated by IDA during Phase I of the UXO ATD analysis (USAEC 1994, 1995; and IDA 1995). These algorithms are believed to provide the best representation of demonstrator ability.

For the *CLOSEST* TMA, a circle of the radius or the critical radius ( $R_{crit}$ ) is centered about the approximate geometric center location of each of the baseline target items in the x-y horizontal plane. The closest demonstrator reported target falling within this circle is matched to that baseline item. If a reported target can be matched to multiple baseline items, a tie-breaking scheme is employed that minimizes the average distance to the items while maximizing the number of matches. If no reported targets are within this circle, the baseline item is scored as undetected. As in Phase I, the Phase II  $R_{crit}$  was designated as 2 meters for ground demonstrators and 5 meters for air demonstrators.

At the JPG survey sites, several of the baseline items were emplaced in close proximity to other baseline items to assess the resolution capabilities of the various systems. Figures 4-3 and 4-4 are cumulative distributions of the relative distances between baseline items and their closest neighbor at the 16A- and 16B-hectare areas, respectively. As shown in these figures, between 37 and 38 percent of the baseline items are within 2 meters of each other. Because of this, demonstrators with larger spatial resolutions may have problems resolving individual baseline item within a group of closely-spaced items and instead may have reported target groups as a single target. Use of *CLOSEST* TMA provides a measure of the system's capability to detect individual UXO items in an area highly populated with UXO and debris.

The *GROUP* TMA was developed for use in determining detection performance, because it is believed to provide the best estimate of demonstrator performance in this category (USAEC 1995; IDA 1995). Each group essentially contains all baseline targets, both ordnance and nonordnance, within a circle of a 2-meter radius. For this TMA, the baseline target set was divided into groups which may consist of one or more baseline targets. A demonstrator is scored as detecting a group if his reported target is within  $R_{crit}$  of at least one baseline item in the group. If no reported targets are within  $R_{crit}$  of a group, that group of targets is scored as undetected. Assuming that closely-spaced baseline items are not detected due to lack of resolution in demonstrator equipment, the *GROUP* TMA provides the best estimate of demonstrator detection performance. Again,  $R_{crit}$  was 2 meters for ground-based demonstrators and 5 meters for airborne demonstrators. Any demonstrator reported target not matched to a baseline ordnance item was scored as a false alarm.

For this performance assessment, the *GROUP* TMA was used to quantify demonstrator detection performance. A different TMA was required for localization, identification, and classification, because the *GROUP* TMA combines ordnance, nonordnance, and items of different size, location, and depth, into a single group. As a result, the *CLOSEST* TMA is used for localization, identification, and classification, because it provides a one-to-one matching between demonstrator reported targets and baseline targets.

#### 4.1.2 Detection Performance

In determining the detection performance of any system, one must consider how that system reacts to both signal and noise. For example, a system with a high probability of detection may not be of practical use if the number of false alarms is excessive, because false alarms require investigation and unnecessary expenditure of resources.

The standard method of comparing the performance between systems employs the Receiver Operating Characteristics (ROC) curve. The ROC curve is a plot of the probability of detection ( $P_D$ ) of a detection system as a function of the probability of false alarm ( $P_{FA}$ ), or alternatively the false alarm rate (FAR). To produce a ROC curve, a detection threshold is applied to the detection system's output, and the corresponding  $P_D$  and  $P_{FA}$  are determined for that threshold. The threshold level is varied across some range of values, and the corresponding  $P_D$  and  $P_{FA}$  values are accumulated and plotted. Figure 4-5 shows a sample ROC plot for two systems, and their underlying signal and noise distributions are shown in Figures 4-6 and 4-7. For this

sample plot, both the signal and noise distributions are assumed to be Gaussian with unity standard deviations and mean signal to noise ratios of 2 and 3, respectively.

For a given detection threshold in Figures 4-6 and 4-7, the number of targets detected is related to the area under the signal distribution curve that is to the right of the threshold level. Likewise, the number of false alarms is related to the area under the noise distribution curve that is to the right of the threshold level. As seen from these curves, both the  $P_D$  and  $P_{FA}$  increase or decrease with a corresponding decrease or increase in the detection threshold, as reflected in the ROC curve (see Figure 4-5).

When the individual demonstrators were scored against the baseline target set for JPG, a single  $P_D$  and  $P_{FA}$  (and FAR ) value was obtained. These values represent a single point on the ROC curve for that system. If the type and standard deviation of both the signal and noise distributions were known, then a ROC curve could be produced for that system. Because the characteristics of these distributions are not known, ROC curves were not produced.

With regard to signals, probabilities of detection are computed from reported targets that match baseline items. As discussed in Section 4.1.1, the *GROUP* TMA was used to match demonstrator reported targets to baseline items to produce the primary detection performance statistics. Within this area, probabilities of detection are computed for the ordnance, nonordnance, and total number of baseline items detected versus the corresponding number of baseline items in the area surveyed. These detection probabilities are defined as follows:

$$\begin{aligned} P_{D,ord} &= \text{Probability of detection for ordnance} \\ &= (\text{number ordnance detected})/(\text{total number ordnance in area surveyed}) \end{aligned}$$

$$\begin{aligned} P_{D,nonord} &= \text{Probability of detection for nonordnance} \\ &= (\text{number nonordnance detected})/(\text{total number nonordnance in area surveyed}) \end{aligned}$$

$$\begin{aligned} P_D &= \text{Probability of detection for total baseline items} \\ &= (\text{number baseline items detected})/(\text{total number baseline items in area surveyed}) \end{aligned}$$

The methods described above for determining probability of detection ( $P_D$ ) may include a percentage of targets detected due to random sensor or environmental noise. In other words, correct identification of an emplaced item could result from a random point. For example, it is likely that a certain percentage of these



targets would fall within  $R_{crit}$  of some of the baseline items (Feller 1968). Therefore, a detection probability (labeled in the tables as  $P_{random}$ ) was calculated for each demonstrator.  $P_{random}$  is a measure of the number of baseline items that would be detected if the total number of reported targets were randomly distributed over the surveyed area, as opposed to being specifically declared by demonstrators. This number is useful to compare with the various probabilities computed above to determine if the  $P_D$  values are statistically different from the detection probability that would result from a random placement of points. If  $P_{random}$  is close to or greater than a demonstrator's  $P_D$ , it is likely that some portion of those detections are due to random target declarations.  $P_{random}$  is discussed in detail in Appendix C and is calculated as follows:

$$P_{random} = 1 - e^{-\lambda}$$

where

$$\lambda = np$$

$n$  = Number of demonstrator reports

$p$  = Probability of having a report within  $R_{crit}$

$$= \frac{\pi R_{crit}^2}{A}$$

$A$  = Area surveyed

The previous statistics are measures of demonstrator ability to detect ordnance and nonordnance. System performance must also include determination of the false alarm rate. In a true performance assessment, one must consider the false alarm rate as well. By lowering the detection or sensor threshold, one can increase the  $P_D$ , but not without a corresponding increase in the number of false alarms. This increase in false alarms ultimately increases the cost of the remediation effort. Accordingly, the number of false alarms reported by a demonstrator, the corresponding FAR, and the probability of false alarms are reported.

During Phase I, a false alarm was defined as a reported target not associated with a baseline target item. However, for Phase II, the remediation efforts on the 16B-acre area showed that the field contained a large number of nonordnance items (see Appendix D). Therefore, this analysis uses a narrower definition of false alarm that is more consistent with the goals of a remediation system. To correspond with ordnance

remediation, a false alarm is defined as a demonstrator reported target not associated with ordnance. To compute the number of false alarms, demonstrator reported targets not matched to the baseline ordnance set are declared false alarms. Because only a small number of nonbaseline ordnance items were remediated in the 16B-hectare area, and they were all located near a firing range, the number of nonbaseline ordnance items in the controlled sites is believed to be negligible. Similarly, the FAR is computed by dividing the number of false alarms,  $N_{FA}$ , by the area surveyed,  $A$  (in square meters):

$$FAR = \frac{N_{FA}}{A}$$

The probability of false alarm,  $P_{FA}$ , is defined as the fraction of area in the site covered by the false alarms, which is:

$$P_{FA} = \frac{N_{FA} \pi R_{crit}^2}{A}$$

One final measure, false alarm ratio, assesses the impact of a system's false alarms on a remediation effort. The false alarm ratio is defined as:

$$\text{False Alarm Ratio} = \frac{\text{Number of False Alarms}}{\text{Number of Ordnance Items Detected}}$$

The statistic defines the number of nonordnance holes that would be excavated for every hole containing an ordnance item. This assumes that all demonstrator reported targets would be investigated and sufficient resources would be available to support this excavation.

#### 4.1.3 Localization Performance

Localization is a measure of how accurately demonstrators can determine the location of buried ordnance in three-dimensional space. Once an object has been detected, its position must be determined horizontally (x, y) and vertically (z, depth).

For this analysis, the location errors for each demonstrator were computed from the set of baseline ordnance items that were determined using the *CLOSEST* TMA. As a result, horizontal location errors will be

constrained by the  $R_{crit}$  (2 meters or 5 meters) used in the detection process. For each detection, the error of the reported target relative to the approximate geometric center of the baseline ordnance item is computed for the horizontal and depth components as follows:

$$\begin{aligned} dx &= x_r - x_b \\ dy &= y_r - y_b \\ dz &= z_r - z_b \end{aligned}$$

where the "r" subscript refers to the demonstrator reported target position and the "b" subscript refers to the baseline target position. A negative value in dx, dy, and dz indicate that the reported target position is to the west and south of, and shallower than, the baseline target.

The errors associated with determining position and depth can have two components: (1) constant offset ( $\bar{dx}$ ,  $\bar{dy}$ ,  $\bar{dz}$ ), and (2) randomly fluctuating error ( $\sigma_x$ ,  $\sigma_y$ ,  $\sigma_z$ ). These components of the error are estimated by the means and standard deviations of dx, dy, and dz, respectively. The radial distance error, r (in the horizontal plane only), and the mean absolute depth error  $|dz|$ , are measures of the average total error in the location estimates that result from the combination of the offset and randomly fluctuating error components. These statistics are computed as follows (where "N" represents the number of baseline ordnance targets detected):

- The mean and standard deviation of the x and y errors of the reported target locations

$$\text{Mean: } \bar{dx} = \frac{\sum dx_i}{N}$$

$$\bar{dy} = \frac{\sum dy_i}{N}$$

$$\text{Standard Deviation: } \sigma_x = \sqrt{\frac{\sum (dx_i - \bar{dx})^2}{N}}$$

$$\sigma_y = \sqrt{\frac{\sum (dy_i - \bar{dy})^2}{N}}$$

- The mean and standard deviation of the radial distance error for the UXO from the center of mass

$$\text{Mean: } \bar{r} = \frac{\sum r_i}{N}$$

$$\text{Standard Deviation: } \sigma_r = \sqrt{\frac{\sum (r_i - \bar{r})^2}{N}}$$

$$r_i = \sqrt{dx_i^2 + dy_i^2}$$

- The mean, standard deviation, and mean absolute depth errors of the UXO

$$\text{Mean: } \bar{dz} = \frac{\sum dz_i}{N}$$

$$\text{Standard Deviation: } \sigma_z = \sqrt{\frac{\sum (dz_i - \bar{dz})^2}{N}}$$

$$\text{Mean Absolute: } |\bar{dz}| = \sqrt{\frac{\sum dz_i^2}{N}}$$

The “N” in the denominator of the above equations represents the number of baseline ordnance targets detected.

#### 4.1.4 Identification and Classification Performance

In any remediation system, the ability to correctly identify and classify a detected target provides valuable information to the remediation process. Because large amounts of both natural and man-made nonordnance are encountered on most ranges, the ability to discriminate between ordnance and nonordnance items (referred

to as identification in this analysis) is very important in reducing the number of nonordnance items (false alarms) that are detected. In addition, estimates of ordnance size and class (such as bomb, projectile, mortar, or cluster) provide guidance on which precautions should be taken during the remediation process.

Phase II demonstrators were requested to identify and classify reported targets by type (ordnance or nonordnance); size (small, medium, or large), and classification (bomb, projectile, mortar, or cluster). To assess demonstrator identification and classification performance, the following statistics were computed from detected baseline items using the *CLOSEST* TMA:

$$P_{CO} = \text{Probability of correct identification of ordnance} \\ = (\text{number ordnance correctly classified})/(\text{number ordnance detected})$$

$$P_{CN} = \text{Probability of correct identification of nonordnance} \\ = (\text{number nonordnance correctly classified})/(\text{number nonordnance detected})$$

$$P_{CS} = \text{Probability of correct size determination of small ordnance} \\ = (\text{number small ordnance correctly classified})/(\text{number small ordnance detected})$$

$$P_{CM_e} = \text{Probability of correct size determination of medium ordnance} \\ = (\text{number medium ordnance correctly classified})/(\text{number medium ordnance detected})$$

$$P_{CL} = \text{Probability of correct size determination of large ordnance} \\ = (\text{number large ordnance correctly classified})/(\text{number large ordnance detected})$$

$$P_{CB} = \text{Probability of correct classification determination of bombs} \\ = (\text{number bombs correctly classified})/(\text{number bombs detected})$$

$$P_{CP} = \text{Probability of correct classification determination of projectiles} \\ = (\text{number projectiles correctly classified})/(\text{number projectiles detected})$$

$$P_{CM_o} = \text{Probability of correct classification determination of mortars} \\ = (\text{number mortars correctly classified})/(\text{number mortars detected})$$

$$P_{CC} = \text{Probability of correct classification determination of clusters} \\ = (\text{number clusters correctly classified})/(\text{number clusters detected})$$

These identification and classification probabilities are not to be confused with the classification ratios presented in the Phase I report (USAEC 1994). The Phase II probabilities measure a demonstrator's ability to correctly identify and classify reported targets, while Phase I classification ratios measured the demonstrator's classification ability using the entire baseline.

In addition to the identification and classification probabilities by category, detection probabilities were also computed from the *CLOSEST* TMA as follows:

$$P_{DO} = \text{Probability of detecting ordnance} \\ = (\text{number ordnance detected})/(\text{number ordnance items in area surveyed})$$

$$P_{DN} = \text{Probability of detecting nonordnance} \\ = (\text{number nonordnance detected})/(\text{number nonordnance items in area surveyed})$$

$$P_{DS} = \text{Probability of detecting small ordnance} \\ = (\text{number small ordnance detected})/(\text{number small ordnance items in area surveyed})$$

$$P_{DMe} = \text{Probability of detecting medium ordnance} \\ = (\text{number medium ordnance detected})/(\text{number medium ordnance items in area surveyed})$$

$$P_{DL} = \text{Probability of detecting large ordnance} \\ = (\text{number large ordnance detected})/(\text{number large ordnance items in area surveyed})$$

$$P_{DB} = \text{Probability of detecting bombs} \\ = (\text{number bombs detected})/(\text{number bomb items in area surveyed})$$

$$P_{DP} = \text{Probability of detecting projectiles} \\ = (\text{number projectiles detected})/(\text{number projectile items in area surveyed})$$

$$P_{DMo} = \text{Probability of detecting mortars} \\ = (\text{number mortars detected})/(\text{number mortar items in area surveyed})$$

$$P_{DC} = \text{Probability of detecting clusters} \\ = (\text{number clusters detected})/(\text{number cluster items in area surveyed})$$

## 4.2 PERFORMANCE ASSESSMENT

### 4.2.1 Performance Assessment Plots

In the individual demonstrator summaries (see Section 5.0), two plot types are presented to graphically display individual demonstrator performance abilities and to allow comparisons among them. In this section, examples of these plots are presented and discussed.

The shape and magnitude of a sensor signal output are functions of both the size and depth (distance from the sensor) of the buried ordnance item. For magnetometer systems, the "size" component is a complicated

function of ferrous mass, diameter, length, and orientation. For electromagnetic induction and GPR sensors, the "size" is effectively related to the cross-sectional area of the buried ordnance item. In both cases, the size component of these types of systems depends to varying degrees on the diameter of the ordnance item.

To illustrate this dependency, a scatter plot of size (as indicated by the diameter of the ordnance) versus depth of the baseline ordnance item, was produced (see Figures 4-8 and 4-9). In these figures, detected ordnance items (as matched by the *CLOSEST* TMA, with the area searched and fence line removed) are indicated by darkened squares; those items not detected are indicated by open squares. The regions corresponding to the three size classes are indicated by dashed lines. To avoid biases from nearby ordnance, only those ordnance items not having another baseline item within 2.0 meters of its horizontal (x, y) location were plotted; as a result, the number of detected and undetected ordnance items will differ from the numbers generated in Section 4.1.4. Figures 4-8 and 4-9 illustrate ordnance detection capabilities with respect to depth and size. These figures show the detection limits of the demonstrator systems. For example, in Figure 4-8, the demonstrator is successful at detecting medium and large targets but has difficulty detecting small targets at most depths. This figure illustrates a relationship for ordnance detection with respect to depth and size. In Figure 4-9, no such relationship exists, as detections appear to occur at random with respect to depth and size.

As a measure of a UXO detection system's effectiveness as it relates to remediation, the  $P_D$  for ordnance items is plotted against the false alarm ratio for each demonstrator in Figure 4-10. A comparison of these two statistics define the fraction of ordnance items that would be remediated and the number of nonordnance holes that would be excavated for every hole containing an ordnance item. The *GROUP* TMA was used to generate these statistics (over the area surveyed and with the data around the fence line removed). This assumption is based on the rationale that, in a remediation effort, all reported targets would have to be investigated. These statistics represent estimates of how well a system would perform if sufficient resources were available to remediate every reported target location, and if the remediator were 100 percent effective.

Good performance in this category is denoted by symbols located in the plot's upper left quadrant. The plot shows two things: (1) a relatively high number of baseline ordnance items were detected, and (2) if remediation was performed based on these detection data, a relatively low number of holes excavated would not contain ordnance. Likewise, poor performance in this category is denoted by symbols located in the plot's lower right quadrant. Statistics found here indicate the opposite: (1) a relatively low number of

baseline ordnance items were detected, and (2) if remediation was performed based on these detection data, a relatively high number of holes excavated would not contain ordnance. Simply stated, the more holes remediated that do not contain ordnance, the more costly the remediation effort.

#### 4.2.2 Confidence Intervals

Because there were a finite number of baseline targets used in Phase II, the performance statistics computed for each demonstrator are estimates of the true statistics because each demonstrator's survey during Phase II represents a single sample drawn from a random process. Due to the random statistical fluctuations, the true performance statistics lie within some interval about this estimate. This interval is referred to as the confidence interval (CI).

Because of these fluctuations, a CI must be computed for the probabilities and means before comparisons between performance statistics can be made. The computation of CI allows one to determine whether or not the observed differences in performance are statistically significant. For the detection and classification probability estimates, the CI is computed as follows:

$$C.I. = P \pm z_{1-\alpha/2} \sqrt{\frac{P(1-P)}{N}}$$

where

- $P$  = Probability of detection or classification
- $N$  = Total number of elements in the test set
- $z_{1-\alpha/2}$  = Standard normal deviate at the  $1-\alpha/2$  level

For estimates of the mean, the CI is computed as follows:

$$C.I. = \mu \pm z_{1-\alpha/2} \frac{\sigma}{\sqrt{N}}$$



where

- $\mu$  = Estimate of the mean
- $\sigma$  = Estimate of the standard deviation
- $N$  = Total number of elements in the test set
- $z_{1-\alpha/2}$  = Standard normal deviate at the  $1-\alpha/2$  level

For a 95 percent CI,  $z_{1-\alpha/2} = 1.96$ .

To illustrate how CI is used in the probability analysis presented in this report, let us assume that there are three demonstrators (A, B, and C) with the following  $P_D$  values,  $P_{\text{random}}$  values, and number of baseline targets (N) in the area they surveyed:

- For A:  $P_D = 0.65$ ,  $P_{\text{random}} = 0.25$ , and  $N = 50$
- For B:  $P_D = 0.35$ ,  $P_{\text{random}} = 0.25$ , and  $N = 50$
- For C:  $P_D = 0.60$ ,  $P_{\text{random}} = 0.25$ , and  $N = 5$

As a first step, we must determine if these  $P_D$  values from each demonstrator are significantly different than the  $P_D$  values that would be obtained by randomly distributing their reported targets over the site (as indicated by their  $P_{\text{random}}$ ). Using the above formula, the 95 percent CI for each demonstrator's  $P_D$  value can be determined as follows:

- For A: CI = 0.13;  $0.52 \leq P_D \leq 0.78$
- For B: CI = 0.13;  $0.22 \leq P_D \leq 0.48$
- For C: CI = 0.42;  $0.23 \leq P_D \leq 1.00$

Based on these numbers, the demonstrator  $P_D$  values are significantly different than their  $P_{\text{random}}$  values if their respective  $P_{\text{random}}$  values do not fall within the CI. For these three demonstrators, only demonstrator A has a  $P_D$  value that is significantly different (at the 95 percent level) than the  $P_{\text{random}}$  value.

**Figure 4-1**  
**Fenceline Extraction for 16A-Hectare Area with Sample Demonstrator Data**

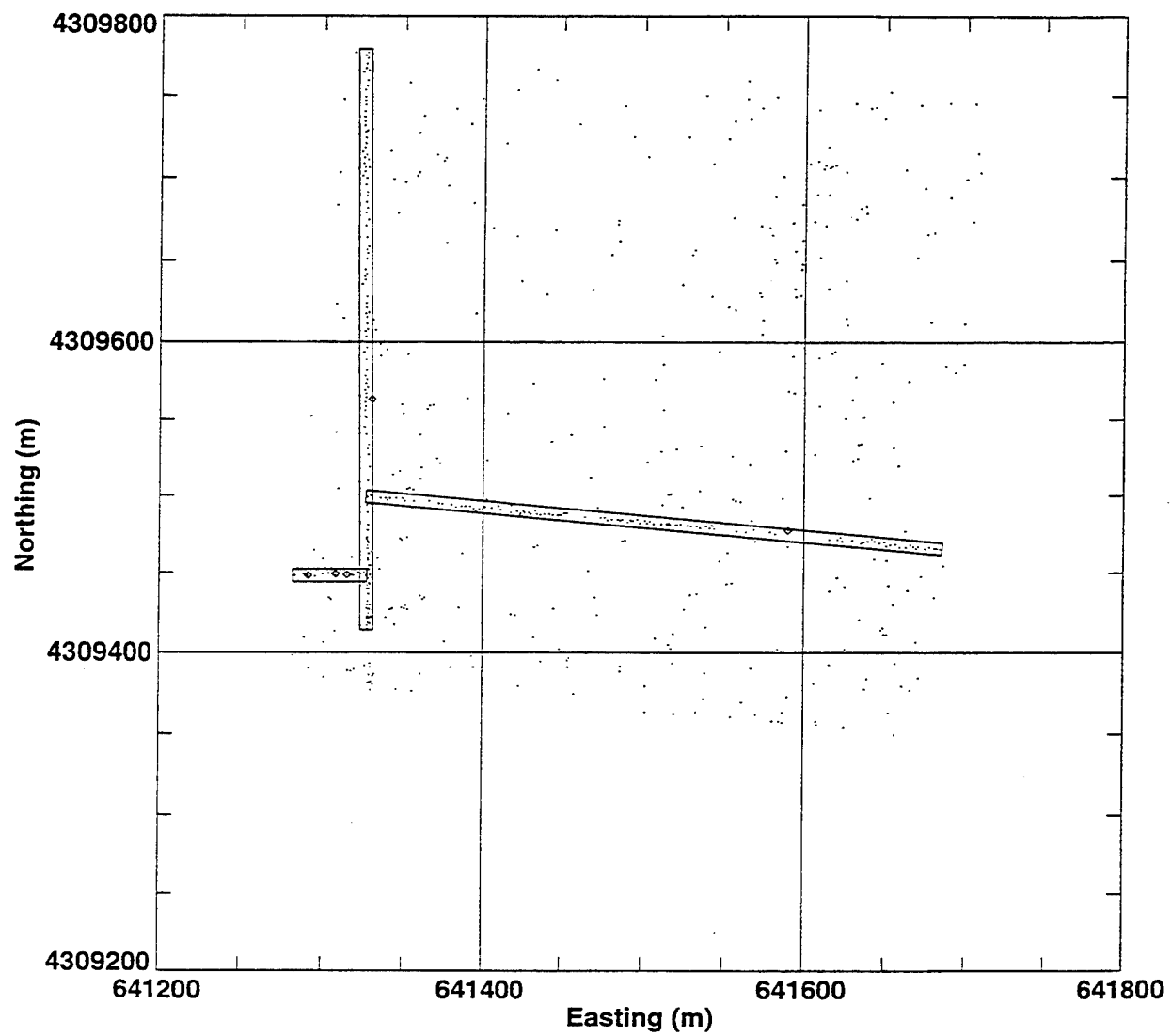
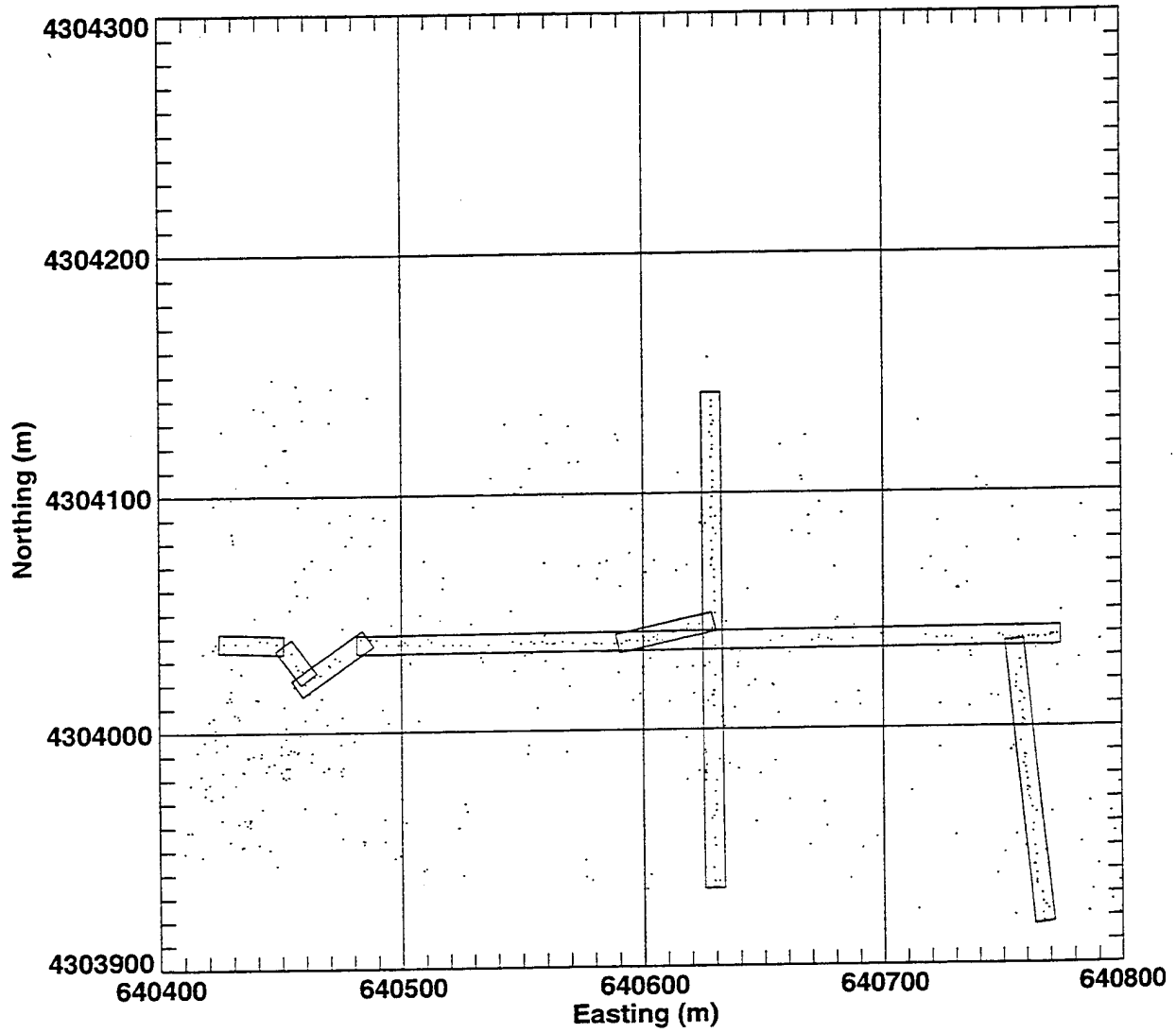
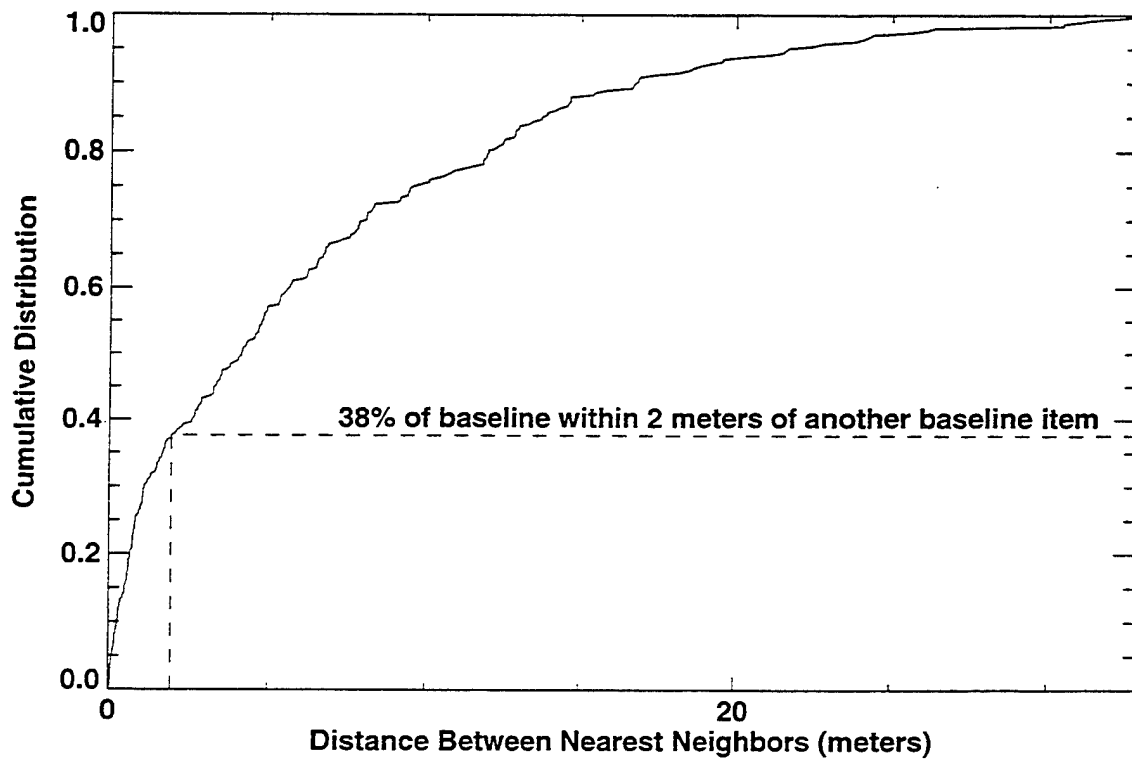


Figure 4-2  
Fenceline Extraction for 16B- and 32-Hectare Area with Sample Demonstrator Data



**Figure 4-3**  
**Cumulative Distribution of Distance Between Nearest Neighbor Baseline Items at 16A-Hectare Area**



**Figure 4-4**  
**Cumulative Distribution of Distance Between Nearest Neighbor Baseline Items at 16B-Hectare Area**

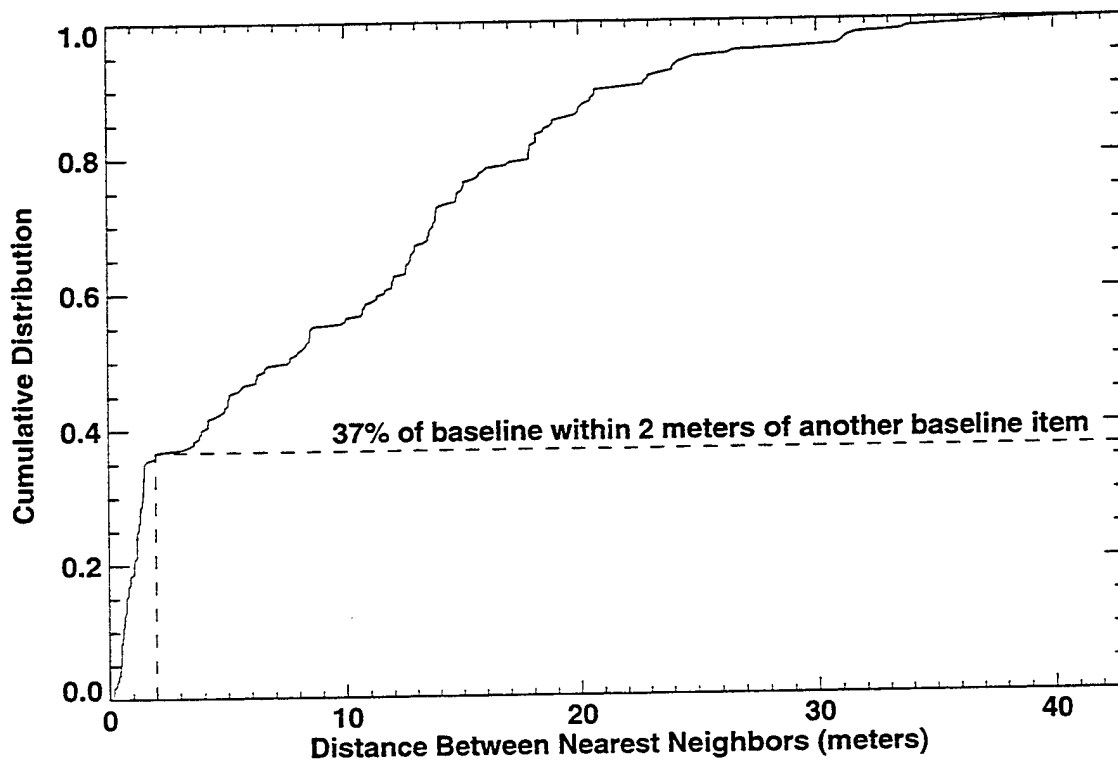


**Figure 4-5**  
**Sample Receiver Operating Characteristics (ROC) Curve**

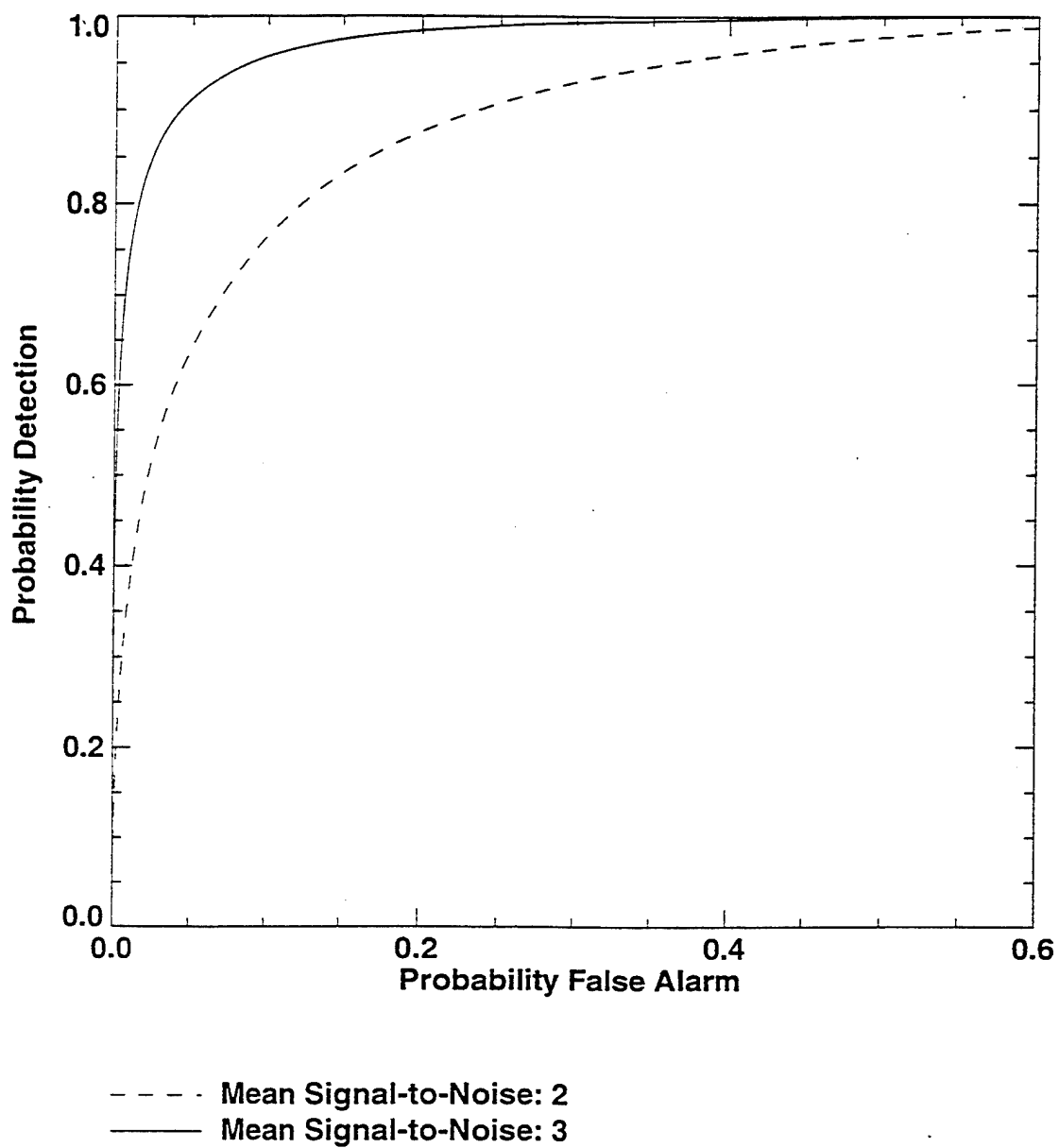


**Figure 4-6**  
**Sample Signal and Noise Distribution with Mean Signal to Noise Ratio (SNR) = 2**

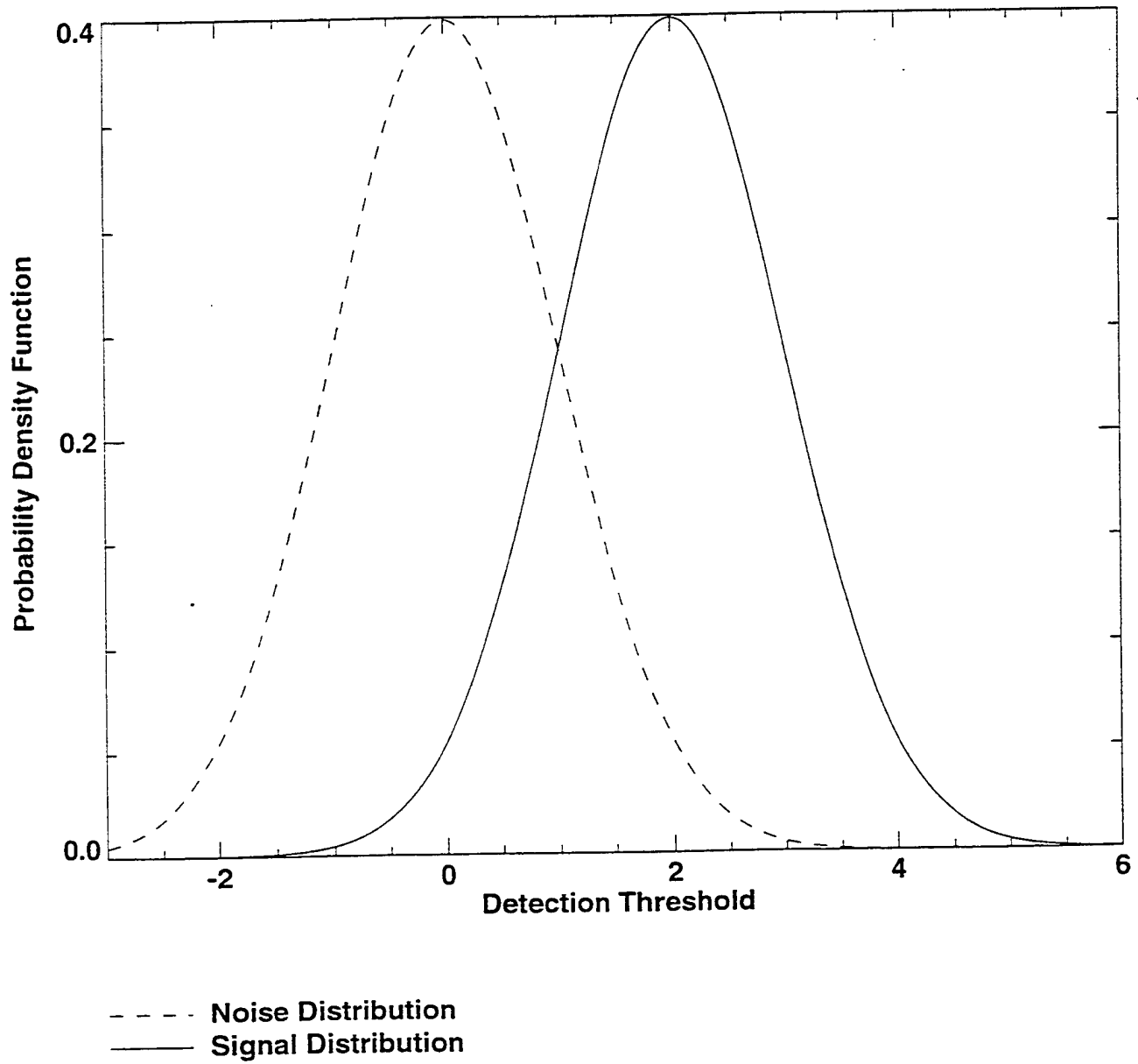


**Figure 4-7**  
**Sample Signal and Noise Distribution with Mean Signal to Noise Ratio (SNR) = 3**

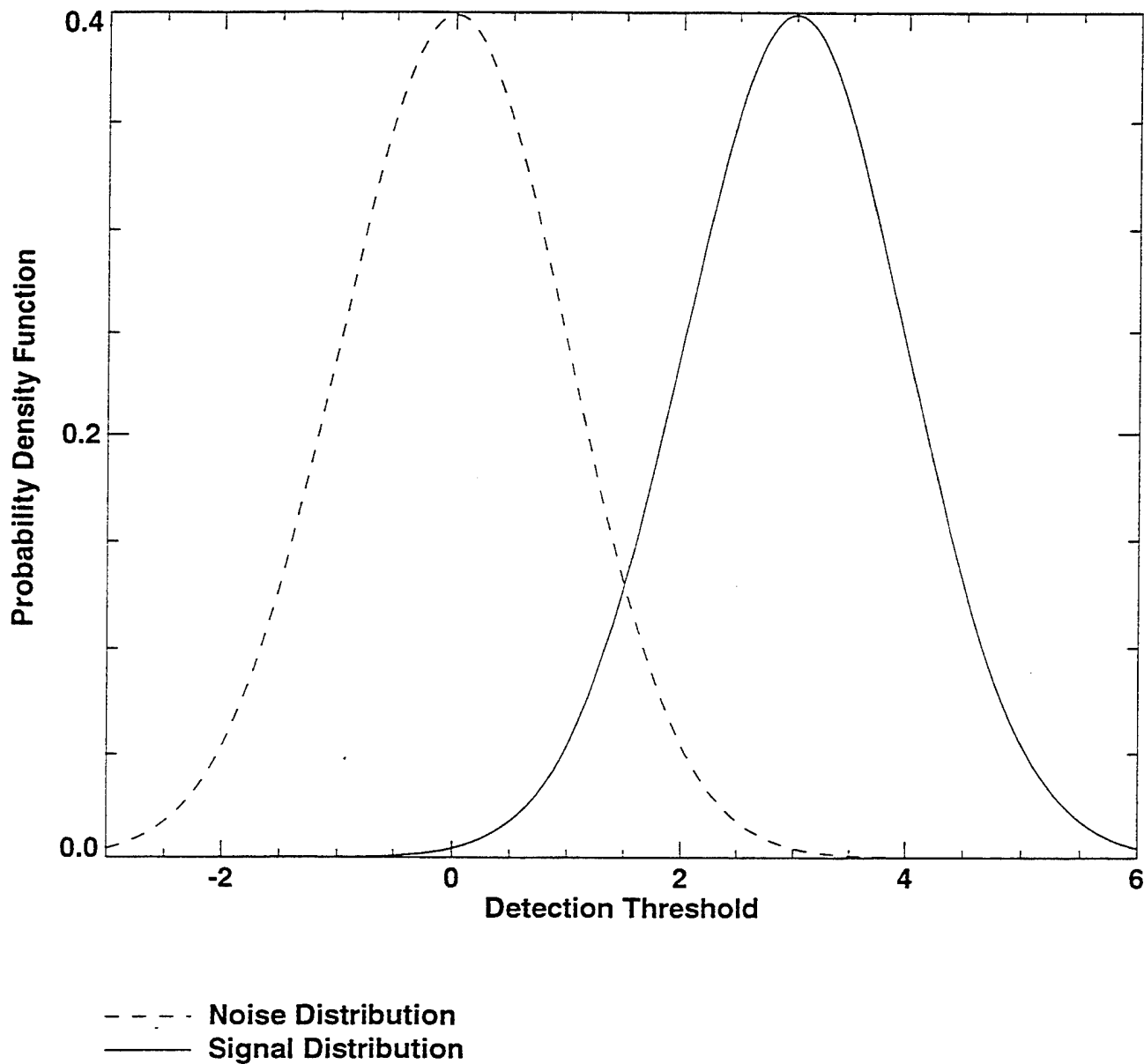






**Figure 4-9**  
**Sample Plot Illustrating Detection as a Function of Depth and Size (Diameter) – No Trend Indicated**  
(only those ordnance items not having another baseline item within 2 meters of its horizontal (x,y) location are shown)

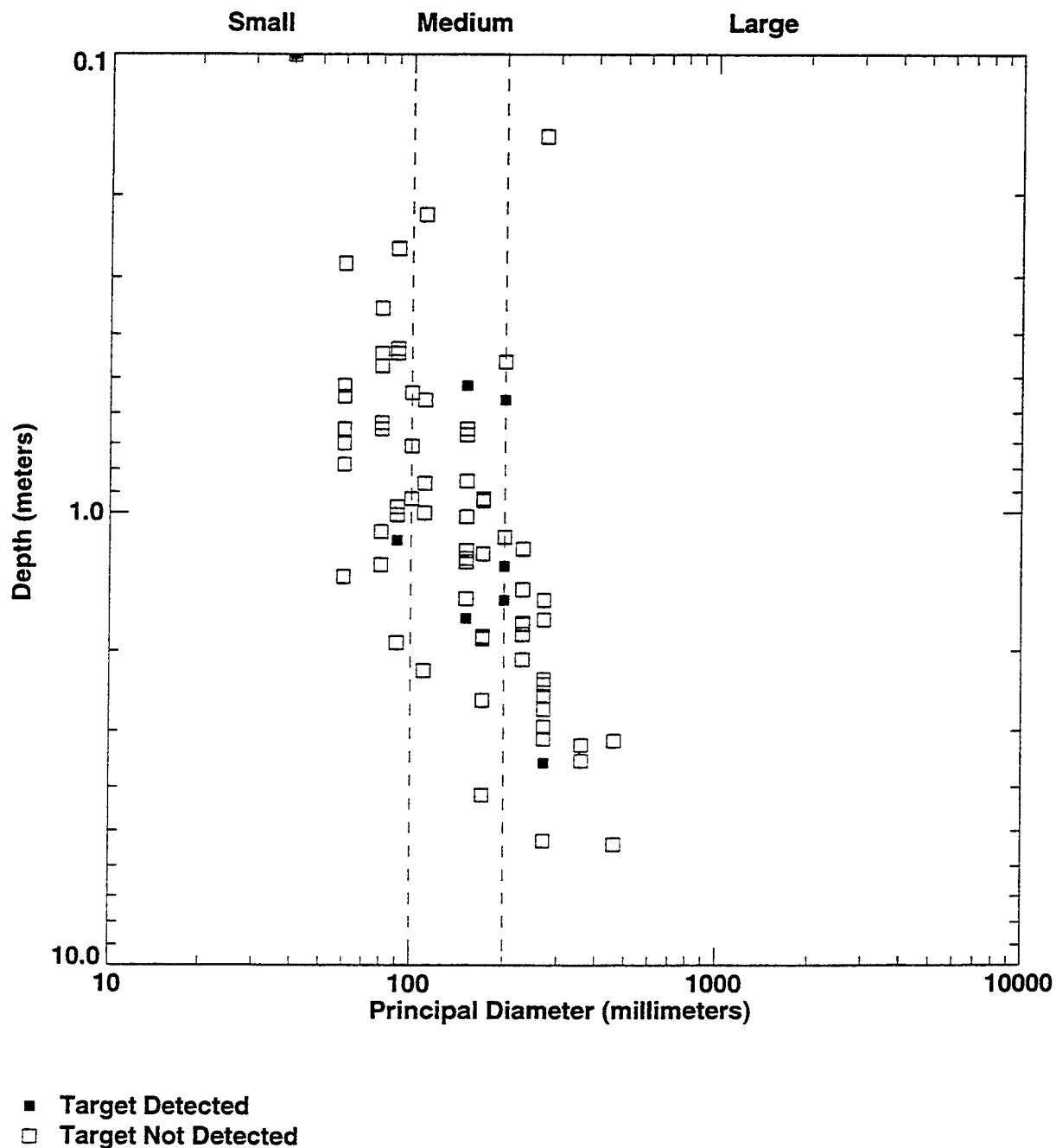
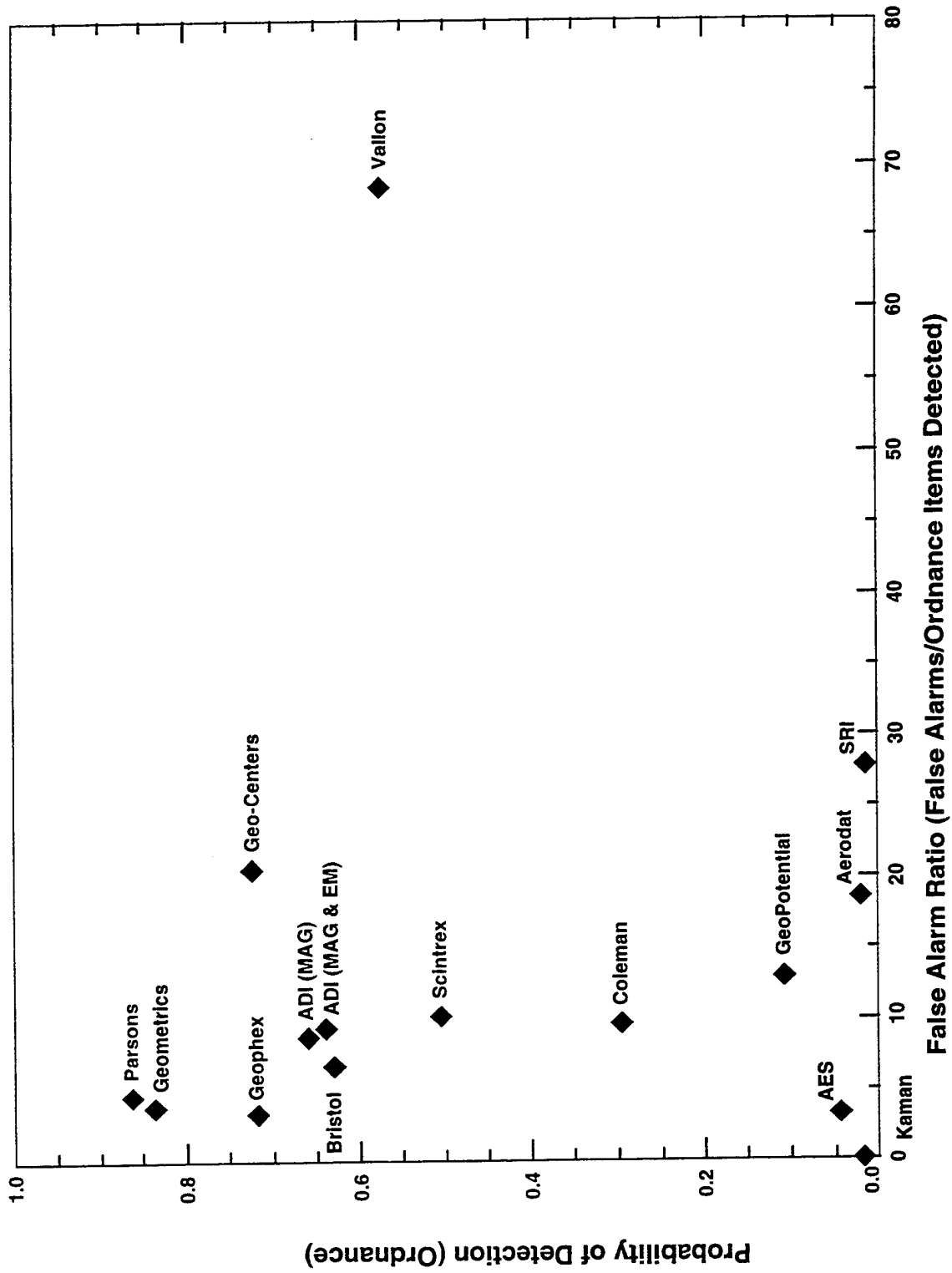


**Figure 4-10**  
**Plot of Demonstrator Probability of Detection (Ordnance) versus False Alarm Ratio**



## **5.0 DEMONSTRATION RESULTS**

During Phase II, 15 UXO detection systems and two remediation systems were demonstrated from May through September 1995. Detection system technologies included eight magnetometer systems, seven electromagnetic induction systems, and five ground-penetrating radar (GPR) systems; in addition, five companies utilized a multi-sensor approach. Of the detection systems, six were man-portable, two were vehicle-towed, four were combined man-portable and vehicle-towed (multimodal), and three were airborne.

### **5.1 MAGNETOMETER SENSOR SYSTEMS**

#### **5.1.1 Aerodat Inc.**

Aerodat Inc. (Aerodat), demonstrated from September 6 through 8, 1995, at the 32-hectare area at JPG. Aerodat also participated in Phase I of the UXO ATD program.

##### **5.1.1.1 Technology Description**

Aerodat used a magnetometer system for its airborne demonstration at JPG (see Figure 5.1.1-1). The magnetometers are mounted on a "bird," which is towed by a helicopter. Aerodat's system consists of five cesium total-field magnetometers and a three-component fluxgate magnetometer, all with a resolution of 0.01 nanotesla. Four of the cesium sensors are arranged in the pods of a rigid X-wing "bird," with one more in the nose, and the fluxgate in the tail. Aerodat states that this configuration provides three-component field and gradient measurements, yielding multiple independent readings for each sample. Data are sampled every 0.1 second, which averages 2 to 3 meters (6 to 9 feet) ground spacing at typical air speeds (Aerodat 1995a).

After acquisition, data reduction occurs as heading and lag corrections are applied as calculated in the pre-survey calibration flights. The diurnal correction is made by directly subtracting the base station measurements. Global positioning satellite (GPS) data are differentially corrected and recorded but can be postprocessed if the real-time link is broken for any reason. The GPS antenna is mounted directly on the bird for greater accuracy of data positioning and anomaly targeting.

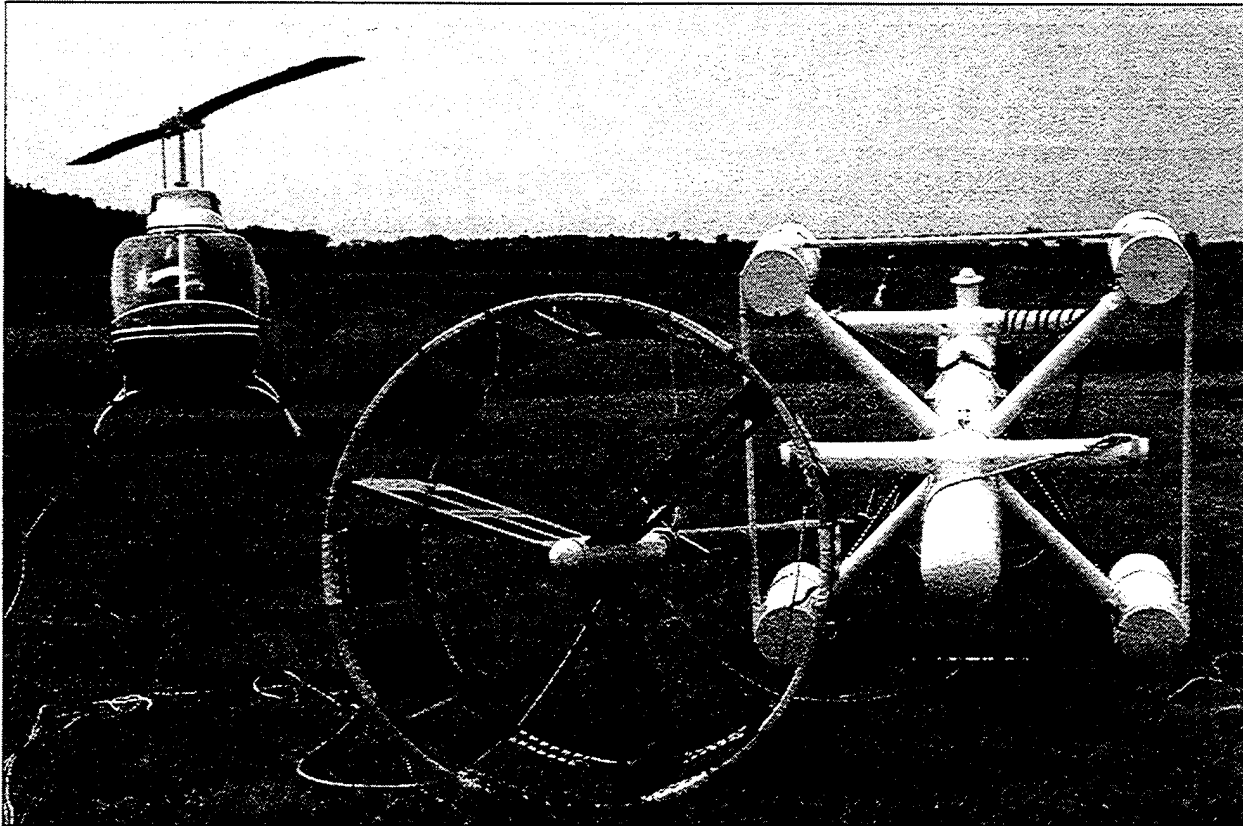


**Figure 5.1.1-1 Aerodat Inc., Airborne Detection System**

The sensors and recording instruments are installed in the helicopter once it is on site. Ground stations for diurnal magnetics and differential GPS measurements are established at the survey site for maximum effectiveness. A low-power, radio modem link is established from the GPS base to the airborne unit to provide real-time updates of position. According to Aerodat, postprocessed differential GPS is adequate for data positioning, but in-flight navigation requires real-time updates to ensure full and even coverage of the area.

Instruments are calibrated off site after installation. This takes place as a cloverleaf pattern is flown at high altitudes so that heading corrections and absolute sensor differences can be calculated. A low pass over a large and obvious target is also flown in two directions to calculate the recording time lag. These test flights also serve to verify the real time GPS link. Once this is completed, the survey is conducted. At JPG, the sensor was towed across the target area in two orthogonal directions, using preprogrammed navigation points from the 32-hectare area. Lines were spaced 10 meters (33 feet) apart. The average survey altitude

was 25 to 30 meters (82 to 98 feet). The altitude is monitored by a laser altimeter mounted in the bird, and a radar altimeter mounted in the helicopter. The laser altimeter provides a more accurate measurement of the sensor height but cannot penetrate foliage and tree cover as the radar can. The radar cannot be mounted in the helicopter, because it disrupts the magnetic readings. The orientation of the bird in flight is measured as a by-product of the fluxgate magnetometer data collection (Aerodat 1995a).

For the demonstration, data were transcribed to a working database for processing and presentation. Data from the base station monitor were used to remove the effects of diurnal variations from the total field data. Vertical and horizontal gradient data were corrected for sensor pitch and roll using an on-board fluxgate magnetometer.

Aerodat indicated the following changes from Phase I: identification of false anomalies caused by sensor pitch-and-roll motions; redesign of the "bird" to provide a three-component field and gradient sensor; and data processing improvements (Aerodat 1995a and b).

#### **5.1.1.2 System Assessment**

This section summarizes the demonstration by Aerodat, based on observations made in the field and information provided by Aerodat.

#### **Requirements for Technology Implementation**

Aerodat used five people to complete its demonstration. Two people were in the aircraft, one processing data and the other flying the helicopter. The remaining personnel served as ground crew. All equipment other than the helicopter was transported to JPG from Aerodat's office in Mississauga, Ontario, Canada.

Support equipment required to perform the survey included a Bell 206 helicopter, equipped with the system-required instrumentation; a van that transported the system equipment; computers; and a GPS base station.

## Operational Capabilities and Limitations

The survey was flown completely in two orthogonal directions. The aircraft ground speed was maintained at about 25 meters per second (82 feet per second). The nominal sensor height was 30 to 35 meters (98 to 115 feet) to ensure the safety of the aircraft and crew. Aerodat stated in its results that the ideal sensor height for this system is less than 10 meters (33 feet) and never more than 15 meters (49 feet). This was not mentioned as a limiting factor in the proposal. Tree cover prevented flying any lower than 30 to 35 meters (98 to 115 feet) throughout the area. According to Aerodat, this survey height reduced the sensitivity of the system to 4 percent. No delays occurred as a result of equipment failure.

### 5.1.1.3 Measured Performance

Aerodat covered the entire 32-hectare area within 13 of the allotted 24 hours. Aerodat identified a total of 78 potential UXO locations at the 32-hectare area. Figure 5.1.1-2 shows Aerodat's target declarations with its airborne magnetometer system at the 32-hectare area (Aerodat 1995b). Aerodat was scored on 100 percent of the total area. Aerodat's performance is shown in Table 5.1.1-1, which presents both detection and localization statistics. Aerodat did not provide type, size, and class information so classification statistics were not computed.

The baseline for computing detection performance included both ordnance and nonordnance items. The detection ratio of 0.02 (cited as  $P_D$  ordnance in Table 5.1.1-1) reflects the number of targets detected by Aerodat compared to the total number of baseline ordnance targets in the area covered. This detection probability is identical to the probability of detection arising from random declarations due to sensor noise and other factors ( $P_{\text{random}} = 0.02$ ). Aerodat's FAR was 2.3 per hectare.

Aerodat had the lowest probability of detection of the four magnetometer systems demonstrated. However, Aerodat's detection results are consistent with those obtained by other airborne demonstrators. These results may be due to the difficulty of magnetometers to detect at the high speed of an airborne system. Aerodat's FAR was low, which may be indicative of a combination of both a high noise level and a high detection threshold.

As part of Phase I, Aerodat had a  $P_D$  of 0.04 for ordnance items. The FAR was 4.2 per hectare. Phase II detection performance decreased slightly with a  $P_D$  of 0.02, although the FAR improved slightly as it decreased from 4.2 in Phase I to 2.3 in Phase II. Aerodat's results are comparable to the results from other airborne systems from Phase I and Phase II.

For most demonstrators, the probability of ordnance detection depends on both the size and depth of the buried ordnance item. Figure 5.1.1-3, which is a scatter plot showing detection performance as a function of size versus depth, illustrates this relationship for Aerodat. In this figure, no clear relationship is evident. The majority of targets were difficult for Aerodat to detect.

The localization error statistics section of Table 5.1.1-1 indicates Aerodat's ability to estimate the locations of the targets declared. Aerodat reported target depths between 0.10 and 0.30 meter (0.33 and 0.98 foot) below ground surface.



**Figure 5.1.1-2**  
**Aerodat Target Declarations**

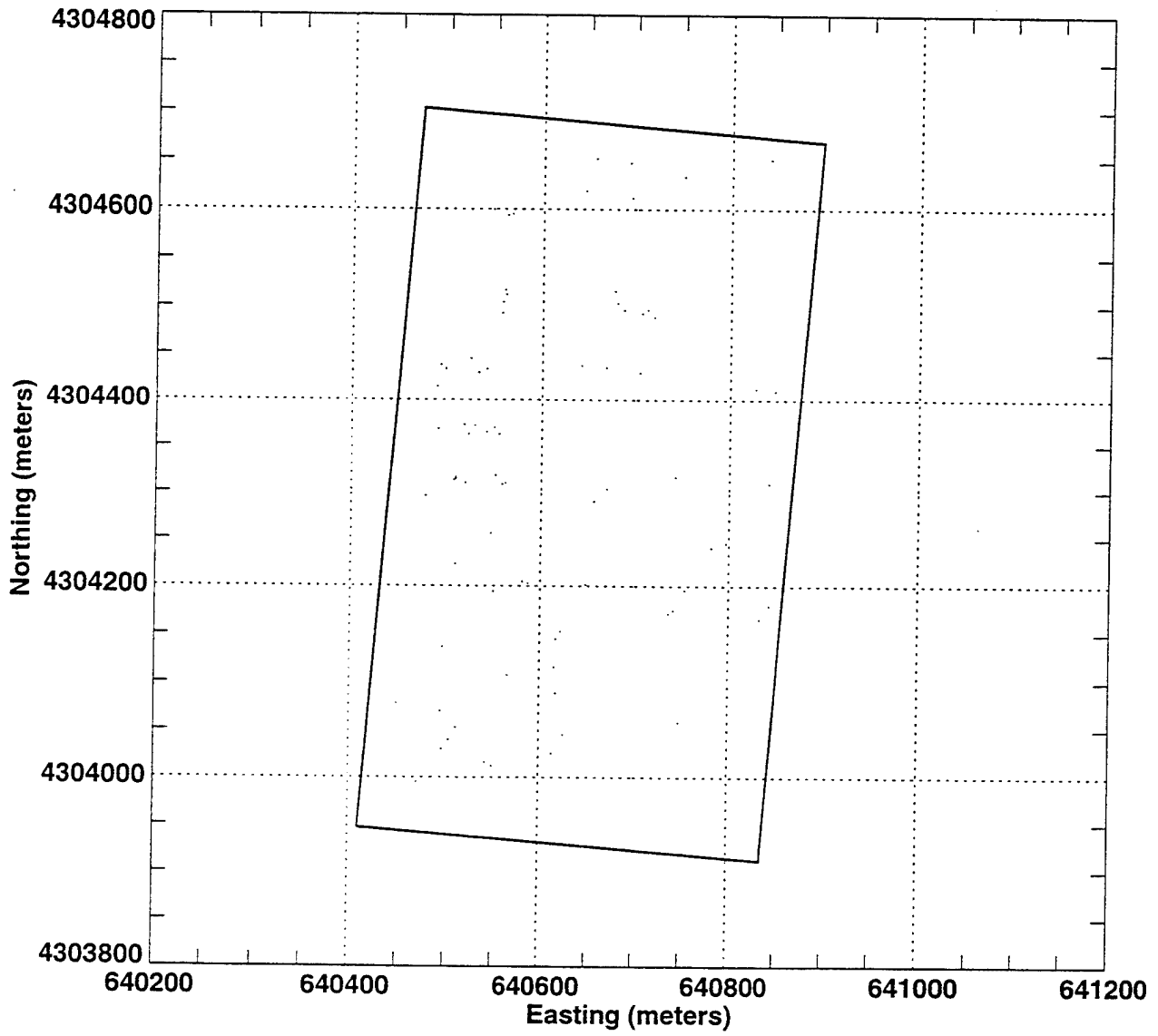


**TABLE 5.1.1-1  
PERFORMANCE STATISTICS FOR AERODAT**

**Detection Statistics**

	Number Baseline	Number Matched	$P_D^a$
Ordnance	201	4	0.02
Nonordnance	20	1	0.05
Total	221	5	0.02
$P_{random}$	0.02		
Number False Alarms	74		
False Alarm Rate	2.3/hectare		
False Alarm Ratio	18.5		
Probability False Alarms	0.0182		

**Localization Statistics**

	Mean (m) <sup>b</sup>	Std. Dev. <sup>c</sup> (m)
Position (x,y)		
dx	-0.37	2.05
dy	0.56	2.15
Radial	2.29	
Depth (z)		
$dz^d$	-1.87	1.00
dz	2.07	

**Identification and Classification Statistics**

	Number Baseline	Number Detected	$P_D^e$	Number Correct	$P_C^f$
Type					
Ordnance	245	4	0.02	0	0
Nonordnance	27	1	0.04	0	0
Size					
Large	41	3	0.07	0	0
Medium	37	1	0.03	0	0
Small	165	0	0	0	NA <sup>g</sup>
Class					
Bomb	23	2	0.09	0	0
Projectile	73	2	0.03	0	0
Mortar	143	0	0	0	NA
Cluster	6	0	0	0	NA

- Notes:
- <sup>a</sup> Probability of detection (based on Group TMA, fence area excluded)
  - <sup>b</sup> Meter
  - <sup>c</sup> Standard deviation
  - <sup>d</sup> Square root of the mean square depth error
  - <sup>e</sup> Probability of detection (based on closest TMA, fence area excluded)
  - <sup>f</sup> Probability of correctly classifying (based on closest TMA)
  - <sup>g</sup> Not applicable



## 5.1.2 Australian Defence Industries, Pty. Ltd.

Australian Defence Industries, Pty. Ltd. (ADI), demonstrated from June 14 through 18, 1995, at the 16B-hectare area at JPG. ADI also participated in Phase I of the UXO ATD program. During Phase II, ADI used two separate man-portable sensor systems for its demonstration: magnetometer and electromagnetic induction. The following sections describe ADI's magnetometer technology, assess ADI's demonstration, and analyze ADI's magnetometer results. For a complete discussion on ADI's electromagnetic induction technology and analysis of both the magnetometer and electromagnetic induction data combined, see Section 5.4.1.

### 5.1.2.1 Technology Description

ADI used a TM-4 magnetometer system for part of its surveying (see Figure 5.1.2-1). The TM-4 magnetometer includes an imaging magnetometer with integrated processing and interpretation software. The TM-4 data acquisition, processing, interpretation, and documentation systems are designed to locate

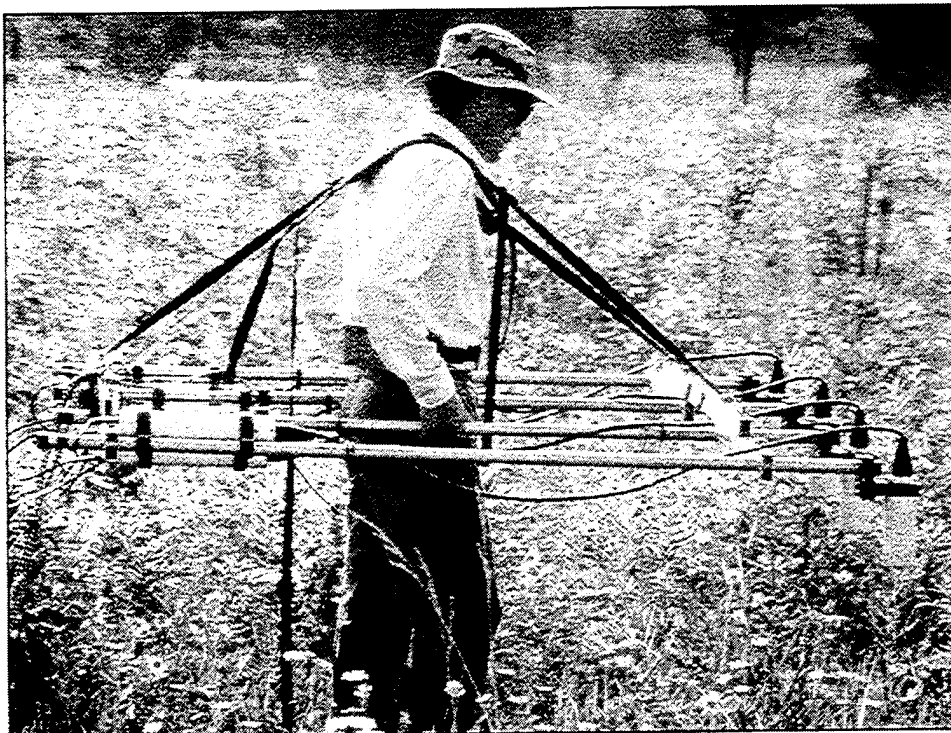


Figure 5.1.2-1 Australian Defence Industries, Pty. Ltd., TM-4 Imaging Magnetometer

ferrous sources. The unit can be used with either single or multiple cesium-vapor magnetometers. The TM-4 magnetometer measures total magnetic field and, according to ADI, is capable of reading the total magnetic field to a sensitivity of 0.011 nanotesla at a rate of 100 times per second. Data are stored in solid-state memory and transferred to a personal computer (PC) in the field. The data are then gridded for image processing and interpretation (ADI 1995a).

ADI indicated the following improvements from Phase I: increased accuracy to the odometer of the TM-4 magnetometer, improved positioning system, new routines for data processing of the TM-4 magnetometer data, and the addition of the electromagnetic induction-sensor system as described in Section 5.4.1 (ADI 1995a).

#### **5.1.2.2 System Assessment**

This section summarizes the ADI magnetometer demonstration, based on observations made in the field.

#### **Requirements for Technology Implementation**

ADI used seven people to complete its demonstration. Two people operated the TM-4 magnetometer in the field. One person carried the sensors, followed by another person who carried a PC tethered to the sensors. The remaining five people operated the two electromagnetic induction-sensor units, alternating to allow for rest periods. All system equipment used for this demonstration was shipped to JPG from ADI headquarters in Australia. ADI rented a utility vehicle locally for transportation. ADI used the support trailer to store equipment and to recharge batteries.

For grid navigation, ADI used four magnetic marking chains. The magnetic chains were placed along east-west grid lines. The survey lines or transects were conducted in a north-south fashion. The TM-4 magnetometer uses a cotton string odometer to track its position. Each time the TM-4 magnetometer passed the marking chains, that particular grid was "marked" in the computer memory.

## Operational Capabilities and Limitations

The TM-4 magnetometer can be used as a single, dual, or quad-sensor unit. The quad-sensor configuration was used for this demonstration. The system is man-portable and is subject to the physical limitations of the operator. The TM-4 magnetometer weighs 10 kilograms (22 pounds), imposing some fitness requirements on the operator. The TM-4 magnetometer is versatile in the field. For example, it can be collapsed to a single unit for surveying inaccessible areas between trees.

### 5.1.2.3 Measured Performance

ADI covered the entire 16B-hectare area with the TM-4 magnetometer in about 32 hours. ADI's results were analyzed in two ways. The TM-4 magnetometer data were analyzed separately, and the magnetometer and electromagnetic induction data were analyzed together, for insight as to the ferrous and the nonferrous items detected (ADI 1995a). Section 5.4.1 discusses of the measured performance of the combined magnetometer and electromagnetic induction data (ADI 1995b).

After removing the fence line area from the area searched, ADI reported 569 targets with the TM-4 magnetometer (see Figure 5.1.2-2) within the 16 hectares. ADI's performance with the magnetometer is shown in Table 5.1.2-1, which presents the following: (1) detection, (2) localization, and (3) classification statistics with respect to type, size, and class for ADI's magnetometer data.

The baseline for computing detection performance for Phase II included both ordnance and nonordnance items. The detection ratio of 0.63 (cited as  $P_D$  ordnance in Table 5.1.2-1) reflects the number of ordnance targets detected by ADI with the TM-4 magnetometer. This  $P_D$  value is significantly different than the probability of detection resulting from random declarations, shown as 0.04 ( $P_{\text{random}}$ ). ADI had a FAR of 31.4 per hectare for the TM-4 magnetometer.

As part of Phase I, ADI deployed the TM-4 magnetometer for data acquisition and had a  $P_D$  of 0.48 for ordnance items; the FAR was 30.1 per hectare. A comparison of Phase I and Phase II detection performance shows that ADI's detection capability improved while the FAR remained essentially the same.

For most demonstrators, the probability of ordnance detection depends on both the size and the depth of the buried ordnance item. Figure 5.1.2-3 presents a scatter plot showing detection performance as a function of size versus depth to illustrate this relationship. ADI was more successful at detecting medium and large targets than smaller targets. Small targets (less than 100-mm diameter) were difficult for ADI to detect at most depths.

The localization error statistics section of Table 5.1.2-1 indicates ADI's ability to estimate the location of the targets declared. ADI reported target depths between 0.39 meter (1.28 feet) above surface to 6.08 meters (19.95 feet) below ground surface. ADI provided type, size, and class information, as shown in the table.

**Figure 5.1.2-2**  
**ADI Magnetometer Target Declarations**

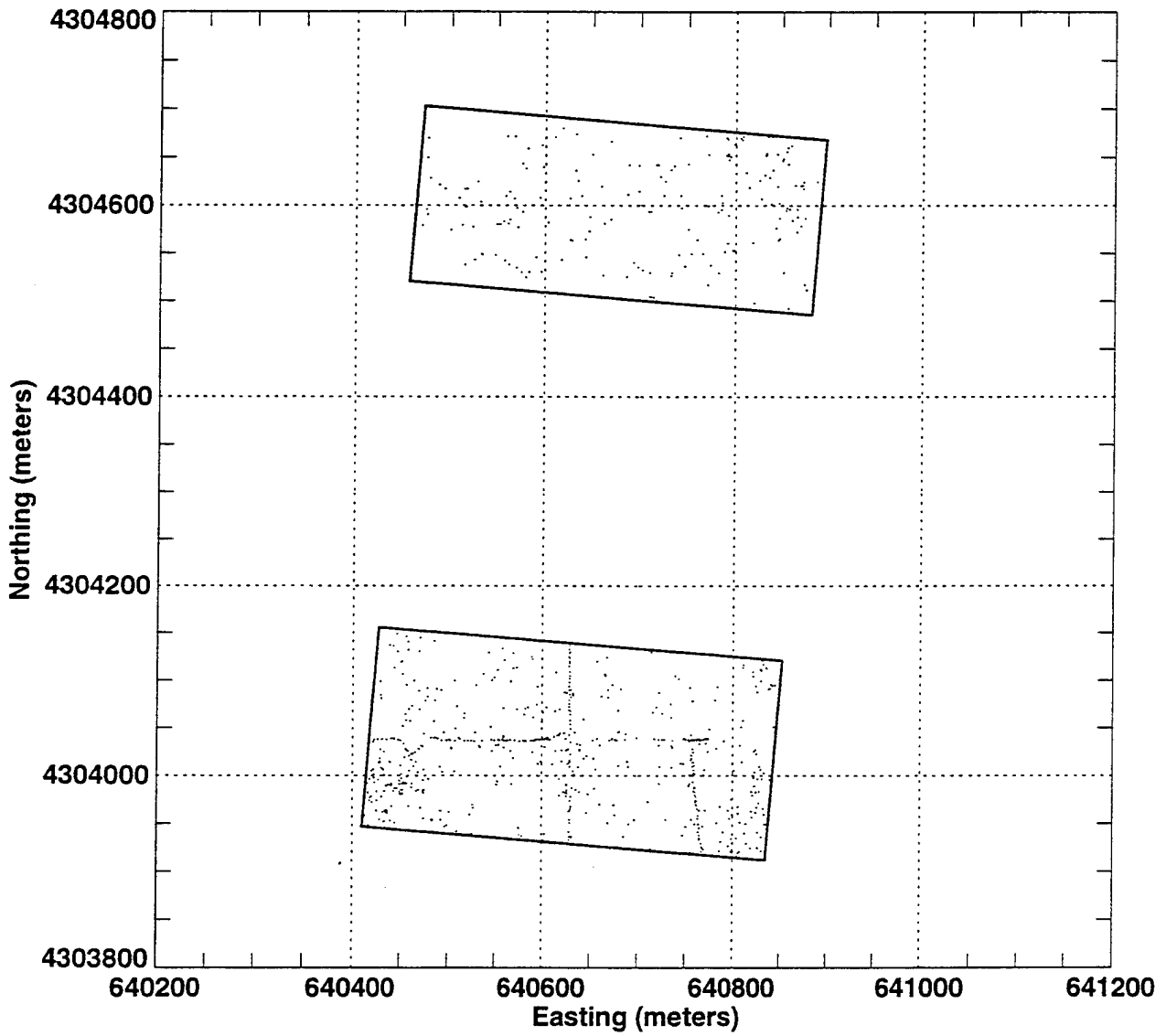




**TABLE 5.1.2-1  
PERFORMANCE STATISTICS FOR ADI (MAGNETOMETER DATA)**

**Detection Statistics**

	Number Baseline	Number Matched	$P_D^a$
Ordnance	92	58	0.63
Nonordnance	8	6	0.75
Total	100	64	0.64
$P_{random}$	0.04		
Number False Alarms	515		
False Alarm Rate	31.7/hectare		
False Alarm Ratio	8.88		
Probability False Alarms	0.0398		

**Localization Statistics**

	Mean (m) <sup>b</sup>	Std. Dev. <sup>c</sup> (m)
Position (x,y)		
dx	-0.05	0.61
dy	-0.23	0.56
Radial	0.74	
Depth (z)		
$dz^d$	0.14	0.67
dz	0.68	

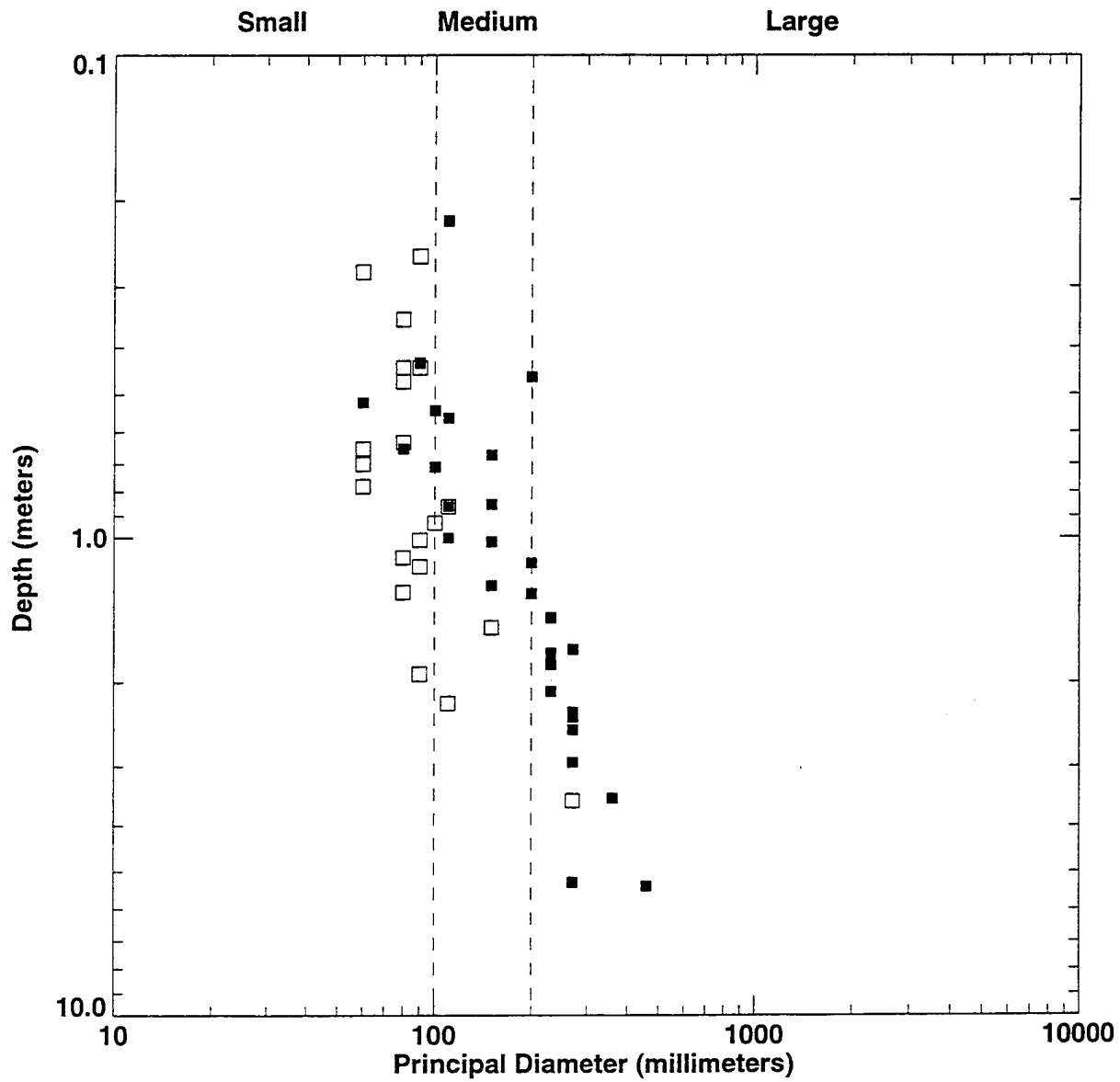
**Identification and Classification Statistics**

	Number Baseline	Number Detected	$P_D^e$	Number Correct	$P_C^f$
Type					
Ordnance	125	60	0.48	45	0.75
Nonordnance	14	9	0.64	1	0.11
Size					
Large	31	20	0.65	13	0.65
Medium	23	14	0.61	8	0.57
Small	69	25	0.36	24	0.96
Class					
Bomb	15	13	0.87	10	0.77
Projectile	51	24	0.47	10	0.42
Mortar	53	20	0.38	7	0.35
Cluster	6	3	0.50	0	0

Notes:

- <sup>a</sup> Probability of detection (based on Group TMA, fence area excluded)
- <sup>b</sup> Meter
- <sup>c</sup> Standard deviation
- <sup>d</sup> Square root of the mean square depth error
- <sup>e</sup> Probability of detection (based on closest TMA, fence area excluded)
- <sup>f</sup> Probability of correctly classifying (based on closest TMA)

Figure 5.1.2-3  
ADI Magnetometer Detection Ability



- Target Detected
- Target Not Detected

### 5.1.3 Geometrics, Inc.

Geometrics, Inc. (Geometrics), demonstrated from July 26 through 30, 1995, at the 16A-hectare area at JPG. Geometrics also participated in Phase I of the UXO ATD program.

#### 5.1.3.1 Technology Description

Geometrics used a ground based multisensor approach to complete its demonstration at JPG. The first system used was the hand-carried G-858 magnetometer; three of these units were used in the demonstration (see Figure 5.1.3-1). The G-858 consists of two cesium magnetometer sensors horizontally separated by 0.76 meter (2.5 feet) and located about 0.46 meter (1.5 feet) above the ground. Data from each sensor are recorded individually on the G-858, along with operator marked fiducials and time. Each magnetometer contains a data control, acquisition, and field display unit. Differential GPS and along-track markers are used to provide sub-meter positioning information. In addition, each operator uses an audio cross-track differential GPS steering indicator to stay on line. Each operator has a headphone with an audio tone that



Figure 5.1.3-1 Geometrics, Inc. G-858 Magnetometer

has a different frequency to indicate left and right. The frequency pulsing rate indicates deviation right or left of the survey line (Geometrics 1995a).

Before conducting the survey, the area to be covered was marked with green survey paint at 30-meter (100-foot) intervals along one side of the grid cell and at 1.5 meter (5.0-foot) intervals along the other side of the grid cell. GPS data and magnetic sensor data was continuously transmitted back to a base station by an RF data link. The data were then processed at the base workstation by the Arete Engineering Technologies Corporation (AETC) team, subcontractor to Geometrics. The data was processed to provide targets for GDE Systems, Inc. (GDE), subcontractor to Geometrics; the GDE team used GPS coordinates to locate the targets. The GDE team concentrated on potential UXO target areas identified by the magnetic data.

The GPR system used an all-terrain vehicle (ATV) to tow a trailer that carried seven broadband antennas over the areas identified by the data team (see Figure 5.1.3-2). The ATV also carried a motor generator; a commercial network analyzer, which is the transmitter and receiver; a computer; and a display. The GPR

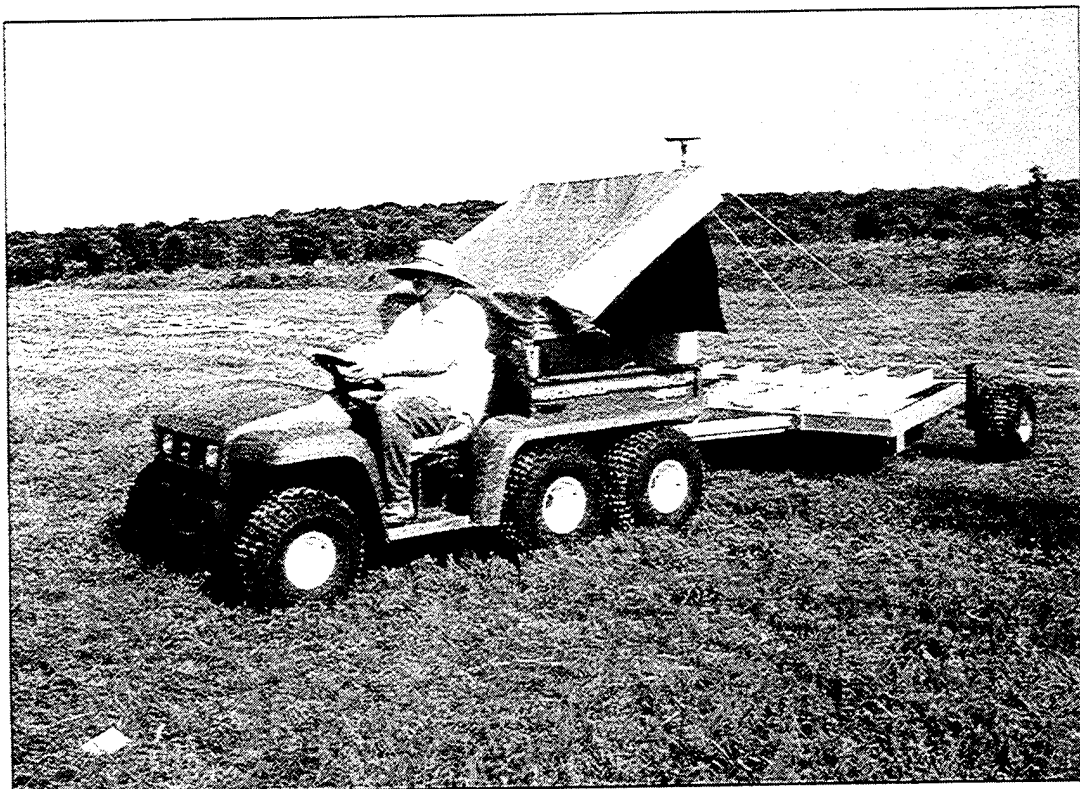


Figure 5.1.3-2 Geometrics Ground Penetrating Radar System

system operates with radio waves at discrete frequencies between 180 and 720 megahertz (MHz), measuring near field reflectance with an antennae array on a ground vehicle. Vehicle motion and array sampling combine to synthesize a data swath, and a computer processes the data into images. The images are plan views in horizontal sections, which are orthogonal to the vertical sections of pulsed GPR (Geometrics 1995a).

System improvements from Phase I included the method of surveying and processing data. Differential GPS was added for navigation across grid cells, and GPR was added to provide a ground-base multisensor approach. During Phase II, Geometrics combined the efforts of AETC and GDE; all three of these companies demonstrated independently during Phase I (Geometrics 1995a).

#### **5.1.3.2 System Assessment**

This section summarizes the Geometrics demonstration, based on observations made in the field.

#### **Requirements for Technology Implementation**

Geometrics used 12 people to complete its demonstration. The three magnetometers were operated by two-person teams. One person carried the magnetometer, while the other person recorded the line numbers and assisted the operator. Personnel on these teams alternated to provide rest periods. One person provided EOD technical support for the demonstration. AETC provided two people for data processing. Three people from GDE performed the GPR survey.

All system equipment used for this demonstration was shipped or brought to JPG by Geometrics. Equipment required for the magnetometer survey included three G-858 units in dual-sensor configuration, three backpack-mounted GPS receivers and antennas, three data radios, three backpack-mounted 12-volt batteries, one laptop PC for data downloading, one ATV for use as a utility vehicle, one magnetic base station, and one GPS base station. The GPR system required the following components: an array of seven antennas, a receiver, a transmitter, a data acquisition computer, and an ATV for towing the GPR. The on-site data processing system consisted of a Sun SPARK workstation, a Windows PC terminal, a black-and-white and color printer, and AETC modeling software.

Support equipment used by Geometrics included several vehicles to transport personnel and supplies. Several spare magnetometer sensors were shipped by overnight delivery to replace faulty sensors. The support trailer supplied electricity to recharge the Geometrics system batteries. Data analysis also took place at the support trailer.

### **Operational Capabilities and Limitations**

The magnetometers used by Geometrics required little maintenance beyond recharging the batteries. Geometrics experienced a delay on the first day because the freight forwarding company temporarily lost the crate containing the backpacks, GPS, and communication equipment. The three magnetometer systems operated simultaneously. Each team surveyed a 30-by-189-meter (100-by-620-foot) section in succession with the other teams. Sensor problems with one of the magnetometers were resolved using replacement sensors shipped by overnight delivery.

According to Geometrics, the magnetometers collect data at a rate of 10 magnetic readings per second with a sensitivity of 0.05 nanotesla. Survey speeds were initially estimated at about 2 hectares (5 acres) per hour for each of the three systems. The extremely hot weather and delays on the first day may have been partially responsible for the slower survey speed. Heavy brush and uneven terrain can also slow the survey speed due to difficulty with maneuverability. Geometrics stated in its results that a single-sensor magnetometer could have penetrated the areas of thick brush better than the dual-sensor magnetometer. The GPR system was proposed to be able to travel at least 10 kilometers (6 miles) per hour. Geometrics found the GPR system to be severely restricted by terrain and vegetative cover. Geometrics stated in its results that there is a need for a portable, hand-carried GPR that would not have to be driven or dragged over the surface.

#### **5.1.3.3 Measured Performance**

Geomatrics surveyed the entire 16A-hectare area with its magnetometer system in the allotted 40 hours (see Figure 5.1.3-3). Geomatrics was unable to cover all of the area with its GPR system and unable to process all of the data collected. As a result, Geomatrics requested that it be scored on its magnetometer data alone (Geomatrics 1995b). Geomatrics reported 521 targets within the 16A-hectare area. Geomatrics' performance is shown in Table 5.1.3-1, which presents the following: (1) detection, (2) localization, and (3) classification statistics with respect to type, size, and class.

The baseline for computing detection performance included both ordnance and nonordnance items. The detection ratio of 0.83 (cited as  $P_D$  ordnance in Table 5.1.3-1) reflects the number of targets detected by Geometrics compared to the total number of baseline ordnance targets in the 16 hectares with the fence line area removed. This detection probability is significantly different than the probability of detection arising from random declarations due to sensor noise and other factors ( $P_{\text{random}} = 0.04$ ). Geometrics had a FAR of 25.2 per hectare.

Geometrics had the highest  $P_D$  (0.83) of all magnetometer systems demonstrated. Geometrics teamed with AETC to perform the data processing which may, in part, account for their performance relative to the other systems demonstrated.

As part of Phase I, Geometrics had a  $P_D$  of 0.21 for ordnance items. The FAR was 7.5 per hectare. A comparison of Phase I and Phase II detection performance shows that Geometrics obtained much higher  $P_D$  values for Phase II, 0.83 as compared to 0.21. However, Geometrics FAR also increased, from 7.5 in Phase I to 26.7 during Phase II.

For most demonstrators, the probability of ordnance detection depends on both the size and depth of the buried ordnance item. Figure 5.1.3-4, which is a scatter plot showing detection performance as a function of size versus depth, illustrates this relationship for Geometrics. Geometrics was successful at detecting targets of all sizes at most depths.

The localization error statistics section of Table 5.1.3-1 indicates Geometrics' ability to estimate the locations of the targets declared. Geometrics reported target depths between 0 and 5.84 meters (0 and 19.16 feet) below ground surface. Geometrics declared all target detections as ordnance. Geometrics did provide size and class information, as shown in the table. Geometrics did not correctly classify any ordnance items.

Figure 5.1.3-3

Geometrics Target Declarations

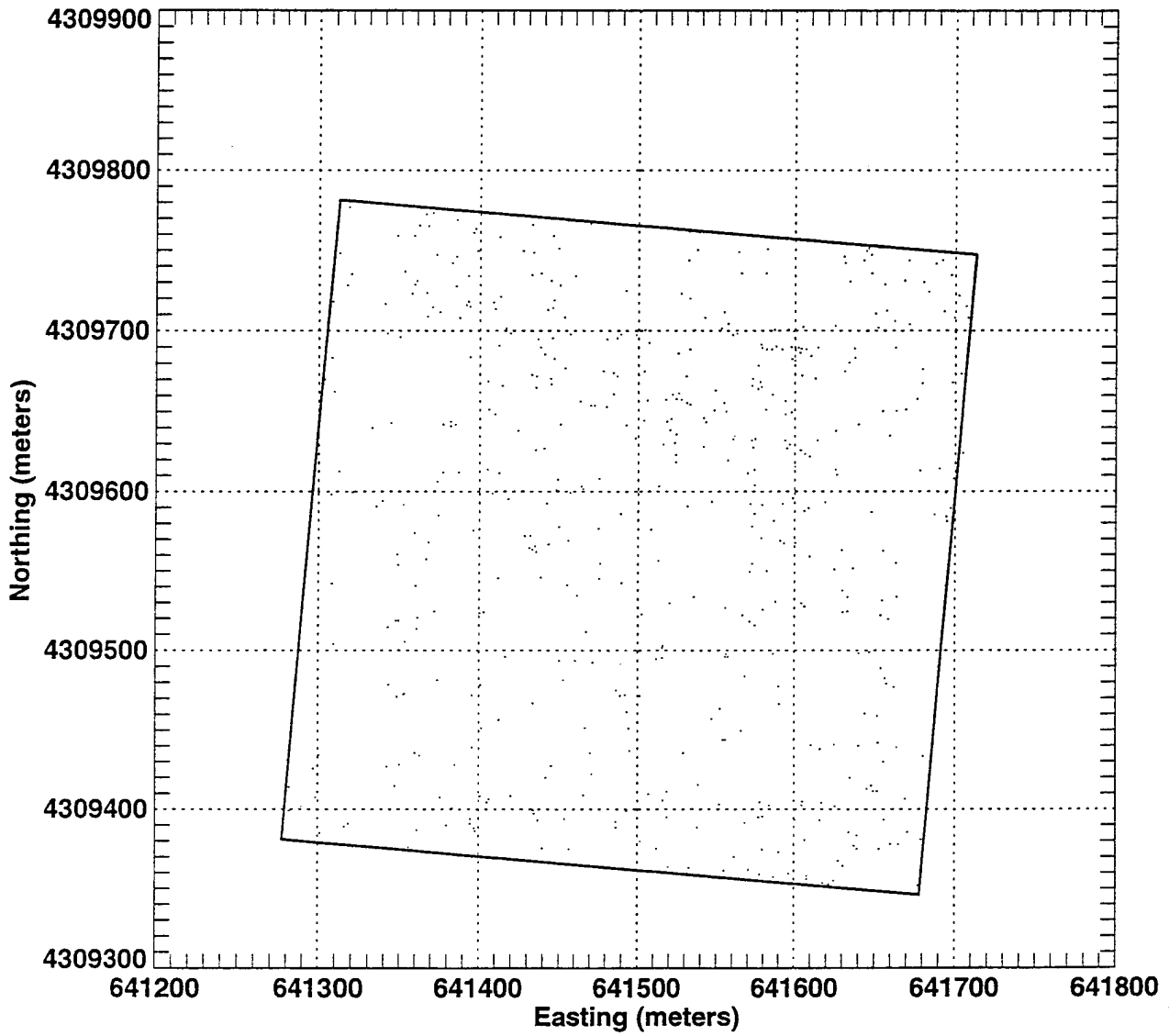




**TABLE 5.1.3-1  
PERFORMANCE STATISTICS FOR GEOMETRICS**

**Detection Statistics**

	Number Baseline	Number Matched	$P_D^a$
Ordnance	127	105	0.83
Nonordnance	41	23	0.56
Total	168	128	0.76
$P_{random}$	0.04		
Number False Alarms	416		
False Alarm Rate	26.7/hectare		
False Alarm Ratio	3.96		
Probability False Alarms	0.0336		

**Localization Statistics**

	Mean (m) <sup>b</sup>	Std. Dev. <sup>c</sup> (m)
Position (x,y)		
dx	-0.11	0.48
dy	0.08	0.60
Radial	0.65	
Depth (z)		
$dz^d$	0.21	0.59
dz	0.62	

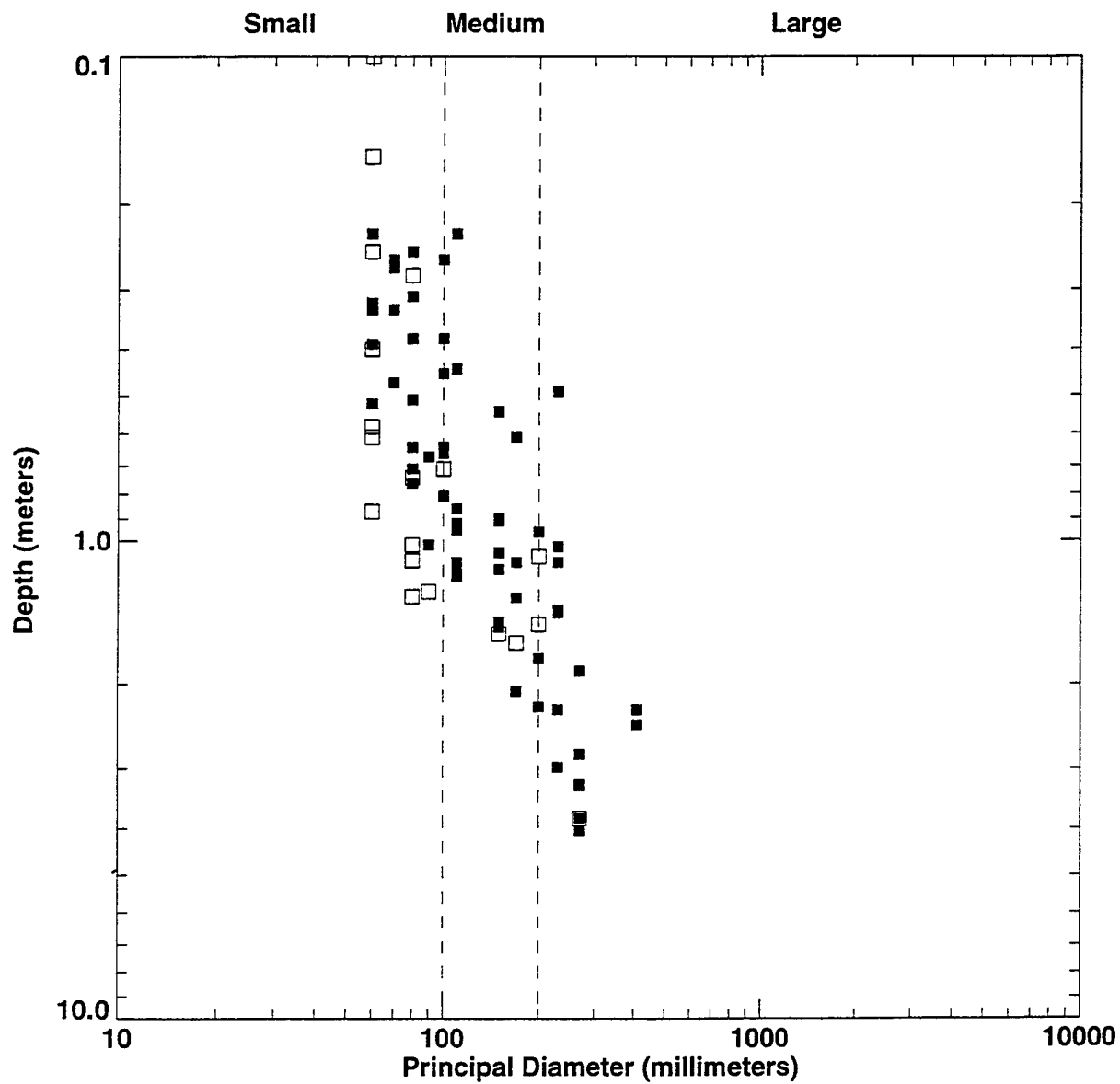
**Identification and Classification Statistics**

	Number Baseline	Number Detected	$P_D^e$	Number Correct	$P_C^f$
Type					
Ordnance	158	99	0.63	99	1.00
Nonordnance	65	31	0.48	0	0
Size					
Large	35	27	0.77	20	0.74
Medium	53	37	0.70	20	0.54
Small	69	35	0.51	28	0.80
Class					
Bomb	21	19	0.90	0	0
Projectile	69	45	0.65	0	0
Mortar	59	31	0.53	0	0
Cluster	9	4	0.44	0	0

**Notes:**

- <sup>a</sup> Probability of detection (based on Group TMA, fence area excluded)
- <sup>b</sup> Meter
- <sup>c</sup> Standard deviation
- <sup>d</sup> Square root of the mean square depth error
- <sup>e</sup> Probability of detection (based on closest TMA, fence area excluded)
- <sup>f</sup> Probability of correctly classifying (based on closest TMA)

Figure 5.1.3-4  
Geometrics Detection Ability



- Target Detected
- Target Not Detected

#### 5.1.4 Polestar Technologies, Inc.

Polestar Technologies, Inc. (Polestar), demonstrated from June 14 through 17, 1995, at the 16A-hectare area at JPG.

##### 5.1.4.1 Technology Description

Polestar's magnetometer system used a magnetic sensor with both total field and vector gradiometer readings (see Figure 5.1.4-1). The magnetometer is designed to incorporate "dual-mode" detection in a single sensor. Navigation was achieved through a precision beacon system (PBS) that offered 0.1 meter position information, even in vegetated and forested conditions. The PBS was designed to prevent the failures that can occur with GPS when satellite communication is disrupted due to terrain, structures, or vegetation.

Polestar's magnetometer system uses five detection heads mounted on a 2.4-meter (8.0-foot) boom positioned 0.5 meters (1.6 feet) apart. The sensors are carried by two people using a backpack harness, one on either end of the boom. An antennae attached to one of the backpack harnesses transmitted

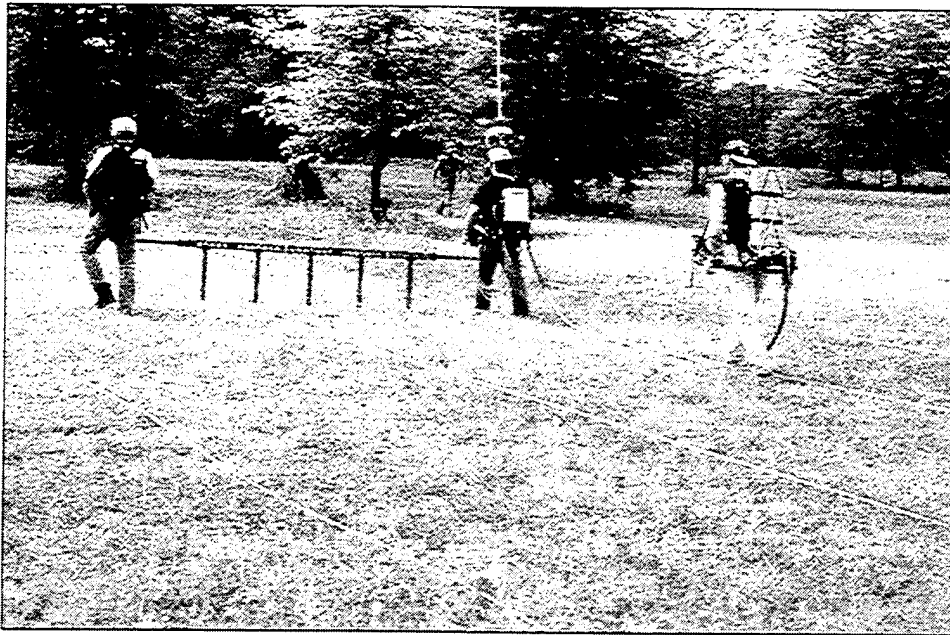


Figure 5.1.4-1 Polestar Technologies, Inc., Magnetometer System

to the PBS for navigation purposes. The sensor system is attached to a computer system carried by a third person; this individual is attached to the magnetometer by a flexible safety tube.

According to Polestar's proposal, the PBS uses a low frequency microwave signal, exhibiting a coverage range of 3.0 kilometers (1.9 miles). Most trees do not interfere with its long wavelength which diffracts around trees. The system's phase detection permits spatial resolution to a fraction of a wavelength, thereby achieving a distance measurement accuracy of less than 15 centimeters (6 inches). Established monuments at the 16A-hectare area were used as base stations, and triangulation was used to track the sensor system. Although Polestar used microwave navigation with its PBS, the system was also equipped to use a GPS.

Polestar stated that the navigation data are stored twice per second, and the six individual axes of each magnetometer are read at 50 Hz. Proprietary data analysis software was used to process both the vector and total magnetic field data. A multiparameter, nonlinear least squares algorithm was used to accurately determine x, y, and z, as well as magnetic mass, inclination, and declination (Polestar 1995a).

#### **5.1.4.2 System Assessment**

This section summarizes the Polestar demonstration, based on observations made in the field.

#### **Requirements for Technology Implementation**

Polestar used nine people to complete its demonstration. At the beginning of the demonstration, three beacons that made up the PBS were placed outside of the 16A-hectare area to assist in navigation on the grid. The magnetometer system required three people for operation. Polestar used two teams, alternating personnel to allow for rest periods. The resting team and the remaining three people were responsible for grid layout.

The grid was laid out by placing stakes every 3 meters (10 feet) along the grid lines. String was then used to visually guide the survey team along a straight path from these stakes.

All system equipment used for this demonstration was shipped or brought to JPG by Polestar. Support equipment used by Polestar included two laptop computers to store and process the data, one minivan to

transport personnel and supplies, and a full-size van to store the equipment in the field. Surveyor stakes and string were used to lay out lanes within the grid area. The support trailer supplied electricity to recharge the Polestar system batteries.

### **Operational Capabilities and Limitations**

Polestar's system appeared to operate best in large open areas. The system had difficulty accessing wooded areas, as the size of the boom precluded maneuvering around more than one or two trees at a time. In addition, low cover in woody areas presented a problem because the PBS antenna, which is 3.7 meters (12.0 feet) high, became caught in the overstory. The grid layout required by the system is labor intensive. The survey equipment is heavy and requires alternating operators under hot and humid conditions.

The system used by Polestar required little maintenance beyond recharging the batteries; delays resulting from battery failure resulted in a total of 44 minutes of downtime during the demonstration. Polestar experienced no other delays in the field as a result of equipment failure.

#### **5.1.4.3 Measured Performance**

Polestar surveyed about 15 hectares of the 16A-hectare area with its magnetometers in 32.5 of the allotted 40 hours. Polestar reported no targets within the 16A-hectare area. In its final report, Polestar stated that the solid-state sensors of the magnetometers were defective. Polestar stated that the three axes of the sensor were improperly located causing a "crosstalk." Polestar noted this problem early, during preprocessing at JPG but thought that calibration and correction could be used to restore the integrity of the data. However, the defect was nonlinear and could not be corrected. The only data provided by Polestar were the navigation results, illustrating the utility of the PBS for field use. As a result, no data analysis was possible (Polestar 1995b).

## **5.1.5 Scintrex, Inc.**

Scintrex, Inc. (Scintrex), demonstrated from July 12 through 17, 1995, at the 16A-hectare area at JPG.

### **5.1.5.1 Technology Description**

Scintrex used two magnetometers called Smartmags for its demonstration (see Figure 5.1.5-1). The Smartmag consists of a staff-mounted cesium-vapor magnetometer and signal processor; a memory console, staff mounted display, and headphones; and a belt-mounted battery pack for the processor. Three different versions of the Smartmag exist: the sweep version, the mapping version, and the survey version, all using slightly different combinations of equipment. The mapping version was used for this demonstration, and it consisted of the magnetometer and processor with a belt-mounted battery pack and memory console. The magnetometer sensor consists of a miniature atomic absorption unit from which a signal proportional to the intensity of the ambient magnetic field is derived. A signal processor converts the signal into the magnetic field strength in nanoteslas for display and recording.

A Trimble real-time kinematic GPS was coupled with the Smartmag to position the survey data. A Trintalk reference station was used to send error corrections to rover units in the field. Total field magnetometer data were collected every 0.1 second, with GPS position updates every second. Survey lines were marked with surveyor staffs placed at each end and painted at 1-meter intervals to ensure that areas were not missed. Scintrex personnel walked the survey lines in a north-to-south direction. East-to-west lines were used to tie the surveyed grid cells together.

As data were collected, they were stored in the system's memory console and subsequently transferred to a PC for permanent storage. A reference magnetometer was set up to record data on the background magnetic field of the earth; these data were then used to correct the magnetometer data collected in the field. The target data was mapped using software supplied by Geosoft, Scintrex subcontractors (Scintrex 1995a).

### **5.1.5.2 System Assessment**

This section summarizes the Scintrex demonstration, based on observations made in the field.



Figure 5.1.5-1 Scintrex, Inc., Smartmag Magnetometer System

### **Requirements for Technology Implementation**

Scintrex used four people to complete its demonstration. Two people operated the two magnetometers used for the survey. One person supported these two teams, keeping track of the area covered and transporting the memory console to the support trailer for downloading. The remaining person, from Geosoft, managed data analysis, which took place at the support trailer.

All system equipment used for this demonstration was shipped or brought to JPG by Scintrex. Support equipment used by Scintrex included several laptop computers to store and process the data, one minivan to transport personnel and supplies, and one car to transport personnel. A surveyor staff and paint lines were used for navigation through the grid area. Electricity supply was provided from the 16A-hectare support trailer to recharge the Scintrex system batteries.

### **Operational Capabilities and Limitations**

The magnetometers used by Scintrex required little maintenance beyond recharging the batteries. Because the Smartmag is man-portable, survey efficiency is subject to the physical limitations of the operator. The data acquisition equipment and battery pack of the Smartmag weigh about 99 kilograms (45 pounds), imposing some fitness requirement on the operator. Although the man-portable system can access wooded areas easily, GPS signals were often lost due to tree cover. As a result, the heavily wooded areas of the 16A-hectare area were not surveyed.

Several delays resulted from equipment difficulties during the demonstration. The GPS took longer than expected to set up the first day, and the cables for one of the roving GPS units operated intermittently. Recurring difficulties in maintaining GPS satellite signals or "lock" in heavily wooded areas also delayed the survey considerably. Generally, four to eight satellites were available. When the operator entered a heavily wooded area, the cover interfered with the satellite signal. The GPS unit would not function unless five satellites were available. Once the satellite lock was lost, the operator stopped the magnetometer and waited until the lock was reestablished.

One of the two magnetometer data recorders had extended memory that lasted for 8 hours. However, the other data recorder had only standard memory configuration, which filled up in 2 hours and required downloading several times daily. Each download of this data recorder took about 40 minutes, and as a result, the system was not functional much of the time. The two Scintrex personnel operating the magnetometers had difficulty managing the operation, navigation, and data downloading with the intermittent support provided. It is likely that more of the area could have been covered with additional personnel and equipment.



### 5.1.5.3 Measured Performance

Scintrex was scored on 5.76 hectares (14.23 acres) of the 16A-hectare area (35.6 percent), which it covered in the allotted 40 hours. Although Scintrex covered slightly less area than it was scored on, grid cells that were covered 50 percent or more were included. Scintrex reported 255 targets within the 16A-hectare area with the fence line area removed (see Figure 5.1.5-2) (Scintrex 1995b).

Scintrex's performance is shown in Table 5.1.5-1, which presents the following: (1) detection, (2) localization, and (3) classification statistics with respect to type, size, and class. The baseline for computing performance included both ordnance and nonordnance items. The detection ratio of 0.50 (cited as  $P_D$  ordnance in Table 5.1.5-1) reflects the number of targets detected by Scintrex compared to the total number of baseline ordnance targets in the area covered within the 16 hectares. This detection probability is significantly different than the probability of detection arising from random declarations due to sensor noise and other factors ( $P_{\text{random}} = 0.06$ ). Scintrex had a FAR of 45.3 per hectare.

Scintrex's  $P_D$  of 0.50 fell in the lower half of the results for magnetometer systems. These results may be in part because of difficulties in the field in maintaining adequate GPS lock as well as the inexperience of one of the two equipment operators. Scintrex also had the second highest FAR of the magnetometer demonstrators.

For most demonstrators, the probability of ordnance detection depends on both the size and the depth of the buried ordnance item. Figure 5.1.5-3 presents a scatter plot showing detection performance as a function of size versus depth for Scintrex. Although Scintrex was able to detect several large targets, small and medium targets were difficult for Scintrex to detect.

The localization error statistics section of Table 5.1.5-1 indicates Scintrex's ability to estimate the location of the targets declared. Scintrex reported target depths between 0.13 and 4.76 meters (0.43 and 15.62 feet) below ground surface. Scintrex provided type, size, and class information as shown in Table 5.1.5-1.

**Figure 5.1.5-2**  
**Scintrex Target Declarations**

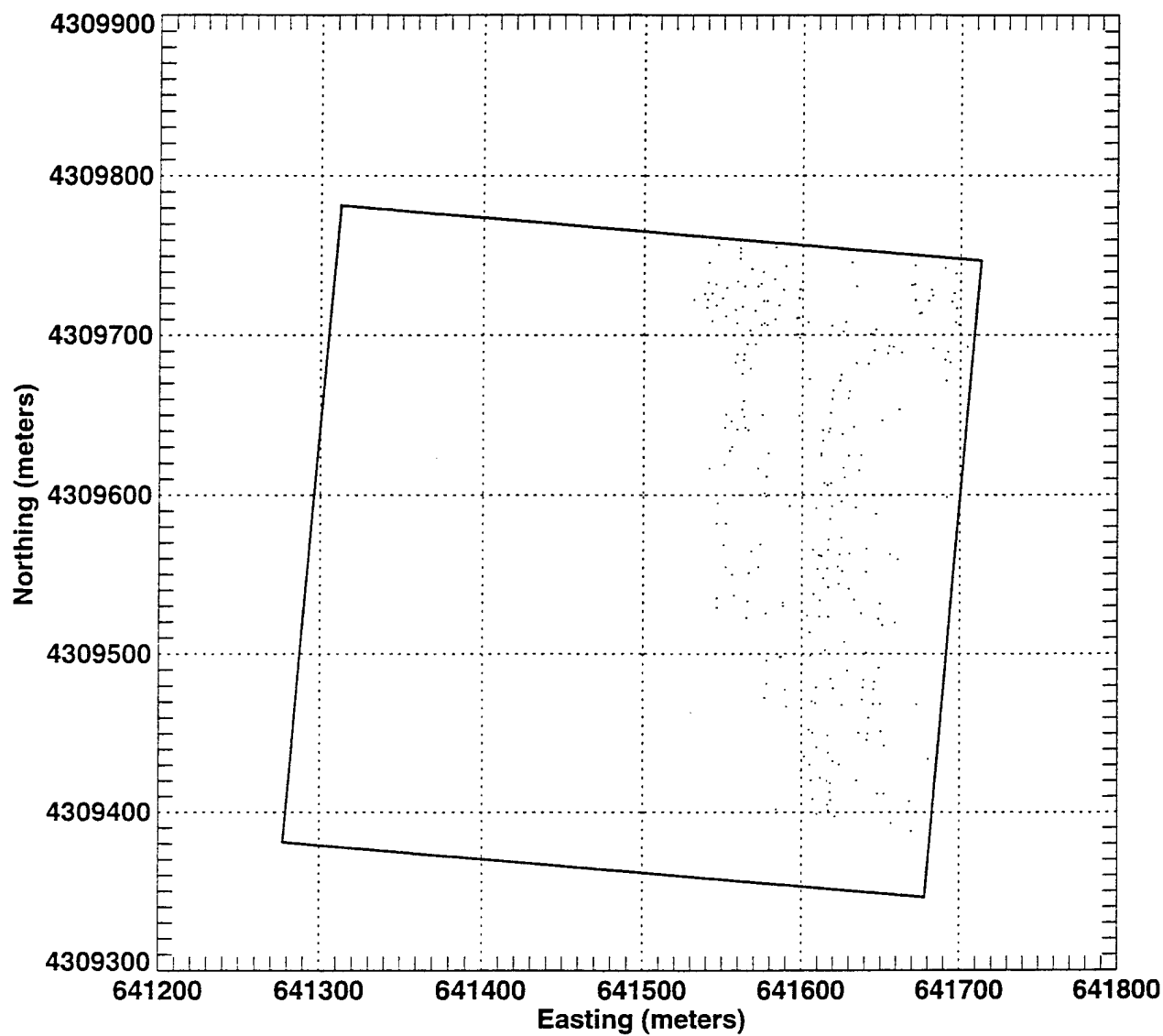


**TABLE 5.1.5-1  
PERFORMANCE STATISTICS FOR SCINTREX**

**Detection Statistics**

	Number Baseline	Number Matched	$P_D^a$
Ordnance	46	23	0.50
Nonordnance	23	12	0.52
Total	69	35	0.51
$P_{random}$	0.06		
Number False Alarms	232		
False Alarm Rate	45.3/hectare		
False Alarm Ratio	10.1		
Probability False Alarms	0.0569		

**Localization Statistics**

	Mean (m) <sup>b</sup>	Std. Dev. <sup>c</sup> (m)
Position (x,y)		
dx	-0.18	0.74
dy	0.47	0.65
Radial	0.94	
Depth (z)		
$dz^d$	0.39	0.79
dz	0.87	

**Identification and Classification Statistics**

	Number Baseline	Number Detected	$P_D^e$	Number Correct	$P_C^f$
Type					
Ordnance	58	21	0.36	20	0.95
Nonordnance	38	16	0.42	0	0.0
Size					
Large	18	8	0.44	4	0.5
Medium	19	9	0.47	9	1.00
Small	21	4	0.19	1	0.25
Class					
Bomb	14	8	0.57	6	0.75
Projectile	25	10	0.40	4	0.40
Mortar	16	3	0.19	1	0.33
Cluster	3	0	0	0	NA <sup>g</sup>

Notes:

- <sup>a</sup> Probability of detection (based on Group TMA, fence area excluded)
- <sup>b</sup> Meter
- <sup>c</sup> Standard deviation
- <sup>d</sup> Square root of the mean square depth error
- <sup>e</sup> Probability of detection (based on closest TMA, fence area excluded)
- <sup>f</sup> Probability of correctly classifying (based on closest TMA)
- <sup>g</sup> Not applicable



## 5.1.6 Vallon GmbH

Vallon GmbH (Vallon), in cooperation with Security Search Products and Sales, demonstrated from July 12 through 17, 1995, at the 16B-hectare area at JPG. Vallon also participated in Phase I of the UXO ATD program.

### 5.1.6.1 Technology Description

Vallon used three magnetometer systems during the demonstration: a vehicle-towed system and two separate man-portable systems. The vehicle-towed system used by Vallon was the MSV-5 multisensor vehicle (see Figure 5.1.6-1). This system uses an ATV to tow a sensor platform with an array of five magnetometers (EL1302A1 ferrous locators) spaced 0.5 meter (1.6 feet) apart. Vallon describes the EL1302A1 as a high sensitivity differential magnetometer used to detect iron. Each sensor is connected to a separate

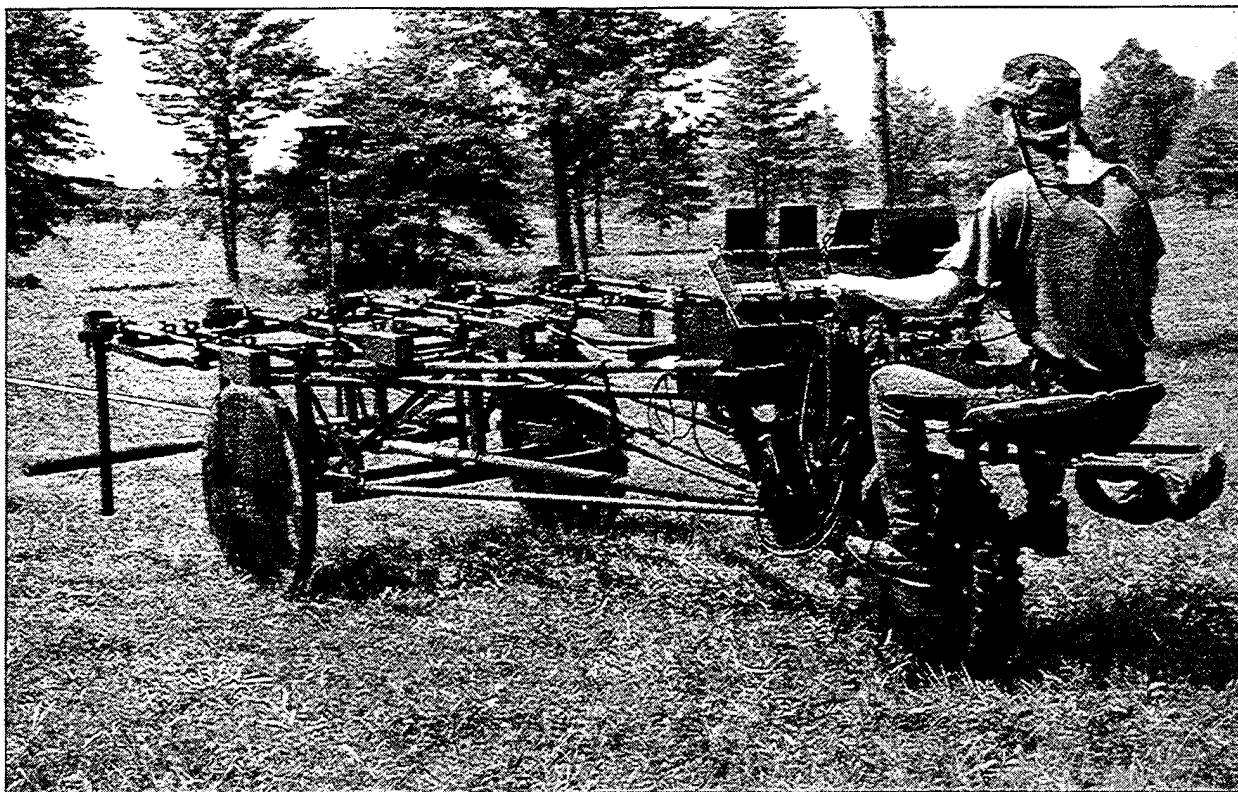


Figure 5.1.6-1 Vallon GmbH Multisensor Vehicle

microcomputer (MC1) for data acquisition. The MSV-5 is ridden by an operator, who keeps the unit on course while the unit is towed by the ATV. A differential GPS provides navigation and GPS tagging for detected targets with accuracy of less than 1 meter (3 feet). To provide accurate direction and distance control, the MSV-5 operator uses a radio link to the GPS navigation system. The MSV-5 is intended to provide accurate positional information with continuous recording.

The second system used by Vallon is called the man-portable detection system (MANPODS). This system consists of a single sensor magnetometer, an operator backpack containing a data acquisition microcomputer (MC1), and a differential GPS for accurate position information. Vallon used two MANPODS at JPG; each were used in inaccessible areas where the MSV-5 could not be used.

The third system used by Vallon was its man-portable sensor positioning system (SEPOS) (see Figure 5.1.6-2). This system is identical to the MANPODS, except that GPS was not employed. In instances when MANPODS could not receive satellite signals, Vallon marked the starting positions with GPS and then used survey tapes to conduct the survey. The SEPOS survey tapes were placed manually. The SEPOS lines were



Figure 5.1.6-2 Vallon Man-Portable Sensor Positioning System

100 meters (328 feet) long and were marked at each meter with a marker detector. Each marker was recorded by the MC1. Vallon used the grid system for navigation with the SEPOS. Vallon walked north to south lines within the grid cells using survey tapes to mark its location and coverage.

The GPS included a base receiver, which was positioned on a known benchmark in the field, one differential receiver on the MSV-5, one receiver on each MANPODS, and two radio repeaters for the differential radio link. As described above, the SEPOS did not use GPS except to mark the starting position for the survey. Vallon developed an algorithm to receive data from the MC1 units and to analyze and process this data to produce target lists and field maps (Vallon 1995a).

Vallon indicated the following improvements from Phase I: (1) use of differential GPS for navigation and GPS tagging of detected targets, (2) a radio link between the driver of the ATV and the GPS navigation for direction and distance control, (3) balancing of the MSV-5 for control over rugged terrain, and (4) increased storage capabilities for the MC1 (Vallon 1995a).

#### **5.1.6.2 System Assessment**

This section summarizes the demonstration by Vallon, based on observations made in the field.

#### **Requirements for Technology Implementation**

Vallon used nine people to complete its demonstration. Two people operated the MSV-5; one person drove the ATV, while the other person steered and operated the system sensors from behind. Six people operated either the MANPODS or the SEPOS, alternating personnel to provide rest periods. The remaining person supervised the operation.

Vallon's sensors and GPS equipment were shipped to JPG. Vallon purchased an ATV locally for use with the MSV-5. Vallon rented a large truck to transport the ATV, MSV-5, and MANPODS equipment. Two minivans were rented to transport personnel and equipment to and from the site. Additional equipment required included a laptop PC for data analysis, four radios for communication in the field, and survey stakes and tapes for marking location in the field. Replacement bolts, wooden support brackets, batteries, and a flat

tire inflator and sealer were purchased locally for repairs to the MSV-5 and ATV. Vallon required an electrical supply to recharge batteries; this was provided at the support trailer.

### **Operational Capabilities and Limitations**

The MSV-5 and GPS can cover about 0.6 to 0.8 hectare (1.5 to 2 acres) per hour depending on the terrain. The data recording for this system is continuous, which prevented data downloading delays. However, poor satellite conditions caused some delays, and the MSV-5 experienced numerous delays due to equipment failure. The ATV that towed the MSV-5 had a flat tire, as well as recurring engine problems. Two bolts also sheared off the MSV-5 during the demonstration and had to be replaced. The MSV-5 is designed for areas that are generally clear of high foliage and large obstacles (such as trees). As a result, the MSV-5 had difficulty operating in areas of uneven terrain and maneuvering the turnarounds (particularly at the beginning of the survey).

Both the MANPODS and the SEPOS operated independently of the MSV-5. The MANPODS were not used to the degree anticipated because Vallon was unable to maintain GPS signals due to the tree cover. Instead, Vallon used the SEPOS (which was used during Phase I) in an effort to increase its coverage. Both the MANPODS and then the SEPOS were used simultaneously with the MSV-5.

All three of the magnetometer systems used by Vallon employed the same sensor and data analysis techniques. The major differences between the systems were with the sensor configuration and the navigation and target locating subsystems.

#### **5.1.6.3 Measured Performance**

Vallon was scored on 8.83 hectares (21.81 acres) of the 16B-hectare area (52.6 percent) for the combined systems during the allotted 40 hours. Although Vallon covered slightly more area than it was scored on, only grid cells covered 50 percent or more were included in the scoring. Vallon provided results for both the GPS and the SEPOS, the data from these two systems were combined for this data analysis. Vallon reported a total of 1,903 targets with the GPS and SEPOS within the 8.83 hectares it was scored on, once the fence line area was removed (see Figure 5.1.6-3) (Vallon 1995b).



Vallon's performance is shown in Table 5.1.6-1, which presents the following: (1) detection, (2) localization, and (3) classification statistics with respect to type, size, and class. The baseline for computing detection performance included both ordnance and nonordnance items. The detection ratio of 0.57 (cited as  $P_D$  ordnance in Table 5.1.6-1) reflects the number of targets detected by Vallon as compared to the total number of baseline ordnance targets in the area covered. The probability of detection arising from random declarations due to sensor noise and other factors was 0.25 ( $P_{\text{random}}$ ) for Vallon, the highest of all demonstrators. Vallon had a FAR of 225.9 per hectare, also the highest of all the demonstrators.

As part of Phase I, Vallon had a  $P_D$  of 0.72 for ordnance items. The FAR was 149 per hectare. A comparison of Phase I and Phase II detection performance shows that Vallon obtained a lower  $P_D$  value for Phase II detection performance data, 0.57 compared to 0.72 for Phase I. Correspondingly, Vallon's FAR also increased, from 149 to 225.9.

For most demonstrators, the probability of ordnance detection depends on both the size and depth of the buried ordnance item. Figure 5.1.6-4, which is a scatter plot showing detection performance as a function of size versus depth, illustrates this relationship for Vallon. Vallon was somewhat successful at detecting targets of all sizes at various depths.

The localization error statistics section in Table 5.1.6-1 indicates Vallon's ability to estimate the locations of the targets declared. Vallon reported target depths between 0 and 6.27 meters (0 and 20.57 feet) below ground surface. Vallon did not provide ordnance type information, declaring all target detections as "unknown." Vallon did provide size and class information.

**Figure 5.1.6-3**  
**Vallon Target Declarations**

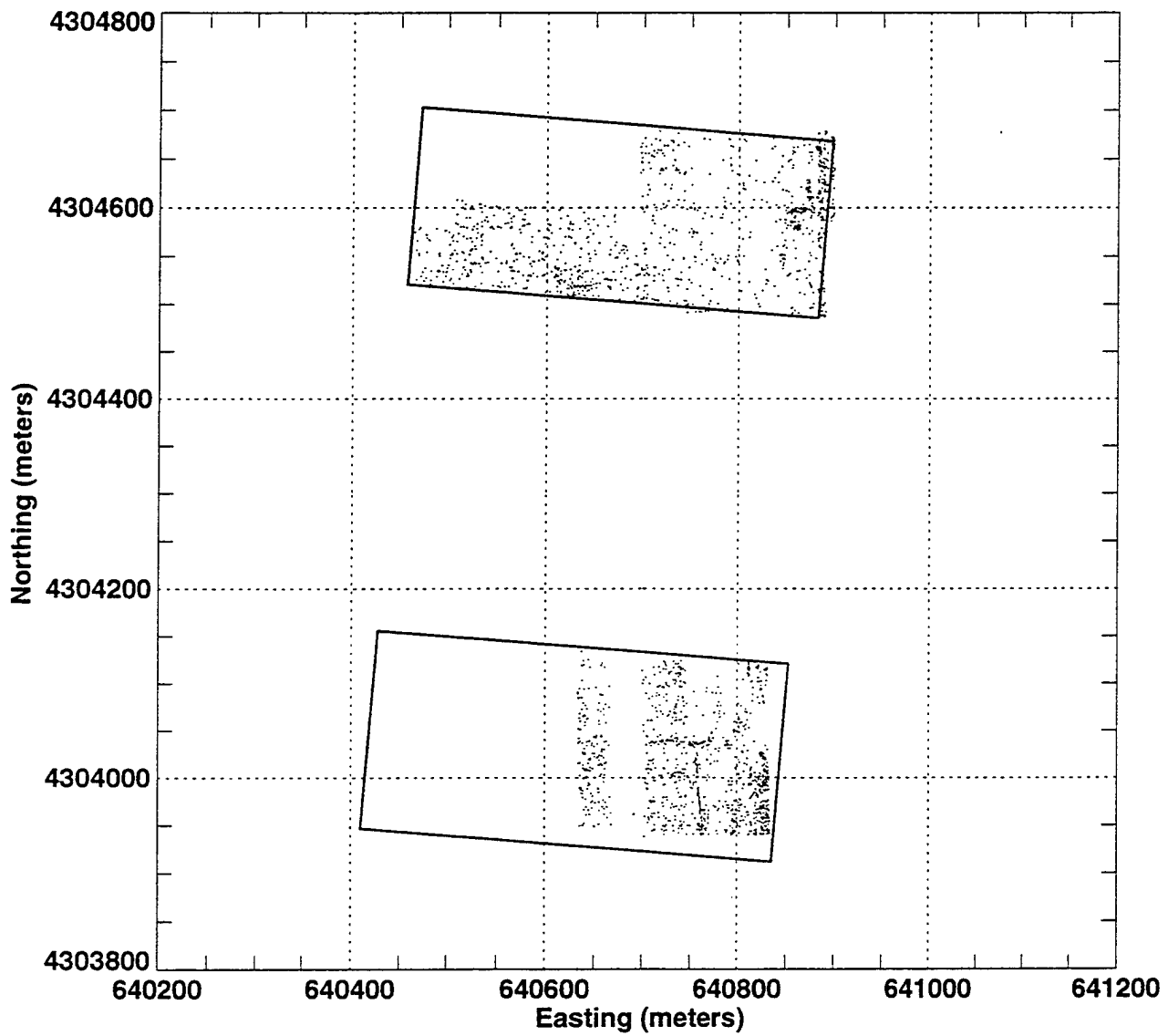


**TABLE 5.1.6-1  
PERFORMANCE STATISTICS FOR VALLON**

**Detection Statistics**

	Number Baseline	Number Matched	$P_D^a$
Ordnance	47	27	0.57
Nonordnance	5	1	0.20
Total	52	28	0.54
$P_{random}$	0.25		
Number False Alarms	1,849		
False Alarm Rate	225.9/hectare		
False Alarm Ratio	68.5		
Probability False Alarms	0.2838		

**Localization Statistics**

	Mean (m) <sup>b</sup>	Std. Dev. <sup>c</sup> (m)
Position (x,y)		
dx	-0.01	0.59
dy	0.13	0.78
Radial	0.83	
Depth (z)		
$dz^d$	0.02	0.99
dz	0.98	

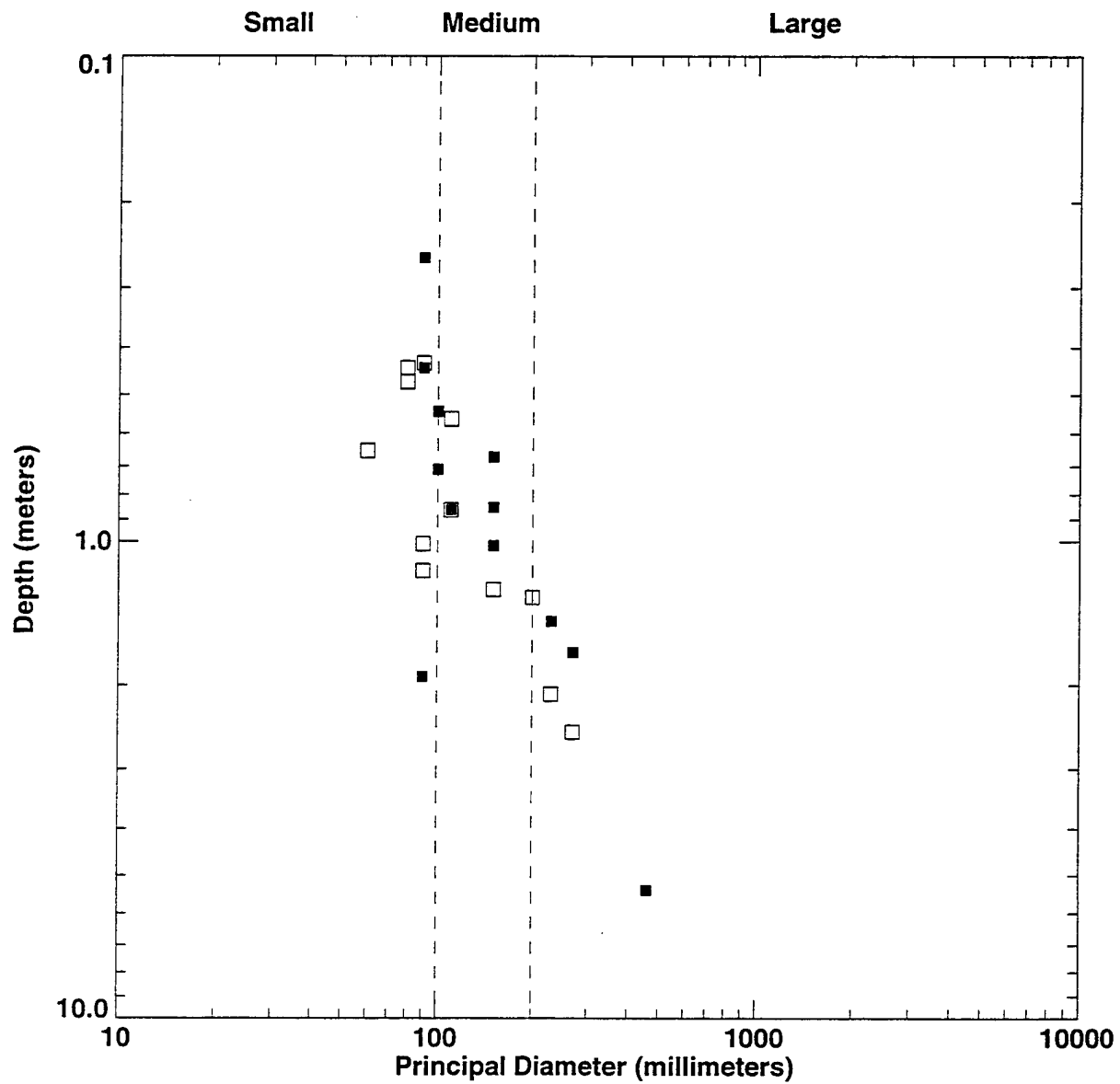
**Identification and Classification Statistics**

	Number Baseline	Number Detected	$P_D^e$	Number Correct	$P_C^f$
Type					
Ordnance	65	31	0.48	0	0
Nonordnance	7	1	0.14	0	0
Size					
Large	11	6	0.55	1	0.17
Medium	14	8	0.57	7	0.88
Small	38	16	0.42	6	0.38
Class					
Bomb	5	3	0.60	1	0.33
Projectile	31	16	0.52	0	0
Mortar	25	9	0.36	0	0
Cluster	4	3	0.75	0	0

**Notes:**

- <sup>a</sup> Probability of detection (based on Group TMA, fence area excluded)
- <sup>b</sup> Meter
- <sup>c</sup> Standard deviation
- <sup>d</sup> Square root of the mean square depth error
- <sup>e</sup> Probability of detection (based on closest TMA, fence area excluded)
- <sup>f</sup> Probability of correctly classifying (based on closest TMA)

Figure 5.1.6-4  
Vallon Detection Ability



- Target Detected
- Target Not Detected

## 5.2 ELECTROMAGNETIC INDUCTION SENSOR SYSTEMS

### 5.2.1 Bristol Aerospace Ltd.

Bristol Aerospace Ltd. (Bristol), demonstrated from June 14 through 18, 1995, at the 16A-hectare area at JPG.

#### 5.2.1.1 Technology Description

Bristol used a remotely operated ATV that towed a pulse induction sensor array (see Figure 5.2.1-1). Bristol describes the sensor platform as able to detect electromagnetic signatures. The sensor uses pulse induction coils to detect the presence of conductive metallic objects. Data are transmitted to a remote-control command station for recording and analysis. At the command station, the sensor data is plotted on a map of the area being scanned using color intensity to show signal strength. A differential GPS receiver mounted

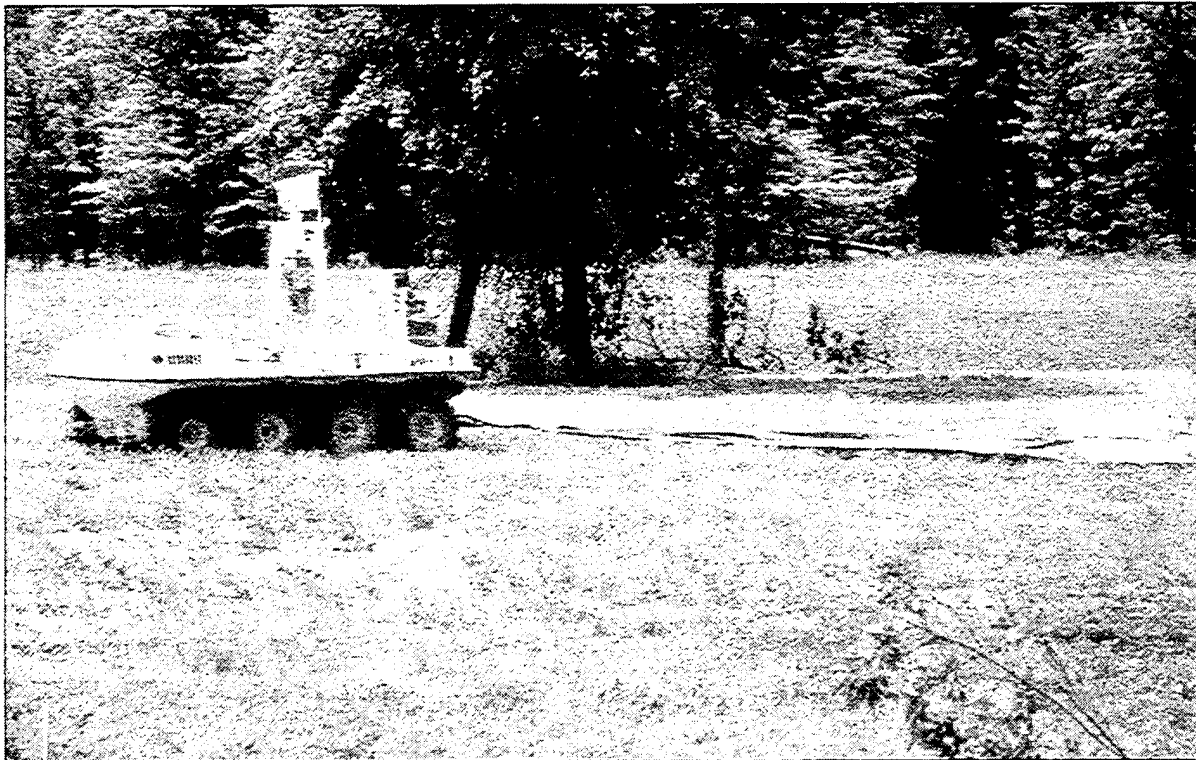


Figure 5.2.1-1 Bristol Aerospace Ltd., Pulse Induction Sensor Array

on the vehicle provides a continuous readout of the location of the vehicle. Bristol stated in its proposal that the vehicle location provided by the GPS is accurate to plus or minus 1 meter (3.3 feet).

When a detection is made by the sensor platform, the system automatically marks the position provided by GPS and alerts the operator in the command station. The electromagnetic signature of the object is displayed on the command station monitor, and the location in universal transverse mercator (UTM) coordinates and detection time are automatically recorded. A video camera is mounted on the vehicle with a pan and tilt mechanism; the video signal is sent back to the operator's monitor in the command station. The vehicle is controlled autonomously via GPS in open terrain, but requires operator guidance around obstacles; guidance is provided via joystick controls and a television monitor.

The towed sensor platform contains two sensor coils; each coil is 2-meters (6.6-feet) wide. A towing "carpet" attaches the platform to the ATV and carries the necessary cables and hoses to the system controller. The detector system automatically unhitches from the ATV if the towed sensor platform becomes obstructed.

The Bristol system functions by electromagnetic pulses from the transmitter coils that generate eddy currents in the buried metal; these currents in turn produce a magnetic field around the object. When the decay of the magnetic field is detected, it induces a voltage in the receiver coils. The received voltage results in a signal that is sent to the operator console for processing. The detector coils create a zone of sensitivity such that any metallic object that passes within its influence is detected (Bristol 1995a).

#### **5.2.1.2 System Assessment**

This section summarizes the demonstration by Bristol, based on observations made in the field.

#### **Requirements for Technology Implementation**

Bristol used five people to complete its demonstration. One to two people observed the progress of the sensor platform. The remaining personnel, located in the command station, remotely operated the system and monitored and recorded its progress.

Bristol shipped the majority of its equipment to JPG from Canada. A flatbed trailer was used to transport the Bristol system including all the spare parts and supplies required for operation and maintenance. This equipment included a command station that contained all computer equipment and monitors; a smaller trailer that contained two gasoline-powered generators serving as electrical supply; and the sensor platform, including the ATV used for towing the system. Locally rented equipment included an additional ATV used to transport personnel around the perimeter of the site as well as a crane, which was used to move the control station on and off the site. Additional equipment, acquired locally, included miscellaneous hardware needed to replace the broken hitch connecting the array to the vehicle.

### **Operational Capabilities and Limitations**

Bristol's ATV can move at a rate of about 10 kilometers per hour (6 miles per hour). The system covered the open areas autonomously, while the operator remotely guided the ATV around obstacles. The system performs best in open terrain, due both to the nature of the remote-controlled system for guidance around obstacles and the size of the sensor platform. The wide turning radius of the vehicle limits maneuverability around trees and in making turns at the end of a swath line. The 2- to 4-meter- (6.6- to 13-foot-) wide sensor platform is unable to access densely wooded areas because it cannot fit between closely spaced trees. In addition, uneven terrain and ground cover caused the detector system to unhitch from the ATV. The system experienced minor delays until the detector system was reattached to the vehicle; however, the detachable configuration prevented damage to the sensor platform from brush or trees.

Numerous delays occurred as a result of equipment failures. Mechanical problems included sensor failure, a broken bolt on the hitch, cable connection failures, a burned-out electrical switch, hydraulic system in-line filter replacement, and steering control failure. Despite about 11 hours of downtime resulting from mechanical problems, Bristol surveyed most of the acreage thoroughly. To increase coverage around trees, the survey was performed in both north-to-south and east-to-west directions.

#### **5.2.1.3 Measured Performance**

Bristol was scored on 13.58 hectares (33.56 acres) of the 16A-hectare area (83.9 percent) covered with its ATV-towed system during the allotted 40 hours. Although Bristol covered slightly more area than it was scored on, only grid cells covered 50 percent or more were included. Figure 5.2.1-2 shows Bristol's target

declarations at the 16A-hectare area (Bristol 1995b). Bristol reported a total of 566 targets with the sensor platform within the 13.58 hectares (33.56 acres), with the fence line area removed. Bristol's performance is shown in Table 5.2.1-1, which presents detection and localization statistics. Bristol did not provide type, size, or class information so classification statistics were not computed.

The baseline for computing detection performance included both ordnance and nonordnance items. The detection ratio of 0.62 ( $P_D$  ordnance) reflects the number of targets detected by Bristol as compared to the total number of baseline ordnance targets in the area covered (Bristol 1995b). This detection probability is significantly different than the probability of detection arising from random declarations due to sensor noise and other factors ( $P_{\text{random}} = 0.05$ ). Bristol had a FAR of 38.2 per hectare.

For most demonstrators, the probability of ordnance detection depends on both the size and depth of the buried item. Figure 5.2.1-3 presents a scatter plot showing detection performance as a function of size versus depth that illustrates this relationship for Bristol. Bristol was successful at detecting some targets of all sizes at a variety of depths.

The localization error statistics section of Table 5.2.1-1 indicates Bristol's ability to estimate the location of the targets declared. Bristol reported all target depths at 0.10 meter (0.33 feet) below ground surface. Bristol did not provide type, size, or class information.



**Figure 5.2.1-2**  
**Bristol Target Declarations**

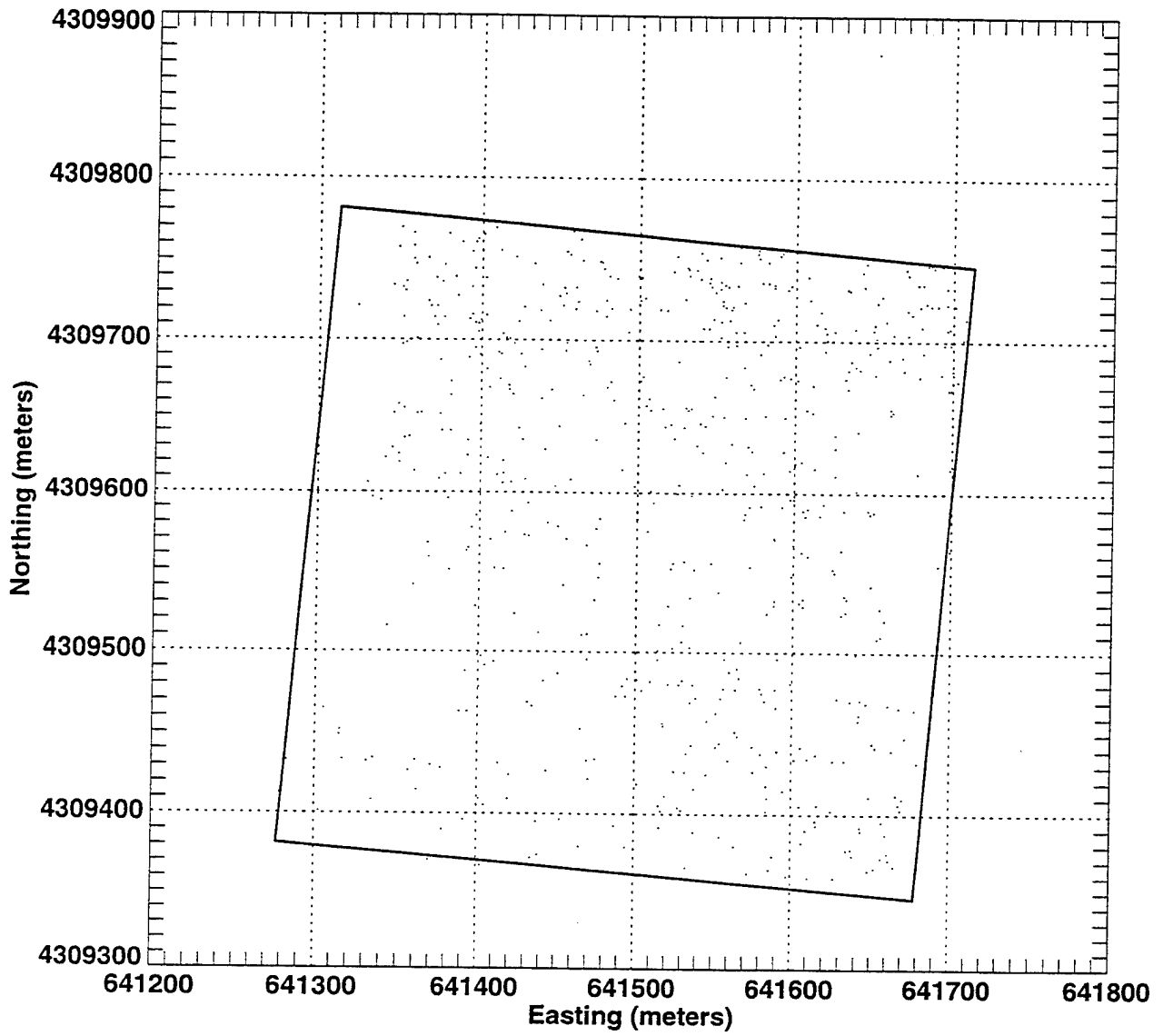


**TABLE 5.2.1-1  
PERFORMANCE STATISTICS FOR BRISTOL**

**Detection Statistics**

	Number Baseline	Number Matched	$P_D^a$
Ordnance	114	71	0.62
Nonordnance	33	19	0.58
Total	147	90	0.61
$P_{random}$	0.05		
Number False Alarms	495		
False Alarm Rate	38.2/hectare		
False Alarm Ratio	6.97		
Probability False Alarms	0.048		

**Localization Statistics**

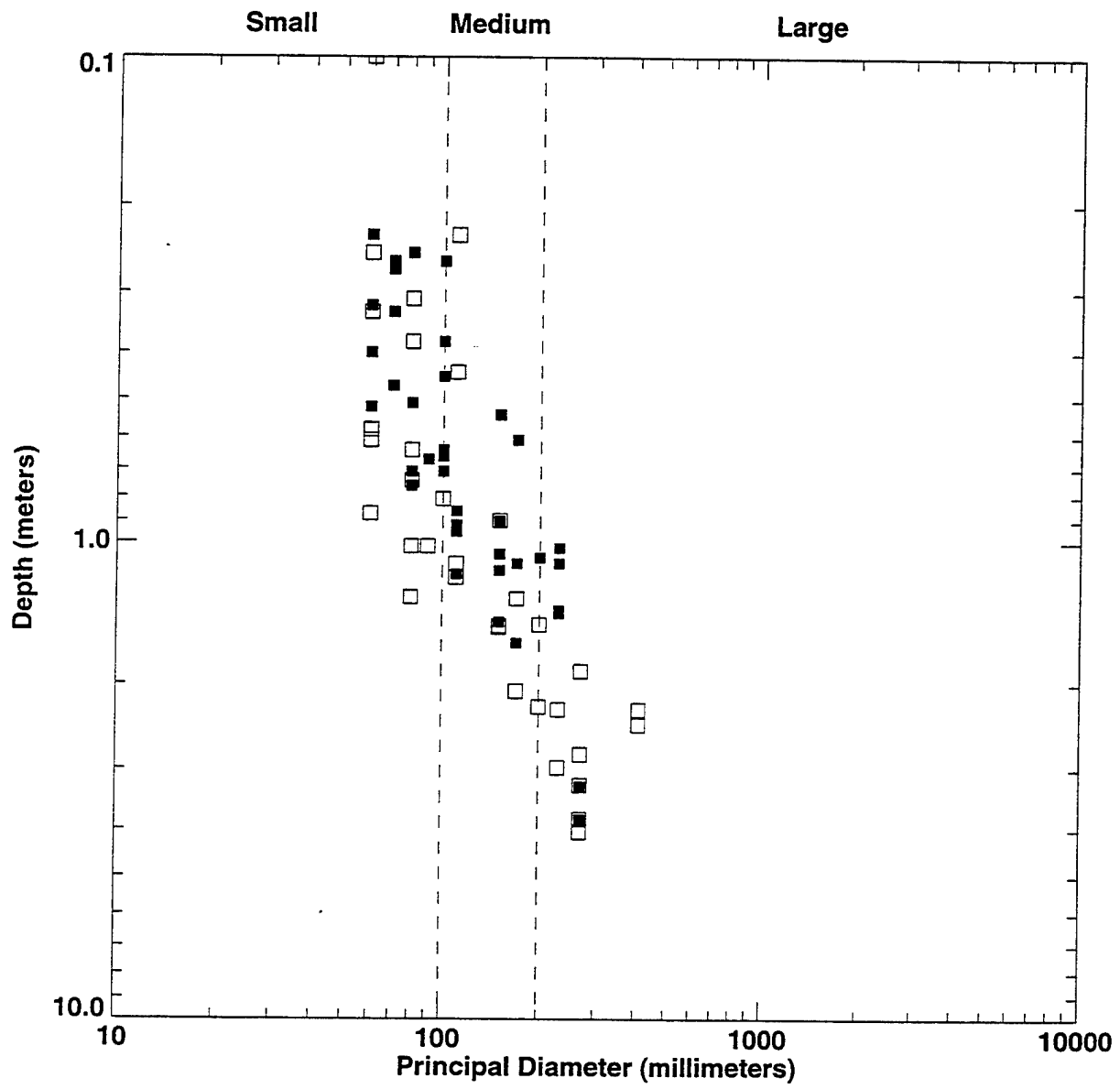
	Mean (m) <sup>b</sup>	Std. Dev. <sup>c</sup> (m)
Position (x,y)		
dx	-0.30	0.80
dy	0.10	0.80
Radial	1.04	
Depth (z)		
dz <sup>d</sup>	-0.66	0.72
dz	0.97	

**Identification and Classification Statistics**

	Number Baseline	Number Detected	$P_D^e$	Number Correct	$P_C^f$
Type					
Ordnance	141	64	0.45	0	0
Nonordnance	55	29	0.53	0	0
Size					
Large	30	13	0.43	0	0
Medium	50	25	0.50	0	0
Small	60	26	0.43	0	0
Class					
Bomb	20	8	0.40	0	0
Projectile	61	31	0.51	0	0
Mortar	52	21	0.40	0	0
Cluster	8	4	0.50	0	0

- Notes:
- <sup>a</sup> Probability of detection (based on Group TMA, fence area excluded)
  - <sup>b</sup> Meter
  - <sup>c</sup> Standard deviation
  - <sup>d</sup> Square root of the mean square depth error
  - <sup>e</sup> Probability of detection (based on closest TMA, fence area excluded)
  - <sup>f</sup> Probability of correctly classifying (based on closest TMA)

**Figure 5.2.1-3**  
**Bristol Detection Ability**



- Target Detected
- Target Not Detected

## 5.2.2 GeoPotential

GeoPotential demonstrated from August 23 through 27, 1995, at the 16A-hectare area at JPG.

### 5.2.2.1 Technology Description

GeoPotential used three electromagnetic induction systems (Aqua-Tronics A6 tracers) during the demonstration (see Figure 5.2.2-1). One electromagnetic system was equipped with a datalogger (OMNIDATA PRO 2000). Each electromagnetic system operates at 117 kilohertz (kHz) and contains both a transmitting antenna and a receiving antenna, which are separated by a 1.22-meter- (4.00-foot-) long handle. The system operates by transmitting an electromagnetic wave into the ground. Conductive objects in the subsurface cause changes in the wave, which then show up as a voltage variation in the receiver. The power output varies from 17 to 270 volts.

The electromagnetic system can be used in search mode, mapping mode, or a combination of the two. Search mode uses audio and visual outputs to map the location of subsurface objects in real time. The



Figure 5.2.2-1 GeoPotential Electromagnetic Induction Instrument

operator then marks the location with paint or stakes, and the coordinates are determined later. The electromagnetic system mapping mode uses the A6 tracer and datalogger to acquire and record electromagnetic measurements used to generate profiles and contour maps. Data are acquired along profiles at 1.5-second intervals when recorded by the datalogger. Profile data are then downloaded from the datalogger to a portable computer where they are edited, gridded, and contoured to produce an electromagnetic profile and contour maps. Data are interpreted to determine the nature of a buried object. The combined search and mapping modes consist of using the search mode to initially locate objects then lay out profiles over the object. The mapping mode is then used to record electromagnetic data from the object for quantitative analysis (GeoPotential 1995a).

#### **5.2.2.2 System Assessment**

This section summarizes the demonstration by GeoPotential, based on observations made in the field.

#### **Requirements for Technology Implementation**

GeoPotential used six people to complete its demonstration. The three electromagnetic systems were operated by three one-person teams. A two-person team measured the locations of the anomalies or items located by each electromagnetic system. The remaining individual analyzed the data and produced the contour maps. All system equipment used for this demonstration was driven to JPG by GeoPotential personnel. Support equipment required to perform the geophysical survey included a laptop computer and printer used to analyze data and produce contour maps. GeoPotential had additional batteries for its survey equipment and did not require on-site recharging of batteries. Data analysis was performed on a GeoPotential work station temporarily set up in the on-site support trailer. Navigation equipment used by GeoPotential included an optical transit, a stadia rod, a measuring wheel, and flagging material.

#### **Operational Capabilities and Limitations**

The electromagnetic system required very little setup or takedown time. The system was operational within 15 minutes, and about the same amount of time was needed to store equipment at the end of each day. GeoPotential reported that its system is limited by weather, such as electrical storms, which would disrupt readings, and extremely cold weather, which would drain batteries.

The GeoPotential proposal stated that it intended to use the electromagnetic system in mapping mode to generate electromagnetic contour maps. However, when GeoPotential began processing data, the field data indicated that ambient electromagnetic noise caused drifting and level shifts in the electromagnetic data. The noise degraded the resulting electromagnetic contour maps, and GeoPotential decided that the combination mode would be more effective. As a result, two of the three systems were used in combination mode to survey the area.

Navigation across the grid was completed using the grid coordinate system on the 16A-hectare area and was aided by spray paint dashes made by Geophex Ltd., (which demonstrated during the same time period) at 1.5-meter (5-foot) intervals in an east-west direction. Surveying was completed in east-west fashion. Line-of-sight traverses were made between flags during data acquisition. All objects located were surveyed to the nearest grid stake with a compass on a stadia rod and a tape line. Without the preexisting grid system at the 16A-hectare area, GeoPotential would have needed to set up its own grid system to track its coverage and measure the location of the detected anomalies.

#### **5.2.2.3 Measured Performance**

GeoPotential covered 13.60 hectares (33.61 acres) of the 16A-hectare area (84.0 percent) with the electromagnetic systems in about 38.5 hours (of 40 hours allotted). Two electromagnetic systems covered about 74 percent of this covered area using the combination mode. The electromagnetic system with the datalogger covered the remaining 26 percent of the covered area in the mapping mode; however, the resulting contour maps were deemed unacceptable for data interpretation and were not submitted for scoring.

GeoPotential resurveyed about 1.3 hectares (3.2 acres) of the area as part of its quality assurance program. Areas previous covered with the datalogger system were resurveyed, and the datalogger system was used to profile the anomalies detected by the other two systems. In this way, GeoPotential was able to compare data and contour maps (GeoPotential 1995b).

GeoPotential reported 168 targets within the 13.60 hectares that it was scored on (see Figure 5.2.2-2). Only grid cells that were covered 50 percent or more were scored. GeoPotential's performance with the electromagnetic system is shown in Table 5.2.2-1, which presents the following: (1) detection, (2) localization, and (3) classification statistics with respect to type, size, and class.

The baseline for computing detection performance included both ordnance and nonordnance items. The detection ratio of 0.11 (cited as  $P_D$  ordnance in Table 5.2.2-1) reflects the number of targets detected by GeoPotential as compared to the total number of baseline ordnance targets in the area they covered. GeoPotential's probability of detection based on only random declarations ( $P_{\text{random}}$ ) is 0.02. GeoPotential had a FAR of 12.0 per hectare. Of the three EM sensors demonstrated, GeoPotential had the lowest  $P_D$  and FAR.

For most demonstrators, the probability of ordnance detection depends on both the size and depth of the buried ordnance item. Figure 5.2.2-3 presents a scatter plot showing detection performance as a function of size versus depth that illustrates this relationship for GeoPotential. This figure shows no clear demarcation for detection as a function of size and depth. All targets were difficult for GeoPotential to detect. The localization error statistics section of Table 5.2.2-1 indicates GeoPotential's ability to estimate the location of the targets declared. GeoPotential reported target depths between 0.01 and 3.50 meters (0.03 and 11.48 feet) below ground surface. Table 5.2.2-1 also indicates GeoPotential's type, size, and class capabilities, all of which were provided.

**Figure 5.2.2-2**  
**GeoPotential Target Declarations**

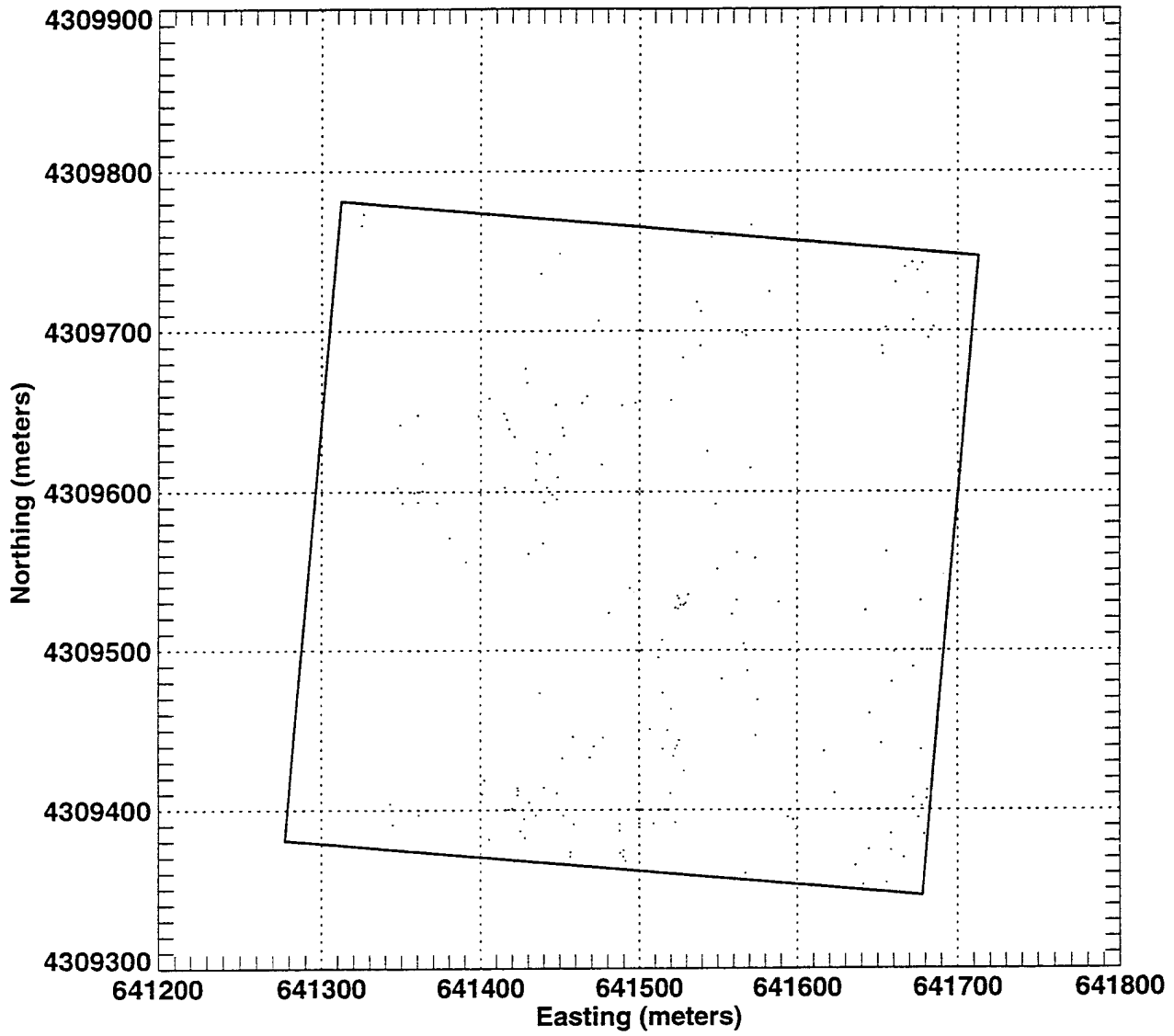




**TABLE 5.2.2-1  
PERFORMANCE STATISTICS FOR GEOPOTENTIAL**

**Detection Statistics**

	Number Baseline	Number Matched	$P_D^a$
Ordnance	113	12	0.11
Nonordnance	29	3	0.10
Total	142	15	0.11
$P_{random}$	0.02		
Number False Alarms	156		
False Alarm Rate	12.0/hectare		
False Alarm Ratio	13.0		
Probability False Alarms	0.0151		

**Localization Statistics**

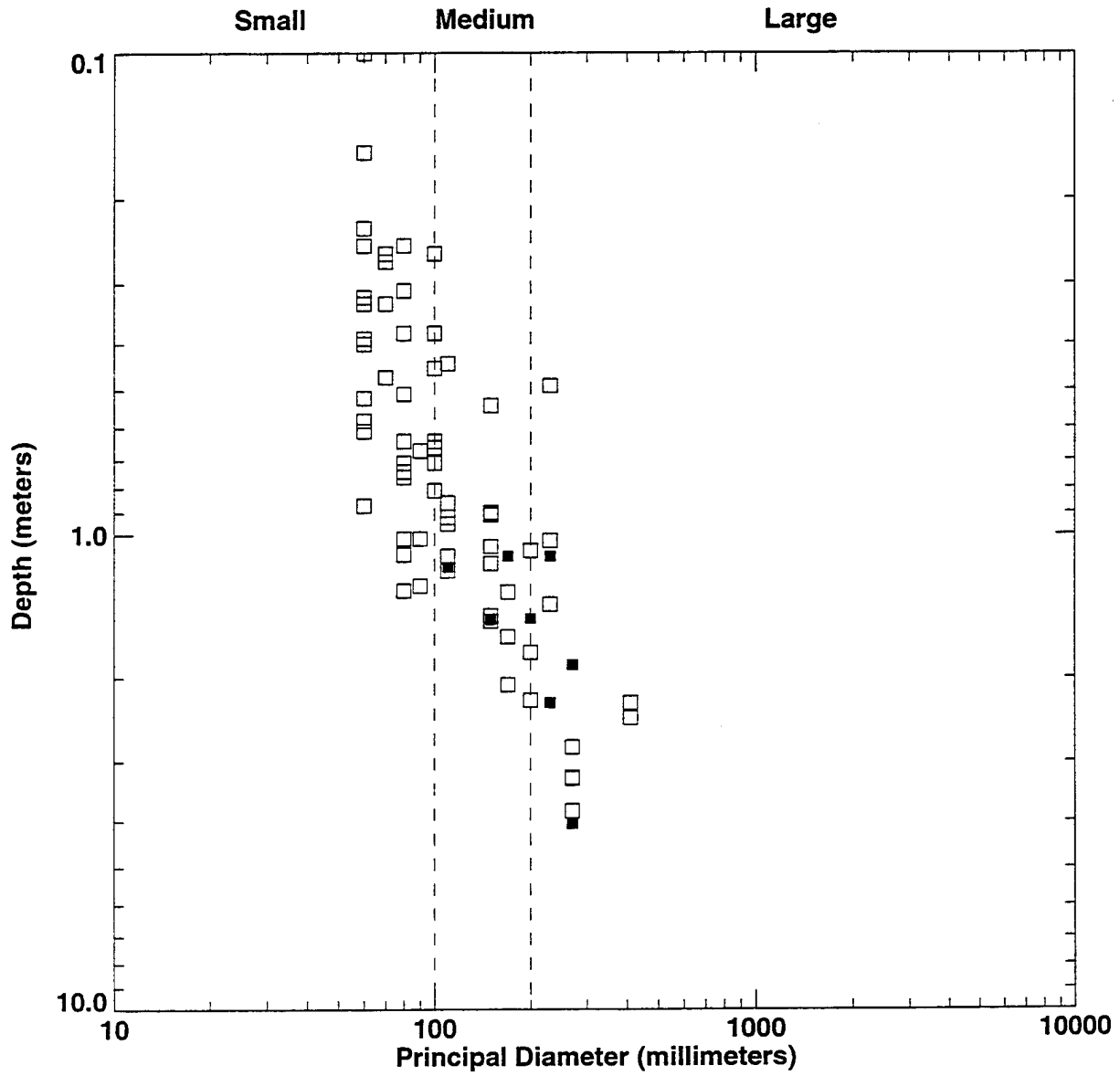
	Mean (m) <sup>b</sup>	Std. Dev. <sup>c</sup> (m)
Position (x,y)		
dx	0.44	0.99
dy	-0.37	0.86
Radial	1.30	
Depth (z)		
$dz^d$	-0.38	0.73
dz	0.80	

**Identification and Classification Statistics**

	Number Baseline	Number Detected	$P_D^e$	Number Correct	$P_C^f$
Type					
Ordnance	142	12	0.08	12	1.00
Nonordnance	50	3	0.06	0	0
Size					
Large	29	5	0.17	0	0
Medium	49	4	0.08	2	0.50
Small	63	3	0.05	1	0.33
Class					
Bomb	16	4	0.25	2	0.50
Projectile	63	5	0.08	3	0.60
Mortar	54	3	0.06	1	0.33
Cluster	9	0	0	0	NA <sup>g</sup>

- Notes:
- <sup>a</sup> Probability of detection (based on Group TMA, fence area excluded)
  - <sup>b</sup> Meter
  - <sup>c</sup> Standard deviation
  - <sup>d</sup> Square root of the mean square depth error
  - <sup>e</sup> Probability of detection (based on closest TMA, fence area excluded)
  - <sup>f</sup> Probability of correctly classifying (based on closest TMA)
  - <sup>g</sup> Not applicable

Figure 5.2.2-3  
GeoPotential Detection Ability



- Target Detected
- Target Not Detected

### 5.2.3 Parsons Engineering Science, Inc.

Parsons Engineering Science, Inc. (Parsons), demonstrated from May 31 through June 4, 1995, at the 16A-hectare area at JPG.

#### 5.2.3.1 Technology Description

Parsons used an electromagnetic induction system with both field and laboratory components. The field components included Geonics EM-61 high sensitivity electromagnetic time-domain metal detectors (see Figure 5.2.3-1), associated dataloggers, and a laptop PC for review and storage of the survey data. The computer laboratory component for data analysis included Intergraph's MGE Grid Analyst.

Parsons used three EM-61 units to conduct a geophysical survey of the site. The EM-61 unit is an electromagnetic induction profiler. This type of instrument measures and records the conductivity of nearby



Figure 5.2.3-1 Parsons Engineering Science, Inc., EM-61 Electromagnetic Unit

materials. A sinusoidal waveform is emitted from the transmitter, causing eddy currents in the subsurface. The intensity of the eddy currents is a function of the ground conductivity and the conductivity of buried material. The eddy currents cause a time-varying secondary electromagnetic field that is measured at the receiver. The EM-61 unit differs from the frequency domain electromagnetic instrument in that no voltage component is included. Therefore, the entire signal measured results from the electromagnetic eddy current induced by the primary field. Parsons stated in its proposal that the EM-61 generates electromagnetic pulses at 150 times per second and records the measured electromagnetic field between each pulse. This configuration allows enough time for the response in the conductive earth to dissipate before measuring the prolonged response of the buried metal. Measurements recorded by the datalogger are transferred to the laptop PC for processing.

After Parsons collected the data at the site, this information was provided to their subcontractor, Sanford, Cohen, and Associates (SC & A) for data interpretation. SC & A performed data analysis using the Huntsville UXO Knowledgebase (UXO-KB) developed for the U.S. Army Corps of Engineers, Huntsville Division. The UXO-KB allows for variations of signal characteristics within a range of acceptable values and allows the range of acceptable values to change daily as more data are added to the system (Parsons 1995a).

#### **5.2.3.2 System Assessment**

This section summarizes the Parsons demonstration, based on observations made in the field.

#### **Requirements for Technology Implementation**

Parsons used eight people to complete its demonstration. The three EM-61 units were operated by two-person teams. On each team, one individual operated the datalogger and instrument, while the second individual was responsible for record keeping and navigation. One person was responsible for data analysis, which took place at the support trailer. The remaining individual served as the field supervisor.

All system equipment used for this demonstration was shipped or brought to JPG by Parsons. Support equipment used by Parsons included two laptop computers to store and process the data, two minivans to transport personnel and supplies, and a panel truck to store the assembled equipment in the field. Surveyor

tapes, pin flags, and string were used for navigation through the grid area. Pin flags were used to mark the beginning and end of a swath line, while the string was used to guide the teams along a straight path. The support trailer supplied electricity to recharge the Parsons system batteries.

### **Operational Capabilities and Limitations**

The EM-61 units used by Parsons required little maintenance beyond recharging the batteries. Parsons experienced no delays due to equipment failure. According to Parsons, its system is limited to a survey speed of 0.6 meter per second (2.0 feet per second). Heavy brush and heavily wooded areas can further slow the survey speed by decreasing maneuverability. Extremely rugged terrain may require the EM-61 antenna system to be carried using a shoulder harness, but this was not necessary at JPG. Such uneven or wooded terrain adversely affects the system by hampering the accurate location of corners and flag locations designating lanes. Parsons also indicated that the system is unable to operate in standing water greater than 15 centimeters (6 inches) deep without modification. Although some areas of standing water were present during the JPG demonstration, Parsons did not indicate that it made any modifications to accommodate these wet areas. Parsons stated that surface interferences such as wire fences can affect data quality within a 3- to 4-meter (10- to 13-foot) radius of the system (Parsons 1995b). Navigation across the grid was completed using the grid coordinate system on the 16A-hectare area.

#### **5.2.4.3 Measured Performance**

Parsons surveyed the entire 16A-hectare area with its EM-61 units in the allotted 40 hours. Parsons reported 602 targets within the 16A-hectare area, once the fence line area was removed (see Figure 5.2.3-2) (Parsons 1995b). Parsons' performance is shown in Table 5.2.3-1, which presents the following: (1) detection, (2) localization, and (3) classification statistics with respect to type, size, and class.

The baseline for computing detection performance included both ordnance and nonordnance items. The detection ratio of 0.85 (cited as  $P_D$  ordnance in Table 5.2.3-1) reflects the number of targets detected by Parsons compared to the total number of baseline ordnance targets in the 16 hectares. This detection probability is significantly different than the probability of detection arising from random declarations due to sensor noise and other factors ( $P_{\text{random}} = 0.05$ ). Parsons had a FAR of 32.5 per hectare.

Parsons had the highest  $P_D$  of all the systems demonstrated for Phase II. Parsons teamed with SC & A to perform the data processing which may, in part, account for their performance relative to the other systems demonstrated.

For most demonstrators, the probability of ordnance detection depends on both the size and depth of the buried ordnance item. Figure 5.2.3-3, which is a scatter plot showing detection performance as a function of size versus depth, illustrates this relationship for Parsons. Parsons was able to detect targets of all sizes and generally appeared to detect all but the deepest targets in each category.

The localization error statistics section of Table 5.2.3-1 indicates Parsons' ability to estimate the location of the targets declared. Parsons reported target depths ranged between 0 and 3 meters (0 and 10 feet) below ground surface. Parsons provided type, size, and class information as shown in Table 5.2.3-1.

**Figure 5.2.3-2**  
**Parson Target Declarations**

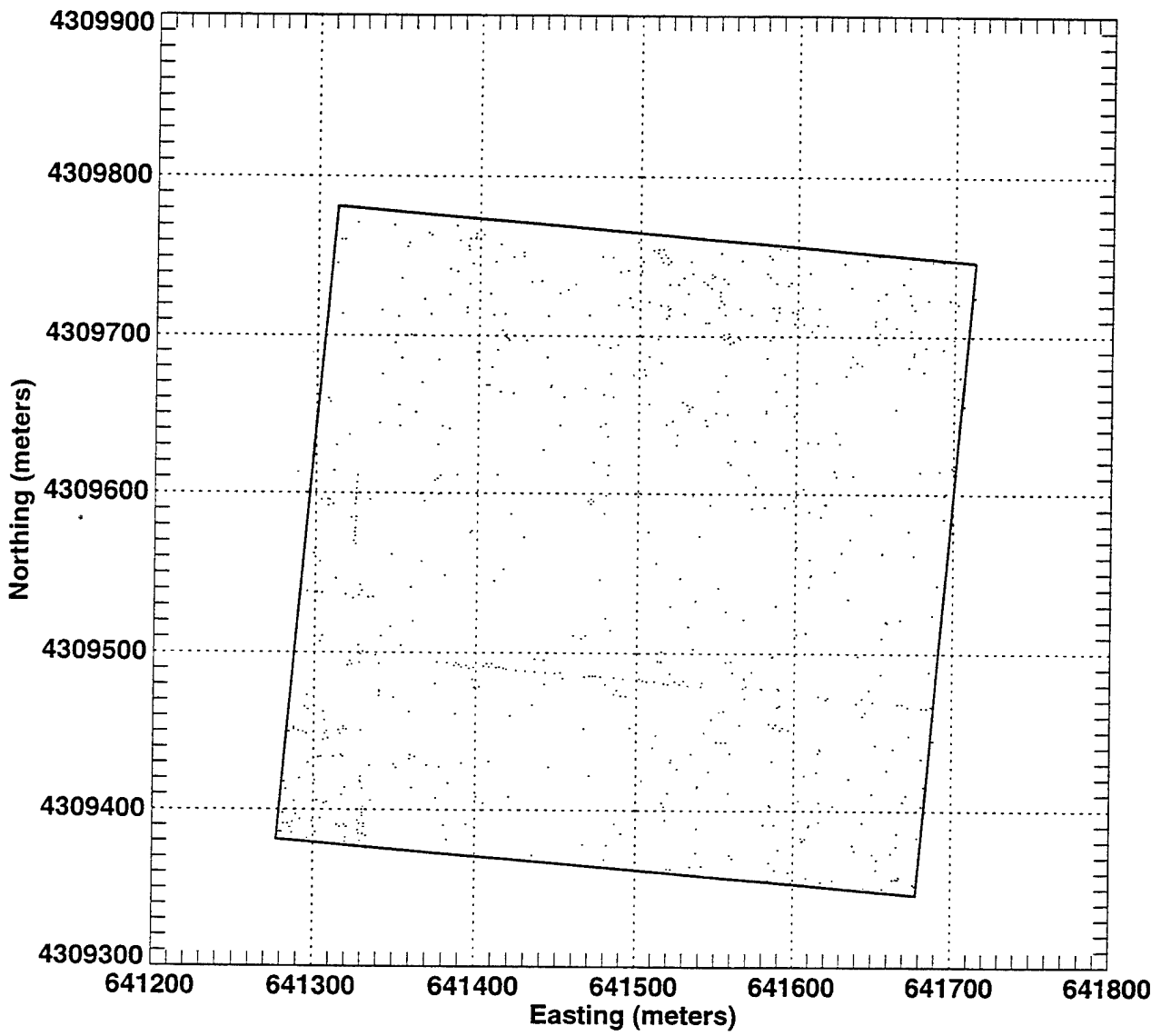


**TABLE 5.2.3-1  
PERFORMANCE STATISTICS FOR PARSONS**

**Detection Statistics**

	Number Baseline	Number Matched	$P_D^a$
Ordnance	127	108	0.85
Nonordnance	41	22	0.54
Total	168	130	0.77
$P_{random}$	0.05		
Number False Alarms	505		
False Alarm Rate	32.5/hectare		
False Alarm Ratio	4.68		
Probability False Alarms	0.0408		

**Localization Statistics**

	Mean (m) <sup>b</sup>	Std. Dev. <sup>c</sup> (m)
Position (x,y)		
dx	-0.03	0.73
dy	0.14	0.54
Radial	0.79	
Depth (z)		
$dz^d$	-0.24	0.68
dz	0.72	

**Identification and Classification Statistics**

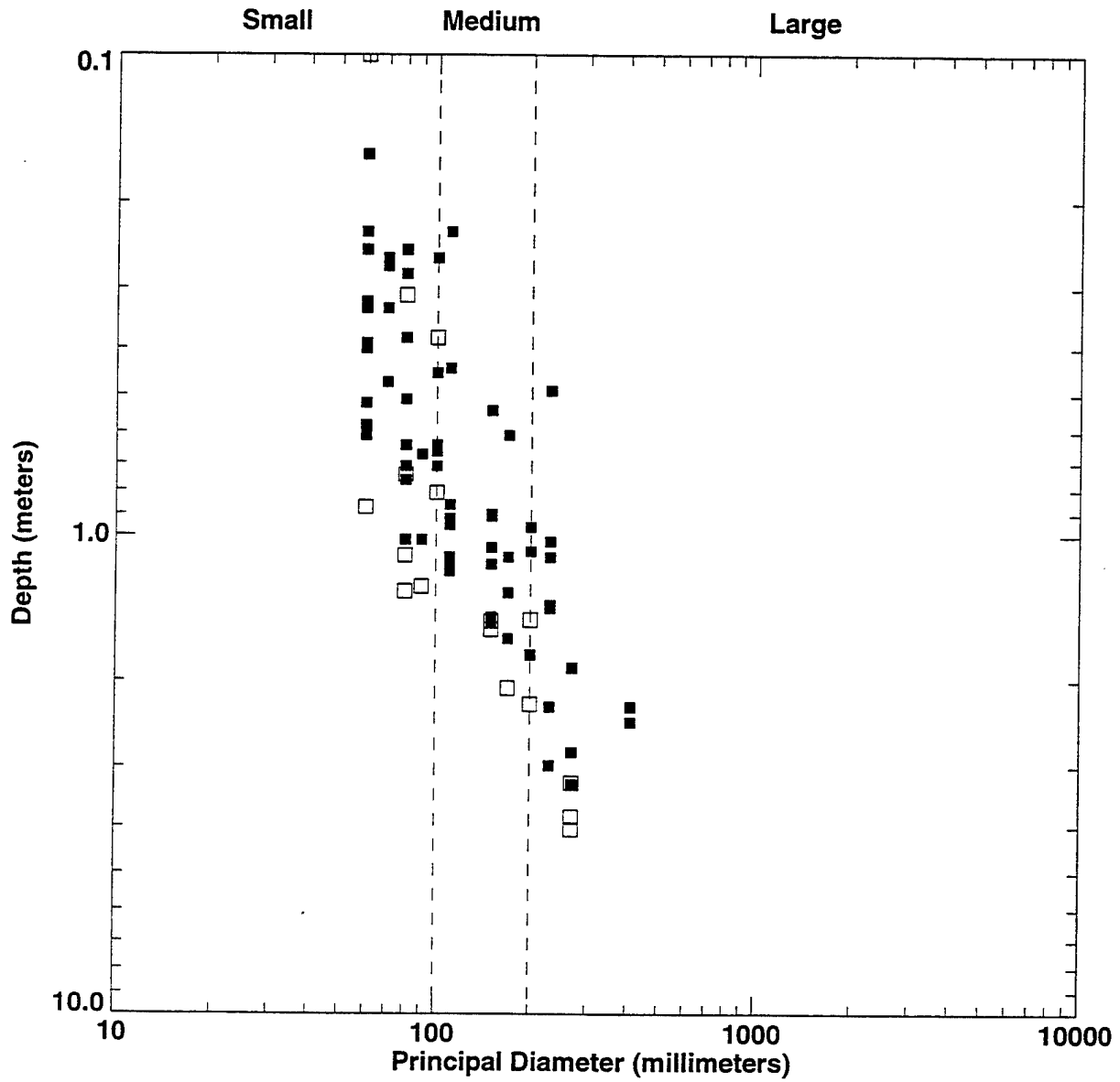
	Number Baseline	Number Detected	$P_D^e$	Number Correct	$P_C^f$
Type					
Ordnance	158	109	0.69	85	0.78
Nonordnance	65	30	0.46	3	0.10
Size					
Large	35	25	0.71	4	0.16
Medium	53	40	0.75	30	0.75
Small	69	44	0.64	10	0.23
Class					
Bomb	21	17	0.81	2	0.12
Projectile	69	47	0.68	27	0.57
Mortar	59	40	0.68	10	0.25
Cluster	9	5	0.56	0	0

**Notes:**

- <sup>a</sup> Probability of detection (based on Group TMA, fence area excluded)
- <sup>b</sup> Meter
- <sup>c</sup> Standard deviation
- <sup>d</sup> Square root of the mean square depth error
- <sup>e</sup> Probability of detection (based on closest TMA, fence area excluded)
- <sup>f</sup> Probability of correctly classifying (based on closest TMA)



Figure 5.2.3-3  
Parson Detection Ability



- Target Detected
- Target Not Detected

## 5.3

### GROUND PENETRATING RADAR SENSOR SYSTEMS

#### 5.3.1

##### Airborne Environmental Surveys, Inc.

Airborne Environmental Surveys, Inc. (AES), demonstrated from May 31 through June 3, 1995, at the 32-hectare area at JPG. AES also participated in Phase I of the UXO ATD program.

#### 5.3.1.1

##### Technology Description

AES used an EMS-20 airborne ground penetrating radar (AGPR) system (see Figure 5.3.1-1). The AGPR system is mounted on a Bell 412 helicopter. The 503-MHz center-frequency AGPR system is coupled to two oppositely polarized, bistatic, helical antennae. The system control, data collection, and GPS navigation hardware are mounted in the passenger compartment. With the oppositely polarized antenna configuration, ground penetration in dry soil should be at least 5 meters, and responses from surface clutter should be highly attenuated. The EMS-20 radar transmissions are analog, these analog signals received by the



Figure 5.3.1-1 Airborne Environmental Surveys, Inc., Airborne Ground Penetrating Radar System

antennae are digitized in an on-board computer and stored on the video channel of a VHS tape via a pulse-code modulator recorder. The helicopter flight path is navigated by a Trimble 3000F Navigator, while a six-channel Trimble Pathfinder Professional with MC-V (rover) is used to record GPS positioning data of the helicopter flight path. AES subcontracted Coleman Research Corporation to analyze the GPR data.

At JPG, AES combined data from its AGPR with a 63-channel digital airborne imaging spectrometer (DAIS). AES subcontracted to Geophysical and Environmental Research Corporation (GER) for the DAIS surveys. The GER DAIS was flown aboard a Piper Navajo airplane (see Figure 5.3.1-2). The DAIS is an airborne unit designed to gather spectral information for environmental studies, geologic mapping, research, and other applications. A Kennedy type scanner is used to acquire the images, which are formed at the entrance slit to the spectrometer. The spectrometer has four wavelengths ranging from 0.35 to 12.5 microns. The locations of anomalies interpreted from these data were determined by referencing the images with ground markers. Before DAIS data analysis, data are subject to preprocessing or correcting, which consist of



Figure 5.3.1-2 Digital Airborne Imaging Spectrometer System

gyro and baseline corrections, inversion of thermal channels, panoramic correction, and time-constant correction (AES 1995a).

AGPR system improvements from Phase I include a 12-channel base station and on-board GPS systems for differential correction of recorded GPS data and for recording positioning data of the GPR, respectively; and a new time recording system taken directly from the GPS to eliminate the possibility of drift (AES 1995a).

### **5.3.1.2 System Assessment**

This section summarizes the demonstration by AES, based on observations made in the field and information provided by AES.

#### **Requirements for Technology Implementation**

AES used five people to complete its demonstration at JPG. Two additional people from GER were on site to conduct the DAIS surveys. Operation of the AGPR system required two AES personnel on site to direct the helicopter with orange flags, while three other AES personnel were in the helicopter. The DAIS surveys were conducted at sunrise, midday, and after sunset to profile thermal activity throughout the day. AES personnel were often not on site during the DAIS surveys.

Support equipment required to perform the survey included a Bell 412 helicopter and a Piper Navajo airplane, equipped with the system-required instrumentation. Additional equipment needed for the survey included a optical color video; a 12-channel Trimble Navigation GPS Pathfinder Community Base Station for differential correction of recorded GPS data; and a laptop computer. White bed sheets were purchased by GER personnel and placed in four locations throughout the area. The bed sheets were used as reference points for the images produced from the DAIS. AES later surveyed the locations of the bed sheets using GPS coordinates; this approach enabled data from the two systems to be compared and evaluated.

#### **Operational Capabilities and Limitations**

AES completed the AGPR survey of the 32-hectare area in about 4 hours. The entire area was surveyed from an altitude of 38 meters (125 feet) above the ground surface, in a cross-grid pattern with flight line

centers separated by 8 meters (26 feet). GER's DAIS system covered relatively large areas within a short time. GER covered the 32-hectare area in 0.5 hour, but additional or redundant data sets were collected to ensure full coverage and data quality. Inclement weather, such as heavy fog and thunderstorms, caused several delays during the demonstration.

The AES system is limited by terrain clutter and soil moisture. Precipitation occurred on several days during the demonstration, and standing water was often present over much of the ground surface. Rainfall during the first 3 weeks of May was reportedly 300 percent above normal. The AES system does not differentiate between buried ordnance and other detected targets such as nonordnance or empty holes, and standing water and wet conditions greatly decrease the effectiveness of the radar. The sensors used in this demonstration were not useful in determining the weight, type, or class of detected objects. Most of the objects were classified as large because of the lower limitation of resolution.

#### **5.3.1.3 Measured Performance**

AES covered the entire 32-hectare area with the two systems in 16 of the allotted 24 hours. AES identified a total of 37 target locations at the 32-hectare area. Figure 5.3.1-3 shows AES's target declarations at the 32-hectare area, with the fence line area removed. Table 5.3.1-1 shows AES's results which includes the following: (1) detection, (2) localization, and (3) classification statistics with respect to type, size, and class.

The baseline for computing detection performance included both ordnance and nonordnance items. The detection ratio ( $P_D$  ordnance) of 0.05 reflects the number of targets detected by AES as compared to the total number of baseline ordnance targets in the area covered with the fence line area removed (AES 1995b). This detection probability is not significantly different than the probability of detection arising from random declarations due to sensor noise and other factors ( $P_{\text{random}} = 0.01$ ). AES had a FAR of 0.9 per hectare.

AES's results were comparable to those of other airborne demonstrators as they showed little of no capability detecting ordnance. In addition, AES's results are comparable to the results from other GPR systems from Phase I and Phase II.

As part of Phase I, AES had a  $P_D$  of 0.01 for ordnance items. The FAR was 1.29 per hectare. A comparison of Phase I and Phase II detection performance shows that AES obtained slightly higher  $P_D$  values for Phase II

(0.05) detection performance data. Similarly, AES's FAR improved, decreasing from 1.29 in Phase I to 0.9 in Phase II, although these differences are not statistically significant.

For most demonstrators, the probability of ordnance detection depends on both the size and depth of the buried ordnance item. Figure 5.3.1-4, which is a scatter plot showing detection performance as a function of size versus depth, illustrates this relationship for AES. The figure shows no relationship between these parameters for AES, which appeared to have difficulty in assessing depth at all.

The localization error statistics section of the table indicates AES's ability to estimate the locations of the targets declared. AES reported target depths between 0.01 and 1.80 meters (0.03 and 5.91 feet) below ground surface. AES provided ordnance type, size, and class information, as shown in the table.

**Figure 5.3.1-3**  
**AES Target Declarations**

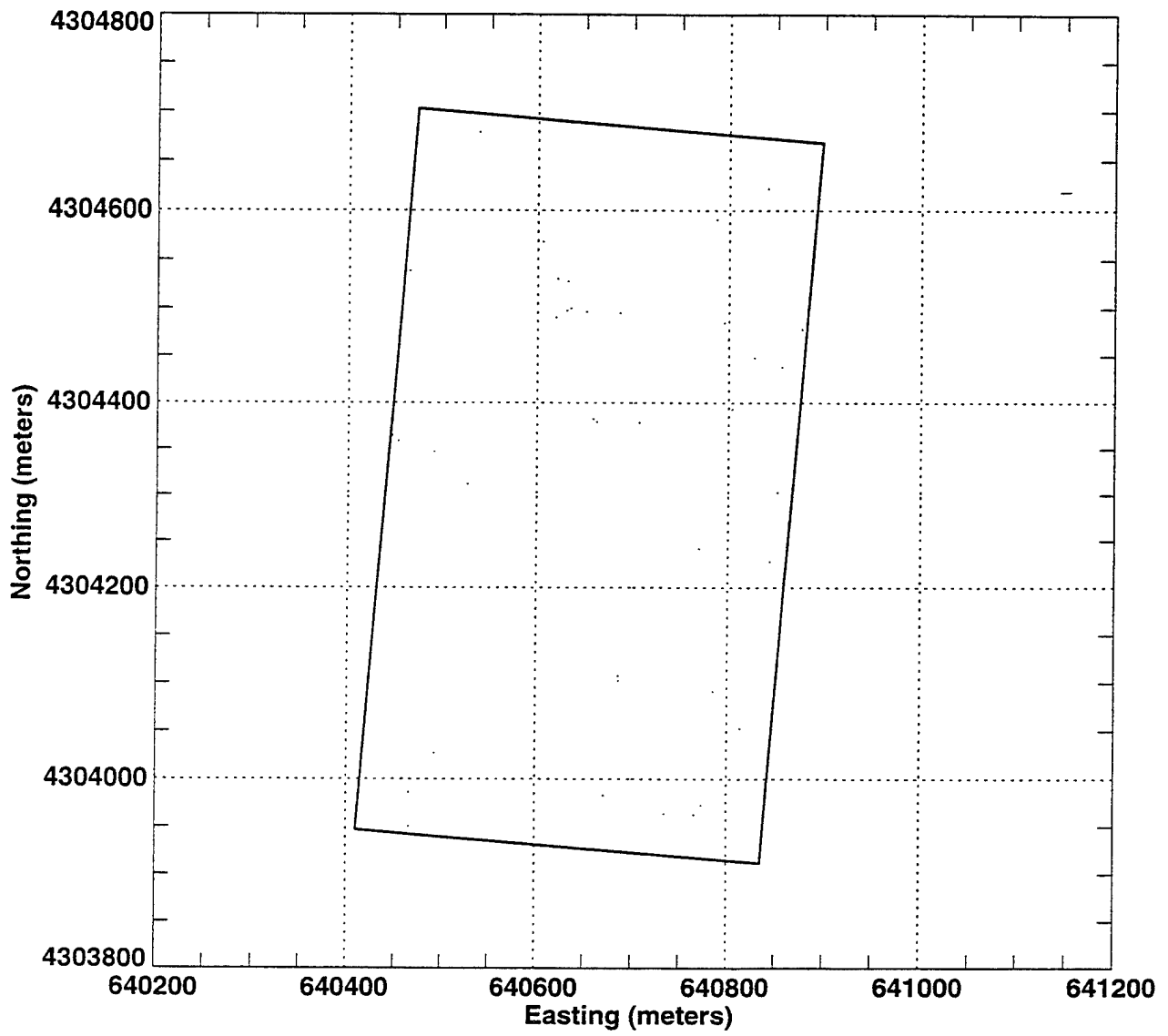


**TABLE 5.3.1-1  
PERFORMANCE STATISTICS FOR AES**

**Detection Statistics**

	Number Baseline	Number Matched	$P_D^a$
Ordnance	201	9	0.05
Nonordnance	20	0	0
Total	221	9	0.04
$P_{random}$	0.01		
Number False Alarms	28		
False Alarm Rate	0.9/hectare		
False Alarm Ratio	3.11		
Probability False Alarms	0.0069		

**Localization Statistics**

	Mean (m) <sup>b</sup>	Std. Dev. <sup>c</sup> (m)
Position (x,y)		
dx	-0.42	2.68
dy	-0.26	2.09
Radial	2.76	
Depth (z)		
$dz^d$	-0.49	0.91
dz	0.99	

**Identification and Classification Statistics**

	Number Baseline	Number Detected	$P_D^e$	Number Correct	$P_C^f$
Type					
Ordnance	245	9	0.04	8	0.89
Nonordnance	27	0	0	0	NA <sup>g</sup>
Size					
Large	41	4	0.10	3	0.75
Medium	37	2	0.05	0	0
Small	165	3	0.02	1	0.33
Class					
Bomb	23	1	0.04	1	1.00
Projectile	73	6	0.08	6	1.00
Mortar	143	2	0.01	0	0
Cluster	6	0	0	0	NA

- Notes:
- <sup>a</sup> Probability of detection (based on Group TMA, fence area excluded)
  - <sup>b</sup> Meter
  - <sup>c</sup> Standard deviation
  - <sup>d</sup> Square root of the mean square depth error
  - <sup>e</sup> Probability of detection (based on closest TMA, fence area excluded)
  - <sup>f</sup> Probability of correctly classifying (based on closest TMA)
  - <sup>g</sup> Not applicable





### 5.3.2 Kaman Sciences Corporation

Kaman Sciences Corporation (Kaman) demonstrated from August 9 through 14, 1995, at the 16A-hectare area at JPG.

#### 5.3.2.1 Technology Description

Kaman used a towed ground penetrating radar (GPR) mounted on a fiberglass and plexiglass sled (see Figure 5.3.2-1). The system is mounted on a four-wheel-drive truck, with the antennas towed on a wheeled sled. Kaman describes its GPR system as a nonintrusive, range-gated synthetic pulse radar system. The system uses separate transmitting and receiving antennas capable of detecting metallic objects and identifying characteristic changes below ground surface. The Kaman GPR system uses a frequency-stepped, wide-band radar capable of detecting metallic objects. Kaman stated in its proposal that it expected target resolution on the order of 0.1 meter (3.94 inches) for depth (Kaman 1995a).

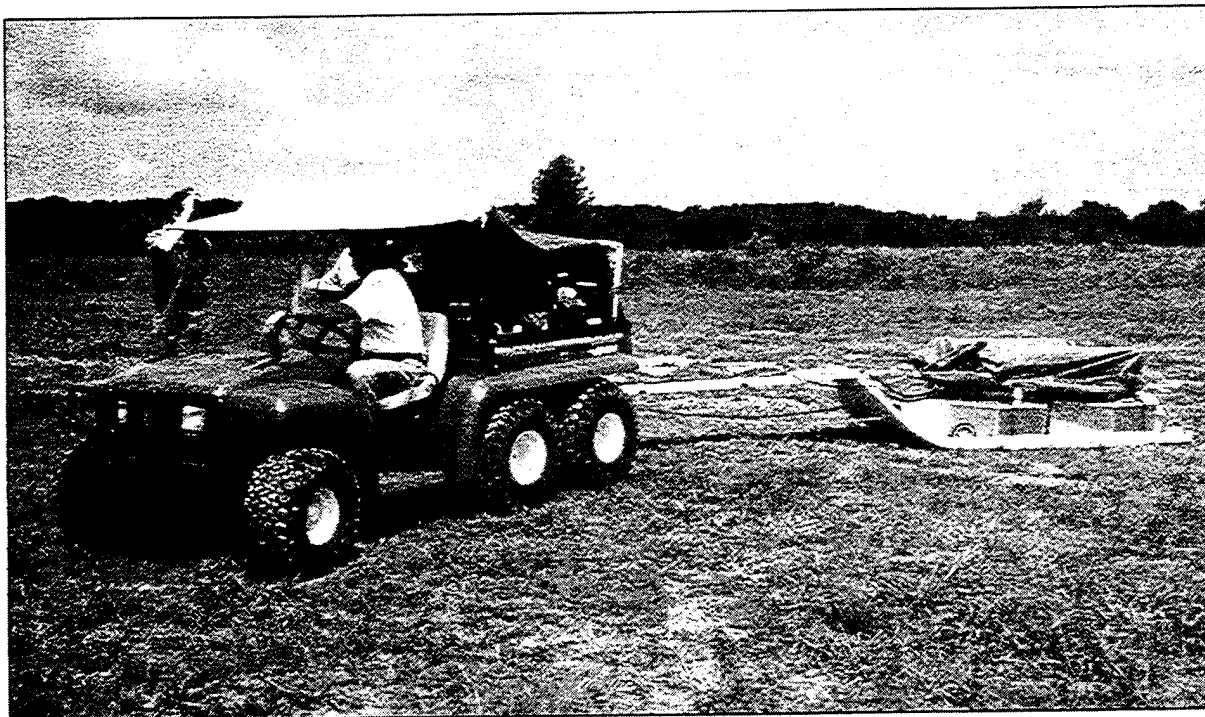


Figure 5.3.2-1 Kaman Sciences Corporation Towed Ground Penetrating Radar

Frequencies were generated by a Hewlett-Packard network analyzer combined with a digital quadrature detector (DQD) giving the GPR receiver a range of between 1 and 3,000 MHz. The optimal range for the system operating at JPG was between 100 and 800 MHz. The DQD combined with a range gate removes direct feedover between the transmitter and receiver as well as strong unwanted reflections. The GPR operates at a dynamic range of greater than 200 decibels. A differential GPS was used for navigation. Differential GPS data was used for location scanning, grid layout, and vehicle guidance. The remote differential GPS was placed and calibrated for use at monument 1 on the grid.

Kaman used the following subcontractors for its technology demonstration: John Hopkins University Applied Physics Laboratory, Program for Miljøovervåkingsteknikk, and SUSAR, Inc. Kaman used discrimination algorithms developed by SUSAR to post-process and analyze the collected data. Kaman and SUSAR use a proprietary technique named the target adaptive matched illumination radar (TAMIR) system, which is intended to eliminate false radar signals. Kaman stated in its proposal that TAMIR has the ability to differentiate between UXO and nonordnance items.

#### **5.3.2.2 System Assessment**

This section summarizes the demonstration by Kaman, based on observations made in the field..

#### **Requirements for Technology Implementation**

Kaman used six people to complete its demonstration. One person drove the ATV, while two people accompanied it, helping to guide the system on the grid. Two people were responsible for data downloading and analysis. The sixth person set up and maintained the GPS system.

Kaman drove its equipment to JPG for the demonstration. Kaman intended to survey the area with its four-wheel-drive pickup truck, however, the truck became stuck in the wet clay soils on the morning of the first day and had to be removed with a tow truck. Kaman then rented a John Deere 6-by-4-wheel ATV locally to survey the site. Two four-wheel-drive pickup trucks were used to transport personnel and supplies and to store the assembled equipment in the field.

Additional support equipment required to perform the geophysical survey included two laptop computers to store and process data, one gas-powered generator to operate the GPR/GPS system, and one 1.2-meter- (4.0-foot-) wide sled that held the GPR transmitter and receiver. Surveyor stakes and tapes, pin flags, and tape measures were used for guidance through the grid, which was surveyed in an east-west direction. The support trailer supplied electricity to recharge the GPR batteries.

### **Operational Capabilities and Limitations**

As described above, the system proposed for use by Kaman proved unusable due to the wet conditions at JPG. Kaman's GPR system, using the ATV as a tow vehicle, has a rate of up to about 1 meter per second (3 feet per second). The system performs best in open terrain. Heavy brush and low areas in the terrain slowed the survey considerably due to access difficulties. Kaman did not survey in the heavily wooded areas of the grid because of the difficult access as well as the loss of GPS reception in these areas. Kaman was also unable to survey in wet low areas because the GPR pulse is rapidly degraded by standing water or high soil moisture content. While in the field, Kaman personnel remarked that the clay soil might present a problem for GPR detection of metal objects.

Several short delays resulted from equipment failures. Kaman experienced a loose electrical connector with one battery terminal, which caused some data loss. The ATV became stuck on a stump, which also caused a delay. In addition, about every 2 hours, the GPR/GPS system had to be shut down for about 5 minutes so that the field generator could be refueled.

#### **5.3.2.3 Measured Performance**

Kaman was scored on 8.51 hectares (21.03 acres) of the 16A-hectare area (52.6 percent) covered with its vehicle towed system during the allotted 40 hours. Although Kaman covered slightly more area than it was scored on, only grid cells covered 50 percent or more were included. Figure 5.3.2-2 shows Kaman's target declarations at the 16A-hectare area (Kaman 1995b). Kaman reported a total of 32 targets with its system within the 8.51 hectares (21.03 acres) scored. Kaman's performance is shown in Table 5.3.2-1, which presents both detection and localization statistics. Kaman did not provide type, size, and class information, so classification statistics were not computed.

The baseline for computing detection performance included both ordnance and nonordnance items. The detection ratio of 0 (cited as  $P_D$  ordnance in Table 5.3.2-1) reflects the number of targets detected by Kaman as compared to the total number of baseline ordnance targets in the area covered. Kaman did not detect, and therefore were unable to classify, any of the 65 ordnance items or 14 nonordnance items that were in the area they surveyed. Kaman had a FAR of 4.2 per hectare. Kaman's results are comparable to the results from other GPR systems from Phase I and Phase II.

For most demonstrators, the probability of ordnance detection depends on both the size and depth of the buried ordnance item. Figure 5.3.2-3, which is a scatter plot showing detection performance as a function of size versus depth, illustrates this relationship for Kaman. This figure shows that Kaman had difficulty detecting targets of all sizes across the spectrum of depths.

Due to the lack of correct declarations, the mean radial accuracy for the targets Kaman declared could not be determined. Kaman reported target depths at 0.50 to 2.50 meters (1.64 to 8.20 feet) below ground surface. Again, due to the results, the mean depth error could not be determined.

**Figure 5.3.2-2**  
**Kaman Target Declarations**

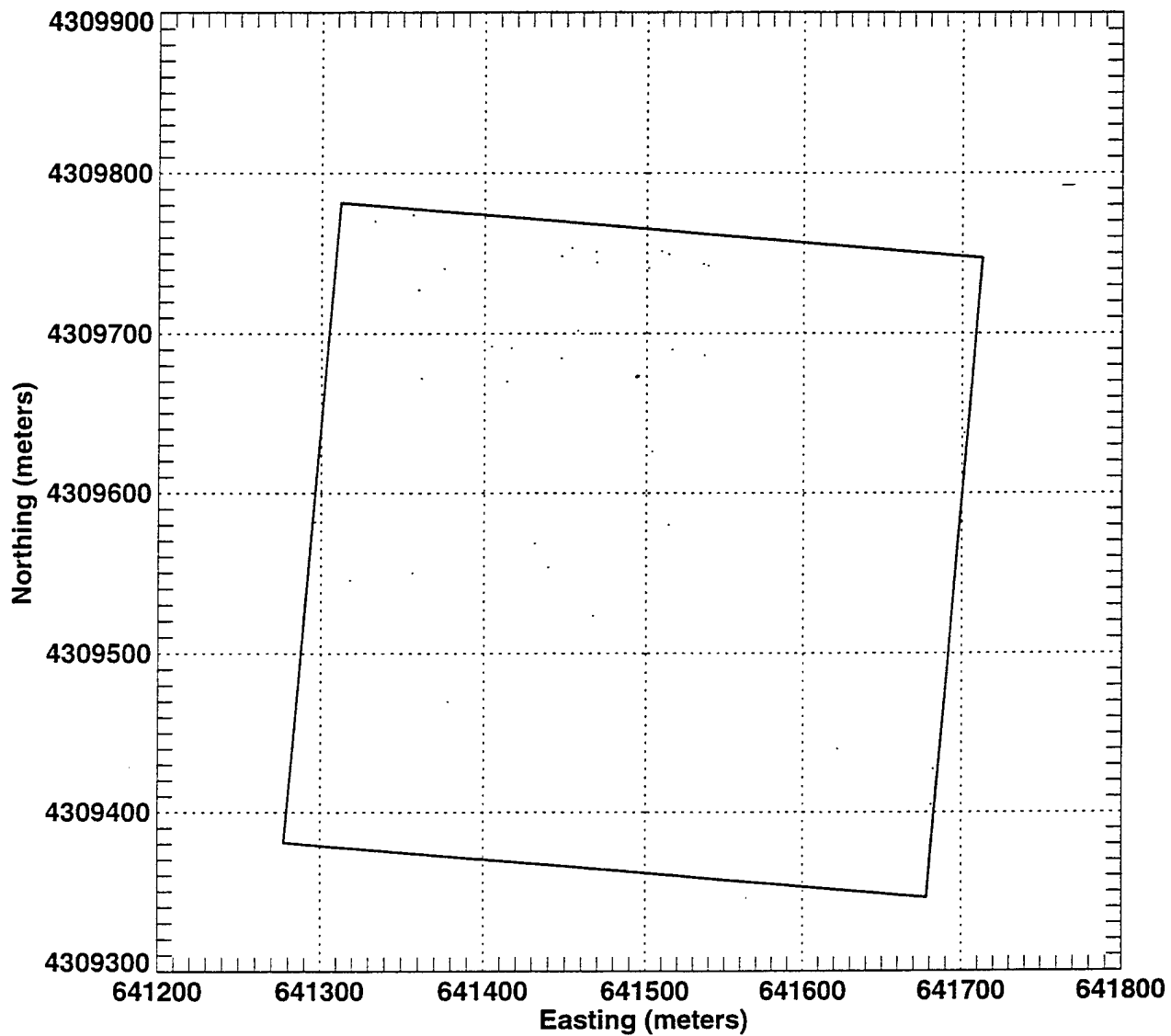


**TABLE 5.3.2-1  
PERFORMANCE STATISTICS FOR KAMAN**

**Detection Statistics**

	Number Baseline	Number Matched	$P_D^a$
Ordnance	65	0	0
Nonordnance	14	0	0
Total	79	0	0
$P_{random}$	0.01		
Number False Alarms	33		
False Alarm Rate	4.2/hectare		
False Alarm Ratio	NA <sup>g</sup>		
Probability False Alarms	0.0053		

**Localization Statistics**

	Mean (m) <sup>b</sup>	Std. Dev. <sup>c</sup> (m)
Position (x,y)		
dx	0	0
dy	0	0
Radial	0	
Depth (z)		
$dz^d$	0	0
dz	0	

**Identification and Classification Statistics**

	Number Baseline	Number Detected	$P_D^e$	Number Correct	$P_C^f$
Type					
Ordnance	77	0	0	0	NA
Nonordnance	23	0	0	0	NA
Size					
Large	14	0	0	0	NA
Medium	31	0	0	0	NA
Small	31	0	0	0	NA
Class					
Bomb	9	0	0	0	NA
Projectile	31	0	0	0	NA
Mortar	32	0	0	0	NA
Cluster	5	0	0	0	NA

**Notes:**

- <sup>a</sup> Probability of detection (based on Group TMA, fence area excluded)
- <sup>b</sup> Meter
- <sup>c</sup> Standard deviation
- <sup>d</sup> Square root of the mean square depth error
- <sup>e</sup> Probability of detection (based on closest TMA, fence area excluded)
- <sup>f</sup> Probability of correctly classifying (based on closest TMA)
- <sup>g</sup> Not applicable





### 5.3.3 SRI International

SRI International (SRI) demonstrated from July 26 through 30, 1995, at the 32-hectare area at JPG. SRI also participated in Phase I of the UXO ATD program..

#### 5.3.3.1 Technology Description

SRI demonstrated an airborne ground penetrating radar (GPR) system. The GPR system is mounted on a Jetstream 31 aircraft ( Figure 5.3.3-1). The transmitters and antennas are housed in a modified luggage pod on the underside of the aircraft. The system control, data collection, and GPS navigation hardware are mounted in two racks in the passenger compartment. SRI incorporated an ultra-wide bandwidth to compensate for the decreased resolution associated with the long wavelengths. SRI also used a low frequency radar (150-500 MHz) in conjunction with the GPR to increase soil penetration. The system used a combination of polarizations, both horizontal and vertical, to reduce the effects of surface clutter. The system uses three-dimensional processing and on-board navigation using GPS information. Positional data are obtained with a differential GPS.

The SRI system integrates radar returns from a linear range of aircraft positions. The system generates a two-dimensional image that shows regions of high and low radar return. The physics of the radar-soil interactions cause the buried targets to appear farther away from the aircraft than they really are.

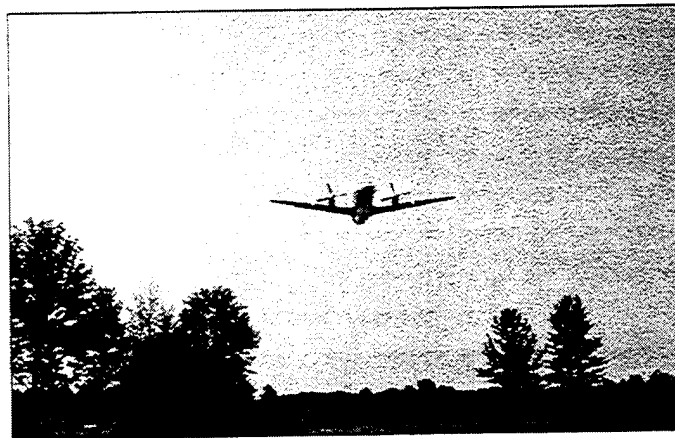


**Figure 5.3.3-1 SRI International Airborne Ground Penetrating Radar System**

The amount of the offset depends on the depth of burial and the characteristics of the soil. During Phase I, SRI used a multi-angle processing approach to determine depth, with poor results. For Phase II, SRI used a stereoscopic viewing approach by analyzing synthetic aperture radar (SAR) data. This approach generates three-dimensional images. This three-dimensional processing is intended to reduce the terrain limitations inherent in the radar system (SRI 1995a).

SRI system improvements from Phase I included the use of dual polarization radar horizontal-horizontal (HH) and vertical-vertical (VV), as apposed to only HH polarization for Phase I. A second major advance was the development of three-dimensional processing.

#### **5.3.3.2 System Assessment**

This section summarizes the demonstration by SRI, based on observations made in the field and information provided by SRI.

#### **Requirements for Technology Implementation**

SRI used six people to complete its demonstration. Two people were on site during setup and takedown; one of these persons was on site during flight times. The remaining four people were either on board the aircraft during the survey or at the airport. Support equipment required to perform the survey included a Jetstream aircraft equipped with the system-required instrumentation. Additional equipment needed for the survey included a laptop computer with a color monitor; a GPS receiver; a radio unit for communication between air and ground personnel; a camera and tripod for photographing panoramic landscape features; and a hand-held GPS 45.

SRI used four large aluminum corner reflectors to enhance the system's ability to identify ground features. These reflectors were assembled on site during the first day of the demonstration; assembly took 8 hours to complete. Tools used in assembling the reflectors were purchased locally. A local person was hired to assist the SRI ground crew during setup and takedown periods. A truck was required to transport the reflectors on site once they were assembled. A utility truck was rented locally and used to transport the reflectors and other equipment during the demonstration.

## **Operational Capabilities and Limitations**

SRI's system is able to cover relatively large areas within a short time. SRI covered the 32-hectare area in 2 hours, but additional or redundant data sets were collected to ensure full coverage and data quality. The site was surveyed at altitudes ranging from 564 to 1,027 meters (1,850 to 3,370 feet) above mean sea level. JPG is located about 80.8 meters (265 feet) above sea level.

SRI indicated that its system is limited by terrain clutter, targets buried greater than 1.0 meter (3.3 feet) below ground surface, and soil moisture. The SRI system does not differentiate between ordnance and other detected targets. Standing water and wet conditions greatly decrease the effectiveness of the radar. In addition, the SRI system cannot determine ordnance type or size.

System limitations with regard to elevation-induced anomalies can be attributed to the nature of synthetic aperture imaging with a side-looking radar. According to SRI, SAR images are intrinsically distorted because the angular sweep of the radar reflections is mapped onto a flat plane. SRI's image generation process accounts for this, but it assumes that the target area is perfectly level and smooth, which in practice is never the case, according to SRI. As a result, the SAR image is affected by additional distortion and by layover, which means that with severe topography the top of the terrain is closer to the aircraft than the bottom of the terrain. Use of the corner reflectors in the survey area lessens this distortion. Although the topography at JPG is not severe, the corner reflectors were used to enhance ground features (SRI 1995b).

### **5.3.3.3 Measured Performance**

SRI covered the entire 32-hectare area within 18 of the allotted 24 hours. SRI did not use the setup day (Tuesday), choosing instead to set up on the first day of the demonstration period (Wednesday). SRI identified a total of 86 potential UXO locations at the 32-hectare area, with the fence line area removed (see Figure 5.3.3-2) (SRI 1995b).

SRI provided the surface, or apparent, locations in the database along with the actual position assuming that the piece of ordnance is buried 1.0 meter (3.3 feet). Each of the 86 detected locations has two entries as endpoints in the target database; one assumes a burial depth of 0.1 meter (0.3 feet), and the other assumes a 1.0-meter (3.3-foot) burial depth with a refractive index of 5. Although SRI requested to be scored based on

these pairs of declarations, the contract required the demonstrator to provide exact target locations. SRI was scored in a similar manner as all other demonstrators consistent with the data reporting requirements. SRI selected a 1.0-meter (3.3-foot) burial depth for the database because it was unlikely that any except the largest items would be detected any more deeply because of the wet soil conditions. According to SRI, the detected item should lie on a straight line between these two target declarations. Because the critical radius used for airborne sensors was 5.0 meters (16.4 feet), and taking the average distance between these two depths into account, one of these two points should encompass a baseline target if it was actually detected.

SRI's performance is shown in Table 5.3.3-1, which presents both detection and localization statistics. SRI did not provide type, size, or class information so classification statistics were not computed. The baseline for computing detection performance included both ordnance and nonordnance items. SRI was scored on 98.6 percent of the total area. The detection ratio of 0.01 (cited as  $P_D$  ordnance in Table 5.3.3-1) reflects the number of targets detected by SRI compared to the total number of baseline ordnance targets in the area they covered. This detection probability is actually lower than the probability of detection arising from random declarations due to sensor noise and other factors ( $P_{\text{random}} = 0.02$ ). If SRI was scored in the manner requested, there would be no effect on the  $P_D$  values; however, the probability of false alarms, false alarm rate, and  $P_{\text{random}}$  would be cut in half. SRI had a FAR of 2.6 per hectare.

As part of Phase I, SRI recorded a  $P_D$  of 0.02 for ordnance items. The FAR was 3.87 per hectare. A comparison of Phase I and Phase II detection performance shows that SRI obtained a slightly lower  $P_D$  value for Phase II detection performance data. SRI's FAR improved slightly, however, from 3.87 in Phase I to 2.6 in Phase II. SRI's results are comparable to the results of other GPR systems from Phase I and Phase II. In addition, SRI's results are comparable to those of other airborne demonstrators as they showed little or no capability to detect ordnance.

For most demonstrators, the probability of ordnance detection depends on both the size and depth of the buried ordnance item. Figure 5.3.3-3, which is a scatter plot showing detection performance as a function of size versus depth, illustrates this relationship for SRI. In this figure, there appears to be no relationship between size and depth as related to detection performance. A relationship is difficult to see because only three target declarations were correct.

The localization error statistics section of Table 5.3.3-1 indicates SRI's ability to estimate the locations of the targets declared. SRI stated that depth information could be provided only by performing more complex analysis than time permitted under this contract. However, in its proposal dated February 17, 1995, SRI stated that it could provide depth information with the stereoscopic approach of analyzing SAR data (SRI 1995a).

Figure 5.3.3-2  
SRI Target Declarations

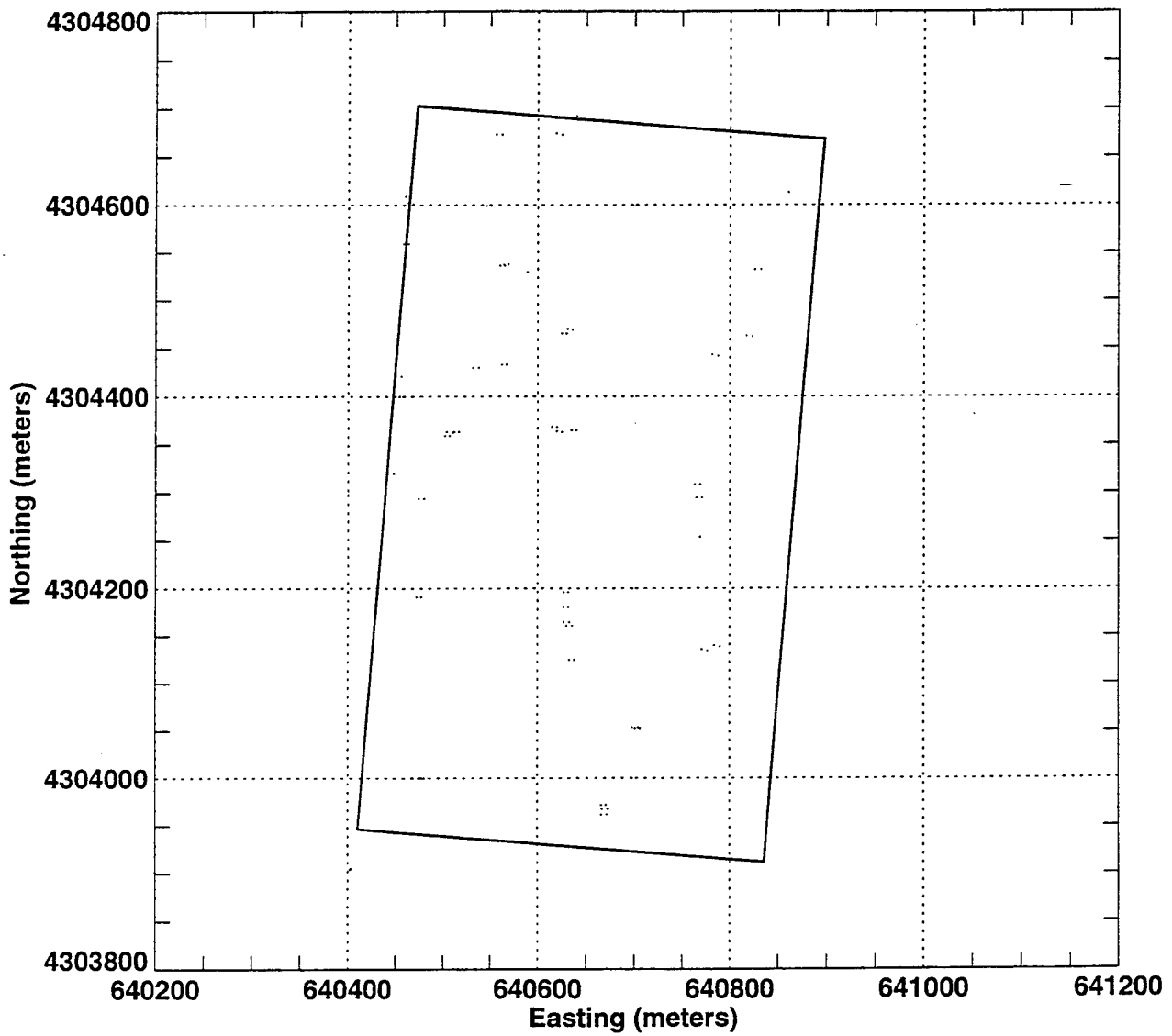


**TABLE 5.3.3-1  
PERFORMANCE STATISTICS FOR SRI**

**Detection Statistics**

	Number Baseline	Number Matched	$P_D^a$
Ordnance	201	3	0.01
Nonordnance	20	0	0
Total	221	3	0.01
$P_{\text{random}}$	0.02		
Number False Alarms	83		
False Alarm Rate	2.6/hectare		
False Alarm Ratio	27.7		
Probability False Alarms	0.0205		

**Localization Statistics**

	Mean (m) <sup>b</sup>	Std. Dev. <sup>c</sup> (m)
Position (x,y)		
dx	1.09	2.56
dy	0.31	3.38
Radial	3.49	
Depth (z)		
$dz^d$	-2.38	0.58
dz	2.42	

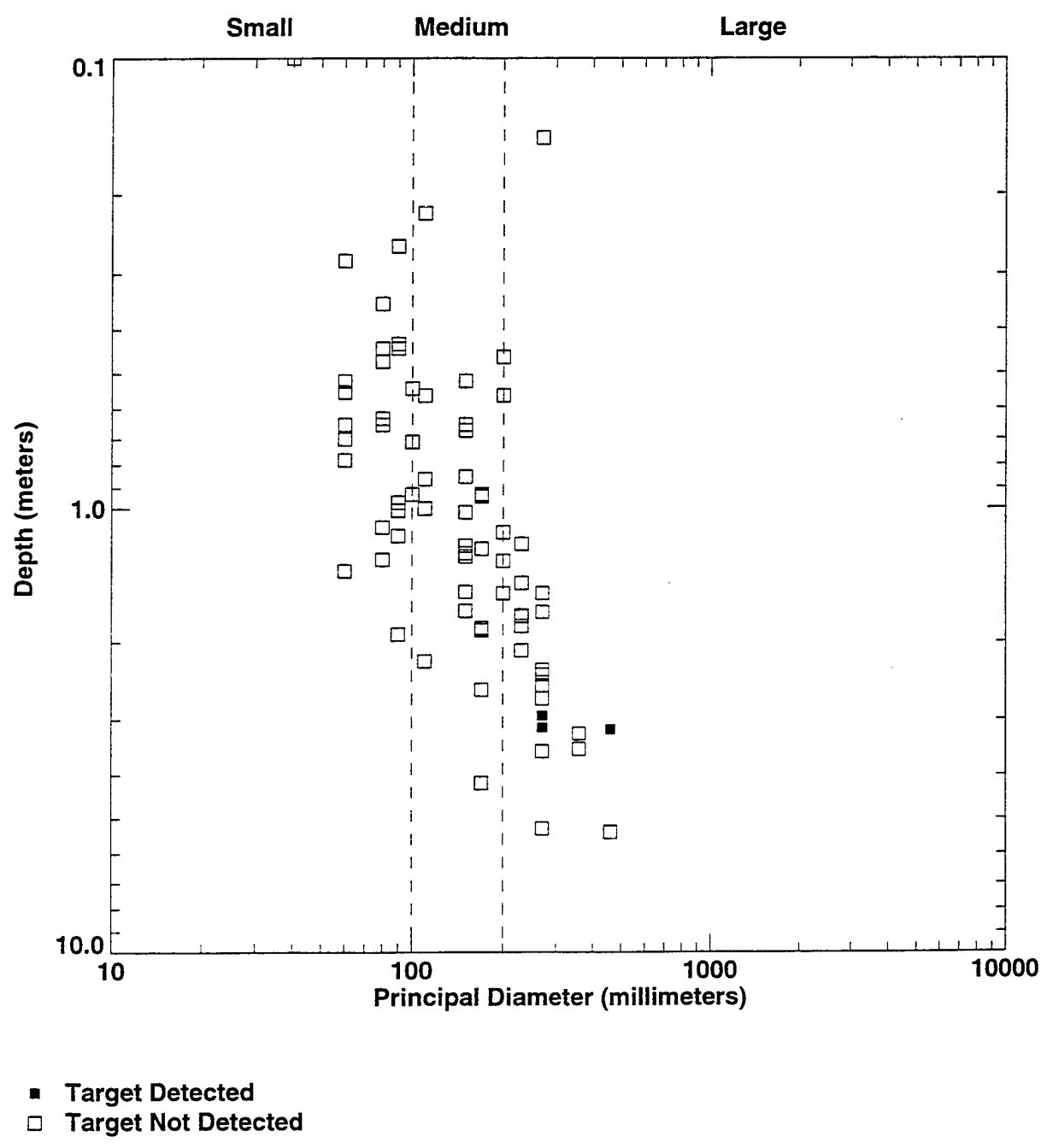
**Identification and Classification Statistics**

	Number Baseline	Number Detected	$P_D^e$	Number Correct	$P_C^f$
Type					
Ordnance	245	3	0.01	0	0
Nonordnance	27	0	0	0	NA <sup>g</sup>
Size					
Large	41	3	0.07	0	0
Medium	37	0	0	0	NA
Small	165	0	0	0	NA
Class					
Bomb	23	3	0.13	0	0
Projectile	73	0	0	0	NA
Mortar	143	0	0	0	NA
Cluster	6	0	0	0	NA

**Notes:**

- <sup>a</sup> Probability of detection (based on Group TMA, fence area excluded)
- <sup>b</sup> Meter
- <sup>c</sup> Standard deviation
- <sup>d</sup> Square root of the mean square depth error
- <sup>e</sup> Probability of detection (based on closest TMA, fence area excluded)
- <sup>f</sup> Probability of correctly classifying (based on closest TMA)
- <sup>g</sup> Not applicable

Figure 5.3.3-3  
SRI Detection Ability





## 5.4

## MAGNETOMETER AND ELECTROMAGNETIC INDUCTION

### 5.4.1

#### Australian Defence Industries, Pty. Ltd.

ADI demonstrated from June 14 through 18, 1995, at the 16B-hectare area at JPG. ADI also participated in Phase I of the UXO ATD program where they demonstrated magnetometer sensor systems only. During Phase II, ADI used two separate man-portable sensor systems for its demonstration: magnetometer and electromagnetic induction. The following sections describe the ADI electromagnetic induction technology, assess ADI's demonstration, and analyze ADI's results for both magnetometer and electromagnetic induction sensor data combined. For a complete discussion on ADI's magnetometer demonstration and analysis of the magnetometer data, see Section 5.1.2.

#### 5.4.1.1

##### Technology Description

ADI used a TM-4 magnetometer system and two EM-61 time-domain electromagnetic induction sensors for its surveying. Each EM-61 unit consists of a transmitter-receiver frame, an electronics backpack, and a hand-held data recorder (see Figure 5.4.1-1). The top coil, mounted 40 centimeters (16 inches) above the

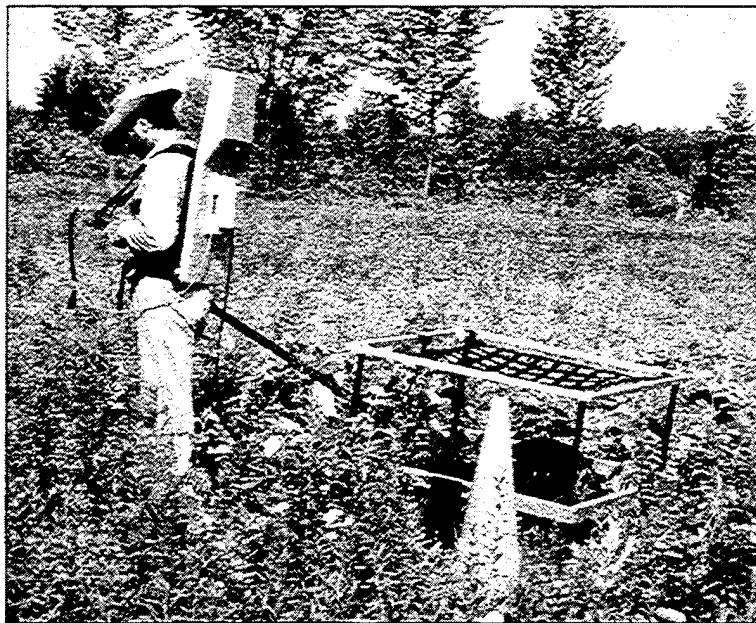


Figure 5.4.1-1 ADI EM-61 Electromagnetic Time-Domain Unit

bottom coil, is a receiver only. The lower coil acts as both a transmitter and receiver. The lower coil is a transmitter when the current is on and a receiver when the current is off. The transmitter, receiver electronics, and controls are contained in a backpack. The data recorder is connected to the electronics in the backpack.

The cart-mounted EM-61 units were towed manually by the ADI field crews. ADI stated that the EM-61 unit measures conductivity so that it can detect nonferrous materials such as aluminum. The EM-61 data set is intended to complement the TM-4 magnetometer data set. The EM-61 unit is also designed to provide lateral location accuracy and discriminate multiple targets. ADI stated that detection by the EM-61 unit should not be affected by varying soil conditions or the proximity of buildings, fences, and power lines. The data are then gridded for image processing and interpretation. The magnetometer and electromagnetic induction data sets are fused to produce a joint interpretation of both ferrous and nonferrous buried ordnance (ADI 1995a).

#### **5.4.1.2 System Assessment**

This section summarizes the ADI demonstration, based on observations made in the field.

#### **Requirements for Technology Implementation**

ADI used seven people to complete its demonstration. Two people operated the TM-4 magnetometer in the field. One person carried the sensors, followed by another person who carried a PC tethered to the sensors. The remaining five people operated the two EM-61 units, alternating to allow for rest periods. All system equipment used for this demonstration was shipped to JPG from ADI headquarters in Australia. ADI rented a utility vehicle locally for transportation. During the demonstration, repair parts such as inner tubes for the tires on the EM-61 wheeled carts were purchased locally. Additional odometers and a replacement circuit board for the EM-61 were also needed and were mailed from the manufacturer. ADI used the support trailer to store equipment and to recharge batteries.

For grid navigation, ADI used four magnetic marking chains. The magnetic chains were placed along east-west grid lines. The survey lines or transects were conducted in a north-south fashion. The EM-61 has an

odometer in the wheel but can also be switched to time-based manual mode. Each time the EM-61 passed the marking chains, that particular grid was "marked" in the computer memory.

### **Operational Capabilities and Limitations**

The cart-mounted EM-61 units were towed manually by the ADI field crews. The cart-mounted EM-61 units had difficulty on the rutted, uneven terrain, and several breakdowns occurred during the demonstration. The most frequent breakdowns included flat tires and broken odometer. A replacement circuit board was also required for one EM-61 unit during the demonstration.

#### **5.4.1.3 Measured Performance**

ADI covered the entire 16B-hectare area with the TM-4 magnetometer in about 32 hours. Because of several breakdowns, the EM-61 units covered about 86 percent of the 16 hectares in 40 hours. ADI's results were analyzed in two ways. The TM-4 magnetometer data were analyzed separately, and the magnetometer and EM-61 data were analyzed together to better determine the ferrous and the nonferrous items detected. Because ADI covered more than 50 percent of all grid cells, both sets of ADI results were scored as 100 percent coverage (ADI 1995b). See Section 5.1.2.3 for a discussion of ADI's magnetometer performance.

After the removal of the fence line from the area searched, ADI reported 598 targets with the combined systems (see Figure 5.4.1-2) within the 16 hectares. ADI's performance with the combined magnetometer and electromagnetic induction systems is shown in Table 5.4.1-1, which presents the following:

(1) detection, (2) localization, and (3) classification statistics with respect to type, size, and class.

The baseline for computing detection performance for Phase II included both ordnance and nonordnance items. The detection ratio of 0.65 (cited as  $P_D$  ordnance in Table 5.4.1-1) reflects the number of ordnance targets detected by ADI with the magnetometer and electromagnetic induction sensor systems combined. These  $P_D$ s are significantly different than the probability of detection resulting from random declarations, shown as 0.05 ( $P_{\text{random}}$ ) for the combined data set. ADI had a FAR of 34.5 per hectare for the combined data set.

For most demonstrators, the probability of ordnance detection depends on both the size and the depth of the buried ordnance item. Figure 5.4.1-3 is a scatter plot showing detection performance as a function of size versus depth illustrating this relationship. ADI was more successful at detecting medium and large targets than smaller targets. Small targets (less than 100-mm diameter) were difficult for ADI to detect at most depths.

The localization error statistics section of Table 5.4.1-1 indicates ADI's ability to estimate the location of the targets declared. ADI reported target depths between 0.39 meter (1.28 feet) above surface to 6.08 meters (19.95 feet) below ground surface. ADI provided type, size, and class information, as shown in the tables.

**Figure 5.4.1-2**  
**ADI Magnetometer & EM Target Declarations**

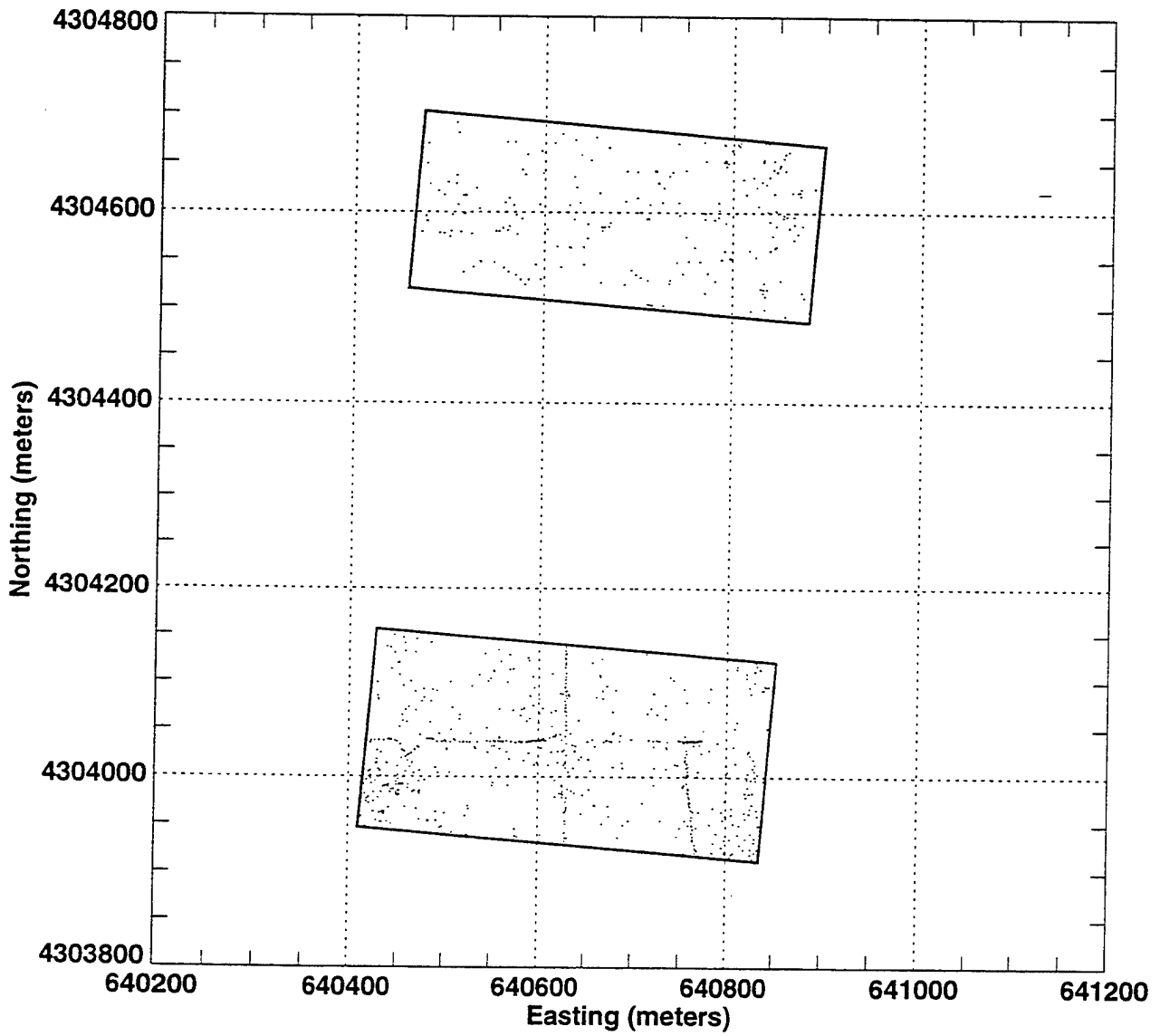


**TABLE 5.4.1-1  
PERFORMANCE STATISTICS FOR ADI (MAGNETOMETER AND EM INDUCTION)**

**Detection Statistics**

	Number Baseline	Number Matched	$P_D^a$
Ordnance	92	60	0.65
Nonordnance	8	6	0.75
Total	100	66	0.66
$P_{random}$	0.05		
Number False Alarms	561		
False Alarm Rate	34.5/hectare		
False Alarm Ratio	9.35		
Probability False Alarms	0.0433		

**Localization Statistics**

	Mean (m) <sup>b</sup>	Std. Dev. <sup>c</sup> (m)
Position (x,y)		
dx	-0.07	0.61
dy	-0.20	0.59
Radial	0.74	
Depth (z)		
$dz^d$	0.12	0.68
dz	0.68	

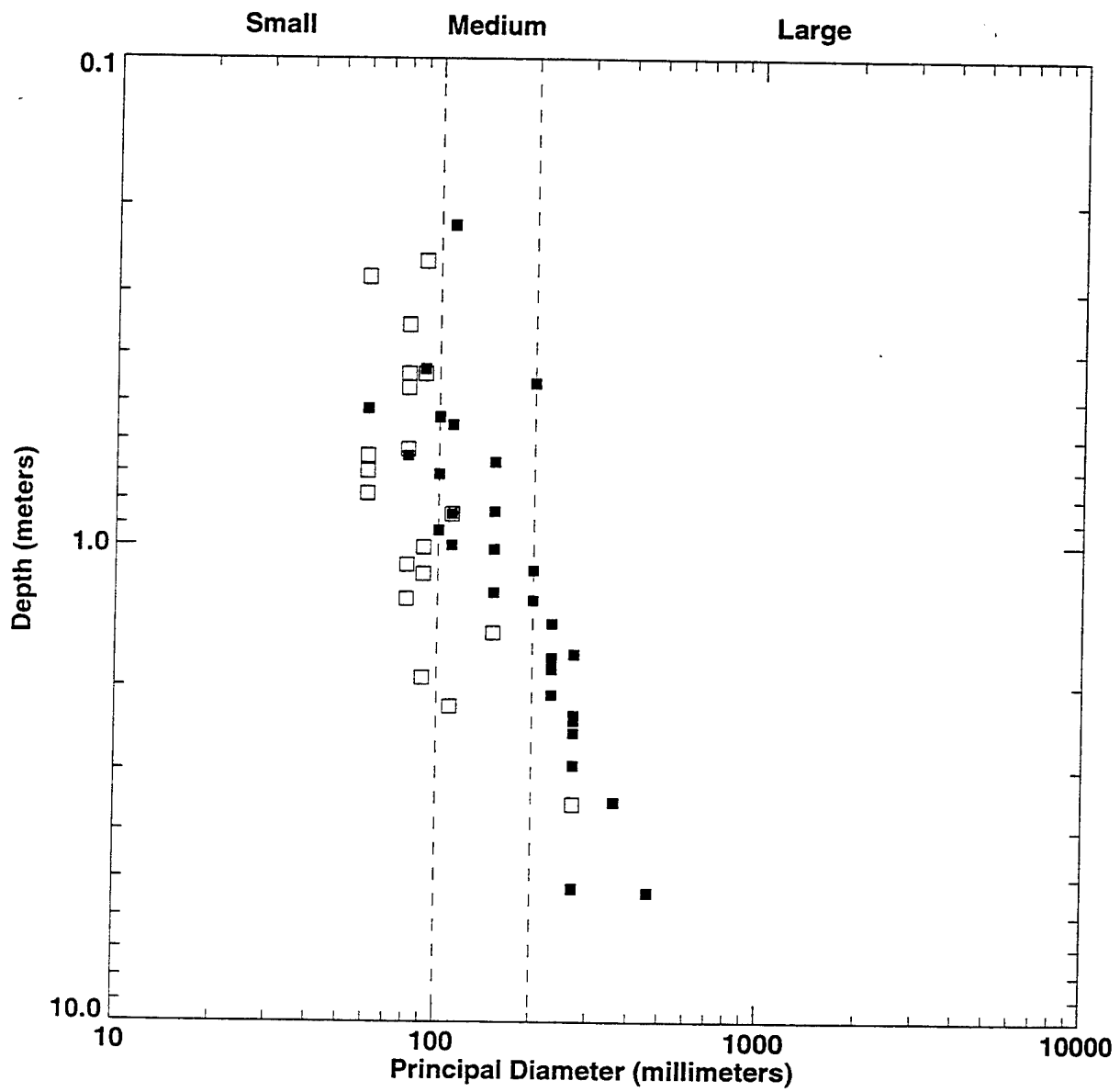
**Identification and Classification Statistics**

	Number Baseline	Number Detected	$P_D^e$	Number Correct	$P_C^f$
Type					
Ordnance	125	62	0.50	45	0.73
Nonordnance	14	9	0.64	1	0.11
Size					
Large	31	20	0.65	13	0.65
Medium	23	15	0.65	8	0.53
Small	69	26	0.38	24	0.92
Class					
Bomb	15	13	0.87	10	0.77
Projectile	51	26	0.51	10	0.38
Mortar	53	20	0.38	7	0.35
Cluster	6	3	0.50	0	0

**Notes:**

- <sup>a</sup> Probability of detection (based on Group TMA, fence area excluded)
- <sup>b</sup> Meter
- <sup>c</sup> Standard deviation
- <sup>d</sup> Square root of the mean square depth error
- <sup>e</sup> Probability of detection (based on closest TMA, fence area excluded)
- <sup>f</sup> Probability of correctly classifying (based on closest TMA)

Figure 5.4.1-3  
ADI Magnetometer & EM Detection Ability



- Target Detected
- Target Not Detected

## 5.4.2 Geo-Centers, Inc.

Geo-Centers, Inc. (Geo-Centers), demonstrated from August 9 through 13, 1995, at the 16B-hectare area at JPG. Geo-Centers also participated in Phase I of the UXO ATD program.

### 5.4.2.1 Technology Description

Geo-Centers used a ground-based, vehicle-towed system and two man-portable systems to complete its demonstration at JPG. The vehicle-towed system is called the surface-towed ordnance locator system (STOLS), which consists of a tow vehicle and tow platform connected by a tow bar (see Figure 5.4.2-1). The tow platform carries eight total-field cesium vapor magnetometers positioned 0.5 meter (1.6 feet) apart along a boom. The magnetometers can be adjusted from 15 to 20 centimeters (6 to 8 inches) above the ground. The eight sensors are arranged in pairs and used as four sets of total-field gradiometers. This total-field magnetometer and gradiometer configuration is used to differentiate small targets from large targets in

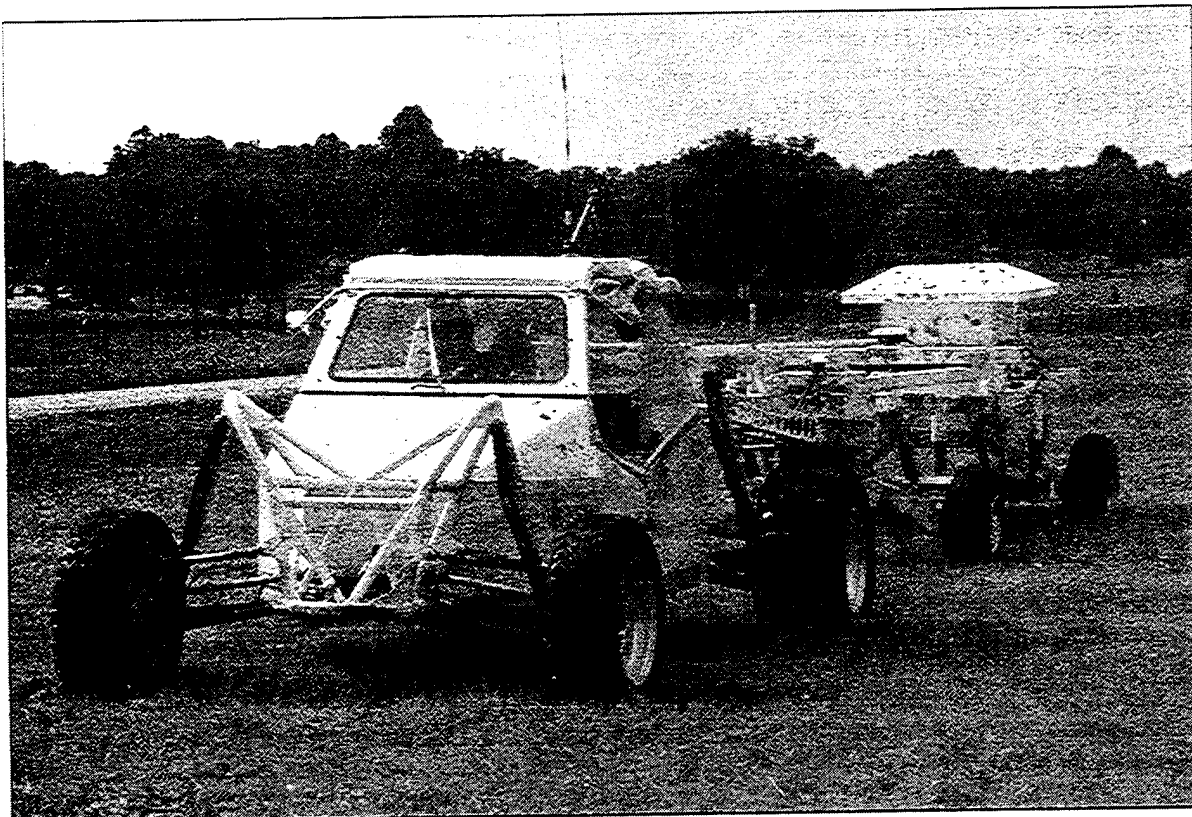
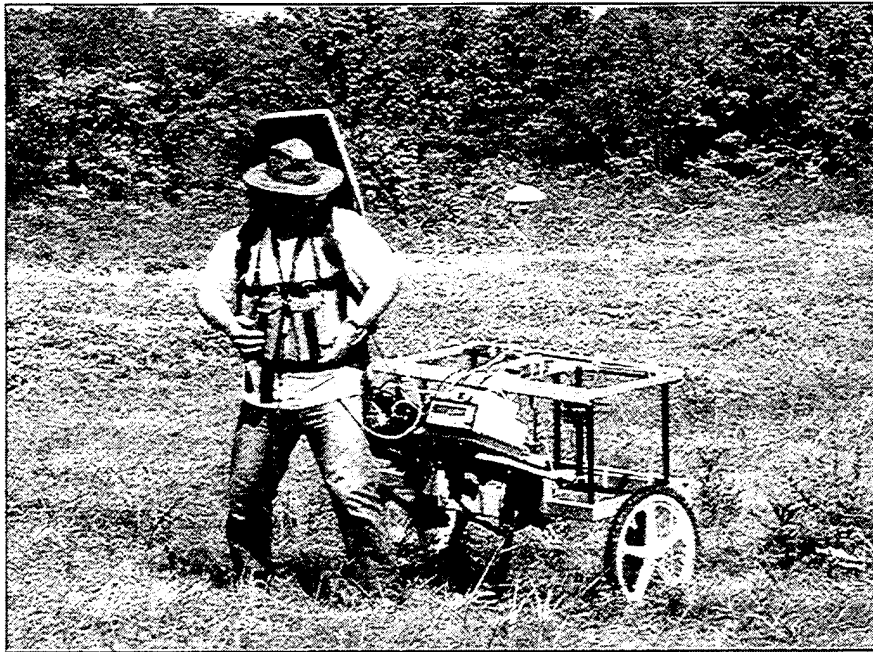


Figure 5.4.2-1 Geo-Centers, Inc., Surface Towed Ordnance Locator System



close proximity. Also included on the platform is the sensor control computer that records the magnetometer data and a GPS dome antenna. High resolution magnetic maps of the surveyed area are produced from the data collected.

The tow vehicle is an off-road two-wheel drive single passenger machine composed of nonmagnetic materials. Geo-Centers stated in its proposal that the STOLS is able to travel in excess of 32 kilometers per hour (20 miles per hour) over rough terrain without adversely impacting the quality of data collected. The system is transported in a fully equipped trailer, which becomes an on-site command center. This trailer is self powered and used for data processing and equipment maintenance and storage. Differential GPS is used for navigational precision to within 0.10 meters (4 inches) for synchronizing and positioning of the multisensor data (Geo-Centers 1995).



**Figure 5.4.2-2 Geo-Centers EM-61 Electromagnetic Unit**

At JPG, two portable, pulsed, induction systems were used to cover areas that could not be accessed by STOLS. Two different types of electromagnetic sensors were used, the EM-61 (see Figure 5.4.2-2) and the Schiebel electromagnetic sensor (see Figure 5.4.2-3), both small coil systems. Two 0.5-meter (1.5-foot) coil EM-61 units were joined together into one sensor system. The Schiebel electromagnetic sensor has an array

of eight 25-centimeter (10-inch) coil sets and is a prototype system. The linear array of small, pulsed induction coils, is designed to resolve and detect all small, shallow metal objects. The array is driven sequentially across each coil to form an array scan. Every eight of these array scans are averaged to form an array output every 64 milliseconds. The output is connected to a PC for setup, display, storage, and analysis.



Figure 5.4.2-3 Geo-Centers Schiebel EM Sensors

#### 5.4.2.2 System Assessment

This section summarizes the Geo-Centers demonstration, based on observations made in the field.

#### Requirements for Technology Implementation

Geo-Centers used nine people to complete its demonstration. Three people drove the STOLS vehicle and operated the man-portable systems, alternating these responsibilities. One person was responsible for the system electronics. One person handled data analysis and the generation of the magnetic maps. The survey

was supervised by one person. The remaining three people were on site for only part of the survey to observe the operations and assist as needed.

All system equipment used for this demonstration was transported to JPG by Geo-Centers in a self-contained trailer. Equipment required in addition to the actual STOLS system included one laptop PC for data downloading, one magnetic base station, and one GPS base station. The GPS also included several radio- frequency (RF) repeater modems needed to broadcast the GPS corrections to the GPS receiver on the STOLS. Support equipment used by Geo-Centers included several vehicles used to transport personnel. System batteries were recharged in the Geo-Centers command station. Data analysis also took place there.

Geo-Centers established a reference magnetometer outside of the 16B-hectare area, in an area that was magnetically clean. These data were recorded at a 10 Hz rate, downloaded to the processing computer after the survey completion, and subtracted from the magnetometer data recorded on the sensor platform.

#### **Operational Capabilities and Limitations**

The STOLS used by Geo-Centers required little maintenance throughout the demonstration, although a rear shock absorber was replaced on the tow vehicle causing a minor delay. Other minor equipment problems included a flat tire on the platform and the reattachment of the skid plate that protects the sensors. The STOLS vehicle became stuck in the mud twice, but it was quickly freed. In wet areas, Geo-Centers added extra tires to the tow vehicle, which improved traction. The STOLS vehicle traversed the terrain and maneuvered around trees with few problems.

The two man-portable electromagnetic systems were only used in a few select areas. The dual EM-61 system developed a broken frame and was modified several times during the demonstration. The Schiebel electromagnetic sensor was only used in two small areas; setup and operation appeared to be time-consuming.

According to Geo-Centers, STOLS magnetometer data are acquired at a rate of about 100,000 magnetometer points per acre. This rate is based on survey speeds of about 5.6 kilometers (3.5 miles) per hour.

### 5.4.2.3 Measured Performance

Geo-Centers surveyed the entire 16B-hectare area with its systems in the allotted 40 hours. Geo-Centers reported 1,409 targets within the 16B-hectare area (see Figure 5.4.2-4) (Geo-Centers 1995). Geo-Centers' performance is shown in Table 5.4.2-1, which presents the following: (1) detection, (2) localization, and (3) classification statistics with respect to type, size, and class.

The baseline for computing detection performance included both ordnance and nonordnance items. The detection ratio of 0.72 reflects the number of targets detected by Geo-Centers compared to the total number of baseline ordnance targets in the 16B-hectare area, with the fence line area removed. This detection probability is significantly different than the probability of detection arising from random declarations due to sensor noise and other factors ( $P_{\text{random}} = 0.10$ ). Geo-Centers had a FAR of 84.0 per hectare.

In Phase I, Geo-Centers had a  $P_D$  of 0.53 for ordnance items. The FAR was 14.3 per hectare. A comparison of Phase I and Phase II detection performance shows that Geo-Centers obtained higher  $P_D$  values for Phase II, but higher FAR values as well.

For most demonstrators, the probability of ordnance detection depends on both the size and the depth of the buried ordnance item. Figure 5.4.2-5, which is a scatter plot showing detection performance as a function of size versus depth, illustrates this relationship for Geo-Centers. Geo-Centers was successful at detecting medium and large targets at all depths, but it had difficulty detecting smaller targets (less than 100-mm diameter) at most depths.

The localization error statistics section of Table 5.4.2-1 indicates Geo-Centers' ability to estimate the location of the targets declared. Geo-Centers reported target depths between 0 and 7.8 meters (0 and 25.6 feet) below ground surface. Geo-Centers declared all target detections as ordnance. Geo-Centers provided size and class information.

**Figure 5.4.2-4**  
**Geo-Centers Target Declarations**

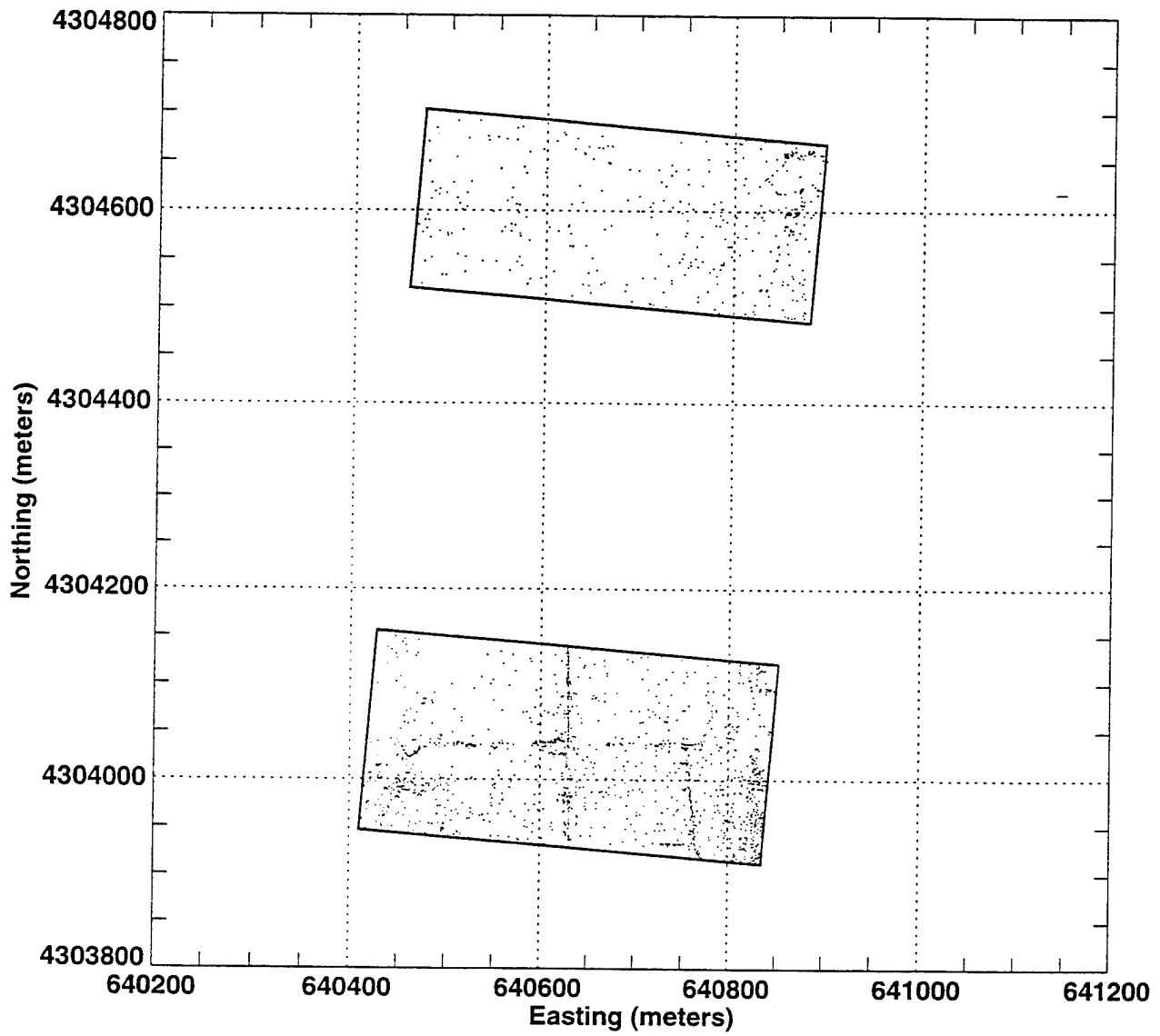


**TABLE 5.4.2-1  
PERFORMANCE STATISTICS FOR GEO-CENTERS**

**Detection Statistics**

	Number Baseline	Number Matched	$P_D^a$
Ordnance	92	66	0.72
Nonordnance	8	8	0.75
Total	100	72	0.72
$P_{random}$	0.10		
Number False Alarms	1,366		
False Alarm Rate	84.0/hectare		
False Alarm Ratio	20.7		
Probability False Alarms	0.1055		

**Localization Statistics**

	Mean (m) <sup>b</sup>	Std. Dev. <sup>c</sup> (m)
Position (x,y)		
dx	0.02	0.63
dy	-0.27	0.67
Radial	0.81	
Depth (z)		
$dz^d$	0.26	0.84
dz	0.88	

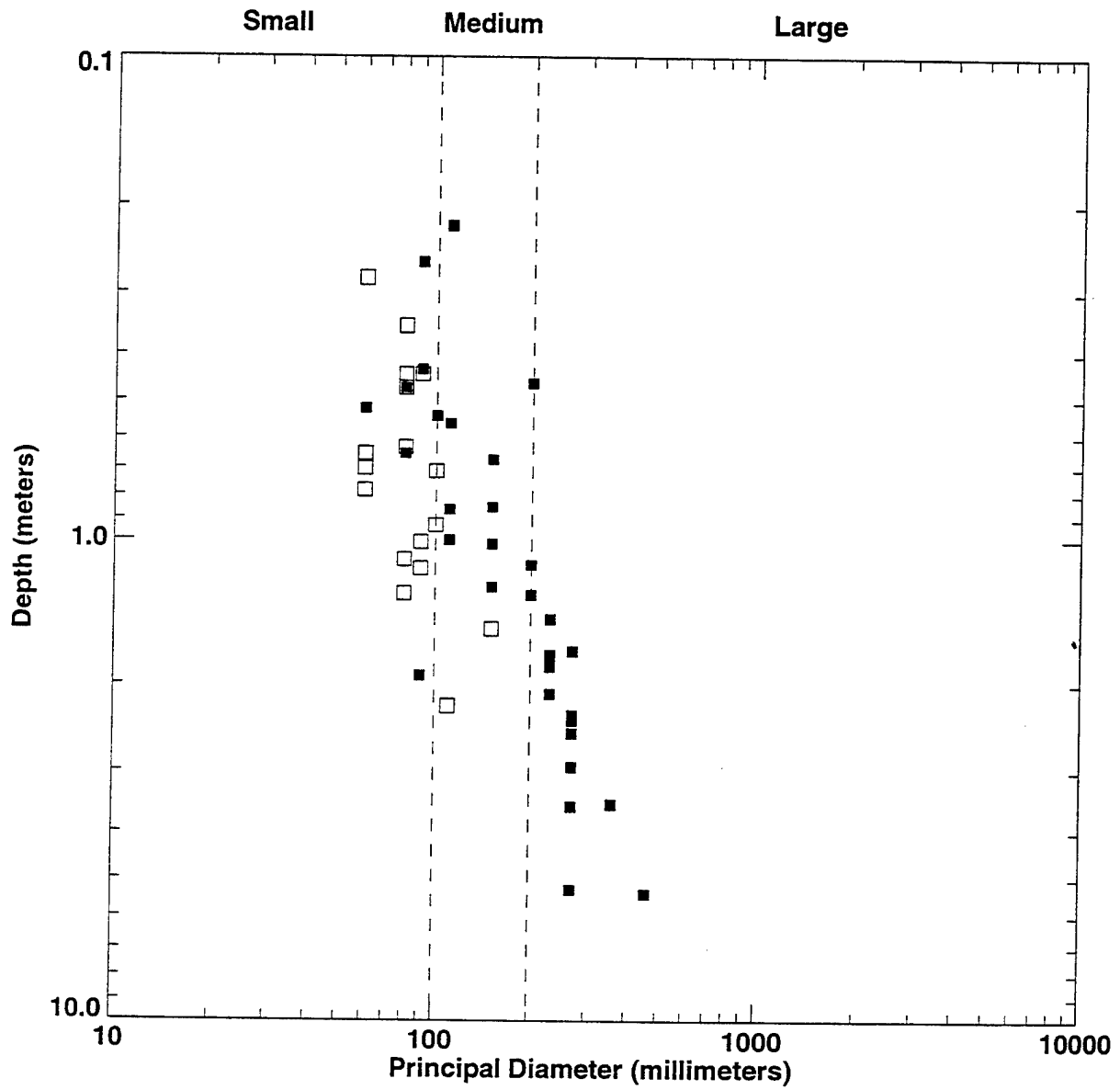
**Identification and Classification Statistics**

	Number Baseline	Number Detected	$P_D^e$	Number Correct	$P_C^f$
Type					
Ordnance	125	68	0.54	68	1
Nonordnance	14	11	0.79	0	0
Size					
Large	31	24	0.77	16	0.67
Medium	23	15	0.65	12	0.80
Small	69	28	0.41	24	0.86
Class					
Bomb	15	15	1.00	14	0.93
Projectile	51	29	0.57	22	0.76
Mortar	53	20	0.38	0	0
Cluster	6	4	0.67	0	0

**Notes:**

- <sup>a</sup> Probability of detection (based on Group TMA, fence area excluded)
- <sup>b</sup> Meter
- <sup>c</sup> Standard deviation
- <sup>d</sup> Square root of the mean square depth error
- <sup>e</sup> Probability of detection (based on closest TMA, fence area excluded)
- <sup>f</sup> Probability of correctly classifying (based on closest TMA)

Figure 5.4.2-5  
Geo-Centers Detection Ability



- Target Detected
- Target Not Detected

### 5.4.3 Geophex Ltd.

Geophex Ltd. (Geophex) demonstrated from August 23 through 27, 1995, at the 16A-hectare area at JPG. Geophex used two man-portable systems for its demonstration.

#### 5.4.3.1 Technology Description

Geophex used four Geometrics G-858 total-field magnetometers and three Geophex electromagnetic GEM-2 units during the demonstration. The G-858 (see Figure 5.4.3-1) consists of a three-axis fluxgate sensor, custom processing electronics, and computer with operating software. According to Geophex, the G-858 provides total-field readings at a rate of 30.7 samples per second with resolution greater than 1 nanotesla. Each G-858 has two cesium magnetometer sensors horizontally separated by 0.76 meter (2.5 feet) and oriented at a 45-degree angle relative to the ground for optimum detection ability. The operator held these sensors about 0.5 meter (1.5 feet) above the ground surface. The data from each sensor are recorded individually on the G-858 along with operator-marked fiducials and time. Each G-858 contains a data control, acquisition, and field display unit (Geophex 1995a).



Figure 5.4.3-1 Geophex Ltd. G-858 Magnetometer



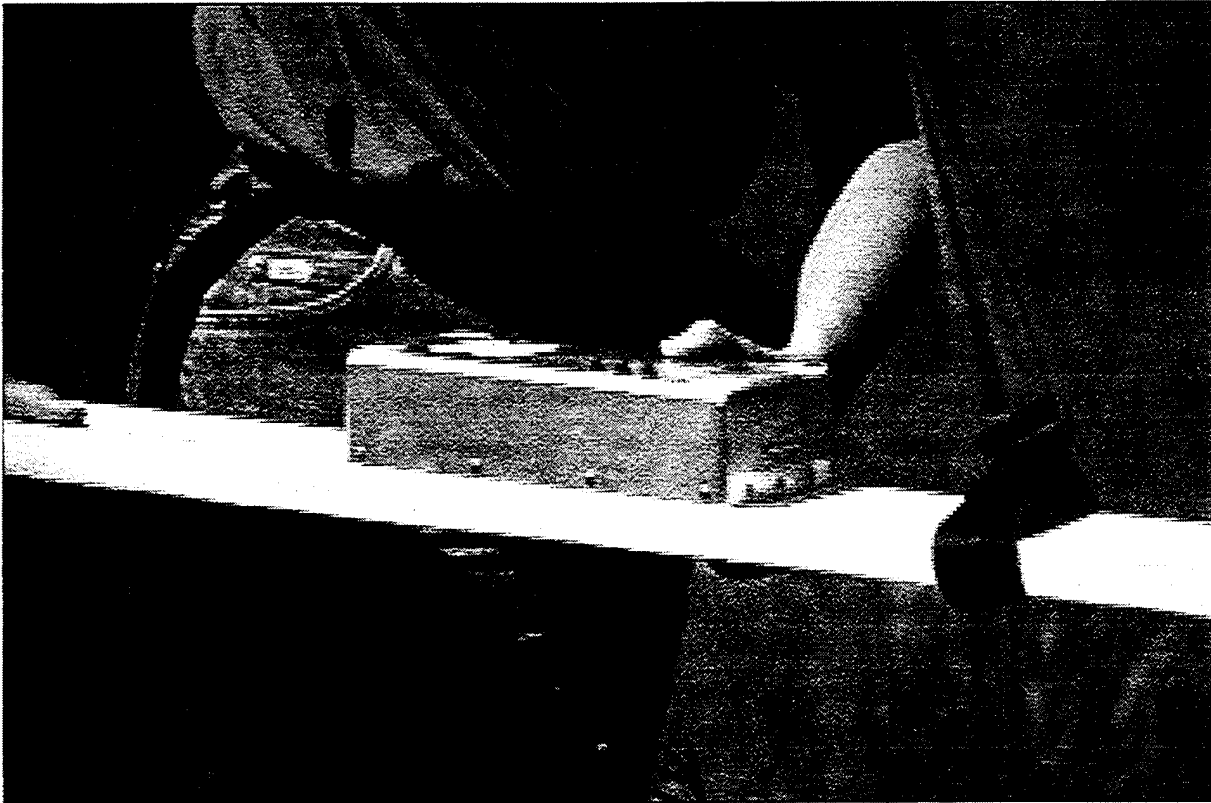


Figure 5.4.3-2 Geophex Ltd. GEM-2 Electromagnetic Unit

The G-858 is used in tandem with three GEM-2 digital, frequency-domain units (see Figure 5.4.3-2), which sense both ferrous and nonferrous materials. The GEM-2 units weigh about 2.0 kilograms (4.4 pounds). The GEM-2 operated simultaneously at two frequencies, 1,350 Hz and 7,290 Hz, using a pulse-width frequency technique. Data are stored in solid-state memory and transferred to a laptop computer in the field. The G-858 measures total magnetic field and changes caused by ferrous material. The GEM-2 measures changes in conductivity to detect ferrous and nonferrous materials. Geophex assimilated magnetic and electromagnetic data for data analysis and processing using a nonlinear inversion algorithm, developed and written by Geophex personnel (Geophex 1995a).

In addition to the G-856 magnetometers and GEM-2 electromagnetic units, Geophex used two Schoensted metal detectors, which were not included in its proposal. These metal detectors were used to verify the existence of subsurface anomalies and the location of metal fencing in the tree lines.

#### **5.4.3.2 System Assessment**

This section summarizes the demonstration by Geophex, based on observations made in the field.

##### **Requirements for Technology Implementation**

Geophex used nine people to complete its demonstration. Geophex personnel alternated as survey crews and support personnel to provide rest periods. Because the G-858 and the GEM-2 were operated by a single person, logistical limitations are a result of human endurance and ability. All system equipment used for this demonstration was driven to JPG by Geophex personnel. Geophex had an ample supply of spare batteries for its survey equipment. No additional equipment was acquired locally.

Geophex originally brought two G-858 magnetometers for this demonstration. However, on the first day of the demonstration, one magnetometer malfunctioned. Geophex received two additional G-858 magnetometers via overnight delivery to complete the last 3 days of the demonstration.

Before conducting the survey, two Geophex personnel cut and cleared thick vegetation and low branches from the site to improve access. The GEM-2 was carried through densely wooded areas much more easily than the G-858 magnetometers. Navigation across the grid was completed using the grid coordinate system on the 16A-hectare area and was aided by spray paint dashes at 1.5-meter (4.9-foot) intervals in the north-south direction. Geophex personnel marked the grid in 30- (north-south) by 60- (east-west) meter (100- by 200-foot) grids prior to surveying. Surveying was completed in east-west fashion.

##### **Operational Capabilities and Limitations**

Both the G-858 and the GEM-2 data were input into a cart-mounted laptop computer powered by a 12-volt car battery. Data were interpreted using two modeling programs developed by Geophex. The data were then gridded for image processing and interpretation. After data review, Geophex determined whether sections of the site needed to be resurveyed. Geophex resurveyed about 2 hectares (5 acres) with G-858 magnetometers.

Data downloading from the dataloggers was completed in the field. Data downloading required 5 to 10 minutes; however, the survey equipment and crew remained in the field to lessen the delay from

downloading. The GEM-2 dataloggers were capable of storing data from about 0.8 hectare (2.0 acres) before downloading was necessary. The G-858 magnetometers were downloaded about every 1.6 hectares (4.0 acres).

#### **5.4.3.3 Measured Performance**

Geophex covered all of the 16A-hectare area with both the G-858 and the GEM-2 in about 37 hours (of 40 hours allotted). Geophex assimilated magnetic (G-858) and electromagnetic (GEM-2) data for analysis and processing to find the spatial position and depth of the larger targets. The interpretations of target size, depth, and confidence levels are based on the final, combined data set (Geophex 1995b). Geophex reported 398 targets within the 16 hectares (see Figure 5.4.3-3). Geophex's performance is shown in Table 5.4.3-1, which presents the following: (1) detection, (2) localization, and (3) classification statistics with respect to type and size. Geophex did not provide class information.

The baseline used to compute detection performance included both ordnance and nonordnance items. The detection ratio of 0.71 (cited as  $P_D$  ordnance in Table 5.4.3-1) reflects the number of targets detected by Geophex as compared to the total number of baseline ordnance targets in the area covered. This detection probability is significantly different than the probability of detection arising from random declarations due to sensor noise and other factors ( $P_{\text{random}} = 0.03$ ). Geophex had a FAR of 19.7 per hectare.

For most demonstrators, probability of ordnance detection depends on both the size and the depth of the buried ordnance item. Figure 5.4.3-4, which is a scatter plot showing detection performance as a function of size versus depth, illustrates this relationship for Geophex. Geophex was more successful at detecting medium and large targets than smaller targets.

The localization error statistics section of Table 5.4.3-1 indicates Geophex's ability to estimate the location of the targets declared. Geophex reported target depths between 0.03 and 5.15 meters (0.10 and 16.90 feet) below ground surface. Table 5.4.3-1 also shows Geophex's type and size capabilities; no class information was provided.

Figure 5.4.3-3  
Geophex Target Declarations

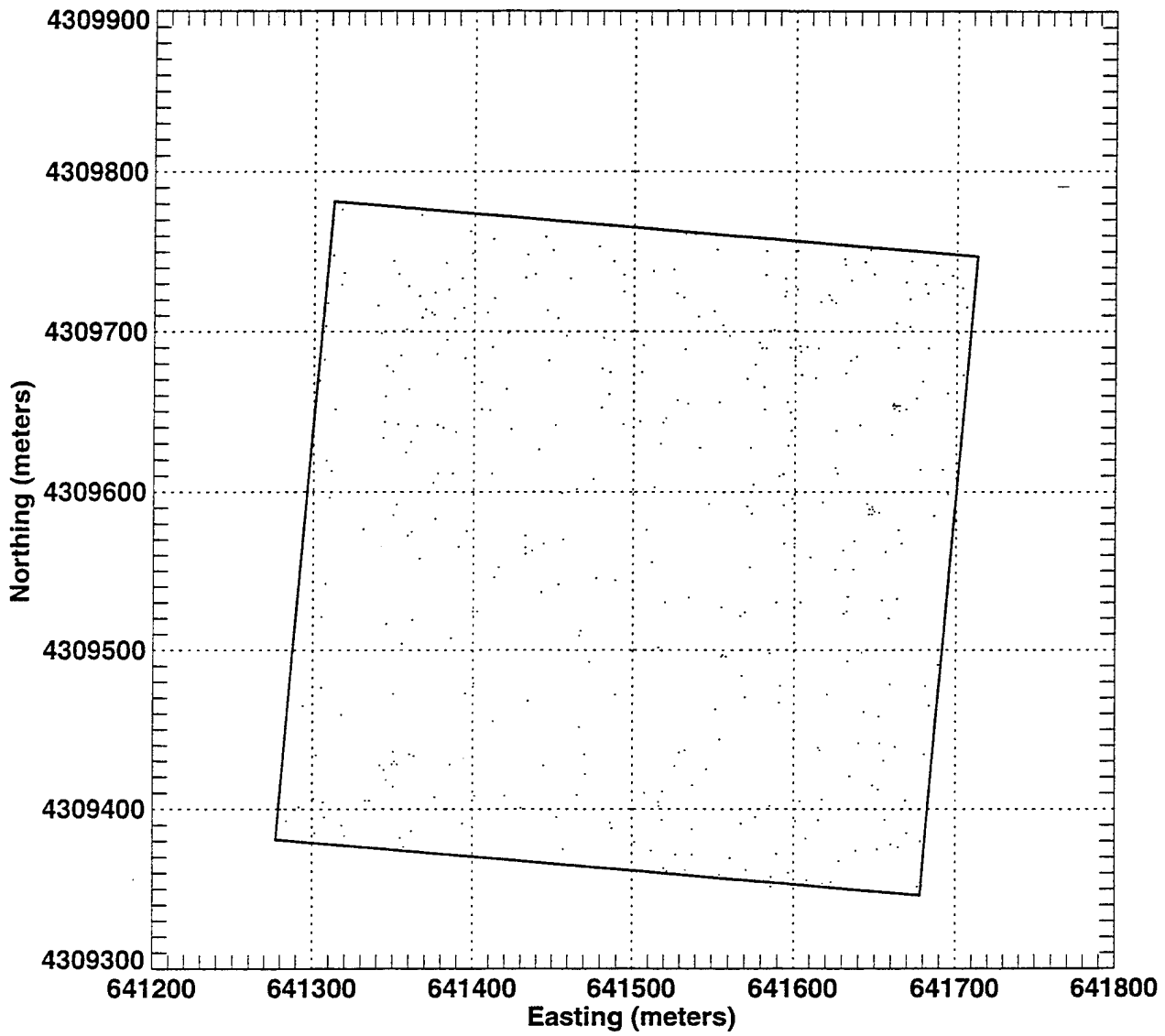


**TABLE 5.4.3-1  
PERFORMANCE STATISTICS FOR GEOPHEX**

**Detection Statistics**

	Number Baseline	Number Matched	$P_D^a$
Ordnance	127	90	0.71
Nonordnance	41	25	0.61
Total	168	115	0.69
$P_{\text{random}}$			0.03
Number False Alarms			307
False Alarm Rate			19.7/hectare
False Alarm Ratio			3.41
Probability False Alarms			0.0248

**Localization Statistics**

	Mean (m) <sup>b</sup>	Std. Dev. <sup>c</sup> (m)
Position (x,y)		
dx	-0.04	0.83
dy	0.01	0.62
Radial	0.91	
Depth (z)		
$dz^d$	0.13	0.61
dz	0.62	

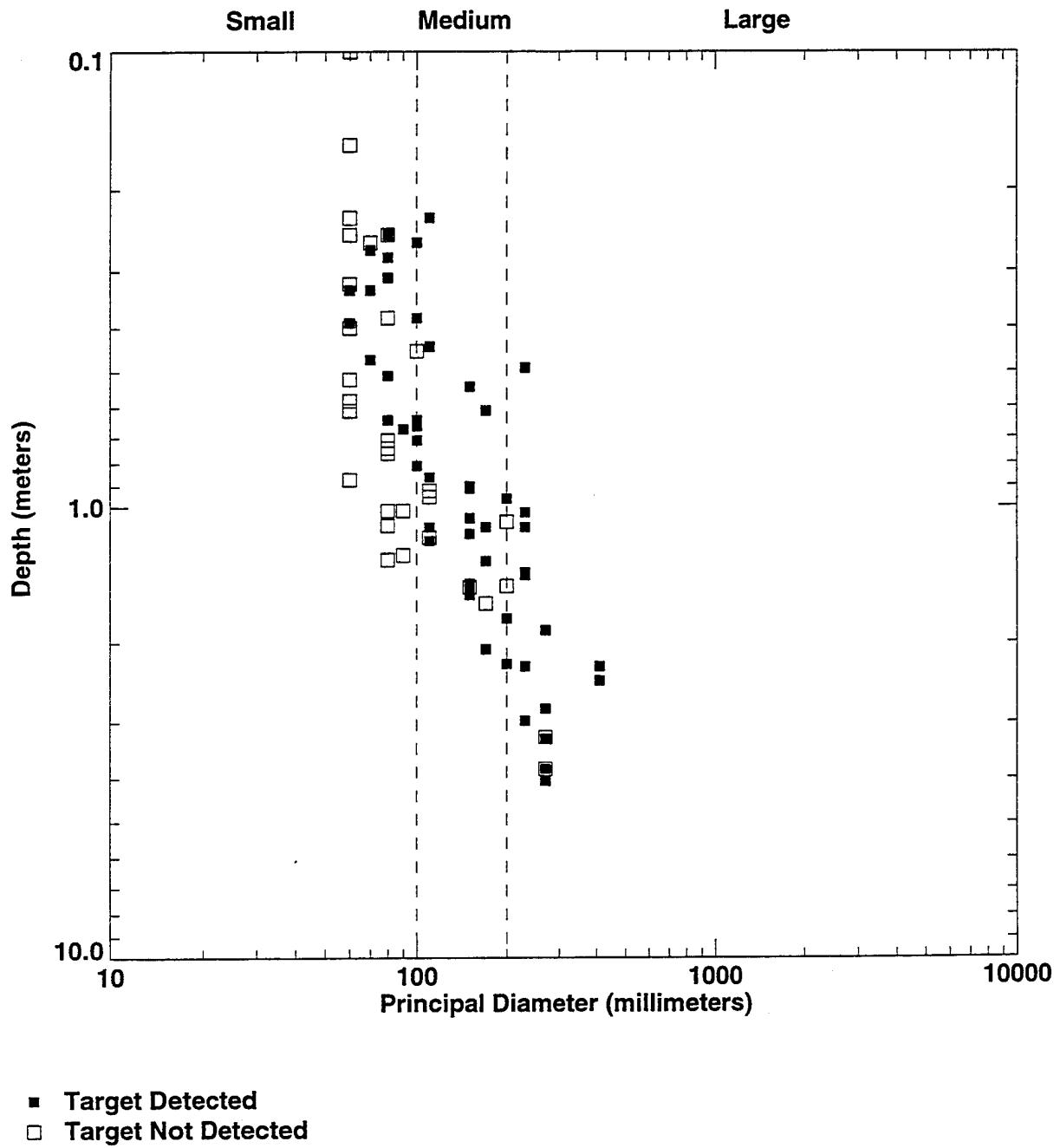
**Identification and Classification Statistics**

	Number Baseline	Number Detected	$P_D^e$	Number Correct	$P_C^f$
Type					
Ordnance	158	90	0.57	86	0.96
Nonordnance	65	31	0.48	7	0.23
Size					
Large	35	25	0.71	22	0.88
Medium	53	37	0.70	14	0.38
Small	69	28	0.41	12	0.43
Class					
Bomb	21	17	0.81	0	0
Projectile	69	40	0.58	0	0
Mortar	59	28	0.47	0	0
Cluster	9	5	0.56	0	0

**Notes:**

- <sup>a</sup> Probability of detection (based on Group TMA, fence area excluded)
- <sup>b</sup> Meter
- <sup>c</sup> Standard deviation
- <sup>d</sup> Square root of the mean square depth error
- <sup>e</sup> Probability of detection (based on closest TMA, fence area excluded)
- <sup>f</sup> Probability of correctly classifying (based on closest TMA)

Figure 5.4.3-4  
Geophex Detection Ability



## 5.5 ELECTROMAGNETIC INDUCTION AND GROUND PENETRATING RADAR SENSOR SYSTEMS

### 5.5.1 Coleman Research Corporation

Coleman Research Corporation (Coleman) demonstrated from June 14 through 18, 1995, at the 16B-hectare area at JPG. Coleman also participated in Phase I of the UXO ATD program.

#### 5.5.1.1 Technology Description

Coleman used the Towed Multi-Sensor Array System (ToMAS) for most of its demonstration at JPG (see Figure 5.5.1-1). According to Coleman, ToMAS is a multisensor detection system capable of detecting metallic and nonmetallic objects and identifying soil characteristic changes. The ToMAS consists of two sensor arrays, including a five-element array of GPR and a three-element array of time-domain

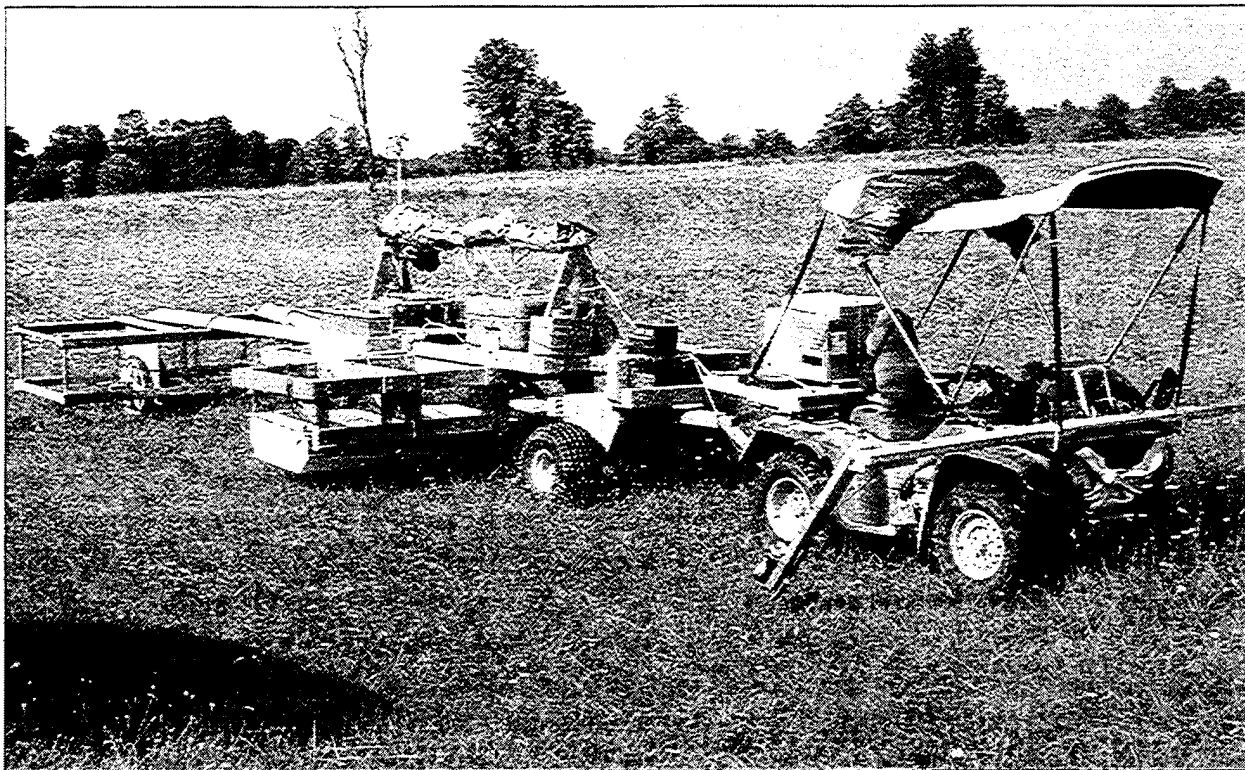


Figure 5.5.1-1 Coleman Research Corporation Towed Multi-Sensor Array System

electromagnetic (TDEM) sensors (also called EM-61 units). The GPR uses a frequency-stepped, wide band radar capable of detecting metallic and nonmetallic objects up to 5 meters (16 feet) deep. The TDEM array detects ferrous and nonferrous metal objects up to 4 meters (13 feet) deep. The sensors cover a 2.44-meter (8.00-foot) scan width. ToMAS is designed to achieve a scan rate of more than 0.8 hectare (2.0 acres) per hour. Data are collected and stored on two distinct media during the scanning process and are later recalled for data post-processing. Coleman uses a data fusion workstation to process and combine the data for two- and three-dimensional displays (Coleman 1995a).

The GPR sensor array portion of ToMAS is a wide band, coherent stepped frequency radar (100 to 1,000 MHz) with receiver and transmitter antennas. The use of a frequency-stepped radar provides greater sensitivity and greater instantaneous dynamic range. The current configuration uses two transmitter and three receiver spiral antennas. The number of receiver and transmitter antennas can be varied as dictated by scan rate requirements and scan width limitations.

The TDEM sensor array used in ToMAS consists of three EM-61 high-sensitivity metal detectors (for a complete description of the EM-61, see Section 5.1.1.1). The EM-61 unit generates electromagnetic pulses at 15 Hz, and performs measurements during the off-time between pulses. The EM-61 system pauses until the response from the conductive earth dissipates, then measures the prolonged metal response from buried metal objects.

Location scanning and grid layout were achieved by combining differential GPS and linear position encoder wheel data. The key components of the differential GPS and data capture system are the differential base station, the remote GPS station, the RF communication link, a linear position encoder wheel, and the data processing computer. The base station computes its current GPS location and compares it to stored reference data. The differences (on a satellite-by-satellite basis) are transmitted to the remote GPS over the RF modem and are used to correct for the majority of the GPS errors. This allows for real-time track accuracies of two meters on moving vehicles. Better accuracy is possible with postfiltering.

The second system used by Coleman was a single EM-61 that was used in areas inaccessible by ToMAS. Coleman used the grid layout to navigate the single EM-61 in these inaccessible areas.



GPR data are processed using fast, two-dimensional synthetic aperture imaging algorithms; the TDEM data are processed through algorithms developed by Coleman for improved lateral and vertical resolution. A data fusion workstation uses synergism between the sensors, physical models, and the position data from the differential GPS navigation system to build and display three-dimensional, multisensor reconstruction of the data (Coleman 1995a).

System improvements from Phase I for Colman's ToMAS include: modifications to the GPR antennae and RF receiver; installation of differential GPS processing algorithms; improved data processing; and the addition of a hand-held EM-61 unit for coverage in areas inaccessible by the ToMAS (Coleman 1995a).

#### **5.5.1.2 System Assessment**

This section summarizes the demonstration by Coleman, based on observations made in the field.

#### **Requirements for Technology Implementation**

Coleman used five people to complete its demonstration. Two people operated the ToMAS, alternating to provide rest periods. The remaining three people analyzed the data and operated the hand-held sensor as needed.

The ToMAS sensors, the ATV, and the GPS equipment were driven to JPG by Coleman personnel in a panel truck. Coleman used two laptop computers to store and process the data, two minivans to transport personnel and supplies, and a panel truck to store the assembled equipment in the field. Coleman marked the area surveyed in the field with spray paint while moving in a helical fashion towards the inside of the grids; the GPS recorded the positional movement of ToMAS. A tarp secured with elastic straps was used to cover the ToMAS. Coleman used the electrical supply provided at the support trailer to recharge the system batteries. No equipment was acquired locally.

#### **Operational Capabilities and Limitations**

The ToMAS can cover about 0.8 hectare (2.0 acres) per hour depending on the terrain. The large trees and deep ruts in part of the area were difficult for the ToMAS to maneuver around. Downloading of the

collected data was required about every 4 hours and took 45 minutes to complete. The ToMAS system experienced numerous delays due to equipment failure. The EM-61 array of the ToMAS had several flat tires as well as wheel bearing failures. Coleman also experienced electronic problems with the ToMAS at one point during the demonstration, and the EM-61 array was not operational for some of the time as well. All of these mechanical problems were corrected on site.

### 5.5.1.3 Measured Performance

Coleman covered all of the 16 hectares with its combined systems during the allotted 40 hours. Coleman reported 280 targets within the 16B-hectare area with the fence line area removed (see Figure 5.5.1-2) (Coleman 1995b). An analysis of Coleman's performance is shown in Table 5.5.1-1, which presents the following: (1) detection, (2) localization, and (3) classification statistics with respect to size and class. Coleman did not provide type information.

The baseline for computing detection performance included both ordnance and nonordnance items. The detection ratio of 0.29 ( $P_D$  ordnance) reflects the number of targets detected by Coleman compared to the total number of baseline ordnance targets in the 16 hectares. This detection probability is significantly different from the probability of detection arising from random declarations due to sensor noise and other factors ( $P_{\text{random}} = 0.02$ ). Coleman had a FAR of 15.9 per hectare. It is not known to what degree Coleman's relatively low score was influenced by the use of GPR.

As part of Phase I, Coleman had a  $P_D$  of 0.40 for ordnance items. Coleman's FAR was 56.0 per hectare. A comparison of Phase I and Phase II detection performance shows that Coleman had a lower  $P_D$  value for Phase II as compared to Phase I. Lower detection performance in Phase II may have been caused by the increased rainfall in May and the affects of soil moisture on GPR performance. Coleman performed Phase I activities in early August 1994 and Phase II activities in June 1995. However, Coleman's FAR improved in Phase II, to 15.9 per hectare as compared to 56.0 in Phase I.

For most demonstrators, the probability of ordnance detection depends on both the size and depth of the buried ordnance item. Figure 5.5.1-3, which is a scatter plot showing detection performance as a function of size versus depth, illustrates this relationship for Coleman. Coleman was able to detect most of the medium targets, but had difficulty detecting small and large targets.

The localization error statistics section of Table 5.5.1-1 indicates Coleman's ability to estimate the locations of the targets declared. Coleman reported target depths between 0.1 and 3.0 meters (0.3 and 9.8 feet) below ground surface. Coleman declared all detections as ordnance. Coleman did provide size and class information as indicated in the table.

Figure 5.5.1-2  
Coleman Target Declarations

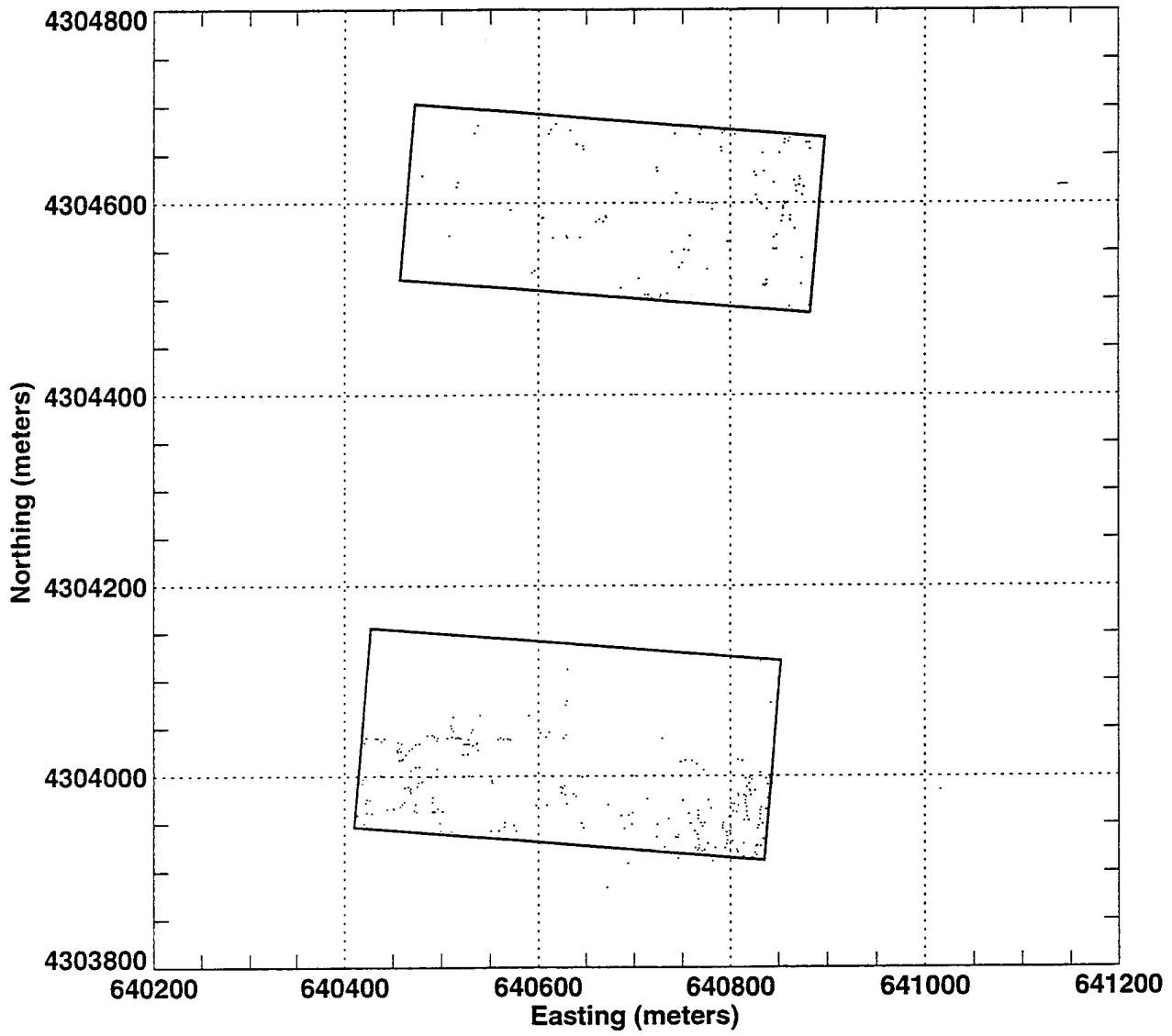


**TABLE 5.5.1-1  
PERFORMANCE STATISTICS FOR COLEMAN**

**Detection Statistics**

	Number Baseline	Number Matched	$P_D^a$
Ordnance	92	27	0.29
Nonordnance	2	8	0.25
Total	100	29	0.29
$P_{random}$	0.02		
Number False Alarms	258		
False Alarm Rate	15.9/hectare		
False Alarm Ratio	9.56		
Probability False Alarms	0.0199		

**Localization Statistics**

	Mean (m) <sup>b</sup>	Std. Dev. <sup>c</sup> (m)
Position (x,y)		
dx	-0.05	1.04
dy	0.30	1.02
Radial	1.41	
Depth (z)		
$dz^d$	-0.36	0.95
dz	1.00	

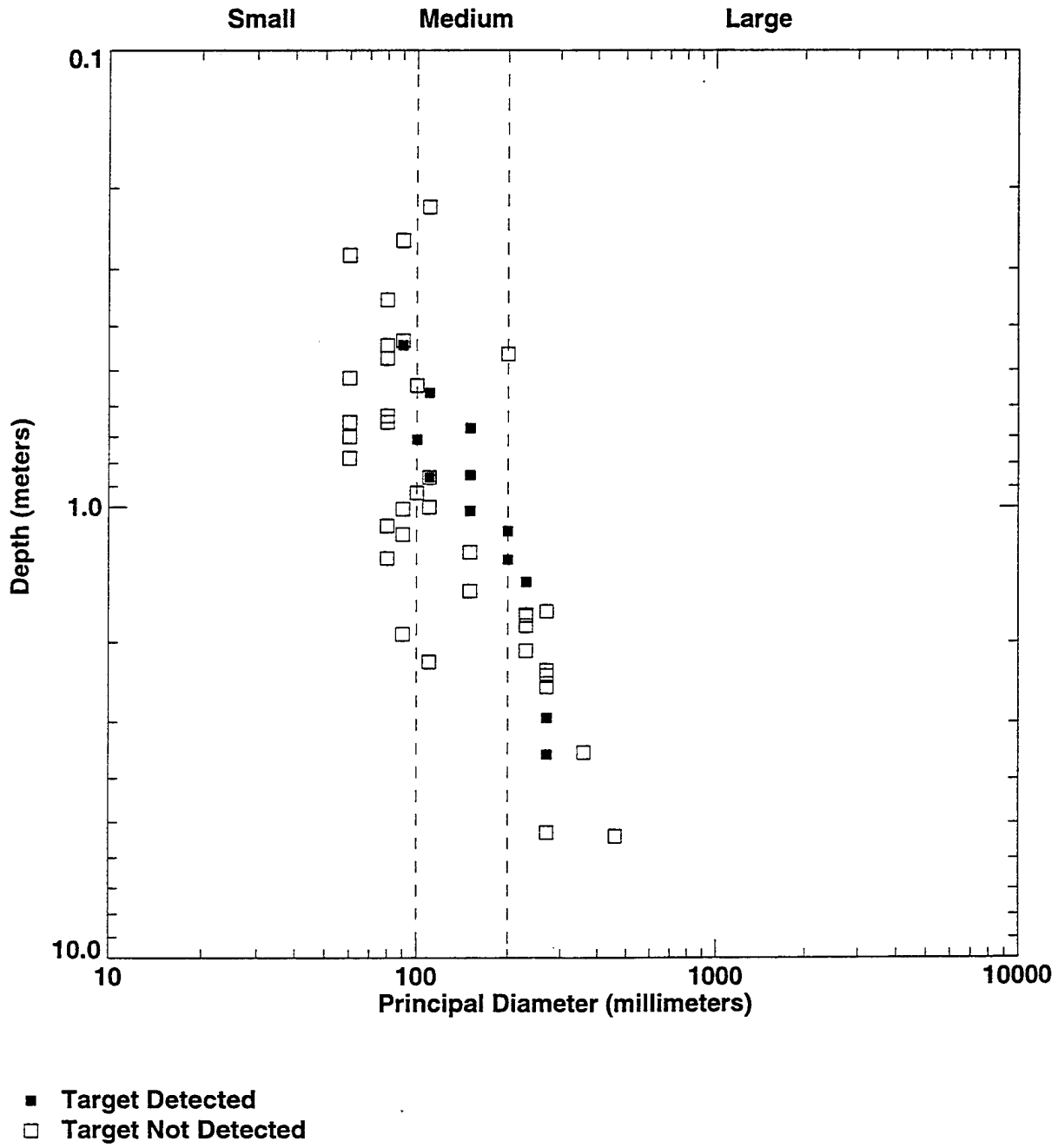
**Identification and Classification Statistics**

	Number Baseline	Number Detected	$P_D^e$	Number Correct	$P_C^f$
Type					
Ordnance	125	29	0.23	29	1.00
Nonordnance	14	2	0.14	0	0
Size					
Large	31	7	0.23	1	0.14
Medium	23	8	0.35	2	0.25
Small	69	13	0.19	12	0.92
Class					
Bomb	15	3	0.2	1	0.33
Projectile	51	15	0.29	13	0.87
Mortar	53	10	0.19	0	0
Cluster	6	1	0.17	0	0

Notes:

- <sup>a</sup> Probability of detection (based on Group TMA, fence area excluded)
- <sup>b</sup> Meter
- <sup>c</sup> Standard deviation
- <sup>d</sup> Square root of the mean square depth error
- <sup>e</sup> Probability of detection (based on closest TMA, fence area excluded)
- <sup>f</sup> Probability of correctly classifying (based on closest TMA)

**Figure 5.5.1-3**  
**Coleman Detection Ability**



## **5.6 REMEDIATION SYSTEMS**

Two remediation systems were demonstrated at JPG for Phase II of the UXO ATD program. Concept Engineering Group, Inc., demonstrated a system called the soft trencher, and Wright Laboratory demonstrated a remote excavating vehicle system.

### **5.6.1 Concept Engineering Group, Inc.**

Concept Engineering Group, Inc. (CEG), demonstrated from September 6 through 8, 1995, at the 16A-hectare area at JPG. CEG's soft trencher was used to demonstrate remediation of known ordnance.

#### **5.6.1.1 Technology Description**

CEG's soft trencher is a mobile, self-propelled, platform-type excavation technology ( see Figure 5.6.1-1). The soft trencher weighs 15,436 kilograms (kg) (34,030 pounds) and is powered by a 275-horsepower Detroit Diesel D-DEC engine, which drives four hydraulic pumps. All of the soft trencher's systems are hydraulically operated. The soft trencher functions manually in the field and is not guided by a ground positioning navigation system. The system is capable of digging trenches up to 1.8 meters (6 feet) wide and 3.0 meters (10 feet) deep, although it can be modified to excavate to about 4 meters (13 feet). The soft trencher has a retractable lift, which removes soil-type materials while excavating, and uses a multistage vacuum and filter system for soil excavation and discharge. A conveyor belt moves soil away from the system and deposits it at the back or side of the machine (CEG 1995a).

The "hood" of the soft trencher uses supersonic air jets and a pneumatic vacuum to transport soil during excavation. The soft trencher uses the high speed air to penetrate and dislodge soil without breaking or puncturing ordnance. The soft trencher consists of a digging assembly that uses the excavation head to loosen the soil with supersonic airjets. The suction tubes combine with a vacuum to aerate materials.

The soft trencher is operated by a remote, portable box equipped with joysticks to allow the operator to control the excavator from distances up to 7.6 meters (25 feet) from the excavator. The system also includes an operator's seat with a conventional steering wheel, accelerator, brakes, and mirror to maneuver the machine to site excavation targets.

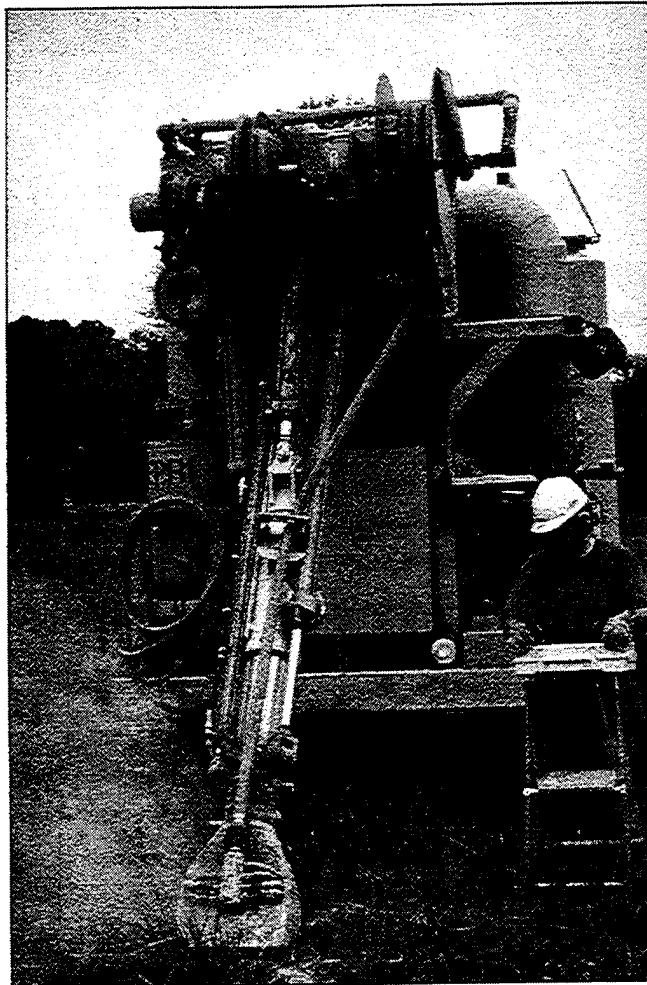


**Figure 5.6.1-1 Concept Engineering Group, Inc.  
Soft Trencher System**

### **5.6.1.2 System Assessment**

This section summarizes the CEG demonstration, based on observations made in the field.

#### **Requirements for Technology Implementation**

Two people were on site for this demonstration. One person drove the vehicle and performed excavation activities. The other observed progress of the excavation activities near the target. CEG personnel used the site trailer for telephone use only.



CEG used local contractors to support its field operations at JPG. Valley Industrial Supply Company Inc., of Madison, Indiana, provided both small and large mechanical parts, including bolts and winches. Sedam Construction Company provided welding support services to weld and reweld cracks in the excavator hood on two separate occasions. Bullock Oil Company provided a 300-gallon diesel tank with fuel.

CEG needed a support vehicle stocked with field supplies such as gloves, drip pans, and measuring tapes, which they did not have. These supplies were all purchased and provided to CEG. No other unique support was provided to CEG other than occasional transport out to the field, which was necessary because CEG did not have a field vehicle.

### **Operational Capabilities and Limitations**

Due to its large size [2.6 meters (8.5 feet) wide, 8.4 meters (27.6 feet) long, and 3.5 meters (11.5 feet) high], the soft trencher has limited maneuvering ability. To navigate in off-road conditions, its rubber tires must be changed to a track mount. The soft trencher was demonstrated during predominantly dry weather; otherwise, the vehicle may have required towing by a large support vehicle such as a bulldozer.

The soft trencher has two types of excavation hoods: cylinder rotating and rectangular. The cylinder rotating hood was used briefly, but this hood was not capable of cutting through the hard, dense, silty clays characteristic of the glacial soils found at JPG. The rectangular hood was more successful because its excavation head has more air pressure. The rectangular hood was also used to physically move soil in and around the excavation area.

In the initial excavation at each target, high grass and weeds caused the intake hood to plug. Additionally, the rectangular excavation hood and the conveyor system also became clogged in the field, because the dense silty clays were sometimes wet and included large angular chert-type rock fragments. These rock and soil formations prevented continuous operations for 10- to 15-minute periods. CEG used a shovel or a large metal rod to remove clogged soils from the hood and conveyor belt.

Two problems occurred with the soft trencher hydraulics. The first involved a cracked hydraulic hose feeding the lower boom extension cylinder. The hose was by-passed, but this reduced excavation depths to about 2 meters (6.6 feet). The second problem involved the inlet fitting to the boom lift cylinder. The inlet

fitting was struck by the top head of the lower boom extension cylinder and forced out of the cylinder head. This could only be repaired by replacing the cylinder head, which could not be done in the field. At this point, the demonstration was terminated.

### **5.6.1.3 Measured Performance**

CEG excavated 14 targets in 18.5 of the 24 hours allotted for its demonstration. Table 5.6.1-1 provides details of the demonstration results. The soft trencher excavated targets consisting of 81-, 105-, 106-, 152-, 155-, and 175-millimeter (mm) projectiles; 8-inch projectiles; and a 250-pound bomb. The targets were excavated in the order in which they appear in Table 5.6.1-1. Due to the limitations of the soft trencher, targets were not removed from the excavation before backfilling. The travel rate to each target was determined from the straight line distance between start and finish points of travel and the time required for that travel. The duration of the target excavation includes downtime associated with repair of the soft trencher (CEG 1995b).

CEG successfully excavated 10 of the 14 targets. A target was considered successfully excavated if it was unearthed and observed entirely by remote excavation. Three of the four targets not successfully excavated were nonbase-line targets (anomalies). After excavation of these targets, it was determined in the field using a Schoenstedt metal detector that no ordnance was apparent in the excavation. Initial detection of the target could possibly have been due to the magnetic signature of the soil.

**TABLE 5.6.1-1**  
**CONCEPT ENGINEERING GROUP, INC.**  
**16A-HECTARE AREA**

Target No.	Target Class	Travel Rate (km/hr)	Depth (meters)	Excavation Duration (hr)	Ordnance Found <sup>a</sup>
972	Unknown	0.09	0.33	1.72	No <sup>b</sup>
222	175-mm projo	1.10	0.70	0.15	Yes
211	250-lb bomb	0.98	0.30	2.22	Yes
1030	106-mm projo	0.55	1.0	0.27	Yes
236	81-mm projo	0.91	1.15	0.15	Yes
213	8-inch projo	3.66	2.44	2.55	Yes
913	Unknown	1.19	1.0	0.45	No <sup>b</sup>
219	155-mm projo	1.14	1.31	0.20	Yes
942	Unknown	0.64	1.0	0.28	No <sup>b</sup>
282	8-inch projo	0.30	1.4	1.30	Yes
242	155-mm projo	1.10	0.90	0.23	Yes
359	105-mm projo	1.04	0.37	0.6	Yes
1016	152-mm projo	4.39	1.0	0.25	Yes
1017	155-mm projo	0.31	1.06	0.08	No <sup>c</sup>
Average		1.24 km/hr		0.75 hr/hole	

**Notes:**

<sup>a</sup> Yes = Ordnance was found during excavation with the soft trencher.

No = Ordnance was not found.

<sup>b</sup> Nonbase-line targets (anomaly) investigated as part of remediation, possibly due to magnetic signature in soil

<sup>c</sup> Soft trencher breakdown; demonstration was terminated

hr Hour  
 km Kilometer  
 lb Pound  
 mm Millimeter  
 projo Projectile

## 5.6.2 Wright Laboratory

Wright Laboratory Remote Excavation Vehicle System (REVS) was demonstrated from September 22 through 25, 1995, at the 16A-hectare area at JPG. Wright Laboratory also participated in Phase I of the UXO ATD program, demonstrating its Autonomous Ordnance Excavator (AOE). Both systems were used to demonstrate remediation of known ordnance.

### 5.6.2.1 Technology Description

The REVS consists of a 36,320 kg (80,071 pounds) remote excavation vehicle and a mobile command station (MCS). Figure 5.6.2-1 shows the REVS excavation vehicle. REVS is designed as a robotic excavator for autonomous control. However, the autonomous operations such as traveling to a target,



Figure 5.6.2-1 Wright Laboratory Remote Excavation Vehicle

vehicle auto leveling, and target overburden soil removal were not demonstrated. Only teleoperated manipulation with an enhanced graphical user interface was demonstrated (Wright Laboratory 1995).

The vehicle features a Caterpillar mobile track system with two wide rubber tracks for travel on paved surfaces. The mobile track system allows travel up to 22.5 kilometers per hour (km/hr) (14 miles per hour). The excavator is powered by a 300-horsepower Cummins diesel engine and equipped with a 5-kilowatt generator. A Caterpillar 225 boom assembly is mounted for excavation operations. A Balderson thumb is installed on the bucket for grasping objects. A real-time GPS and a Modular Azimuth Positioning System (MAPS) are installed on the vehicle to provide precise positioning of the excavator at the target location. MAPS provides the remote operator with the proper orientation of the vehicle during travel and excavation. Linear displacement transducers are built into the excavator's hydraulic cylinders, referred to as actuators, to determine the overall position of the boom, stick, and bucket. This information is returned to the MCS and graphically displayed to the remote operator.

The MCS houses the remote operator station to control teleoperation. The base vehicle for the MCS is a Chevrolet Multi-Stop van. A telescoping, 9.1-meter- (30-foot-) high mast turret camera system provides a 300-degree view and maintains proper orientation of the directional antennae for an optimal communication link with the vehicle. The REVS is capable of 0.62-kilometer (1-mile) line of sight operations. The MCS is equipped with a base-station GPS to provide differential correction of the vehicle location. A Sun Sparc 20 workstation provides the graphic user interface for computer control of outrigger deployment, on-board camera selection, and engine throttle. It also provides real-time graphic orientation of the vehicle. Before each excavation, the latitude, longitude, and depth of the target is entered into the workstation on board the MCS. The MCS requires two operators, one teleoperator for control of the REVS and one operator for the computer interface control. A joystick controller provides the teleoperator with multiple levels of control.

#### **5.6.2.2 System Assessment**

This section summarizes the CEG demonstration, based on observations made in the field.

## **Requirements for Technology Implementation**

Wright Laboratory used five people to conduct its demonstration. Two people operated the vehicle and controlled the computer interface. The other three people included a project leader and two design engineers for electrical and mechanical problem solving. At least one person remained at the excavation area to observe the vehicle during excavation. As a precaution, the observer stopped excavation activities several times during the demonstration so that the REVS could be repositioned near the excavation.

Wright Laboratory personnel used the support trailer for telephone use only. The support tent at the 16A-hectare area was used to store equipment and a support vehicle (a six-wheeled John Deere Gator).

The REVS was used to backfill two shallow excavations that resulted from the excavation of two anomalies, Targets No. 128 and 149. Several small pieces of metal were identified at Target No. 128 and are the possible remains of old farm equipment. Target No. 149 was possibly identified from magnetic properties of the soil. Although the vehicle is equipped with a bulldozer blade, the on-board cameras did not show an overview or positioning of the vehicle near the excavation, making teleoperation of backfilling activities difficult. A local excavation company was subsequently hired to backfill the remaining target excavations.

## **Operational Capabilities and Limitations**

Navigation across the grid was conducted by the remote teleoperator and aided by on-board cameras and MAPS. MAPS provided a computer-graphic aerial view of the 16A-hectare area showing the location of the target and the vehicle. The on-board cameras provided the immediate view for navigation around obstacles. However, smaller obstacles, such as grid stakes, could not be seen by the vehicle operator and were often run over.

The vehicle was equipped with four on-board fixed-lens cameras. During the demonstration, the camera attached to the boom located directly above the bucket failed and had to be replaced with the front-facing overview camera on top of the vehicle, since Wright Laboratory personnel did not have a spare camera. Several times throughout the demonstration, the communication link between the vehicle and MCS was lost, and the REVS computer had to be rebooted. Each incident resulted in about 10 to 15 minutes of downtime.

During remediation of the second target, Target No. 1031, the vehicle operator grasped the target with the Balderson thumb to remove it from the excavation. During removal, the bucket was closed onto the thumb bending the thumb actuator. Wright Laboratory personnel indicated that this is a design flaw because the thumb actuator should retract when excessive force is added to the bucket. The thumb was removed from the vehicle, and the actuator was secured to the boom with a chain.

The vehicle's bucket had teeth about 0.35-meter- (1.1-foot-) long. During every target excavation, these teeth displaced the target so that the azimuth and declination could not be determined. Very often the target could not be identified by the REVS cameras, but were located during field examination using a Schoenstedt metal detector. REVS was unable to remotely locate targets smaller than 106 mm in the clayey native soil at JPG. Larger targets (250- and 500-pound bombs) were also masked by clay and could not be identified until a field investigation was performed with a Schoenstedt metal detector.

Two problems occurred with the REVS hydraulics. Personnel first had to replace an O-ring on a leaking fitting, and when a second O-ring on the stick cylinder failed, Wright Laboratory personnel did not have a replacement O-ring, and the demonstration was terminated.

### **5.6.2.3 Measured Performance**

Wright Laboratory excavated 11 targets in 23.5 of the 24 hours allotted for its demonstration. Table 5.6.2-1 details the results of the REVS demonstration. REVS remediated targets consisting of 60-mm mortars, 106- and 155-mm projectiles, and 250- and 500-pound bombs. The targets were remediated in the order in which they appear in Table 5.6.2-1. The travel rate to each target was determined from the straight line distance between start and finish points of travel and the time required for that travel. The duration of the target excavation includes downtime associated with rebooting the computers on board the vehicle when necessary and searching the excavation with the Schoenstedt metal detector.

REVS remotely excavated 5 of the 11 targets. A target was considered remotely excavated if it was observed and remediated entirely by video surveillance. A target was considered manually excavated if it was located using a metal detector.

**TABLE 5.6.2-1  
WRIGHT LABORATORY  
16A-HECTARE AREA**

Target No.	Target Class	Travel Rate (km/hr)	Depth (meters)	Excavation Duration (hr)	Excavation Method <sup>a</sup>
306	250-lb bomb	2.1	2.98	1.45	Manual
1031	250-lb bomb	2.1	1.11	0.67	Remote
307	250-lb bomb	1.5	2.37	1.55	Manual
346 <sup>b</sup>	106-mm projo	1.5	0.47	0.08	Remote
350 <sup>c</sup>	60-mm mortar	2.9	0.03	0.17	Manual
319	106-mm projo	2.7	0.23	0.07	Manual
304	250-lb bomb	1.8	1.40	0.23	Remote
1033	500-lb bomb	4.4	2.80	0.72	Remote
1017	155-mm projo	2.9	1.06	0.25	Manual
1004	155-mm projo	5.5	0.54	0.05	Remote
205	500-lb bomb	3.7	3.81	1.03	Manual
Average		2.83 km/hr		0.57 hr/hole	

**Notes:**

- <sup>a</sup> Remote = Ordnance was identified on video surveillance during excavation.  
Manual = Ordnance was found using a Schoenstedt metal detector.
- <sup>b</sup> Target No. 346 was found while removing overburden soil for the excavation of Target No. 307.
- <sup>c</sup> Adjacent targets No. 351 and 352 were also removed during excavation of Target No. 350 and were found using a Schoenstedt metal detector.

hr     Hour  
 km    Kilometer  
 lb     Pound  
 mm    Millimeter  
 projo Projectile



## 6.0 COMPARISONS AND CONCLUSIONS

The overall objective of the Phase II demonstration was to evaluate individual sensor performance and overall technology performance to provide useful information for UXO technology end-users. Specifically, demonstrators were to determine target location; localize ordnance below the surface; identify and classify ordnance with respect to type, size, and class of ordnance; and in the case of remediation demonstrators, excavate targets.

### 6.1 PERFORMANCE STATISTICS SUMMARY

Tables 6-1 and 6-2 summarize individual demonstrator performance statistics grouped by the sensor technology employed. Performance statistics for the individual demonstrators were evaluated by detection, localization, identification, and classification.

#### Detection Performance

When assessing the detection performance of a system, both the UXO detection capability and the number of false alarms must be considered. In Figure 6-1, the  $P_D$  values for ordnance items are plotted for each demonstrator. Figure 6-2 presents a similar plot showing the FAR values in number per hectare, for each of the demonstrators. These statistics are combined in Figure 6-3, which plots  $P_D$  versus  $P_{FA}$ . In this plot, demonstrators with better detection performances are located toward the upper left corner of the plot; those with the poorer detection performance are located toward the lower right corner. Two of the Phase II performers had  $P_D$  values greater than 0.8 and  $P_{FA}$  values less than 0.05.

Demonstrators using ground-based magnetometer sensors (ADI, Geometrics, Scintrex, and Vallon) had a probability of detection for ordnance in the range of 0.50 to 0.83. The detection capability of magnetometer sensors appears to be based on the operation of the equipment and data processing. Geometrics recorded the highest  $P_D$  (0.83) using a hand-held magnetometer; Geometrics also employed advanced data processing. When results for the four ground-based magnetometer sensor systems are compared, it appears that Geometrics' advanced data processing may account for its higher  $P_D$  value. The one airborne demonstrator (Aerodat) using magnetometer sensors had little or no detection capability (0.02).

**TABLE 6-1  
DEMONSTRATOR DETECTION AND LOCALIZATION BY SENSOR TYPE**

Sensor Type	Demonstrator	Detection			Localization			System	
		$P_D$ (Ord)	False Alarm Rate (no./hectare)	Probability False Alarm ( $P_{FA}$ )	$P_{random}$	Horizontal (Radial) (m)	Vertical ( Depth ) (m)		Vertical (Mean) (m)
Magnetometer (MAG)	Geometrics	0.83	26.7	0.03	0.04	0.65	0.62	0.21	3.96
	ADI (MAG)	0.63	31.7	0.04	0.04	0.74	0.68	0.14	8.88
	Vallon	0.57	225.9	0.28	0.25	0.83	0.98	0.02	68.5
	Scintrex	0.50	45.3	0.06	0.06	0.94	0.87	0.39	10.1
	Aerodat	0.02	2.3	0.02	0.02	2.29	2.07	-1.87	18.5
Electromagnetic (EM)	Parsons	0.85	32.5	0.04	0.05	0.79	0.72	-0.24	4.68
	Bristol	0.62	38.2	0.05	0.05	1.04	0.97	-0.66	6.97
	GeoPotential	0.11	12.0	0.02	0.02	1.30	0.80	-0.38	13.0
Ground-Penetrating Radar (GPR)	AES	0.05	0.9	0.01	0.01	2.76	0.99	-0.49	3.11
	SRI	0.01	2.6	0.02	0.02	3.49	2.42	-2.38	27.7
	Kaman	0.00	4.2	0.01	0.01	NA	NA	NA	NA
Magnetometer and Electromagnetic	Geo-Centers	0.72	84.0	0.11	0.10	0.81	0.88	0.26	20.7
	Geophex	0.71	19.7	0.02	0.03	0.91	0.62	0.13	3.41
	ADI (MAG and EM)	0.65	34.5	0.04	0.05	0.74	0.68	0.12	9.35
EM and GPR	Coleman	0.29	15.9	0.02	0.02	1.41	1.00	-0.36	9.56

Note: NA Not applicable

**TABLE 6-2  
DEMONSTRATOR IDENTIFICATION AND CLASSIFICATION (TYPE, SIZE, AND CLASS) BY SENSOR TYPE**

Sensor Type	Demonstrator	Type		Size			Class					Survey Site	
		Ordnance	Nonordnance	Large	Medium	Small	Bombs	Projectiles	Mortars	Clusters			
Magnetometer	Geometrics <sup>1</sup>	1.00	0.00	0.74	0.54	0.80	NA	NA	NA	NA	NA	NA	16A
	ADI (MAG)	0.75	0.11	0.65	0.57	0.96	0.77	0.42	0.35	0.00	0.00	0.00	16B
	Vallon <sup>2</sup>	NA	NA	0.17	0.88	0.38	0.33	0.00	0.00	0.00	0.00	0.00	16B
	Scintrex	0.95	0.00	0.50	1.00	0.25	0.75	0.40	0.33	NA	NA	NA	16A
	Aerodat <sup>2</sup>	NA	NA	NA	NA	NA	NA	NA	NA	NA	NA	NA	32
	Parsons	0.78	0.10	0.16	0.75	0.23	0.12	0.57	0.25	0.00	0.00	0.00	16A
Electromagnetic (EM)	Bristol <sup>2</sup>	NA	NA	NA	NA	NA	NA	NA	NA	NA	NA	NA	16A
	GeoPotential <sup>1</sup>	1.00	0.00	0.00	0.50	0.33	0.50	0.60	0.33	NA	NA	NA	16A
	AES	0.89	NA	0.75	0.00	0.33	1.00	1.00	0.00	NA	NA	NA	32
Ground-Penetrating Radar (GPR)	SRI <sup>2</sup>	NA	NA	NA	NA	NA	NA	NA	NA	NA	NA	NA	32
	Kaman <sup>2</sup>	NA	NA	NA	NA	NA	NA	NA	NA	NA	NA	NA	16A
	Geo-Centers <sup>1</sup>	1.00	0.00	0.67	0.80	0.86	0.93	0.76	0.00	0.00	0.00	0.00	16B
Magnetometer and EM	Geophex <sup>2</sup>	0.96	0.23	0.88	0.38	0.43	NA	NA	NA	NA	NA	NA	16A
	ADI (MAG and EM)	0.73	0.11	0.65	0.53	0.92	0.77	0.38	0.35	0.00	0.00	0.00	16B
EM and GPR	Coleman <sup>1</sup>	1.00	0.00	0.14	0.25	0.92	0.33	0.87	0.00	0.00	0.00	0.00	16B

Notes:

NA Not applicable

<sup>1</sup> Demonstrator reported all target declarations as "ordnance."

<sup>2</sup> Demonstrator did not provide type, size, and class information for declarations or listed them as "unknown."

Three demonstrators used EM induction sensors: GeoPotential, Parsons, and Bristol. The range of  $P_D$  values for EM induction sensors is 0.11 to 0.85. Parsons used an EM-61 and advanced data processing to obtain a  $P_D$  of 0.85, which was the highest  $P_D$  for all the systems demonstrated.

Three demonstrators used a combination of magnetometer and EM induction sensors: Geo-Centers, Geophex, and ADI. The results of these demonstrators are comparable to the results of magnetometer and EM induction sensors used alone. There may be an advantage in fusing data from the two technologies, as evident by the narrow range of  $P_D$  values (0.65 to 0.72) observed for these demonstrators.

GPR sensor equipment was used by three demonstrators: AES, SRI, and Kaman. The range of  $P_D$  values for GPR sensors is 0.00 to 0.05. GPR sensor system results are consistent with results from Phase I that showed these systems as having little or no detection capability. GPR systems may have performed poorly due in part to the soils at JPG, which have a high clay content. In addition, weather conditions before and during all three Phase II GPR demonstrations contributed to a high soil moisture content, which typically diminishes GPR performance. The two airborne demonstrations (AES and SRI) showed no detection capability during Phase I or II. Coleman demonstrated a combination of EM induction and GPR sensors. It is not known to what degree Coleman's relatively low score was influenced by the use of GPR.

FAR values for the Phase II demonstrators ranged from 0.9 to 225.9 false alarms per hectare. No direct relationship exists between false alarm rate and  $P_D$ , although both are important parameters in determining the best technology for UXO remediation.

To provide a single evaluation rating that incorporates both the  $P_D$  and the false alarm rate, an optimal performance value was computed. This function is derived by computing the distance in probability space of the demonstrator's performance ( $P_D$ ,  $P_{FA}$ ) relative to the optimal system performance ( $P_D = 1.00$ ,  $P_{FA} = 0$ ). This value provides another metric to evaluate demonstrator performance, and it considers missed detection on an equal basis with false alarms. Low values indicate better performance. Optimal performance evaluation values are presented in Table 6-3 and are plotted in Figure 6-4. Figure 6-4 shows a 'natural' break in the demonstrator rankings at four different intervals that are similar to the distribution bins presented in the Phase I report (USAEC 1995). The best performers are shown as Parsons and Geometrics, followed by Geophex, Geo-Centers, ADI, and Bristol.

**TABLE 6-3  
DEMONSTRATOR OPTIMAL PERFORMANCE EVALUATION**

Demonstrator	Optimal Performance Evaluation	Probability of Detection	Probability of False Alarms
Parsons	0.16	0.85	0.04
Geometrics	0.18	0.83	0.03
Geophex	0.29	0.71	0.02
Geo-Centers	0.30	0.72	0.11
ADI (MAG & EM)	0.35	0.65	0.04
ADI (MAG)	0.37	0.63	0.04
Bristol	0.38	0.62	0.05
Scintrex	0.50	0.50	0.06
Vallon	0.51	0.57	0.28
Coleman	0.71	0.29	0.02
GeoPotential	0.89	0.11	0.02
AES	0.96	0.05	0.01
Aerodat	0.98	0.02	0.02
SRI	0.99	0.01	0.02
Kaman	1.00	0.00	0.01

**Localization Performance**

Figure 6-5 shows the horizontal position (or radial) errors for the demonstrators. Results for the ground-based systems ranged from 0.65 to 1.30 meters. Airborne systems show horizontal position errors from 2.29 to 3.49. The sparse number of detections for airborne demonstrators probably affects the significance of these estimates. Furthermore, for airborne demonstrators, it is not clear whether these location errors are due to random declarations, as indicated by the low detection probabilities (see Figure 6-1).

Depth errors for most of the ground-based demonstrators appear to be statistically indistinguishable from zero (at the 95 percent confidence level). However, demonstrators that used EM sensors (Parsons, Bristol, and GeoPotential) appear to have estimated depths that are shallower than the actual target depth, as evidenced by the negative depth errors in the individual demonstrator tables.

One explanation for these results is that EM sensors are probably receiving stronger signals from the tops of the buried ordnance items. The manner in which the actual signal is received is a complicated function of the configuration of the sensor, the sensor orientation and position relative to the buried UXO, the structure and orientation of the buried UXO, and the intervening soil. A simplistic explanation for the shallower depth estimates require an understanding of the way the sensors function. Conductivity sensors function by inducing surface currents in material that generate an EM field; the strength of the induced field is then measured by the sensor. The strength of the generated signal decreases rapidly with distance from the object (depth). As a result, the top of the ordnance item would tend to generate a stronger signal than the bottom. If this difference in signal strength is not accounted for, a shallower depth estimate will be given. In addition, shallower depth estimates will become more exaggerated when the UXO item is oriented on end (nose up or down) as was the case with many of the emplaced UXO items at the Phase II areas.

#### **Identification and Classification Performance**

Demonstrators providing identification and classification information were scored on their ability to determine the type (ordnance or nonordnance); size (large, medium, or small); and class (bomb, mortar, projectile, or cluster) for detections. A score was given for each possible classification category (type, size, and class). Figures 6-6 through 6-8 indicate each of the demonstrator's performance in correctly determining type, size, and class, respectively. As described in Section 5.0, not all of the demonstrators provided information in all three identification and classification categories. Table 6-3 summarizes the identification and classification information provided by the individual demonstrators. Some demonstrators typed all target declarations as ordnance; these demonstrators are indicated by the "ordnance only" entry in the table.

**TABLE 6-4  
DEMONSTRATOR IDENTIFICATION AND CLASSIFICATION INFORMATION PROVIDED**

Demonstrator	Area Surveyed	Type	Size	Class
Bristol	16A	No	No	No
Geometrics	16A	(ordnance only)	Yes	No
Geophex	16A	Yes	Yes	No
GeoPotential	16A	Yes	Yes	Yes
Kaman	16A	No	No	No
Parsons	16A	Yes	Yes	Yes
Scintrex	16A	Yes	Yes	Yes
ADI (MAG & EM)	16B	Yes	Yes	Yes
ADI (MAG)	16B	Yes	Yes	Yes
Coleman	16B	(ordnance only)	Yes	Yes
Geo-Centers	16B	(ordnance only)	Yes	Yes
Vallon	16B	No	Yes	Yes
Aerodat	32	No	No	No
AES	32	Yes	Yes	Yes
SRI	32	No	No	No

Figure 6-6 shows that demonstrator performance in determining ordnance objects was significantly better than their respective ability in determining nonordnance objects. Although there were significantly more ordnance than nonordnance items employed for Phase II, the performance differences shown in Figure 6-6 are statistically significant at the 95 percent confidence level.

Figure 6-7 shows that demonstrators were collectively better at estimating the size of the emplaced ordnance than they were at determining the class of target detected. For demonstrators providing size estimates, about two-thirds of their probabilities of classification were greater than 0.5. As shown in Figure 6-8, demonstrators were not as successful in determining class as size. In addition, none of the demonstrators were able to correctly classify clusters, even though many of them could detect a cluster.

## 6.2 ADDITIONAL PERFORMANCE STATISTICS

One goal of any UXO system performance assessment is to determine how well a system locates, identifies, and classifies ordnance for remediation. As discussed in Section 4.1.4, this assessment quantifies a demonstrator's ability to provide information that would be cost-effective for remediation. Figure 6-9 presents a scatter plot of the two performance statistics for each demonstrator: probability of detection (ordnance) and false alarm ratio. Because of the relatively poor performance in discriminating between ordnance and nonordnance, all demonstrator declarations were treated as ordnance detections for this figure.

Better performance is found in the upper left region of this plot, which corresponds to the highest fraction of ordnance remediated with the lowest number of nonordnance (or empty) holes remediated. As with the  $P_D$  versus  $P_{FA}$  plot (see Figure 6-3), the three demonstrators with the highest  $P_D$  values (Parsons, Geometrics, and Geophex) surveyed the 16A-hectare area. The better performing demonstrators from the 16B-hectare area generally had lower fractions of detected ordnance remediated and much higher ratios of nonordnance to ordnance targets remediated. These results may be due to the fact that the 16B-hectare area contained more metallic scrap than the 16A-hectare area (see Appendix D).

As described in Section 3.0, a number of plastic mines were emplaced in the 16A- and the 16B-hectare areas. Although magnetometer systems were not expected to detect these mines, some demonstrators claimed that their systems had this detection capability. To determine whether these claims were valid, demonstrators were scored separately in comparison with a baseline target set containing these mines. Appendix E lists the results of this scoring. All of the measures of effectiveness described in this report, with the exception of those in Appendix E, were computed using a baseline target set that did not contain plastic mines. None of the demonstrators, except Vallon, had  $P_D$  values for mines that were statistically different from the  $P_D$  that would be obtained from a random report of targets.

Vallon, which used only magnetometer sensors, detected 55 percent (7 out of 12) of the mines. As discussed in Appendix E, one possible reason for this unexpectedly high detection probability is that Vallon's survey team observed two of the plastic mines that migrated to the surface. This situation may have invited closer scrutiny of that area during the survey and post-test analysis.



### 6.3 OPERATIONAL SUMMARY

Systems demonstrated during Phase II of the controlled site UXO-ATDs had various implementation requirements. The demonstrators also had different support needs, both on site and locally. Some of the systems were almost entirely self-sufficient, while others depended on the support trailers for space to perform data analysis. All of the systems demonstrated during Phase II used the support trailers to some degree, although if the trailers had not been available, the demonstrators most likely would have provided their own support equipment. In any case, the various support needs must be considered when implementing these systems in a remote location.

In addition to on-site support, the demonstrators also used local supplies and services to varying degrees. Some demonstrators shipped all of their equipment to JPG or transported it by truck. Several of the demonstrators required ATVs that were either rented or purchased locally. In many cases, replacement parts and tools were required from local support services during the demonstrations. Two demonstrators experienced equipment breakdowns that required machining or welding for repair. In one instance, a tow truck was required to remove a survey vehicle that became stuck in the mud on site. The local support services used by various demonstrators often enabled demonstration activities to continue; however, in a remote location, such support services might not be as readily available.

The capabilities and limitations of the various technologies were influenced by several factors. The type of system demonstrated, the terrain at the demonstration areas, and the weather conditions before and during the demonstrations all affected system efficiency. Man-portable systems were the most successful in accessing all areas of the site, because these systems could easily maneuver around and through forested areas. Vehicle-towed systems often had difficulty driving through the deeply rutted areas of the demonstration sites. Similarly, densely forested areas were not accessible to vehicle-towed systems.

The airborne system demonstrated by Aerodat was affected by the forested terrain in that the tree level prevented Aerodat from flying over the demonstration area at its optimal elevation. The two other airborne demonstrators, AES and SRI, stated that their GPR systems had limited capability due to the wet ground conditions during the demonstrations.

Several man-portable and vehicle-towed systems experienced difficulties in maintaining the GPS satellite reception during the demonstration period, primarily in areas with heavy tree cover.

Both remediation systems were demonstrated at JPG under dry conditions. If the conditions had not been dry, both the Wright Laboratory and CEG vehicles could have become immobilized in the wet heavy clay soils. Even with the dry ground conditions, CEG had to avoid deeply rutted or low areas when maneuvering its soft trencher, which is top heavy and unstable when traveling on uneven terrain.

In general, vehicle-towed systems were more prone to breakdowns than either the man-portable or the airborne systems. Demonstrators that brought replacement parts were better prepared for field operations than those that had to have equipment or parts shipped via overnight delivery. The two remediation systems experienced numerous equipment breakdowns, as discussed in Section 5.0. Depending on the type of repairs required, these breakdowns were time-consuming, and resulted in lost demonstration time. For example, the final breakdown for CEG ended its demonstration, because the repair could not be made in the field. Remediation systems experienced difficulty in remote operations.

Areal coverage for the technologies varied widely. Table 6-5 lists the coverage (area scored) for detection demonstrators. Airborne systems provided the best coverage, as might be expected, but their coverage rate was negated by poor detection results. The combined man-portable and vehicle-towed systems provided good area coverage, with three out of the four demonstrators covering the full 16 hectares assigned. Four of the six man-portable systems covered all of the area. Neither of the vehicle-towed systems covered the entire area.

The ease of using the different systems varied greatly. For the most part, vehicle-towed, airborne, and remediation systems were operated by experienced personnel. However, both Vallon and Scintrex used personnel who had no previous experience operating the equipment. Although these inexperienced operators required some training, they were able to work independently within a day or so. The quick training time is significant because it increases the potential for the equipment's future use by inexperienced personnel.

**TABLE 6-5  
SUMMARY OF DEMONSTRATOR AREA COVERAGE**

Demonstrator	Coverage (percent)	Demonstrator	Coverage (percent)	Demonstrator	Coverage (percent)
Aerodat	100	Geo-Centers	100	Parsons	100
AES	100	Geometrics	100	Polestar	93.8
ADI	100	Geophex	100	SRI	100
Bristol	83.9	GeoPotential	84	Scintrex	36
Coleman	100	Kaman	52.6	Vallon	52.5

Several systems included real-time data analysis. For example, Geometrics collected additional data with the GPR system in areas where ordnance was detected by the first system (although data collected by the GPR system was not included for data analysis). Such real-time data analysis also permitted the demonstrators to determine whether the system was functioning properly.

As expected, the various man-portable, vehicle-towed, combined, and airborne systems each had specific capabilities and limitations. While the man-portable systems proved to be durable and were able to access the entire site successfully, the systems were limited by the speed and stamina of the operator. The vehicle-towed systems were able to cover the site quickly but were often subject to breakdowns that caused time-consuming delays.

#### 6.4 SUMMARY AND CONCLUSIONS

Several conclusions can be drawn from the performance statistics. In general, Phase II data indicate the following trends or conclusions:

- Magnetometer and EM induction sensors outperformed the GPR sensors.
- Air demonstrators continued to demonstrate the same poor performance shown by Phase I demonstrators.
- A technology demonstration employing several different sensor types can potentially increase performance in both detection and classification (see Table 6-1).
- The combined sensor systems were also superior to either system alone for classifying ordnance items by both size and class.

A wide range of detection performance was exhibited by the Phase II demonstrators. The higher  $P_D$  values of certain demonstrators (compared to Phase I  $P_D$  values) may be due to several factors, including (1) the use of advanced data evaluation techniques, (2) the experience level of the demonstrators, and (3) improved navigational capability.

With respect to operational analysis, the man-portable systems proved to be durable and were able to access most areas; however, systems were limited by the speed and stamina of the operator, the climatic conditions, and the terrain. Vehicle-towed systems covered the area more quickly than man-portable systems, but they were hindered by breakdowns and terrain. The combined sensor systems took advantage of the strengths of each system while compensating for their weaknesses. Airborne systems had the best coverage and speed of all the systems, but they lagged far behind in their detection, localization, identification, and classification ability. The two remediation systems successfully demonstrated their ability to excavate buried ordnance; however, both systems experienced numerous breakdowns, operated slowly, and had difficulty operating remotely.

Several conclusions can be inferred from a comparison between detection abilities of the various demonstrators at the 16A- and 16B-hectare areas.  $P_D$  values at these two areas are generally quite similar, indicating that in terms of detecting ordnance, demonstrators at both areas had similar performance capability. However, demonstrator FAR values were greater at the 16B-hectare area, most likely due to the larger amount of nonordnance clutter present at the site (see Appendix D). Demonstrators at the 16B-hectare area identified more of the detected ordnance correctly than those at the 16A-hectare area, possibly as a result of the previous experience demonstrators gained at the 16A-hectare area during Phase I.

Because the specific performances of systems at JPG are related to the environmental conditions and imposed operational restrictions at the site, demonstration results at JPG may not be directly transferable to other sites. However, Government and private industry will be able to use the data from these demonstrations to allocate their resources for developing more effective systems for defense-related UXO cleanup efforts. In addition, environmental restoration managers at government installations will have an independent source of information that can help them identify potentially appropriate and cost-effective technologies given the site-specific conditions and the limitations of those technologies.

Figure 6-1  
Individual Demonstrator Probability of Detection (Ordnance)

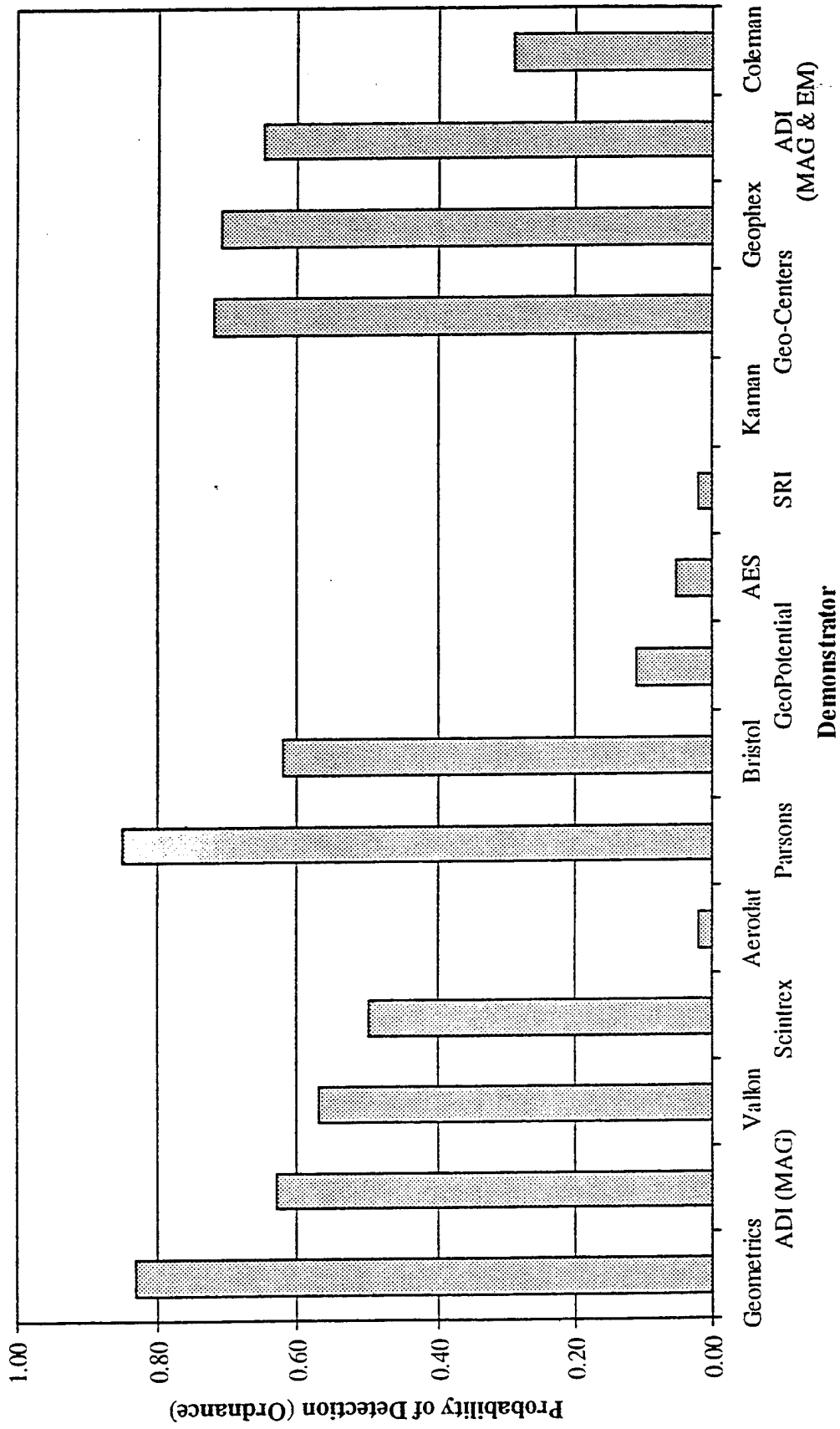


Figure 6-2  
Individual Demonstrator False Alarm Rate

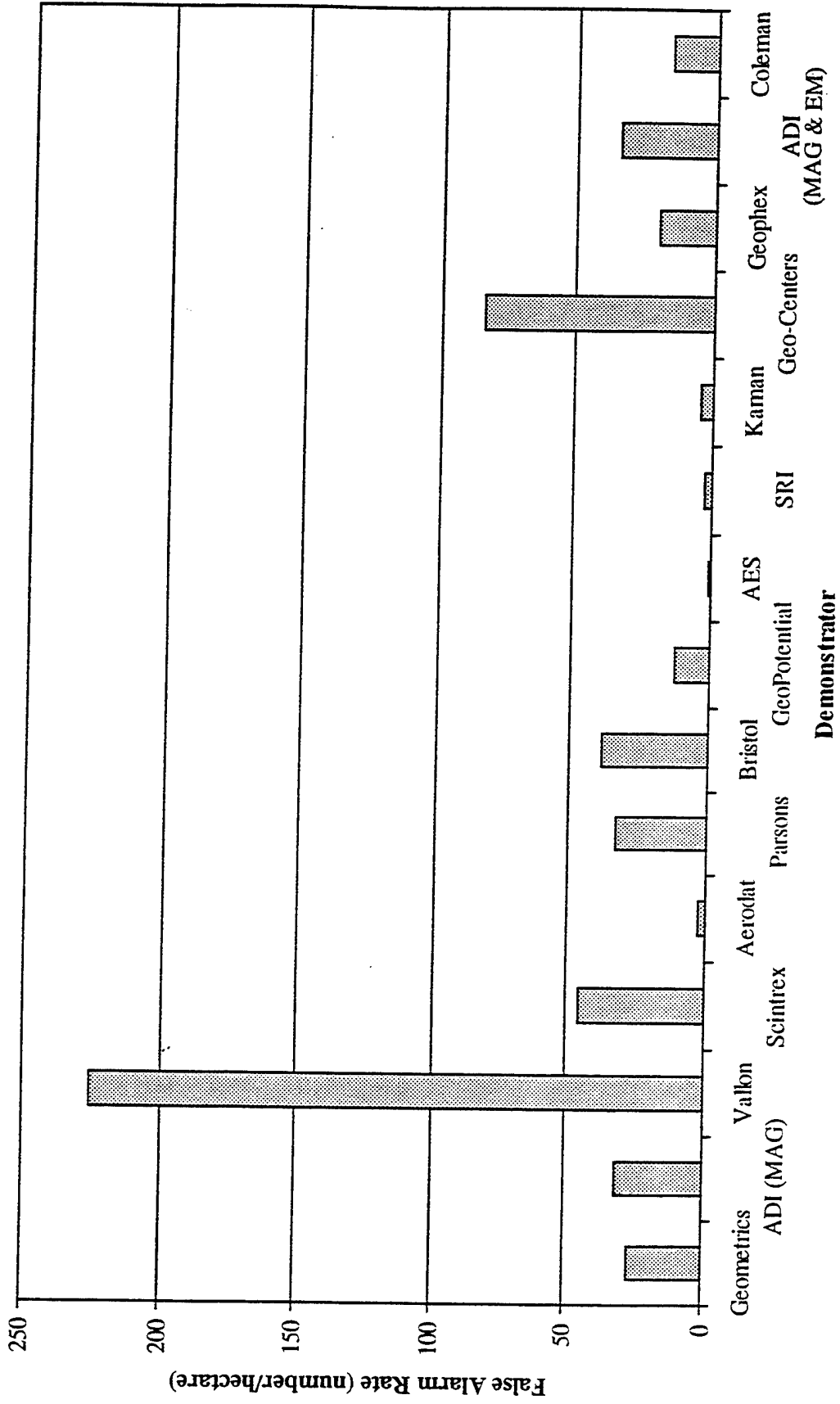
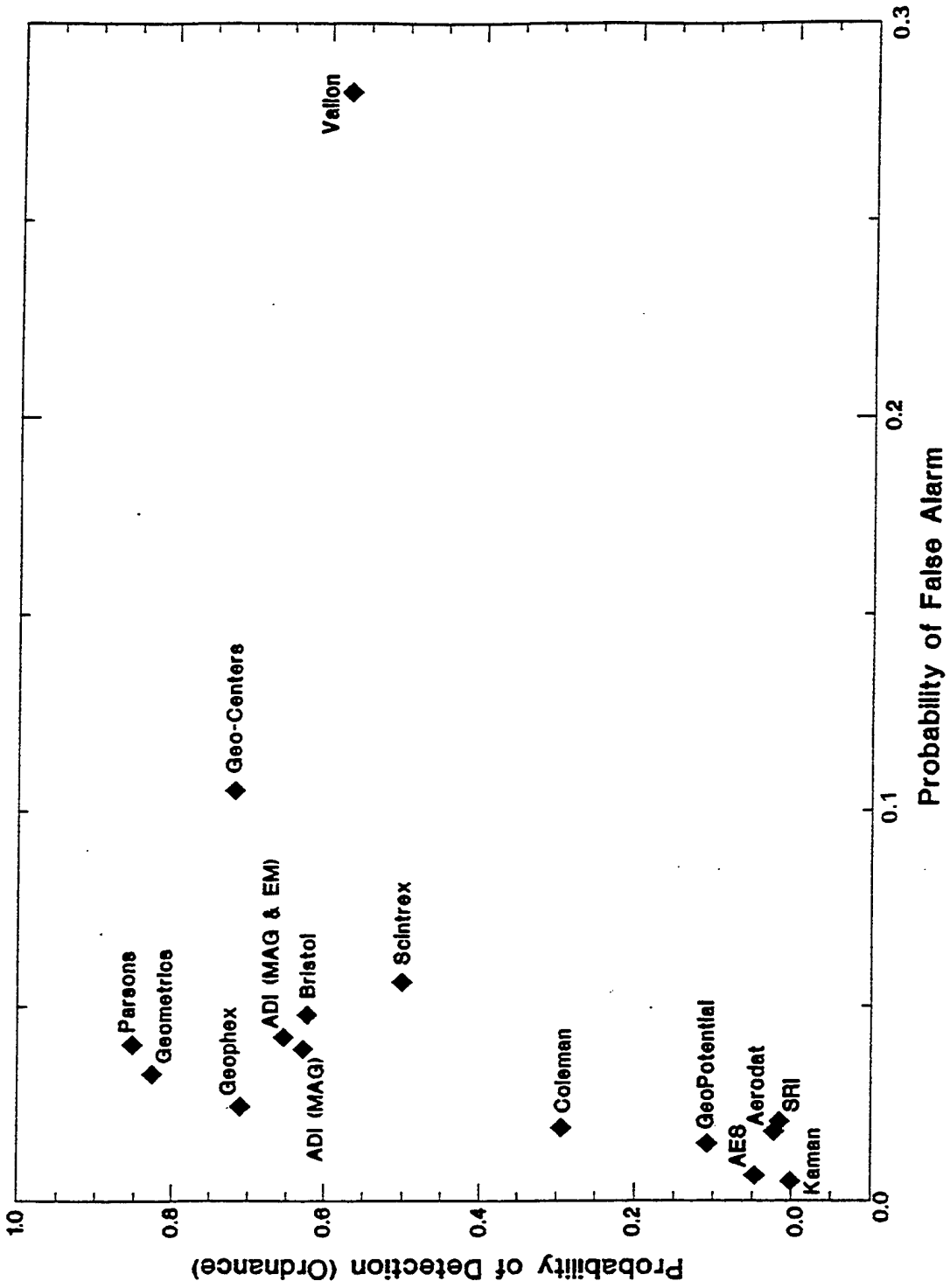


Figure 6-3  
 Plot of Demonstrator Probability of Detection (Ordnance) versus Probability of False Alarm



**Figure 6-4**  
**Optimal Performance Statistics by Demonstrator**

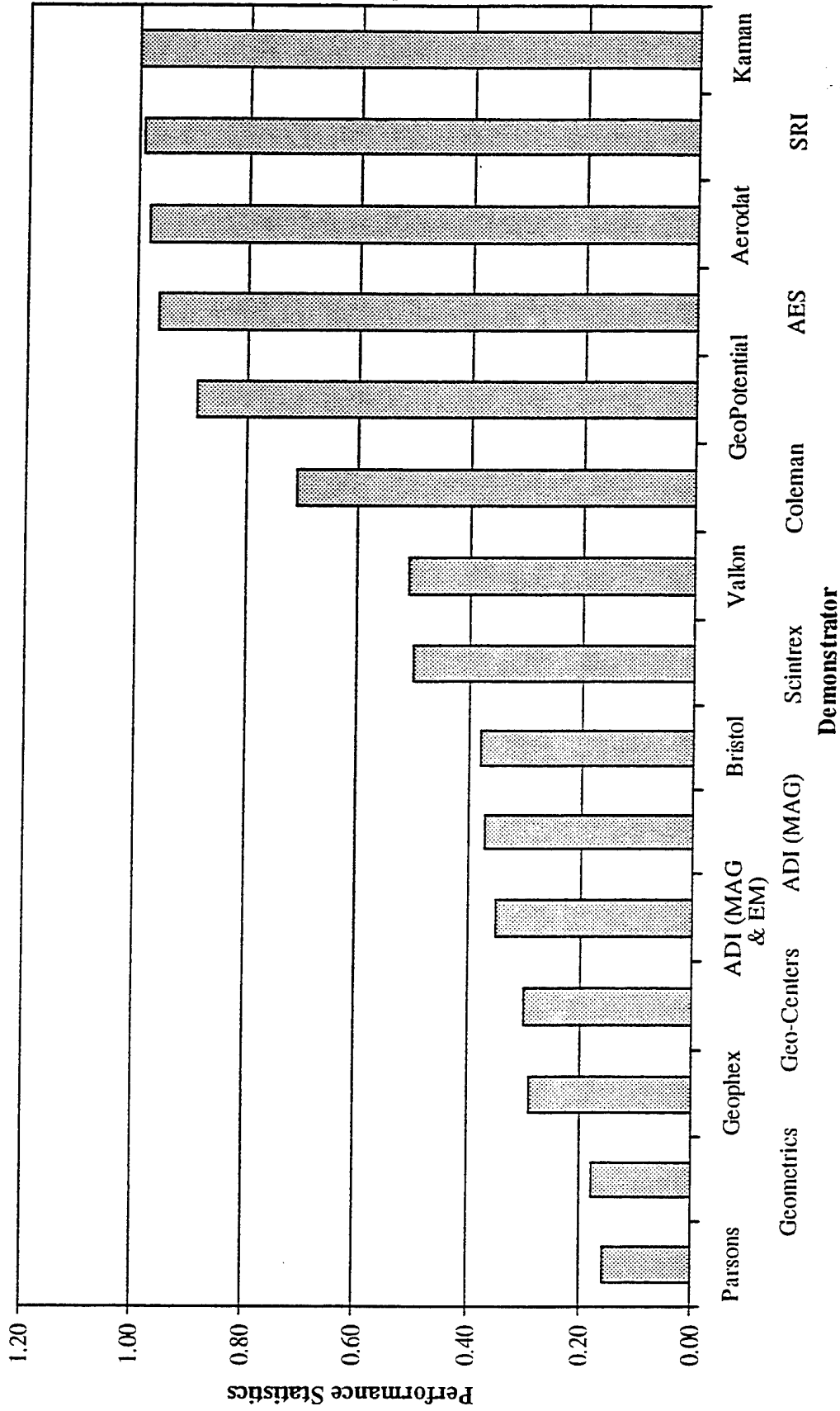
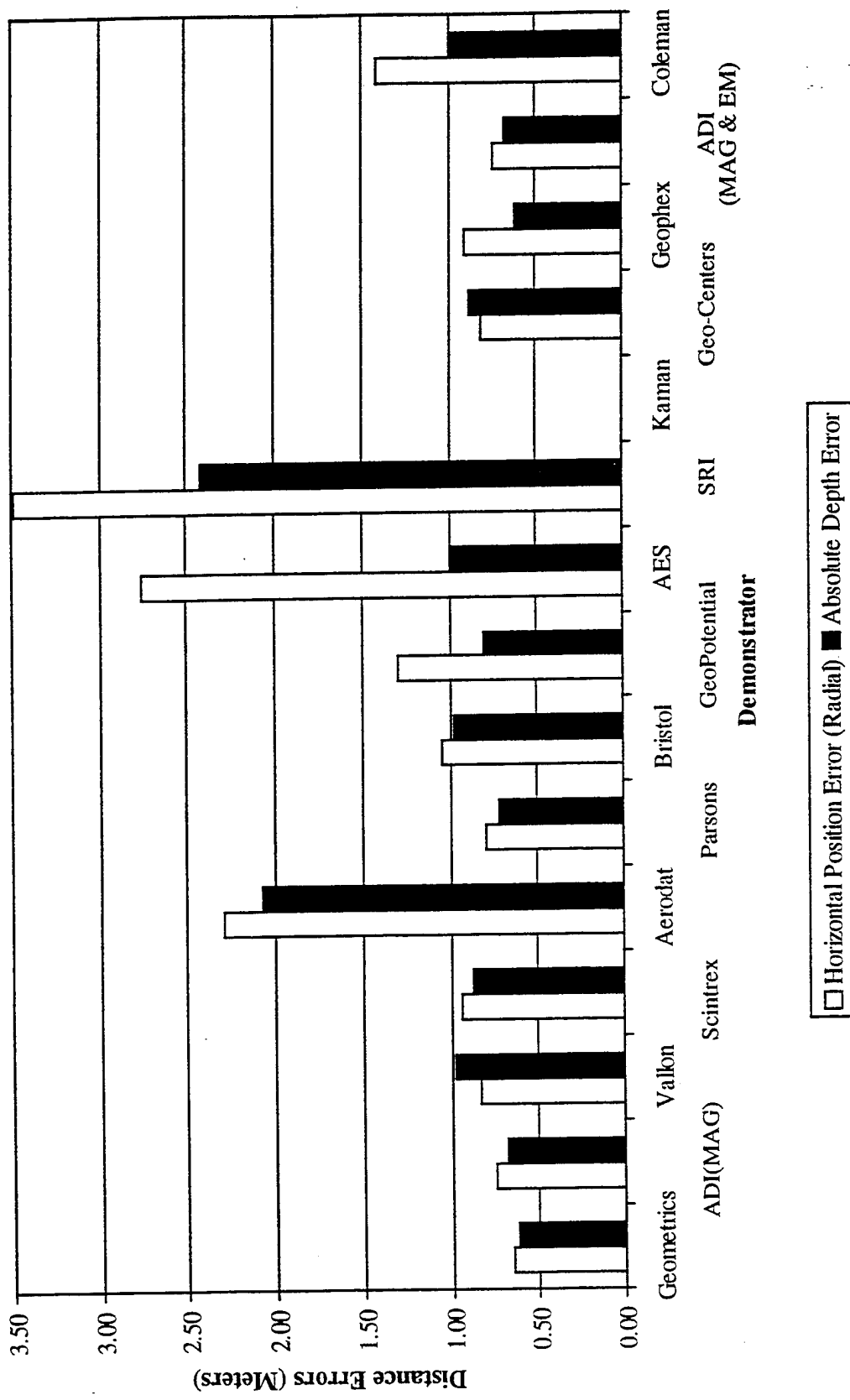
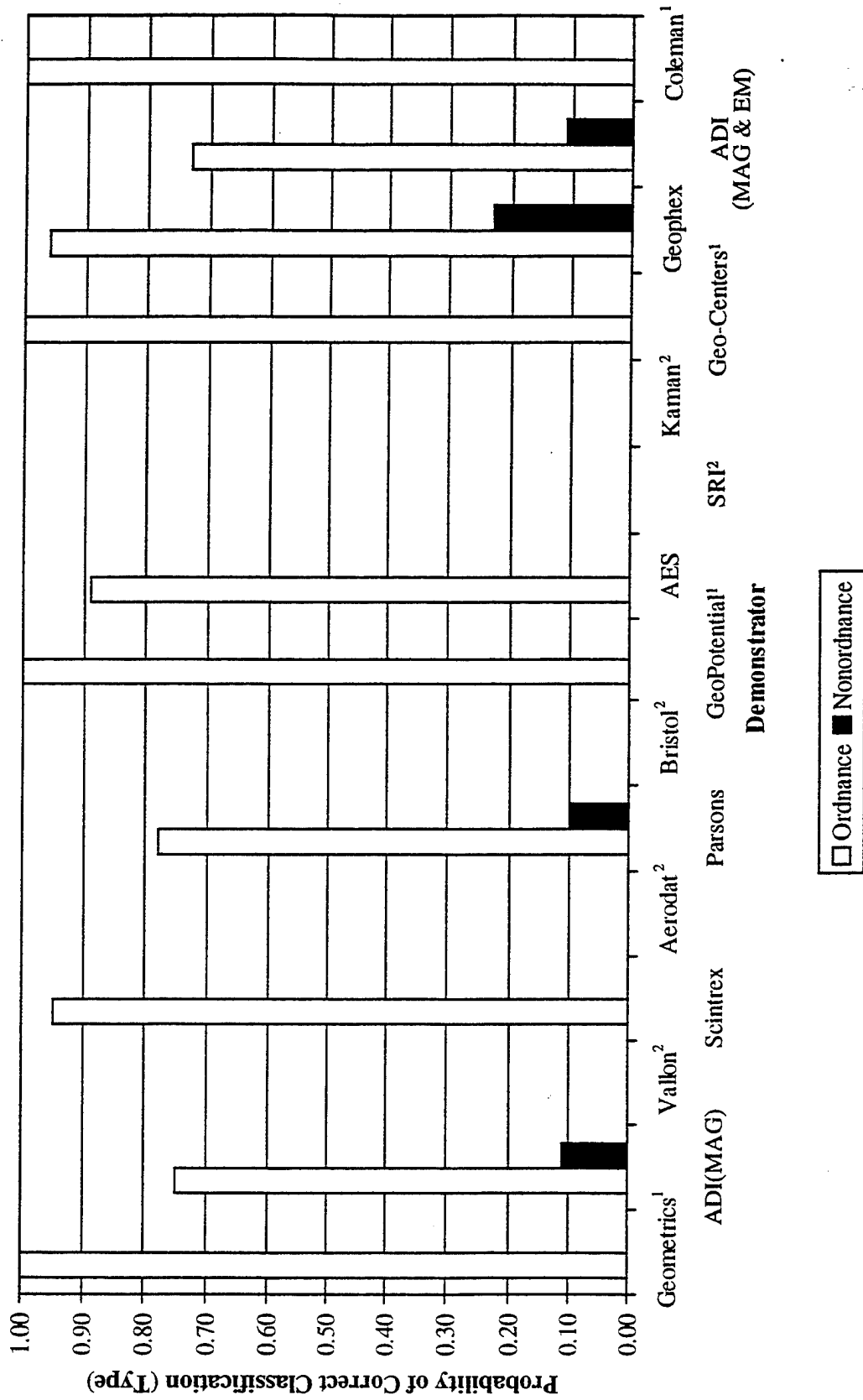




Figure 6-5  
Individual Demonstrator Localization Performance



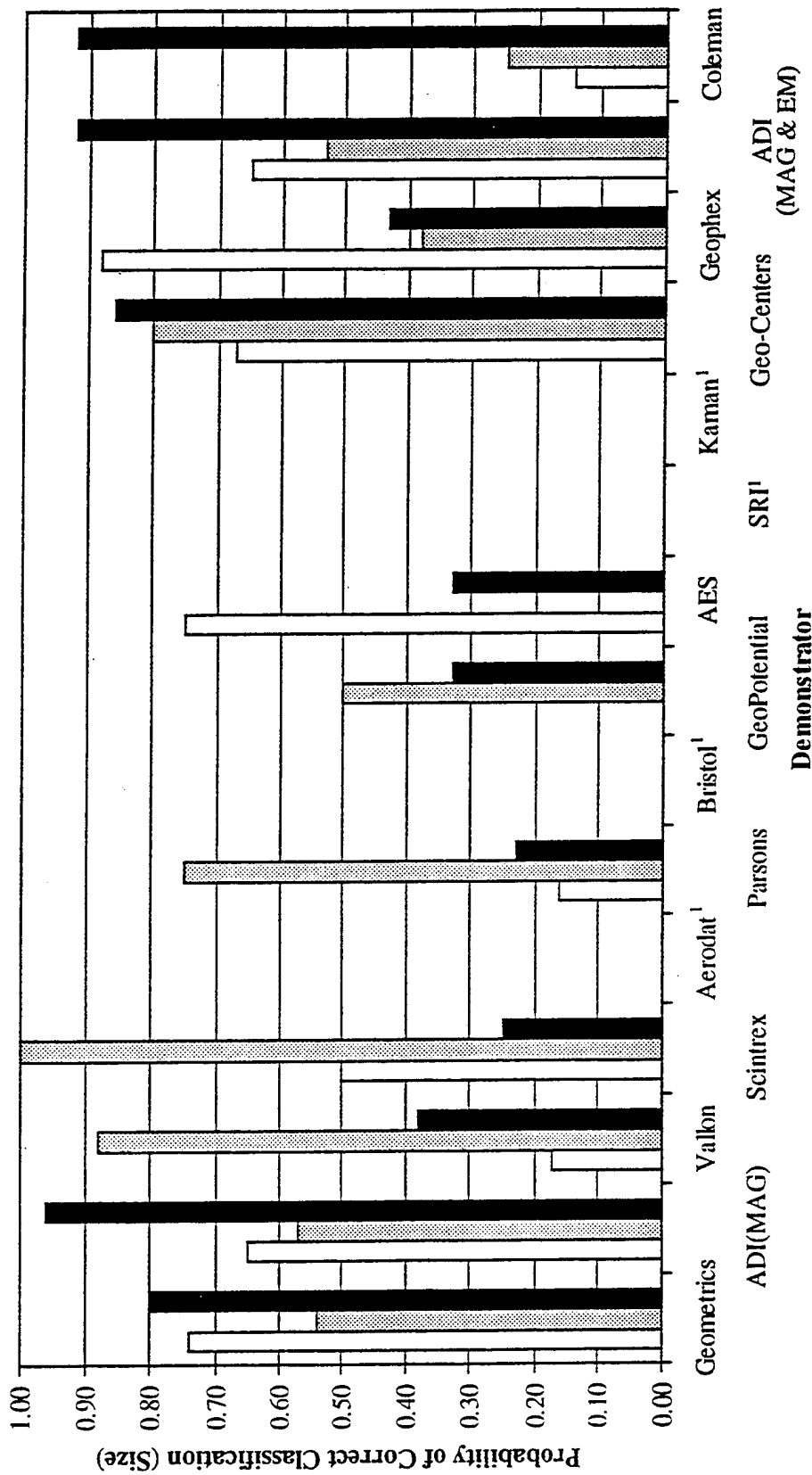
**Figure 6-6**  
**Individual Demonstrator Probability of Correct Identification (Classification by Type)**



Notes: <sup>1</sup> Demonstrator reported all target declarations as "ordnance"

<sup>2</sup> Demonstrator did not provide type information for declarations or listed as "unknown"

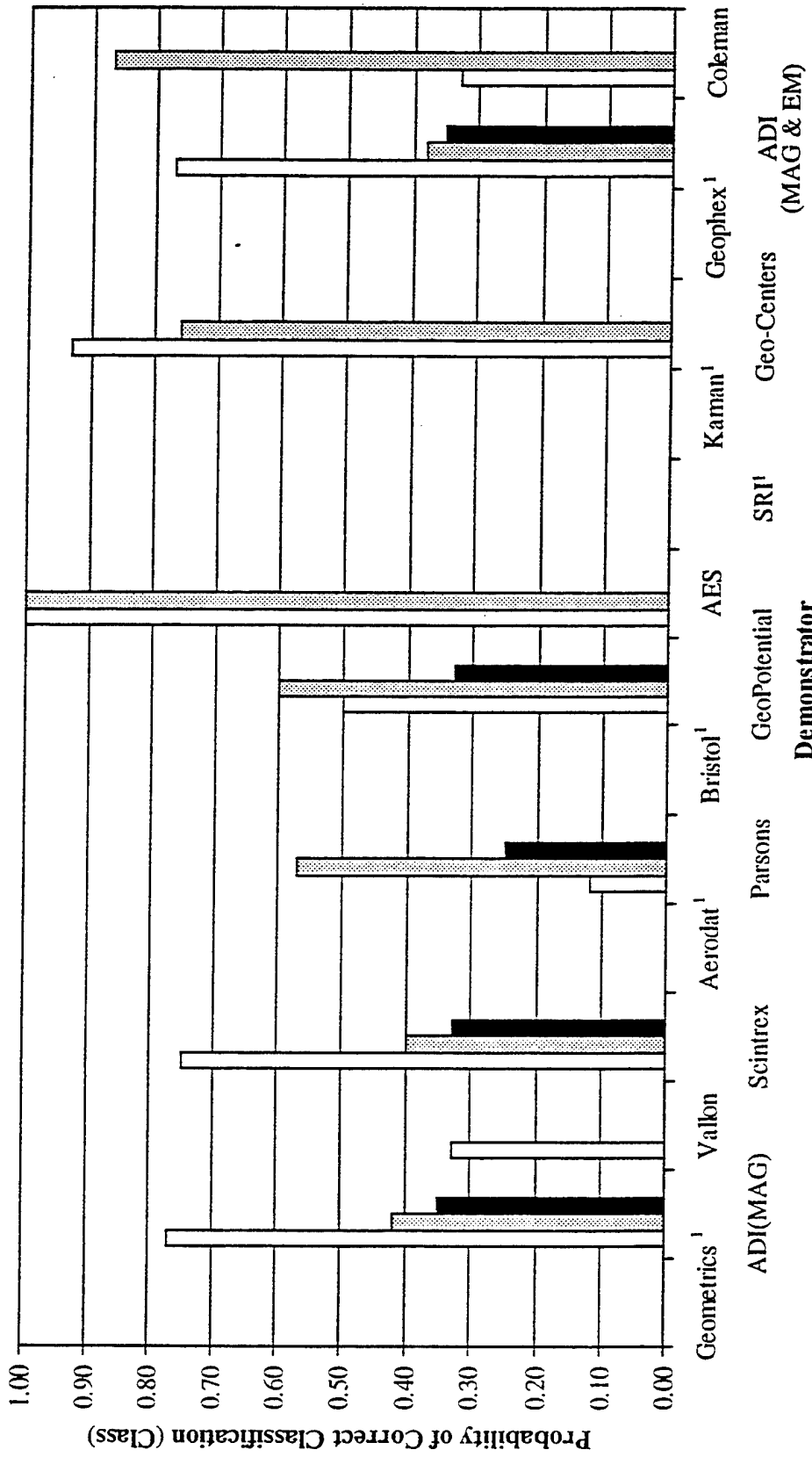
Figure 6-7  
Individual Demonstrator Probability of Correct Classification by Size



□ Large    ▨ Medium    ■ Small

Notes: <sup>1</sup> Demonstrator did not provide size information for declarations or listed as "unknown"

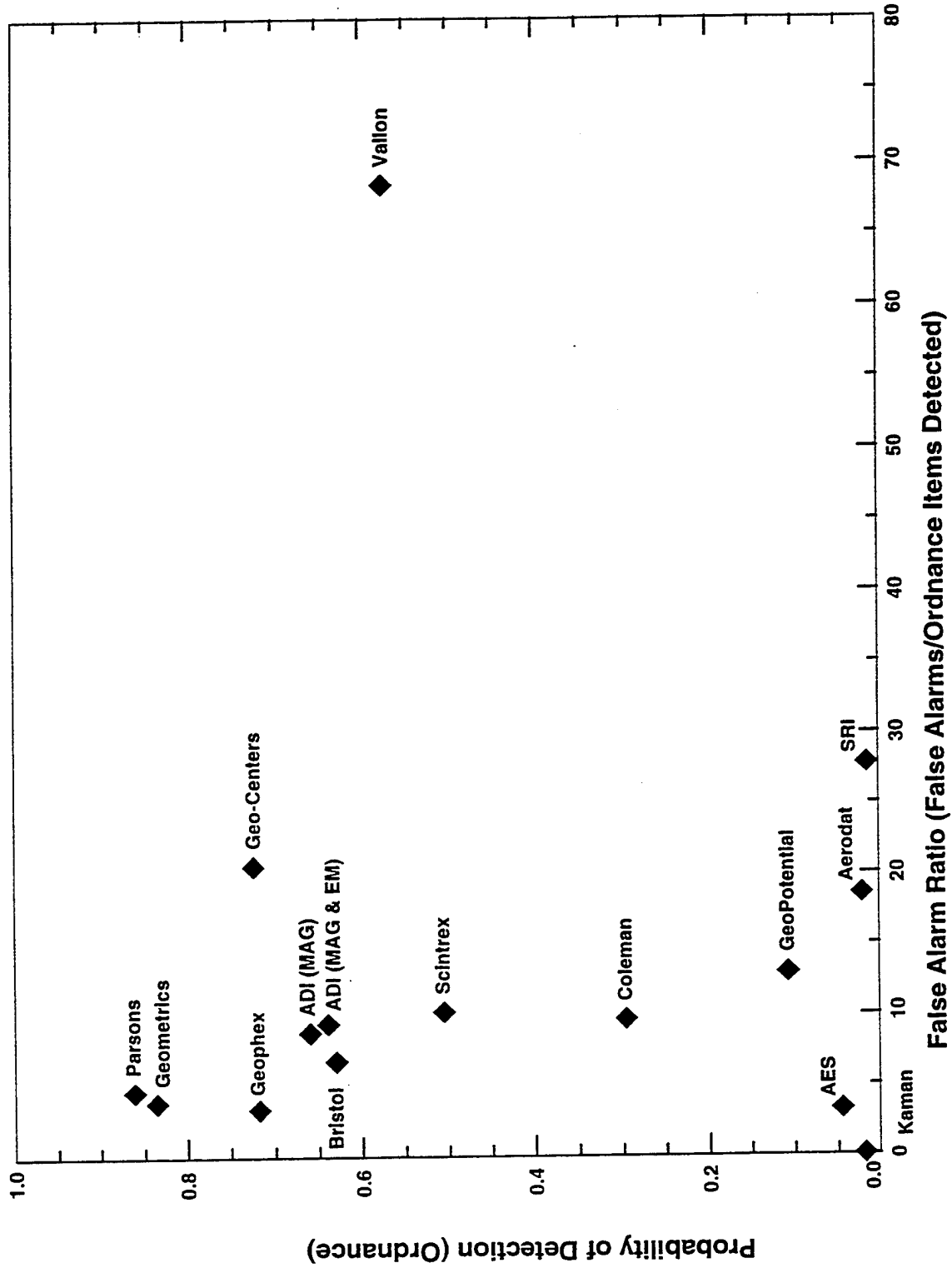
Figure 6-8  
Individual Demonstrator Probability of Correct Classification by Class



Legend:  
 □ Bomb  
 ▨ Projectile  
 ■ Mortar  
 ▩ Cluster

Notes: <sup>1</sup> Demonstrator did not provide class information for declarations or listed as "unknown"

**Figure 6-9**  
**Plot of Demonstrator Probability of Detection (Ordnance) versus False Alarm Ratio**



## REFERENCES

- Aerodat, Inc. (Aerodat). 1995a. "Proposal for a Helicopterborne Magnetic Gradiometer Array Survey for UXO Detection: Jefferson Proving Ground - Phase II." Q410. February 17.
- Aerodat. 1995b. "Report on a UXO Detection Demonstration using a Helicopter Magnetic Gradient System; Jefferson Proving Ground, Indiana, U.S.A." J95309. October 13.
- Airborne Environmental Surveys (AES). 1995a. "Airborne Multiple Sensor Demonstration to Detect Inert Ordnance at the Jefferson Proving Ground, Indiana."
- AES. 1995b. "Airborne Ground Penetrating Radar and Digital Airborne Imaging Spectrometer Survey for the Phase II UXO Detection, Identification, and Remediation Advanced Technology Demonstrations at the Jefferson Proving Ground, Indiana." June 30.
- Anslinger, C. Michael. 1993. "A Phase I Archeological Surface Reconnaissance of Two Land Parcels Located Within the U.S. Army Jefferson Proving Ground Near Jefferson and Ripley Counties, Indiana." *Contract Publication Series 93-79*. Cultural Resource Analysts, Inc. November.
- Australian Defence Industries Pty Ltd. (ADI). 1995a. "Jefferson Proving Ground Technology Demonstration Request for Quotation." ADI Reference No. SS9548.
- ADI. 1995b. "Final Report UXO Detection, Identification, and Remediation Advanced Technology Demonstration Jefferson Proving Ground, Indiana." ADI Reference No. 180507B.
- Bristol Aerospace Ltd. (Bristol). 1995a. "Unexploded Ordnance Detection, Identification, and Remediation Phase II Advanced Technology Demonstration Program." U007-0295. February 21.
- Bristol. 1995b. "UXO Detection, Identification, and Remediation Advanced Technology Demonstration at Jefferson Proving Ground, Indiana." Report No. 95.15. July 17.
- Coleman Research Corporation (Coleman). 1995a. "Detection, Identification, and Remediation Technology Demonstration: Volume 1 - Technical Proposal." COP 610/95-010. February.
- Coleman. 1995b. "Phase II Detection, Identification, and Remediation Advanced Technology Demonstrations at the Jefferson Proving Ground, Demonstration Results Report." COG 95-178. July 17.
- Commerce Business Daily (CBD). 1994. CBD Synopsis Soliciting Demonstrators for Detecting, Locating, and Classifying, or Excavating UXO. December 12.
- Concept Engineering Group, Inc. (CEG). 1995a. "Demonstration of Excavation of Unexploded Ordnance with Supersonic Air Jets and Pneumatic Vacuum Transport at Jefferson Proving Ground." February 21.
- CEG. 1995b. "Final Report Demonstration of Excavation of Unexploded Ordnance with Supersonic Air Jets and Pneumatic Vacuum Transport at Jefferson Proving Ground." October 5.

- Feller, William. 1968. "An Introduction to Probability Theory and Its Application." Volume I. Wiley Interscience. New York.
- Geo-Centers, Inc. (Geo-Centers). 1995a. "Environmental Characterization with Magnetics and STOLS™." November 12.
- Geo-Centers. 1995b. "New Multi-Sensor, Multi-Modal STOLS Technology for UXO Detection and Characterization at Jefferson Proving Ground, Madison, Indiana: Final Report." GC-FR-2898. September.
- Geometrics, Inc. (Geometrics). 1995a. "Proposal to PRC to Unexploded Ordnance Demonstration Program, Phase II Technology Demonstration at the Jefferson Proving Ground." February 18.
- Geometrics. 1995b. "Jefferson Proving Ground Demonstration Report." August 28.
- Geophex, Ltd. (Geophex). 1995a. "Jefferson Proving Ground Technology Demonstration a Technical Proposal." February.
- Geophex. 1995b. "Jefferson Proving Ground UXO Technology Demonstration by Geophex, Ltd." September.
- GeoPotential. 1995a. "Technical Proposal Unexploded Ordnance Advanced Technology Demonstration Program." February 14.
- GeoPotential. 1995b. "Survey Data Analysis Report Unexploded Ordnance Advanced Technology Demonstration Program, Demonstration Period: August 23, 1995, through August 30, 1995." September 28.
- Indiana Department of Natural Resources (IDNR). No date. "An Inventory of Special Plants and Natural Areas within the U.S. Army Jefferson Proving Ground in Southeastern Indiana."
- Institute for Defense Analysis (IDA). 1995. "Demonstrator Performance at the Unexploded Ordnance Advanced Technology Demonstration at Jefferson Proving Ground (Phase I) and Implications for UXO Clearance." IDA Log No. HQ 95-47047/1. October.
- Jefferson Proving Ground. 1980. "Jefferson Proving Ground, Munitions Test Facility for United States Army Test and Evaluation Command." U.S. Government Printing Office 1980-624-200.
- Kaman Sciences Corporation (Kaman). 1995a. "Jefferson Proving Ground Demonstration Technical Proposal." Proposal No. P6F5-X5003. February 21.
- Kaman. 1995b. "Advanced Technology Demonstration Jefferson Proving Ground Test Results." October 19.
- Parsons Engineering Science, Inc. (Parsons). 1995a. "Technical Proposal."
- Parsons. 1995b. "Report on the UXO Detection, Identification, and Remediation Advanced Technology Demonstration at the Jefferson proving Ground, Indiana." 95-D-0009. July.

- Polestar Technologies, Inc. (Polestar). 1995a. "Man-Portable Ordnance Detector Using Schiebel Magnetometers and Precision Beacon System (PBS)." Proposal No. P T-95-P-1036. February 21.
- Polestar. 1995b. "Survey Data Analysis Report (Revised) Unexploded Ordnance (UXO) Detection, Identification, and Remediation Advanced Technology Demonstrations at Jefferson Proving Ground, Madison, Indiana." PT-TR-95-1036. October.
- PRC Environmental Management, Inc. (PRC). 1994. "Task 3: Preparation of Demonstration Site, Jefferson Proving Ground, Madison, Indiana, Geotechnical Investigation Report." February.
- PRC. 1995a. "Site Operations Plan for the UXO Detection, Identification, and Remediation Advanced Technology Demonstration at the Jefferson Proving Ground, Indiana." May.
- PRC. 1995b. "Draft Demonstration Work Plan for the UXO Detection, Identification, and Remediation Advanced Technology Demonstration at the Jefferson Proving Ground, Indiana." June.
- Scintrex. 1995a. "Unexploded Ordnance Detection, Identification, and Remediation Phase II Advanced Technology Demonstration Program Jefferson Proving Ground, Madison, Indiana: Technical Proposal." February 20.
- Scintrex. 1995b. "Survey Data Analysis Report." September.
- SRI International (SRI). 1995a. "Demonstration of Fixed-Wing-Mounted Ultra-Wideband Ground Penetrating Radar." ESD 95-13. February 17.
- SRI. 1995b. "Unexploded Ordnance Detection and Identification - Live Site Advanced Technology Demonstration Program - Phase II." SRI Project 6568. September 1.
- U.S. Air Force/Wright Laboratory (Wright Laboratory). 1995. Facsimile Regarding a Technology Description of the Remote Excavation Vehicle System. From Walter M. Waltz, Captain, U.S. Air Force. To Carol Richardson, Controlled Site Manager, PRC. July 10.
- U.S. Army Environmental Center (USAEC). 1994. "Unexploded Ordnance Advanced Technology Demonstration Program at Jefferson Proving Ground (Phase I)." Report No. SFIM-AEC-ET-CR-94120. December.
- USAEC. 1995. "Evaluation of Individual Demonstrator Performance at the Unexploded Ordnance Advanced Technology Demonstration Program at Jefferson Proving Ground (Phase I)." Naval Explosive Ordnance Disposal Technology Division. Report No. SFIM-AEC-ET-CR-95033. March.
- U.S. Department of Agriculture (USDA). 1985a. "Soil Survey of Ripley County and Part of Jennings County, Indiana." Soil Conservation Service in Cooperation with Purdue University Agricultural Experiment Station and Indiana Department of Natural Resources, Soil and Water Conservation Committee. April.
- USDA. 1985b. "Soil Survey of Jefferson County Indiana." Soil Conservation Service in Cooperation with Purdue University Agricultural Experiment Station and Indiana Department of Natural Resources, Soil and Water Conservation Committee. May.



U.S. Geological Survey (USGS). 1990. 7.5-Minute Series Topographic Map of the Madison, Indiana-Kentucky Quadrangle.

U.S. House of Representatives (USHR). 1992a. HR5504, Conference Report No. 102-408. October 5.

USHR. 1992b. HR5504, Conference Report No. 102-627. October 5.

USHR. 1992c. Department of Defense Appropriations Bill 1993. Report of the Committee on Appropriations (to accompany HR5504). Report No. 102-627. June 29.

Vallon GmbH (Vallon). 1995a. "Technology Demonstration Proposal for Jefferson Proving Ground - Phase II." February 17.

Vallon. 1995b. "Test Report of JPG II UXO Technology Demonstration, Data Recording with MC1 Detection System, Ferrous Locator EL 1302A1, Navigation System SEPOS®, and Navigation System GPS." September 14.

## APPENDIX A

### PERFORMANCE MEASUREMENT ALGORITHM DESCRIPTIONS

*Information contained in this appendix was compiled from documents generated by the Institute for Defense Analysis (IDA)*

This appendix describes how baseline items are matched with demonstrator declarations to determine  $P_{closest}$  and  $P_{group}$ . Demonstrator declarations at locations where no baseline target exists, also referred to as false alarms, are computed for each matching method. The following terminology is used when describing performance measurement algorithms:

- Baseline item -- An inert ordnance or nonordnance object emplaced on site to measure demonstrator detection capability
- Demonstrator declaration -- A detection reported by a demonstrator
- $R_{group}$  -- Maximum radius of the circle that defines a group of baseline items; the group radius should be larger than the expected sensor resolution.
- $R_{crit}$  -- Maximum horizontal distance allowed between a baseline item and a demonstrator declaration of that item for that item to be considered detected;  $R_{crit}$  is intended to indicate the demonstrator's location accuracy, which may be different from the sensor resolution;  $R_{crit}$  is constrained by the intended size of excavation during remediation.

#### COMPUTATION OF $P_{closest}$

The  $P_{closest}$  algorithm measures demonstrator performance by finding one-to-one matches between baseline items and demonstrator declarations. As the name implies, this algorithm matches each baseline item with the demonstrator declaration that is horizontally closest to it. Initially, all baseline items within a critical radius ( $R_{crit}$ ) of a demonstrator declaration are identified.  $R_{crit}$  is used to define a circle centered on each demonstrator declaration. A tie occurs when more than one baseline item lies within the circle. These ties are broken by attempting to match the demonstrator declaration with the baseline item that is closest to it, while simultaneously maximizing the number of detected baseline items.

To start the matching process, all demonstrator declarations are reviewed and all baseline items are considered for a possible match; if a demonstrator declaration lies within  $R_{crit}$  of a baseline item, that declaration is retained as a potential match. All potential matches are retained on a linked list associated with

each baseline item. An algorithm sorts this list according to the computed distance between the demonstrator declaration and the baseline item, with the demonstrator declaration closest to the baseline item listed first, followed by the second closest and so on. After this first iteration, the lists are reviewed to make sure that different baseline items are not matched to the same demonstrator declaration. If the same demonstrator declaration appears as the first entry in two or more lists, then the duplicate demonstrator declaration is removed from all but one of the lists.

To resolve potential duplicate matches, the algorithm compares the lists of each baseline item to the lists of all the other baseline items in a series of two-by-two comparisons. If two baseline items have the same demonstrator declaration at the head of their potential matches list, three situations are possible. The situation and their corresponding solutions are given below.

- **Situation 1.** Both baseline items have potential matches with more than one demonstrator declaration (that is, each list is less than 2).

*Solution: Minimize the sum of the distances between the baseline items and the demonstrator declarations. For example, in the following situation demonstrator declaration d1 could be matched to either baseline item A or B.*

<u>Baseline A</u>	<u>Baseline B</u>
d1 1.5 ft	d1 2.0 ft
d2 2.0 ft	d3 3.0 ft

- *Option 1:*  
*Baseline A—d1 distance = 1.5ft*  
*Baseline B—d3 distance = 3.0ft*  
*sum of the distances = 4.5 ft*

- *Option 2:*  
*Baseline A—d2 distance = 2.0ft*  
*Baseline B—d1 distance = 2.0ft*  
*sum of the distances = 4.0 ft*

- *Option 2 produces the smaller sum of the distance. Therefore, d1 is removed from the Baseline A list.*

- **Situation 2.** Only one baseline item has more than one potential demonstrator declaration match.

*Solution: The baseline item that has only one potential demonstrator match would remain matched to its single demonstrator declaration. The baseline item that has multiple potential demonstrator matches would remove the first declaration on its list.*

- **Situation 3.** Neither baseline item has more than one potential match to a demonstrator declaration in its list (that is, the one demonstrator declaration is the only declaration on both of the lists).

*Solution: The baseline item closest to the demonstrator declaration is matched to that declaration. The other baseline item will have its single demonstrator declaration removed from its list and will become an undetected baseline item.*

In all cases, resolving a tie removes a demonstrator declaration from the head of one of the baseline item potential matches list. Notice that this two-by-two method of tie breaking does not globally optimize the distance from demonstrator declaration to baseline item by, for example, finding all baseline items with the same demonstrator declaration at the head of its list before beginning the tie-breaking process. This method favors the demonstrator by nearly maximizing the number of matches.

The process of breaking one tie may create another tie. Therefore, the method of searching for and resolving ties is repeated until no further ties are found. Eventually, a loop through all baseline items will be free of ties. When this occurs, the process is complete, and the first declaration on each baseline item list is the final selected match. At this point,  $P_{closest}$  can be calculated as follows:

$$P_{closest} = \frac{\text{Baseline items with a demonstrator match}}{\text{Total baseline items emplaced}}$$

The number of false alarms is the number of demonstrator declarations that were not matched to a baseline item (IDA 1994).

### COMPUTATION OF $P_{group}$

If the sensor resolution is not adequate to resolve some of the closer spaced baseline items,  $P_{closest}$  may not accurately describe a demonstrator's detection capability. A more accurate measure of demonstrator performance may be  $P_{group}$ .

A group of baseline items separated by a distance that is less than the sensor resolution will most likely be detected as only one object. An accurate measure of detection performance should take into account the effect of sensor resolution if the test involves the detection of closely spaced objects. The  $P_{group}$  method of computing demonstrator performance counts such groups as only one "item" when computing probabilities of

detection. It credits a demonstrator with detecting a group of objects, and does not count as missed the individual baseline items within a group.  $P_{group}$  is computed by dividing the number of groups of baseline ordnance items within  $R_{crit}$  of a demonstrator declaration by the total number of baseline groups emplaced as follows:

$$P_{group} = \frac{\text{Number of groups detected}}{\text{Total groups emplaced}}$$

In Figure A-1, the circle represents the demonstrator declaration and the x's represent three closely spaced baseline items. In this case,  $P_{group}$  counts one detection out of one possibility for the group.

The  $P_{group}$  algorithm consists of three steps:

- **Step 1.** Determine demonstrator matches to individual baseline items; this step uses the  $P_{closest}$  algorithm to find one-to-one matches with individual baseline items.
- **Step 2.** Group the baseline items according to a grouping radius. This step assembles groups of baseline items according to the grouping radius ( $R_{group}$ ). A group can consist of one or more baseline items. The grouping algorithm initially places each baseline item into a group of its own—that is each baseline item is considered a group. Each baseline item is then visited in turn, and all other baseline items are considered for inclusion in the initial baseline item's group. The first baseline item is denoted as the *offering target* and the second baseline item is the *considered target*. If the *considered target* falls within  $R_{group}$  of the *offering target*, the *considered target* is added to the *offering target's* list of potential group members. The *offering target* considers all other baseline items for inclusion in its group, creating a list of all potential group candidates. The algorithm then checks the list for candidates that have previously been included in another group (the single item group itself). Candidates included in another group are removed from the list; those that are not are permanently added to the *offering target's* group.

The algorithm then rechecks all the baseline items to ensure that any baseline items in a group by themselves are not within  $R_{group}$  of another baseline item. If a lone baseline item is found within  $R_{group}$  of another baseline item, it is added to the other baseline item's group unless the addition increases beyond  $R_{group}$  the radius of the circle that encompasses all of the baseline items belonging to that group.

Situations may occur in which delineations between baseline item groups are not clear. For example, two groupings for the same baseline item set are shown in Figures A-2 and A-3. All four baseline items in the highlighted area cannot be included in the same group, because the radius of the circle encompassing such a group exceeds the  $R_{group}$ . The figures show two possible ways to break these baseline items into two groups. Unfortunately, the single baseline item difference in the grouping will change the measure of demonstrator performance. In the example shown in Figure A-2, the demonstrator is credited with one detection and one false alarm because both detections are applied to the same group.

- **Step 3.** Translate individual matches found in the first step to group matches based on the grouping produced in Step 2. This step in computing  $P_{\text{group}}$  involves counting the number of groups detected using the results of the first two steps. If a demonstrator has declared an ordnance item with  $R_{\text{crit}}$  of a baseline item, then the demonstrator is credited with finding the group that contains that baseline item, and that group is marked as found. If the group has already been marked as found, any further detections of that group are not counted. Because of the way the algorithm is implemented, the demonstrator declaration may not be within  $R_{\text{crit}}$  of the average  $(x, y)$  location of the baseline items in the group. The number of false alarms is the number of demonstrator declarations not within  $R_{\text{crit}}$  of a baseline item group.

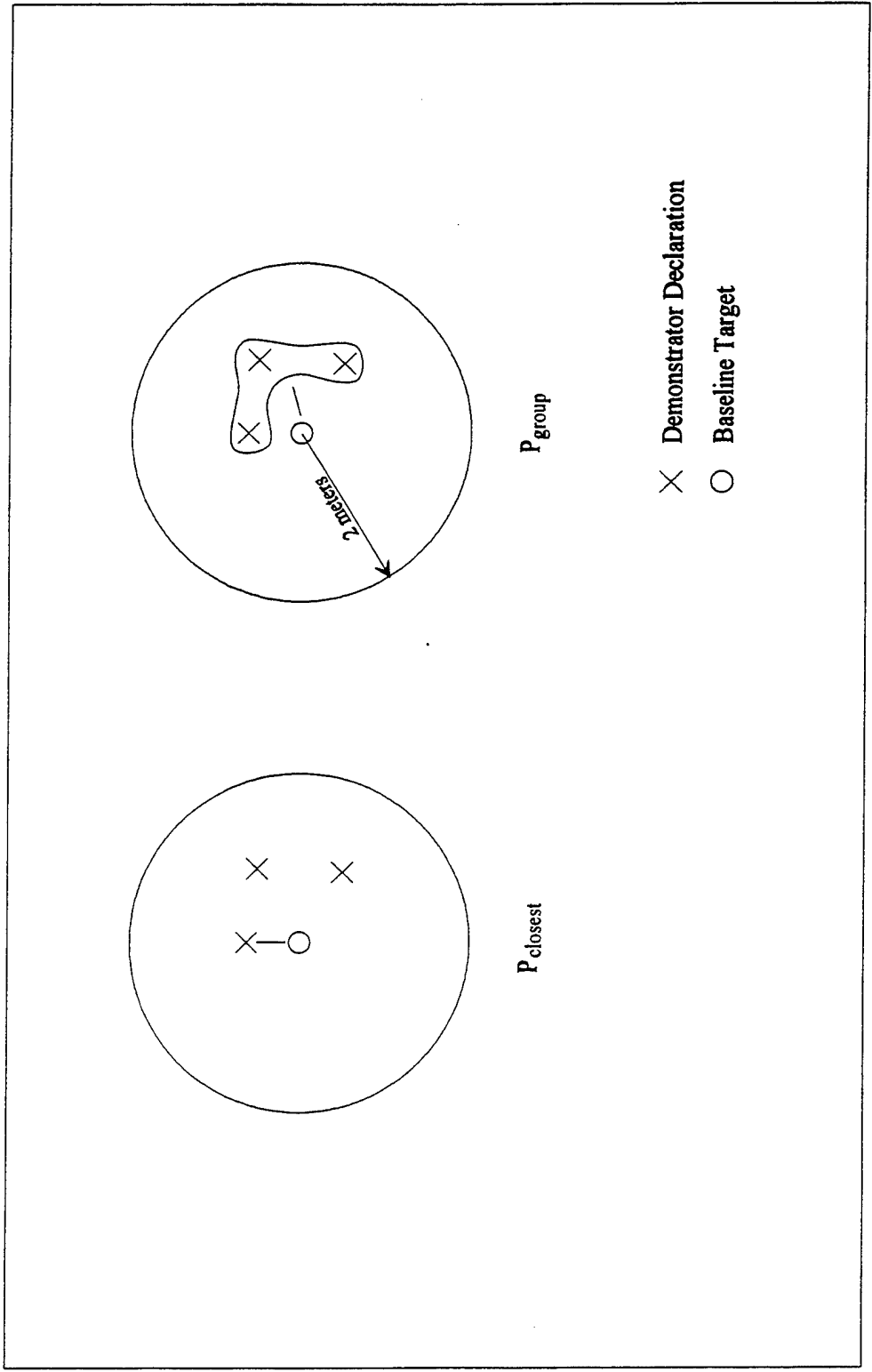


Figure A-1. Two methods of scoring three baseline targets within a 2 meter critical radius or one demonstrator declaration.

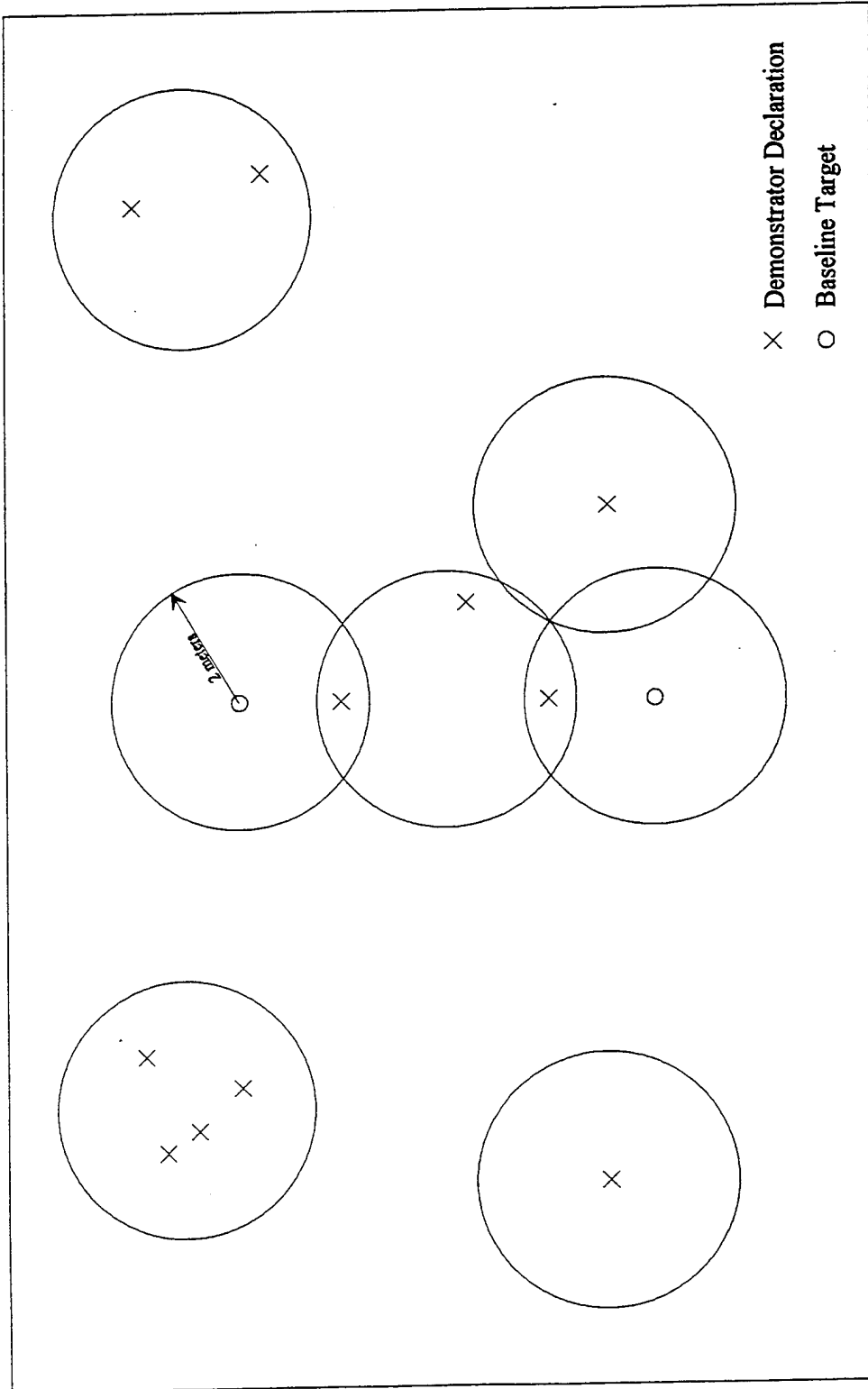


Figure A-2. An example of an ambiguous grouping that results in a decrease in demonstrator probability of detection.



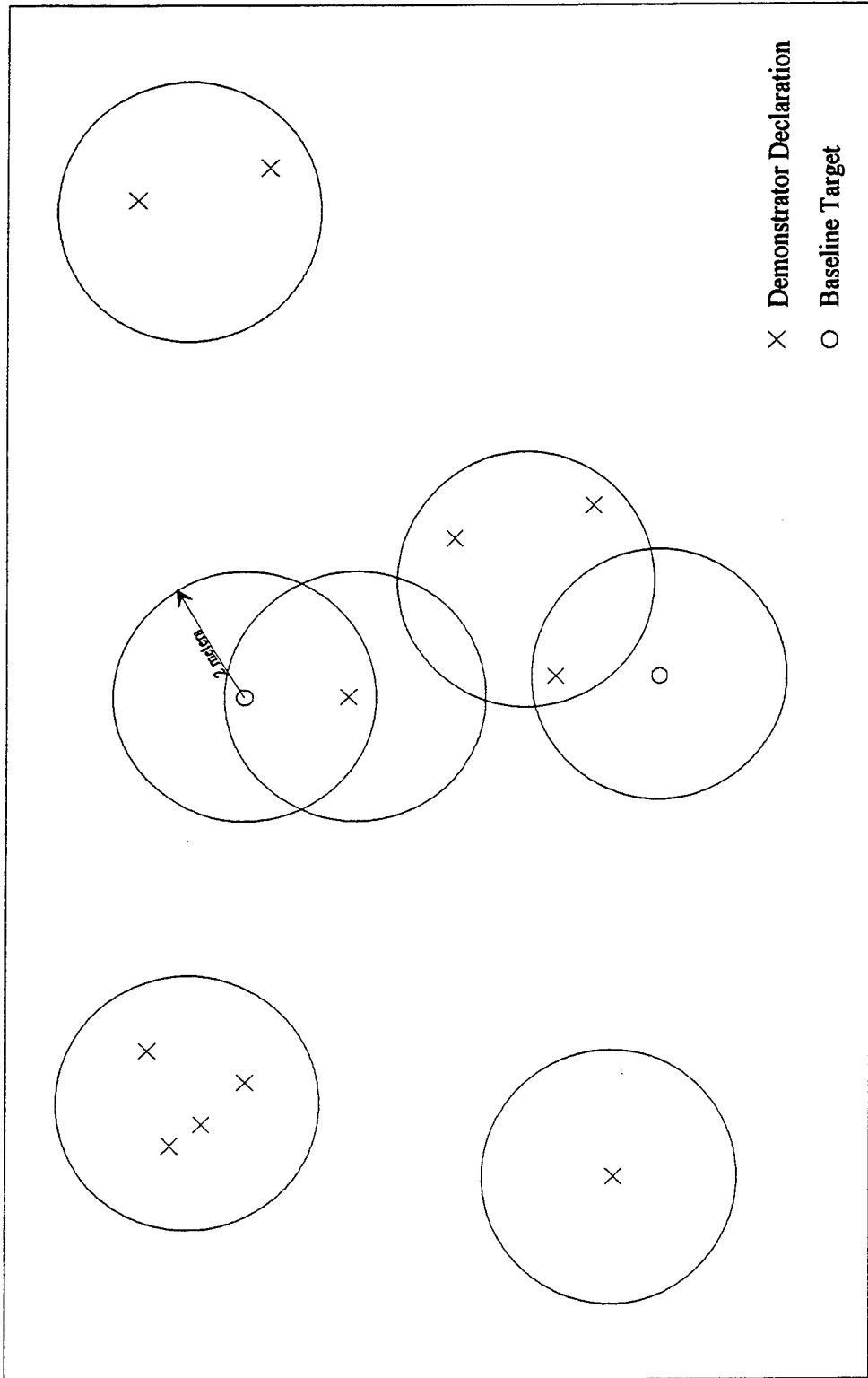


Figure A-3. An example of a second grouping of the same baseline shown in Figure A-2.

**APPENDIX B**  
**FENCE LINE AREA EXTRACTIONS**  
**16A- AND 16B-HECTARE AREAS**

Plotted target reports obtained from some demonstrators (including ADI, Geo-Centers, and Coleman) showed fairly straight lines typical of buried pipelines or fences. Subsequent excavations revealed that these lines correspond to buried or partially buried fence wire. The presence of the fence wire made it necessary to exclude from scoring all demonstrator data, as well as baseline targets, within a specified distance of the fence segments. This approach ensured that demonstrators were not penalized when they detected the fence.

To exclude the fence line areas, fence segments in the 16A- and 16B- hectare areas were first identified using ADI's data. The size of the area around each fence segment was then determined to exclude fence line data from the scoring process. For this step, the data were examined, and rectangles were centered about each of the fence segments. Since some scatter was observed in the points describing the fence segments, the widths of these rectangles were adjusted until all of the data points appeared to be within the rectangles. This process resulted in a 4-meter-wide rectangular area of exclusion.

After all demonstrator reports outside the rectangles were excluded from the data set, the residual variance of the points about the fitted lines was computed for all fence segments. The standard deviations ranged from 0.7 to 1.0 meter. About 2 standard deviations (2 meters) on either side, or a 4-meter-wide rectangle, will include 95 percent of the points.

The above analysis accounts for only the fence line segments and any deviations from the theoretical straight line drawn to subdivide the rectangles. However, when scoring each of the demonstrators, a critical radius of 2 meters was centered about each of the baseline targets to account for factors such as errors in navigation or sensor response. For example, Parsons stated that the output of its sensor is influenced by surface objects, such as wire fences, located within a 3- to 4-meter radius of the sensor. As a result, demonstrator reports that identify target locations near the sides of these rectangles may result from portions of the fence that are within this critical radius. To ensure that these false reports are not scored, the sides of the rectangles were increased by an additional 2 meters (the critical radius) on either side of the fence for a total rectangle width of 8 meters.

When the scoring algorithm was applied to the demonstrator data, any baseline targets or demonstrator data falling within the rectangles were not considered in the performance assessment. To exclude these targets and data, the location  $(x_i, y_i)$  of each report and baseline item was filtered to see if it met the following criteria:

$$\begin{aligned} \min (X_1, X_2) - 4.0 &\leq x_i \leq \max (X_1, X_2) + 4.0 \\ \min (Y_1, Y_2) - 4.0 &\leq y_i \leq \max (Y_1, Y_2) + 4.0 \end{aligned}$$

Points meeting these criteria were then tested to determine if they were horizontally within 4 meters of the straight line fence equation  $(y = mx + b)$  described above. The perpendicular distance ( $d_{\perp}$ ) from any point  $(x_i, y_i)$  to a straight can then be determined if the line fits of the following form:

$$Ax + By + C = 0$$

The perpendicular distance was calculated using the following equation:

$$d_{\perp} = \frac{Ax_i + By_i + C}{\pm\sqrt{A^2 + B^2}}$$

where

$$\begin{aligned} A &= m \\ B &= -1 \\ C &= b \end{aligned}$$

If  $d_{\perp}$  was less than or equal to 4.0, the point was excluded from consideration in the performance assessment.

## APPENDIX C

### DERIVATION OF $P_{\text{random}}$

Assessing the detection performance of any system requires considering not only how well it detects the desired UXO targets, but also how many false alarms occur in the process. A system with a high probability of detection and a high rate of false alarms would probably not be feasible for use in the field because for every true target found and remediated, excessive resources (such as time, money, and personnel) would be expended to remediate the false detections. The most desirable systems have both high probabilities of detection and low false alarm rates.

The detection probabilities of the various demonstrator systems can be quantified accurately based on the large number of emplaced targets. However, quantification of the false alarm rate for these systems presents problems. Typically, in a controlled test, any sensor responses not associated with the known baseline target set are declared as false alarms. This approach assumes that the rest of the field is free from UXO objects. A large percentage of demonstrator reports not associated with baseline targets on the 16B-hectare (40B-acre) area corresponded to various man-made items (such as plow points or wire) and UXO items (some live) that were not emplaced for this test. Because of these extraneous items, false alarm rates cannot be accurately quantified without remediating a large number of each demonstrator's reports.

However, a comparison of the number of reported targets from the various demonstrators shows a wide range in the number of potential targets. Figures C-1, C-2, and C-3 present plots of the number of target reports by demonstrator for the 16A-hectare (40A-acre), 16B-hectare (40B-acre), and 32-hectare (80-acre) areas, respectively. In these figures, the numbers differ by an order of magnitude within the same site and, in many instances, with the same type of sensor (for example, magnetometer). Assuming similar test conditions, the question remains, "Why are the number of reports so different?"

For demonstrators with large numbers of reports, possible causes must be examined. One possible cause for the reports may be that lower noise levels allow more of the smaller or deeper targets to be detected. The lower noise levels could be due to lowered sensor levels, better signal processing, or more advanced post-processing of the data. Higher noise levels (due to sensor noise, electromagnetic interference, or motion contamination) may also result in more false reports due to spurious noise spikes, particularly if the noise were not Gaussian. This latter case is addressed in the following derivation.

If the number of demonstrator reports is assumed to be due to random noise, the number of targets that would be detected randomly must be determined. To quantify this hypothesis, a measure of effectiveness,  $P_{random}$ , was developed.  $P_{random}$  represents the probability of detection due to the random distribution of demonstrator reports.

To develop this measure, the site area  $A$  is divided into individual cells with an area equal to  $\pi R_c^2$ , as defined by the critical radius  $R_{crit}$ . For a single random declaration, the probability of hitting a specific cell is equal to  $\pi R_c^2 / A$ . This process is repeated for the number of trials ( $n$ ), which corresponds to the number of demonstrator reports. Experiments of this type have a wide range of application and are known in probability theory as Bernoulli trials. Bernoulli trials are defined as repeated independent trials with only two outcomes (for example, hit or miss) for each trial, and their respective probabilities remain constant throughout the trials (Feller 1968). After  $n$  trials, a particular cell may contain from 0 to  $n$  reports. According to Feller, the probability of a cell containing exactly  $k$  reports after  $n$  Bernoulli trials is denoted by  $b(k;n,p)$  and is defined by the following equation:

$$b(k;n,p) = \binom{n}{k} p^k q^{n-k}$$

where

$$\binom{n}{k} = \frac{n!}{(n-k)!k!}$$

$$p = \text{Probability of hit} = \frac{\pi R_c^2}{A}$$

$$q = \text{Probability of miss} = 1 - p$$

Using the above equation, the probability of having no reports in a particular cell ( $k = 0$ ) is  $q^n$ , and the probability of having at least one report within a cell is  $1 - q^n$ . This equation is referred to as the binomial distribution.

For most of the cases considered in this report,  $n$  is very large (typically 100 to 2,000), and  $p$  is very small (0.00008). In these situations, it is convenient to use the Poisson approximation of the binomial distribution. The Poisson approximation for the probability of a cell containing exactly  $k$  reports after  $n$  Bernoulli trials is calculated using the following equation:

$$p(k,\lambda) \approx b(k,n,p)$$
$$= e^{-\lambda} \frac{\lambda^k}{k!}$$

The probability of having no reports in a particular cell ( $k = 0$ ) is  $e^{-\lambda}$ , and the probability of having at least one report within a cell is  $1 - e^{-\lambda}$ , which is equal to  $P_{random}$ .

**FIGURE C-1**  
**16A-HECTARE (40A-ACRE) AREA**  
**TARGET REPORTS BY DEMONSTRATOR**

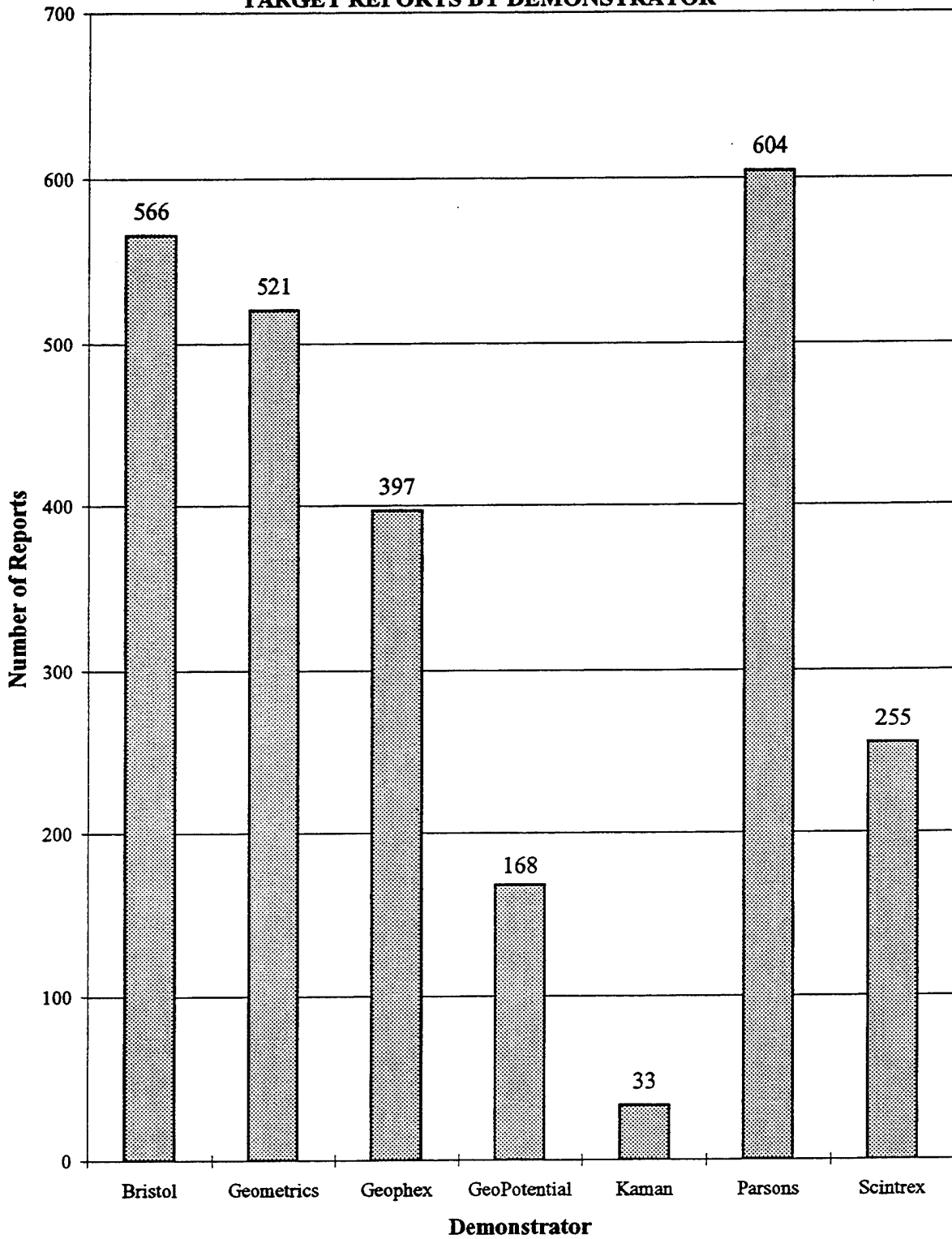


**FIGURE C-2**  
**16B-HECTARE (40B-ACRE) AREA**  
**TARGET REPORTS BY DEMONSTRATOR**

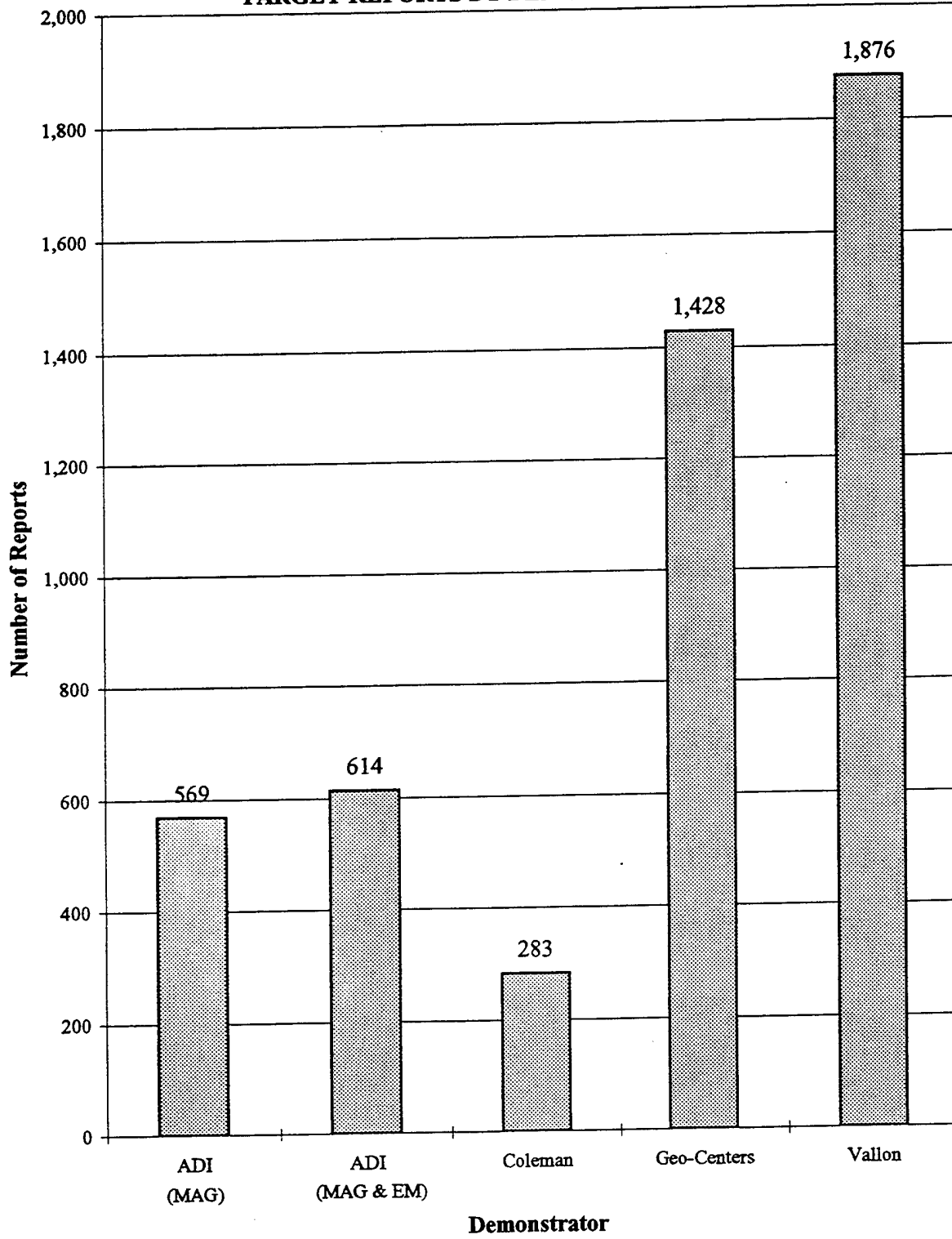
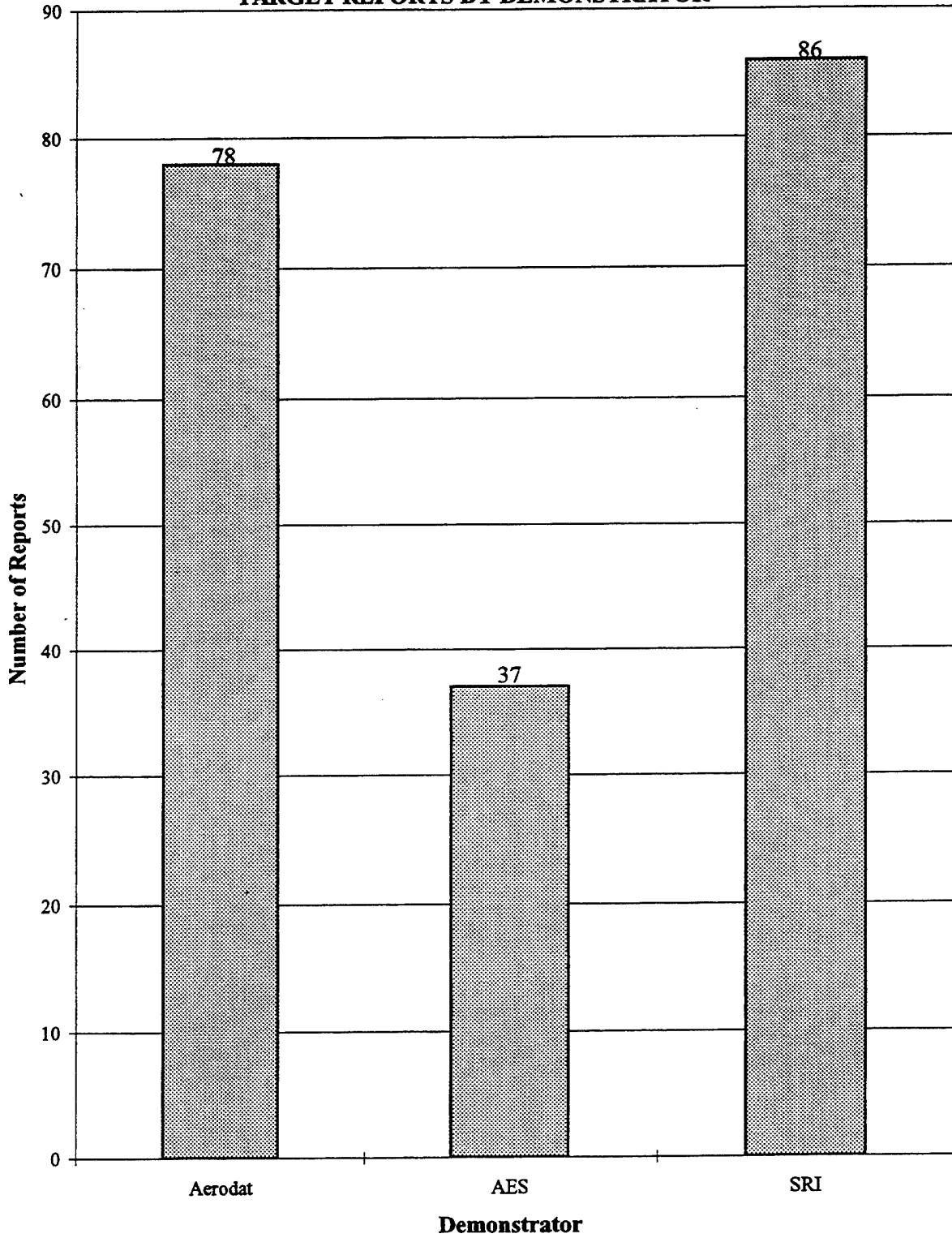




**FIGURE C-3**  
**32-HECTARE (80-ACRE) AREA**  
**TARGET REPORTS BY DEMONSTRATOR**



**APPENDIX D**  
**JPG CONTROLLED SITE 16B-HECTARE DEMONSTRATION AREA**  
**TARGET ANOMALY INVESTIGATION**

During Phase I of the UXO ATD controlled site test, the 16A-hectare area was surveyed by ground-based systems, and the 32-hectare area was surveyed by airborne systems. Locations where several of the demonstrators had coincidental reports were remediated to determine whether the reports were accurate. The 32-hectare area was not remediated due to the sparse number of reports from the airborne systems.

During Phase II, a portion of the 32-hectare area (the 16B-hectare area) was set aside for ground-based surveys. On the 16B-hectare area, a large number of demonstrator reports were not aligned with known baseline targets. To investigate whether these reports corresponded to real objects, a limited number of report locations were remediated.

For this investigation, the four ground demonstrators from the 16B-hectare area were selected. Next, locations were selected if at least three of the four ground demonstrators reported targets within a 2-meter radius of each other but not within a 2-meter radius of any known baseline object. This analysis yielded 42 holes that were subsequently remediated. Of these 42 holes, 38 contained man-made debris, and two holes contained live UXO items; in all, 40 holes (or 95.2 percent) contained metallic items. The results for each remediation are listed in Table D-1.

Because of the high yield from this remediation, 16 additional reports were selected using the following criteria: the individual demonstrator reports were (1) isolated (that is, not within a 2-meter radius of the other demonstrators) and (2) not within a 2-meter radius of a known baseline object. Of these 16 single reports, nine holes yielded man-made objects, and one hole yielded an ordnance item; in all, 10 holes (or 62.5 percent) contained metallic items.

Based on these results, the 16B-hectare area appears to be cluttered with man-made debris. As a result, the definition of false alarm was modified to include only those reports not associated with ordnance items. The ordnance items found were located in the western portion of the area near the edge of the firing range. Due to the location and small percentage of UXO items found during this remediation, the number of nonbaseline UXO items still within this area is believed to be negligible.

**TABLE D-1**  
**16B-HECTARE DEMONSTRATION AREA**  
**TARGET ANOMALY INVESTIGATION**

Target Location Number <sup>a</sup>	Demonstrator	Easting <sup>b</sup>	Northing <sup>b</sup>	Date Excavated	Target Depth (Meters)	Anomaly Detected	Comments <sup>c</sup>
003	At least three demonstrators detected the target.	640478.580	4304628.400	11/14/95	0.15	One metal horseshoe piece	None
011	At least three demonstrators detected the target.	640516.930	4304616.890	11/14/95	Not applicable (NA)	No target anomalies	Probable false alarm from the 105- millimeter (mm) howitzer round located about 0.61 meter north-northwest of target 011.
012	At least three demonstrators detected the target.	640516.330	4304617.460	11/14/95	About 0.05	One non-baseline 105-mm howitzer round with a M-51 fuze <sup>d</sup>	Azimuth and orientation are not available because the 105-mm howitzer round was disturbed during excavation.
013	At least three demonstrators detected the target.	640514.380	4304617.050	11/14/95	NA	No target anomalies	Probable false alarm from the 105-mm howitzer round located about 0.61 meter east of target 013.
027	At least three demonstrators detected the target.	640610.250	4304670.700	11/13/95	0.10	One 0.30- by 0.15-meter metal plow point	None
081	Only Coleman Research Corporation (Coleman) detected the target.	640822.500	4303996.600	11/17/95 <sup>e</sup>	0.46	Two 0.05-meter metal nails	None
085	At least three demonstrators detected the target.	640742.050	4304609.880	11/13/95	0.15	One 0.25- by 0.15-meter metal plow point	None
099	At least three demonstrators detected the target.	640710.340	4304504.550	11/14/95	0.30	One metal bracket	None

**TABLE D-1**  
**16B-HECTARE DEMONSTRATION AREA**  
**TARGET ANOMALY INVESTIGATION**  
**(CONTINUED)**

Target Location Number <sup>a</sup>	Demonstrator	Easting <sup>b</sup>	Northing <sup>b</sup>	Date Excavated	Target Depth (Meters)	Anomaly Detected	Comments <sup>c</sup>
100	At least three demonstrators detected the target.	640711.600	4304503.880	11/14/95	0.30	One 0.15-meter metal rebar	None
101	At least three demonstrators detected the target.	640714.610	4304503.290	11/14/95	0.30	One 0.30- by 0.10-meter metal plow point	None
102	At least three demonstrators detected the target.	640717.060	4304500.120	11/14/95	About 0.20	One metal yoke lead used on horse drawn implement	None
118	Only Australian Defense Industries, Pty. Ltd. (ADI), detected the target.	640791.510	4304560.650	11/17/95	NA	No target anomalies	Within a 1.22-meter radius, no metallic objects were detected.
138	Only ADI detected the target.	640788.490	4304551.650	11/17/95	NA	No target anomalies	Within a 1.22-meter radius, no metallic objects were detected.
139	Only ADI detected the target.	640791.560	4304560.410	11/17/95	NA	No target anomalies	Within a 1.22-meter radius, no metallic objects were detected.
146	At least three demonstrators detected the target.	640832.770	4304651.980	11/13/95	0.30	One 0.61 meter section of wire	None
157	At least three demonstrators detected the target.	640872.920	4304624.120	11/14/95	0.15	Two pieces of sheet metal less than 0.30 meter square each	None
162	At least three demonstrators detected the target.	640827.500	4304606.470	11/13/95	0.08	One 0.30-meter square clump of wire	None

**TABLE D-1  
16B-HECTARE DEMONSTRATION AREA  
TARGET ANOMALY INVESTIGATION  
(CONTINUED)**

Target Location Number <sup>a</sup>	Demonstrator	Easting <sup>b</sup>	Northing <sup>b</sup>	Date Excavated	Target Depth (Meters)	Anomaly Detected	Comments <sup>c</sup>
165	At least three demonstrators detected the target.	640854.870	4304597.250	11/13/95	0.08	One 1.22-meter section of rusted wire cable	None
166	At least three demonstrators detected the target.	640854.230	4304594.620	11/13/95	0.76	One 0.61-meter section of metal rebar about 0.02-meter wide and 0.006-meter thick	None
169	At least three demonstrators detected the target.	640860.790	4304583.980	11/13/95	0.15	One 0.91-meter piece of black wire	The black wire was located 1.22-meter south of the surveyed location.
178	At least three demonstrators detected the target.	640847.190	4304565.050	11/13/95	0.15	One 0.25- by 0.15-meter metal plow point	The plow point was located 0.46-meter southwest of the surveyed location.
179	At least three demonstrators detected the target.	640845.850	4304563.740	11/13/95	0.15	One 0.20- by 0.25-meter piece of sheet metal and a few dime-sized pieces of sheet metal	None
195	Only Coleman detected the target.	640831.200	4303963.900	11/17/95	0.61	Numerous small pieces of 0.02- to 0.05-meter metal rebar	None
224	Only ADI detected the target.	640455.220	4304019.660	11/17/95	1.07	One non-baseline 155-mm projectile <sup>e</sup>	Azimuth and orientation are not available because the 155-mm projectile was disturbed during excavation.
227	Only Coleman detected the target.	640808.200	4303981.300	11/17/95	0.76	One 0.10-meter metal spike or nail	None

**TABLE D-1  
16B-HECTARE DEMONSTRATION AREA  
TARGET ANOMALY INVESTIGATION  
(CONTINUED)**

Target Location Number <sup>a</sup>	Demonstrator	Easting <sup>b</sup>	Northing <sup>b</sup>	Date Excavated	Target Depth (Meters)	Anomaly Detected	Comments <sup>c</sup>
247	Only Coleman detected the target.	640861.200	4304492.200	11/17/95	0.15	One metal horseshoe	The horseshoe was located 1.22 meter southeast of the surveyed location. Beneath the survey stake, no metallic objects were detected. Excavation at this location was stopped at 1.22-meter feet below ground surface (bgs).
264	At least three demonstrators detected the target.	640418.380	4303996.570	11/13/95	0.61	One piece of fragmented metal	None
266	Only Coleman detected the target.	640770.800	4303947.700	11/17/95	0.30	One 0.05-meter piece of metal rebar	None
300	At least three demonstrators detected the target.	640480.310	4303996.480	11/13/95	0.61	The target location anomalies consist of (1) M-39 mortar fins and base plates, (2) aluminum metal blocks (about 0.61 meter long by 0.30 meter wide by 0.10 meter thick), and (3) unidentified metal debris below these metallic objects <sup>d</sup>	The metal debris apparently resulted from the U.S. Army's use of this location as a waste disposal pit. The metal was not removed from this location because the waste metal volume would exceed 2 cubic meters.
305	At least three demonstrators detected the target.	640462.550	4303987.830	11/13/95	0.08	One green, rectangular metal lid from a military vehicle	None
331	At least three demonstrators detected the target.	640425.830	4303973.960	11/13/95	0.15	Two pieces of wire	None

**TABLE D-1  
16B-HECTARE DEMONSTRATION AREA  
TARGET ANOMALY INVESTIGATION  
(CONTINUED)**

Target Location Number <sup>a</sup>	Demonstrator	Easting <sup>b</sup>	Northing <sup>b</sup>	Date Excavated	Target Depth (Meters)	Anomaly Detected	Comments <sup>c</sup>
337	At least three demonstrators detected the target.	640420.960	4303972.590	11/13/95	0.15	One piece of wire	None
343	At least three demonstrators detected the target.	640412.980	4303958.500	11/13/95	0.08	One non-baseline 60-mm M-49 mortar round <sup>d</sup>	Azimuth: flat. Orientation: East. The markings on the mortar were 1955 and PT319.
372	At least three demonstrators detected the target.	640529.290	4304045.350	11/13/95	0.30	One piece of fragmented metal	None
390	Only Geo-Centers, Inc. (Geo-Centers), detected the target.	640584.100	4303956.800	11/17/95	0.02	One 0.30-meter section of barbed wire	The barbed wire was detected at 0.91-meter north of the surveyed location. Beneath the survey stake, no metallic objects were detected. Excavation at this location was stopped at 1.22-meter bgs.
392	Only ADI detected the target.	640492.080	4304009.480	11/17/95	NA	No target anomalies detected	Within a 1.22-meter radius, no metallic objects were detected.
406	At least three demonstrators detected the target.	640510.100	4303942.700	11/13/95	0.20	Small pieces of metal fence and nails less than 0.02-meter long	The fence was connected to the fence detected at target location 407.
407	At least three demonstrators detected the target.	640509.040	4303941.470	11/13/95	0.20	Metal fence and wire	None
528	At least three demonstrators detected the target.	640623.070	4303982.650	11/13/95	About 0.20	Two pieces of bailing and barbed wire	Both pieces of wire were detected 0.61-meter south of the surveyed location.

**TABLE D-1  
16B-HECTARE DEMONSTRATION AREA  
TARGET ANOMALY INVESTIGATION  
(CONTINUED)**

Target Location Number <sup>a</sup>	Demonstrator	Easting <sup>b</sup>	Northing <sup>b</sup>	Date Excavated	Target Depth (Meters)	Anomaly Detected	Comments <sup>c</sup>
667	At least three demonstrators detected the target.	640747.810	4303937.870	11/13/95	About 0.15	One 0.30-meter metal bracket	None
686	At least three demonstrators detected the target.	640759.860	4303949.480	11/13/95	Surface	One 3.66-meter piece of barbed wire	None
706	At least three demonstrators detected the target.	640831.320	4304120.460	11/13/95	0.15	One 0.61-meter section of metal rebar	None
725	At least three demonstrators detected the target.	640820.620	4303983.370	11/13/95	0.30	Two pieces of 0.02-meter wire cable	The two pieces of wire cable stretched between target numbers 725 and 752. Target location numbers 725 and 752 were staked by the surveyors about 0.30-meter apart.
726	At least three demonstrators detected the target.	640821.550	4303979.640	11/13/95	0.08	One 1.07-meter piece of metal wire	The piece of wire stretched between target locations 726 and 753. Target locations 726 and 753 were staked by the surveyors less than 0.30-meter apart.
731	At least three demonstrators detected the target.	640822.590	4303997.940	11/13/95	0.30	Two pieces of wire	None
734	At least three demonstrators detected the target.	640840.110	4303996.240	11/13/95	0.30	Two pieces of metal fence post	None
746	Only ADI detected the target.	640830.950	4303936.040	11/17/95	0.91	One piece of 0.08-meter metal rebar and several 0.08-meter metal bolts	None



**TABLE D-1**  
**16B-HECTARE DEMONSTRATION AREA**  
**TARGET ANOMALY INVESTIGATION**  
**(CONTINUED)**

Target Location Number <sup>a</sup>	Demonstrator	Easting <sup>b</sup>	Northing <sup>b</sup>	Date Excavated	Target Depth (Meters)	Anomaly Detected	Comments <sup>c</sup>
752	At least three demonstrators detected the target.	640820.540	4303983.100	11/13/95	0.30	Two pieces of 0.02-meter wire cable	The two pieces of wire cable stretched between target locations 725 and 752, which were staked by the surveyors about 0.30-meter apart.
753	At least three demonstrators detected the target.	640821.570	4303979.660	11/13/95	0.08	One 1.07-meter piece of wire	The piece of wire stretched between target locations 726 and 753, which were staked by the surveyors less than 0.30-meter apart.
756	At least three demonstrators detected the target.	640815.150	4303929.380	11/13/95	Surface	Two pieces of concrete with metal rebar and wire	None
757	At least three demonstrators detected the target.	640807.840	4303920.850	11/13/95	0.15	Six pieces of green metal fence post ranging from 0.30 to 2.44 meters long	None
771	At least three demonstrators detected the target.	640799.700	4303922.770	11/13/95	0.15	One piece of metal fence strap	None
779	At least three demonstrators detected the target.	640834.640	4303949.190	11/13/95	0.15	One horseshoe	None
785	At least three demonstrators detected the target.	640832.940	4303965.590	11/13/95	0.08	One 0.30-meter square metal piece and one 1.83-meter wire piece	None
960	Only Geo-Centers detected the target.	640780.300	4303938.300	11/17/95	NA	No target anomalies detected	Within a 1.22-meter radius, no metallic objects were detected.

**TABLE D-1  
16B-HECTARE DEMONSTRATION AREA  
TARGET ANOMALY INVESTIGATION  
(CONTINUED)**

Target Location Number <sup>a</sup>	Demonstrator	Easting <sup>b</sup>	Northing <sup>b</sup>	Date Excavated	Target Depth (Meters)	Anomaly Detected	Comments <sup>c</sup>
1641	Only Geo-Centers detected the target.	640855.100	4304493.200	11/17/95	0.30	Numerous 0.02- to 0.05-meter metal nails and rebar	Additional metal and rebar were detected 0.46-meter southwest of the surveyed location.
1668	Only Geo-Centers detected the target.	640857.700	4304526.000	11/17/95	NA	No target anomalies detected	Within a 1.22-meter radius, no metallic objects were detected.
1756	Only Geo-Centers detected the target.	640874.500	4304595.300	11/17/95	0.30	One metal handle	None

Notes:

- a Target anomaly detected by one of three demonstrators (ADI, Coleman, or Geo-Centers) with a high confidence level.
- b The target location number was based on ADI target declaration number.
- c All target locations were swept with a Schoensted metal detector within a 4-foot (1.22-meter) radius of the surveyed location.
- d All target locations excavated on November 17, 1995, were high probability targets declared by only one of three demonstrators.
- e Item excavated assumed to be a result of previous U.S. Army active operations at JPG.

**APPENDIX E**  
**MINE DETECTION STATISTICS**

Mine detection capabilities were not the focus of the Phase II UXO ATDs; however, both the 16A- and 16B-hectare areas contained small mine fields. The 16A-hectare area contained 15 emplaced mines, and the 16B-hectare area contained 12 mines.

Demonstrator mine detection capabilities are shown in Table E-1; only three demonstrators detected mines: Parsons Engineering Science, Inc.; Bristol Aerospace Ltd.; and Vallon GmbH (Vallon). Vallon had the highest probability of detection, most likely because two mines were visually located on the surface of the demonstration area during the course of the survey.

**TABLE E-1  
MINE DETECTION STATISTICS**

Demonstrator	Area Surveyed (Hectares)	No. of Mines	No. of Mines Detected	Probability of Detection ( $P_D$ )
Aerodat Inc.	32	12	0	0.00
Airborne Environmental Surveys	32	12	0	0.00
Australian Defense Industries, Pty. Inc.	16B	12	0 <sup>a</sup> 0 <sup>b</sup>	0.00 0.00
Bristol Aerospace Ltd.	16A	15	3	0.20
Coleman Research Corporation	16B	12	0	0.00
Geo-Centers, Inc.	16B	12	0	0.00
Geometrics, Inc.	16A	15	0	0.00
Geophex Ltd.	16A	15	0	0.00
Geopotential	16A	15	0	0.00
Kaman Sciences Corporation	16A	15	0	0.00
Parsons Engineering Science, Inc.	16A	15	1	0.07
Polestar Technologies, Inc.	16A	15	NR	NR
SRI International	32	12	0	0.00
Scintrex, Inc.	16A	12	0	0.00
Vallon GmbH	16B	12	7 <sup>c</sup>	0.58

Notes:

- a Electromagnetic survey results
- b Magnetometer survey results
- c Two mines were visually located by Vallon during the demonstration.
- NR No data reported

**APPENDIX F**  
**DEMONSTRATOR COST**

Table F-1 presents the costs of surveying a hectare of land at one of the three JPG control sites. Cost data were determined by dividing the individual demonstrator cost by the number of hectares the demonstrator surveyed. Remediation demonstrator costs per hectare were not calculated because those demonstrators remediated selected targets, rather than a specific area. In addition, because the Wright Laboratory REVS demonstration was performed by a government agency, no cost information was provided.

**APPENDIX F  
DEMONSTRATOR COST**

Demonstrator	Demonstration Area (Hectares)	Area Scored		Cost (\$)	Cost per Hectare (\$)
		Hectares	Acres		
<b>Airborne Systems:</b>					
Airborne Environmental Surveys	32	32	80	352,935	11,029
Aerodat Inc.	32	32	80	39,894	1,250
SRI International	32	32	80	137,240	4,289
<b>Ground Systems:</b>					
Australian Defence Industries, Pty. Inc.	16B	16	40	90,002	5,625
Geophex Ltd.	16A	16	40	58,457	3,529
GeoPotential	16A	13.6	33.6	25,990	1,911
Parsons Engineering Science, Inc.	16A	16	40	54,065	3,379
Polestar Technologies, Inc.	16A	16	40	166,293	10,393
Scintrex, Inc.	16A	5.8	14.2	41,643	7,180
<b>Vehicle Systems:</b>					
Bristol Aerospace Ltd.	16A	13.6	33.6	99,806	7,339
Kaman Sciences Corporation	16A	8.5	21	245,285	28,587
<b>Combined Systems:</b>					
Coleman Research Corporation	16B	16	40	78,862	4,929
Geo-Centers, Inc.	16B	16	40	151,819	9,489
Geometrics, Inc.	16A	16	40	296,997	18,562
Vallon GmbH ( in cooperation with Security Search Products)	16B	16	40	66,308	4,144
<b>Remediation:</b>					
Concept Engineering Group	16A	<sup>1</sup>	<sup>1</sup>	70,459	NA
Wright Laboratory REVS	16A	<sup>1</sup>	<sup>1</sup>	<sup>2</sup>	NA

**Notes:**

- <sup>1</sup> Remediation demonstrations not scored.
- <sup>2</sup> Government demonstration cost not provided.
- NA not available

## GLOSSARY

### Abbreviations and Acronyms

ADI	Australian Defence Industries Pty Ltd.
Aerodat	Aerodat, Inc.
AES	Airborne Environmental Surveys
AETC	Arete Engineering Technologies Corporation
AGPR	Airborne ground penetrating radar
ATD	Advanced Technology Demonstration
ATV	All-terrain vehicle
ANSI	American National Standards Institute
Bristol	Bristol Aerospace Limited
Coleman	Coleman Research Corporation
CEG	Concept Engineering Group, Inc.
DAIS	Digital airborne imaging spectrometer
DRA	Demonstrator reference area
DWP	Demonstration work plan
EM	Electromagnetic
FAR	False alarm rate
Geo-Centers	Geo-Centers, Inc.
GER	Geophysical and Environmental Research Corporation
Geometrics	Geometrics, Inc.
Geophex	Geophex, Ltd.
GDE	GDE Systems, Inc.
GIS	Geographic information system
GPR	Ground-penetrating radar
GPS	Global positioning system
HEAT	High Explosive Anti-Tank
IDNR	Indiana Department of Natural Resources
IDA	Institute for Defense Analysis
JPG	Jefferson Proving Ground
Kaman	Kaman Sciences Corporation
ManPODS	Man-portable detection system
MAPS	Modular azimuth positioning system
MCS	Mobile command station
MOE	Measures of effectiveness
NAVEODTECHDIV	Naval Explosive Ordnance Disposal Technology Division
NEPA	National Environmental Policy Act
OPTEVFOR	Operational Test and Evaluation Forces
PBS	Precision beacon system

PC  
Parsons  
Polestar  
PRC  
projo  
PVC  
QA  
QAPP  
QC  
REVS  
SAR  
SEPOS  
SRI  
SHERP

STOLS  
TAMIR  
TDEM  
TMA  
ToMAS  
USAEC  
USDA  
USGS  
UTM  
UXO  
Vallon

#### Units and Measures

°C  
°F  
ft  
hr.  
Hz  
in.  
kg  
kHz  
km  
lb.  
m  
MHz  
mm

Personal computer  
Parsons Engineering Science, Inc.  
Polestar Technologies, Inc.  
PRC Environmental Management, Inc.  
Projectile  
Polyvinyl chloride  
Quality assurance  
Quality assurance program plan  
Quality control  
Remote excavation vehicle system  
Synthetic aperture radar  
Sensor positioning system  
SRI International  
Safety, Health, and Emergency Response  
Plan  
Surface-towed ordnance locator system  
Target adaptive matched illumination radar  
Time domain electromagnetic  
Target matching algorithm  
Towed multi-sensor array system  
U.S. Army Environmental Center  
U.S. Department of Agriculture  
U.S. Geological Survey  
Universal transverse mercator  
Unexploded ordnance  
Vallon GmbH

degrees Centigrade  
degrees Fahrenheit  
feet  
hour  
hertz  
inch(es)  
kilogram  
kilohertz  
kilometer  
pound  
meter  
megahertz  
millimeter